

# Chronic inflammation and pharmacological interventions in cardiovascular diseases, volume II

**Edited by**

Xianwei Wang, Min Zhang and Zufeng Ding

**Published in**

Frontiers in Pharmacology



## FRONTIERS EBOOK COPYRIGHT STATEMENT

The copyright in the text of individual articles in this ebook is the property of their respective authors or their respective institutions or funders. The copyright in graphics and images within each article may be subject to copyright of other parties. In both cases this is subject to a license granted to Frontiers.

The compilation of articles constituting this ebook is the property of Frontiers.

Each article within this ebook, and the ebook itself, are published under the most recent version of the Creative Commons CC-BY licence. The version current at the date of publication of this ebook is CC-BY 4.0. If the CC-BY licence is updated, the licence granted by Frontiers is automatically updated to the new version.

When exercising any right under the CC-BY licence, Frontiers must be attributed as the original publisher of the article or ebook, as applicable.

Authors have the responsibility of ensuring that any graphics or other materials which are the property of others may be included in the CC-BY licence, but this should be checked before relying on the CC-BY licence to reproduce those materials. Any copyright notices relating to those materials must be complied with.

Copyright and source acknowledgement notices may not be removed and must be displayed in any copy, derivative work or partial copy which includes the elements in question.

All copyright, and all rights therein, are protected by national and international copyright laws. The above represents a summary only. For further information please read Frontiers' Conditions for Website Use and Copyright Statement, and the applicable CC-BY licence.

ISSN 1664-8714  
ISBN 978-2-8325-4018-3  
DOI 10.3389/978-2-8325-4018-3

## About Frontiers

Frontiers is more than just an open access publisher of scholarly articles: it is a pioneering approach to the world of academia, radically improving the way scholarly research is managed. The grand vision of Frontiers is a world where all people have an equal opportunity to seek, share and generate knowledge. Frontiers provides immediate and permanent online open access to all its publications, but this alone is not enough to realize our grand goals.

## Frontiers journal series

The Frontiers journal series is a multi-tier and interdisciplinary set of open-access, online journals, promising a paradigm shift from the current review, selection and dissemination processes in academic publishing. All Frontiers journals are driven by researchers for researchers; therefore, they constitute a service to the scholarly community. At the same time, the *Frontiers journal series* operates on a revolutionary invention, the tiered publishing system, initially addressing specific communities of scholars, and gradually climbing up to broader public understanding, thus serving the interests of the lay society, too.

## Dedication to quality

Each Frontiers article is a landmark of the highest quality, thanks to genuinely collaborative interactions between authors and review editors, who include some of the world's best academicians. Research must be certified by peers before entering a stream of knowledge that may eventually reach the public - and shape society; therefore, Frontiers only applies the most rigorous and unbiased reviews. Frontiers revolutionizes research publishing by freely delivering the most outstanding research, evaluated with no bias from both the academic and social point of view. By applying the most advanced information technologies, Frontiers is catapulting scholarly publishing into a new generation.

## What are Frontiers Research Topics?

Frontiers Research Topics are very popular trademarks of the *Frontiers journals series*: they are collections of at least ten articles, all centered on a particular subject. With their unique mix of varied contributions from Original Research to Review Articles, Frontiers Research Topics unify the most influential researchers, the latest key findings and historical advances in a hot research area.

Find out more on how to host your own Frontiers Research Topic or contribute to one as an author by contacting the Frontiers editorial office: [frontiersin.org/about/contact](https://frontiersin.org/about/contact)

# Chronic inflammation and pharmacological interventions in cardiovascular diseases, volume II

## Topic editors

Xianwei Wang — Xinxiang Medical University, China

Min Zhang — BHF Centre of Research Excellence, School of Cardiovascular Medicine & Sciences, Faculty of Life Sciences & Medicine, King's College London, United Kingdom

Zufeng Ding — University of Arkansas for Medical Sciences, United States

## Citation

Wang, X., Zhang, M., Ding, Z., eds. (2023). *Chronic inflammation and pharmacological interventions in cardiovascular diseases, volume II*. Lausanne: Frontiers Media SA. doi: 10.3389/978-2-8325-4018-3

# Table of contents

- 04 **Editorial: Chronic inflammation and pharmacological interventions in cardiovascular diseases, volume II**  
Aiwei Yan, Xiaoping Wang, Can Cui, Min Zhang and Xianwei Wang
- 07 **Association between fibrinogen/albumin ratio and arterial stiffness in patients with type 2 diabetes: A cross-sectional study**  
Chun-mei Chen, Chun-feng Lu, Wang-shu Liu, Zhen-hua Gong, Xue-qin Wang, Feng Xu, Jian-feng Ji and Xing-xing Fang
- 15 **Systematic investigation of the underlying mechanisms of GLP-1 receptor agonists to prevent myocardial infarction in patients with type 2 diabetes mellitus using network pharmacology**  
Guorong Deng, Jiajia Ren, Ruohan Li, Minjie Li, Xuting Jin, Jiamei Li, Jueheng Liu, Ya Gao, Jingjing Zhang, Xiaochuang Wang and Gang Wang
- 28 **A prospective randomized comparative placebo-controlled double-blind study in two groups to assess the effect of the use of biologically active additives with Siberian fir terpenes for the biological age of a person**  
Faniya Maganova, Mikhail Voevoda, Vladimir Popov and Alexey Moskalev
- 35 **Meta-analysis and trial sequential analysis of ezetimibe for coronary atherosclerotic plaque compositions**  
Bofeng Chai, Youlu Shen, Yuhong Li and Xiaoyu Wang
- 44 **A novel glycyrrhizin acid-coated stent reduces neointimal formation in a rabbit iliac artery model**  
Shuai Teng, Zhaowei Zhu, Yang Li, Xinqun Hu, Zhenfei Fang, Zhenjiang Liu and Shenghua Zhou
- 53 **Fucoidan inhibits apoptosis and improves cardiac remodeling by inhibiting p53 transcriptional activation through USP22/Sirt 1**  
Shuai Wang, Jie Bai, Yilin Che, Weikun Qu and Jing Li
- 63 **Identification of the biological processes, immune cell landscape, and hub genes shared by acute anaphylaxis and ST-segment elevation myocardial infarction**  
Zekun Peng, Hong Chen and Miao Wang
- 82 **Inhibition of GSDMD activation by Z-LLSD-FMK or Z-YVAD-FMK reduces vascular inflammation and atherosclerotic lesion development in ApoE<sup>-/-</sup> mice**  
Bao-Li Zhang, Peng Yu, En-Yong Su, Chun-Yu Zhang, Shi-Yao Xie, Xue Yang, Yun-Zeng Zou, Ming Liu and Hong Jiang
- 94 **Evaluating the role of serum uric acid in the risk stratification and therapeutic response of patients with pulmonary arterial hypertension associated with congenital heart disease (PAH-CHD)**  
Jun Luo, Yuanchang Li, Jingyuan Chen, Haihua Qiu, Wenjie Chen, Xiaoqin Luo, Yusi Chen, Yingjie Tan and Jiang Li





## OPEN ACCESS

EDITED AND REVIEWED BY  
Eliot Ohlstein,  
Drexel University, United States

## \*CORRESPONDENCE

Xianwei Wang,  
✉ wangxianwei1116@126.com

<sup>†</sup>These authors have contributed equally to this work

RECEIVED 16 October 2023

ACCEPTED 02 November 2023

PUBLISHED 13 November 2023

## CITATION

Yan A, Wang X, Cui C, Zhang M and Wang X (2023), Editorial: Chronic inflammation and pharmacological interventions in cardiovascular diseases, volume II.  
*Front. Pharmacol.* 14:1322371.  
doi: 10.3389/fphar.2023.1322371

## COPYRIGHT

© 2023 Yan, Wang, Cui, Zhang and Wang. This is an open-access article distributed under the terms of the [Creative Commons Attribution License \(CC BY\)](#). The use, distribution or reproduction in other forums is permitted, provided the original author(s) and the copyright owner(s) are credited and that the original publication in this journal is cited, in accordance with accepted academic practice. No use, distribution or reproduction is permitted which does not comply with these terms.

# Editorial: Chronic inflammation and pharmacological interventions in cardiovascular diseases, volume II

Aiwei Yan<sup>1,2†</sup>, Xiaoping Wang<sup>1,2†</sup>, Can Cui<sup>1</sup>, Min Zhang<sup>3</sup> and Xianwei Wang<sup>1,2\*</sup>

<sup>1</sup>Henan Key Laboratory of Medical Tissue Regeneration, Xinxiang Medical University, Xinxiang, China,

<sup>2</sup>Department of Human Anatomy and Histoembryology, Xinxiang Medical University, Xinxiang, China,

<sup>3</sup>School of Cardiovascular and Metabolic Medicine & Sciences, King's College London BHF Centre of Research Excellence, London, United Kingdom

## KEYWORDS

chronic inflammation, cardiovascular diseases, pharmacological interventions, cell-based therapies, cellular and molecular mechanisms

## Editorial on the Research Topic

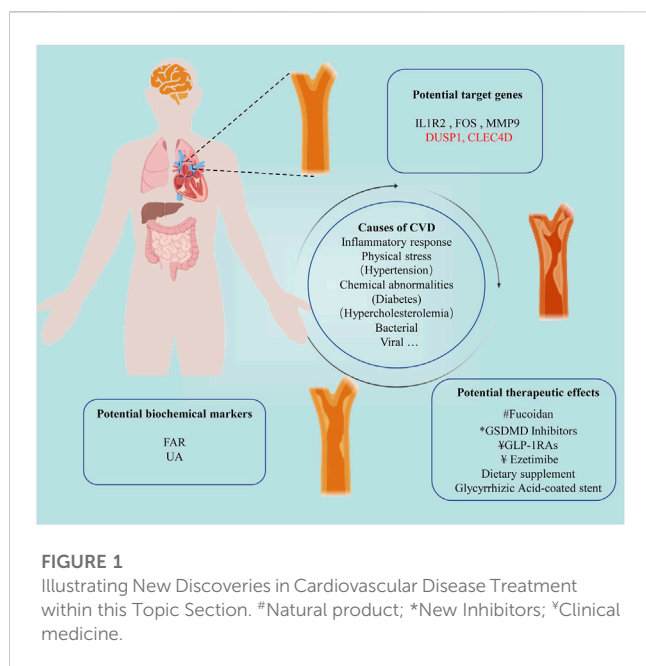
Chronic inflammation and pharmacological interventions in cardiovascular diseases, volume II

## Introduction

Cardiovascular diseases encompass a variety of diseases affecting the heart and vascular system, including coronary artery disease, hypertension, and diverse cardiac disorders. These pathologies are frequently associated with numerous risk factors such as hypertension, high cholesterol, and diabetes (Prousi et al., 2023). Research has elucidated that these factors can often instigate chronic inflammation which can induce a series of adverse physiological reactions, thereby facilitating the occurrence and progression of cardiovascular diseases (Ferrucci and Fabbri, 2018; Goswami et al., 2021).

Presently, to counteract the detrimental effects of chronic inflammation on the cardiovascular system, researchers have initiated the exploration and implementation of various pharmacological intervention strategies (Li et al., 2023). Predominantly focusing on the utilization of anti-inflammatory drugs to attenuate the severity of chronic inflammation and its associated risks, these interventions aim to offer a more secure treatment regimen for patients with cardiovascular diseases (Delbaere et al., 2023).

In the first series of studies centered on “*Chronic Inflammation and Pharmacological Interventions in Cardiovascular Diseases*”, a large number of studies were conducted. Given the sustained interest and critical importance of this area, we have initiated the second round of thematic discussions and eventually accepted eight original research papers and one review (Figure 1).



## Traditional techniques in cardiovascular disease treatment

Within this anthology of nine contributions, the mechanisms of clinical drug interventions in cardiovascular health continue to be unraveled with attention. To illustrate, [Maganova et al.](#) has delineated the beneficial effects of the dietary supplement fir terpenoids in enhancing cerebral blood flow and ameliorating arterial conditions indicative of biological aging. Concurrently, [Wang et al.](#) has cast a spotlight on the salutary properties of the natural entity FO in bolstering cardiac function. This is achieved through a marked reduction in Ang II-induced apoptosis, facilitated by the modulation of USP22/Sirt1 signaling pathways. Besides, [Zhang et al.](#) assessed the effect of GSDMD inhibitor Z-LLSD-FMK or Z-YVAD-FMK in diminishing vascular inflammation and hindering lesion progression in ApoE<sup>-/-</sup> mice, a process orchestrated through the suppression of GSDMD activation. Drug-eluting stents (DES) have become a specific non-pharmacological therapeutic tool for the treatment of cardiovascular diseases ([Crea, 2020](#)). Augmenting the narrative on innovative medical devices, [Teng et al.](#) has presented a pioneering glycyrrhizin acid (GA)-coated stent, lauded for its inhibition of intimal hyperplasia and facilitation of re-endothelialization, thereby marking a significant breakthrough in cardiovascular therapy. Notably, when benchmarked against rapamycin-eluting stents, GA-eluting variants demonstrated a more extensive endothelial coverage, indicating a promising lead in therapeutic efficacy.

## Exploring cardiovascular therapies with big data

In the ongoing efforts to elucidate the intricacies of drug-disease interactions, big data analytics have emerged as an indispensable

tool, underpinning a significant portion (5 out of 9) of the investigations encapsulated in this topic, leveraging this approach alongside detailed analyses of related disease reports to foster novel research avenues.

A notable investigation conducted by [Chen et al.](#) utilized a meticulous cross-sectional exploration of 413 individuals suffering from type 2 diabetes (T2D), uncovering a distinct positive correlation between the Fibrinogen albumin ratio (FAR) level in male patients and both brachial-ankle pulse wave velocity (baPWV) and arterial rigidity, thereby spotlighting potential avenues for further research in this area. [Luo et al.](#) embarked on a detailed analysis involving 225 individuals with coronary heart disease juxtaposed with a control group comprising 40 healthy individuals. Their focal point was discerning the interplay between serum uric acid (UA) levels and the severity as well as the treatment responsiveness in patients with PAH and congenital heart disease (PAH-CHD). The finding that serum UA could potentially function as a feasible and cost-effective biomarker for risk categorization and scrutinizing PAH-specific medicinal interventions stands as a testament to the depth of their investigation.

In parallel, [Deng et al.](#) employed network pharmacology to explore the underlying mechanisms through which GLP-1RAs reduce the incidence of myocardial infarction (MI) in T2DM patients. They underscored the multi-faceted role of GLP-1RAs in attenuating MI by modulating key biological targets and processes, and influencing cellular signaling pathways associated with atheromatous plaque development, myocardial remodeling, and thrombogenesis. Besides, [Peng et al.](#) undertook a holistic characterization of the peripheral whole blood transcriptome in individuals experiencing acute anaphylaxis and ST-segment elevation myocardial infarction (STEMI). This endeavor led to the identification of shared biological processes and immune cell landscapes, bringing to light critical hub genes, namely DUSP1 and CLEC4D.

Lastly, a meta-analytical systematic review and sequential trial scrutiny helmed by [Chai et al.](#) evaluated the influence of zetimide on the genesis of coronary atherosclerotic plaque composition. Their conclusions underscored zetimide's potency in curtailing fibro-fatty plaque (FFP) formations, albeit without notable effects on fibrous plaque (FP), necrotic core (NC) or altering dense calcification (DC) dynamics.

These studies provide valuable insights and solutions to unsolved clinical questions. Instead of solely relying on basic laboratory research for validation, current investigations leverage big data analysis techniques, utilizing large-scale samples and a comprehensive perspective to address clinical issues, thereby ensuring the reliability and holistic understanding of the conclusions reached.

## Conclusion

Each investigation within this thematic compilation delineates critical pathways and prospective therapeutic strategies, shedding new light on advancements in the field of pharmacological interventions for cardiovascular diseases. These endeavors notably provide new insights for innovative treatments targeting chronic inflammation, thereby ushering in a new frontier in mitigating the adversities associated with these ailments.

## Author contributions

AY: Writing–original draft. XW: Writing–original draft, Conceptualization. CC: Writing–original draft. MZ: Writing–review & editing. XW: Writing–review & editing.

## Conflict of interest

The authors declare that the research was conducted in the absence of any commercial or financial relationships that could be construed as a potential conflict of interest.

## References

- Crea, F. (2020). The growing non-pharmacological armamentarium for the treatment of cardiovascular diseases: from drug-coated balloons to drug-eluting stents, extracorporeal membrane oxygenation, and stem cells. *Eur. Heart J.* 41, 3593–3597. doi:10.1093/eurheartj/ehaa854
- Delbaere, Q., Chapet, N., Huet, F., Delmas, C., Mewton, N., Prunier, F., et al. (2023). Anti-inflammatory drug candidates for prevention and treatment of cardiovascular diseases. *Pharm. (Basel)* 16, 78. doi:10.3390/ph16010078
- Ferrucci, L., and Fabbri, E. (2018). Inflammageing: chronic inflammation in ageing, cardiovascular disease, and frailty. *Nat. Rev. Cardiol.* 15, 505–522. doi:10.1038/s41569-018-0064-2
- Goswami, S. K., Ranjan, P., Dutta, R. K., and Verma, S. K. (2021). Management of inflammation in cardiovascular diseases. *Pharmacol. Res.* 173, 105912. doi:10.1016/j.phrs.2021.105912
- Li, X., Sun, C., Zhang, J., Hu, L., Yu, Z., Zhang, X., et al. (2023). Protective effects of paeoniflorin on cardiovascular diseases: a pharmacological and mechanistic overview. *Front. Pharmacol.* 14, 1122969. doi:10.3389/fphar.2023.1122969
- Prousi, G. S., Joshi, A. M., Atti, V., Addison, D., Brown, S. A., Guha, A., et al. (2023). Vascular inflammation, cancer, and cardiovascular diseases. *Curr. Oncol. Rep.* 25, 955–963. doi:10.1007/s11912-023-01426-0

The author(s) declared that they were an editorial board member of Frontiers, at the time of submission. This had no impact on the peer review process and the final decision.

## Publisher's note

All claims expressed in this article are solely those of the authors and do not necessarily represent those of their affiliated organizations, or those of the publisher, the editors and the reviewers. Any product that may be evaluated in this article, or claim that may be made by its manufacturer, is not guaranteed or endorsed by the publisher.



## OPEN ACCESS

## EDITED BY

Xianwei Wang,  
Xinxiang Medical University, China

## REVIEWED BY

Feng Hu,  
Nanchang University, China  
Renying Xu,  
Shanghai Jiao Tong University, China

## \*CORRESPONDENCE

Feng Xu,  
✉ xufeng5205529@163.com  
Jian-feng Ji,  
✉ jjf1971@ntu.edu.cn  
Xing-xing Fang,  
✉ 48776592@qq.com

<sup>†</sup>These authors have contributed equally to this work

## SPECIALTY SECTION

This article was submitted to  
Cardiovascular and Smooth Muscle  
Pharmacology,  
a section of the journal  
Frontiers in Pharmacology

RECEIVED 09 December 2022

ACCEPTED 31 December 2022

PUBLISHED 12 January 2023

## CITATION

Chen C-m, Lu C-f, Liu W-s, Gong Z-h,  
Wang X-q, Xu F, Ji J-f and Fang X-x (2023),  
Association between fibrinogen/albumin  
ratio and arterial stiffness in patients with  
type 2 diabetes: A cross-sectional study.  
*Front. Pharmacol.* 13:1120043.  
doi: 10.3389/fphar.2022.1120043

## COPYRIGHT

© 2023 Chen, Lu, Liu, Gong, Wang, Xu, Ji  
and Fang. This is an open-access article  
distributed under the terms of the [Creative  
Commons Attribution License \(CC BY\)](#).  
The use, distribution or reproduction in  
other forums is permitted, provided the  
original author(s) and the copyright  
owner(s) are credited and that the original  
publication in this journal is cited, in  
accordance with accepted academic  
practice. No use, distribution or  
reproduction is permitted which does not  
comply with these terms.

# Association between fibrinogen/albumin ratio and arterial stiffness in patients with type 2 diabetes: A cross-sectional study

Chun-mei Chen<sup>1†</sup>, Chun-feng Lu<sup>2†</sup>, Wang-shu Liu<sup>2†</sup>,  
Zhen-hua Gong<sup>3</sup>, Xue-qin Wang<sup>2</sup>, Feng Xu<sup>2\*</sup>, Jian-feng Ji<sup>3\*</sup> and  
Xing-xing Fang<sup>4\*</sup>

<sup>1</sup>Department of Geriatrics, Affiliated Hospital 2 of Nantong University and First People's Hospital of Nantong City, Nantong, China, <sup>2</sup>Department of Endocrinology, Affiliated Hospital 2 of Nantong University and First People's Hospital of Nantong City, Nantong, China, <sup>3</sup>Department of Burn and Plastic Surgery, Affiliated Hospital 2 of Nantong University and First People's Hospital of Nantong City, Nantong, China, <sup>4</sup>Department of Nephrology, Affiliated Hospital 2 of Nantong University and First People's Hospital of Nantong City, Nantong, China

**Background:** Fibrinogen albumin ratio (FAR) is significantly correlated with the severity and prognosis of cardiovascular disease (CVD). Arterial stiffness is an early lesion of CVD, but no studies have examined the correlation between arterial stiffness and FAR. This study aimed to examine the relationship between FAR and arterial stiffness in patients with type 2 diabetes (T2D), as measured by brachial-ankle pulse wave velocity (baPWV).

**Methods:** In this cross-sectional investigation, patients with T2D were enrolled between January 2021 and April 2022. In each patient, the levels of fibrinogen and albumin in the serum, and baPWV in the serum were measured. A baPWV greater than 1800 cm/s was utilized to diagnose arterial stiffness.

**Results:** The study included 413 T2D patients. The mean age of these participants was  $52.56 \pm 11.53$  years, 60.8% of them were male, and 18.6% of them had arterial stiffness. There were significant differences in baPWV level and proportion of arterial stiffness ( $p < .001$ ) between the four subgroups categorized by the FAR quartile. The relationships between the FAR and baPWV and arterial stiffness were significantly favorable in the overall population and subgroups of elderly men and non-elderly men ( $p < .01$ ), while they were insignificant in subgroups of elderly and non-elderly women ( $p > .05$ ). To investigate the correlation between the FAR and baPWV, the arterial stiffness and the FAR in male T2D patients, respectively, multivariable logistic regression analysis and multiple linear regression analysis were developed. The lnFAR and lnbaPWV had a significant relationship in the multiple linear regression analysis fully adjusted model. After adjusting for potential covariables, multivariable logistic regression analysis revealed that the FAR was independently associated with arterial stiffness [OR (95% CI), 1.075 (1.031–1.120)]. In addition, receiver operating characteristic analysis indicated that the best FAR cutoff value for detecting arterial stiffness in male T2D patients was 76.67 mg/g.

**Conclusion:** The level of FAR had an independent and positive correlation with baPWV and arterial stiffness in male patients with T2D, but not in female patients.

## KEYWORDS

type 2 diabetes, fibrinogen/albumin ratio, brachial-ankle pulse wave velocity, inflammation, coagulation

## Introduction

The rate of type 2 diabetes (T2D) is rising each year, posing a significant threat to public health, as a result of China's rapid economic development, lifestyle changes, and ageing population (Li et al., 2020). In 2015, cardiovascular problems accounted for the majority of the approximately five million fatalities attributed to T2D and associated consequences worldwide (Zheng et al., 2018). Consequently, the management of cardiovascular disease (CVD) is a crucial aspect of the treatment of T2D. Arterial stiffness, or decreased arterial elasticity, is the earliest lesion of CVD (Zhang et al., 2020). Brachial-ankle pulse wave velocity (baPWV), a reproducible, non-invasive, and easy quantitative measurement of arterial elasticity, is a significant predictor of CVD, myocardial damage, and cardiovascular events (Sheng et al., 2014). Thus, identifying early screening markers of elevated baPWV and initiating early intervention may be advantageous for enhancing cardiovascular outcomes in T2D patients.

Both fibrinogen and albumin are produced in the liver; fibrinogen is implicated in inflammation and clotting cascades (Sörensen et al., 2011), whereas albumin has an inhibitory function in inflammation, platelet activation, and aggregation (Deveci and Gazi, 2021). Albumin and fibrinogen are useful biomarkers of inflammation and hemodynamic changes, respectively. The Fibrinogen/Albumin Ratio (FAR), which combines the two indicators, was more effective than any single indicator in predicting the prognosis of multiple tumors (Geer and Shen, 2009; Yang et al., 2014; Wen et al., 2015). Moreover, FAR performed better than fibrinogen and albumin in determining the severity of acute myocardial infarction (AMI) and predicting the short-term prognosis of patients (Erdoğan et al., 2016; Zhao et al., 2019). A prospective cohort investigation conducted in China revealed that CVD patients with high FAR levels and diabetes had a poorer 5-year prognosis (Wang et al., 2022). The role of FAR in assessing CVD had been thoroughly established in earlier studies, but no investigation had looked at the connection between FAR and the early lesion of CVD, arterial stiffness. Evaluation of FAR will assist in managing CVD throughout T2D if the association between FAR and arterial stiffness in T2D patients is found to exist.

Therefore, this observational study was carried out to investigate the relationship between FAR and baPWV in T2D patients.

## Methods

### Study participants

The current study included T2D patients who were hospitalized in the endocrinology department of the second affiliated hospital of Nantong University from January 2021 to April 2022. T2D was diagnosed using the American Diabetes Association criteria (American Diabetes Association, 2014). Exclusion criteria included any one or more of the following: type 1 diabetes, acute diabetic complications, receiving steroid therapy, taking any anticoagulant, malignant diseases, chronic hepatopathy, atrial fibrillation, peripheral artery disease, heart failure, acute infections, blood diseases, and autoimmune diseases. Figure 1 exhibits the detailed study flowchart. In total, 413 T2D patients

were ultimately included in this study. Each participant provided written, informed consent and the study was conducted following the Declaration of Helsinki.

### Basic data collection

Checking medical records allowed for the collection of information on demographics, drinking and smoking habits, past medication usage, and disease diagnoses. The medication history was particularly focused on the use of drugs for T2D, hypertension, and dyslipidemia.

### Anthropometric assessments

Each subject was measured for anthropometric characteristics, including weight, height, and blood pressure. Body mass index (BMI) was determined by the following formula: weight (kg)/height (m<sup>2</sup>). The average of the two blood pressure readings was recorded for further analysis after being measured twice with a standard mercury sphygmomanometer.

### Laboratory examinations

After a 12-h overnight fast, samples of blood and fresh first-void morning urine were obtained. FAR was determined by dividing the serum fibrinogen level by the serum albumin level after measuring the levels of serum fibrinogen and albumin. The estimated glomerular filtration rate (eGFR) was computed utilizing the CKD-EPI creatinine-cystatin C equation (2012) (Inker et al., 2012).

### Brachial-ankle pulse wave velocity (baPWV)

As previously described, each subject's baPWV was measured by a trained technician utilizing an automated system (BP-203RPE III device, Omron, Japan) (Wu et al., 2019). Each subject lay down for detection in the supine position after at least five minutes of rest. For analysis, the baPWV value with the higher difference between the right and left sides was selected. A baPWV  $\geq 1800$  cm/s was utilized to define arterial stiffness (Takashima et al., 2014).

### Statistical analyses

SPSS statistical software version 18.0 (IBM SPSS Inc., United States) was utilized for the analysis of the data. A *p* value  $< .05$  was considered as statistical significance. Continuous variables with skewed and normal distributions and categorical variables were presented as the mean  $\pm$  standard deviation (SD), frequencies with percentages, and medians with interquartile range, respectively. For analysis, the data on fibrinogen and albumin levels were ln-transformed due to their skewed distributions. Comparisons of continuous variables with skewed and normal distributions and categorical variables were conducted between groups using the Kruskal–Wallis test and the one-way analysis of variance, and the chi-square test, respectively.



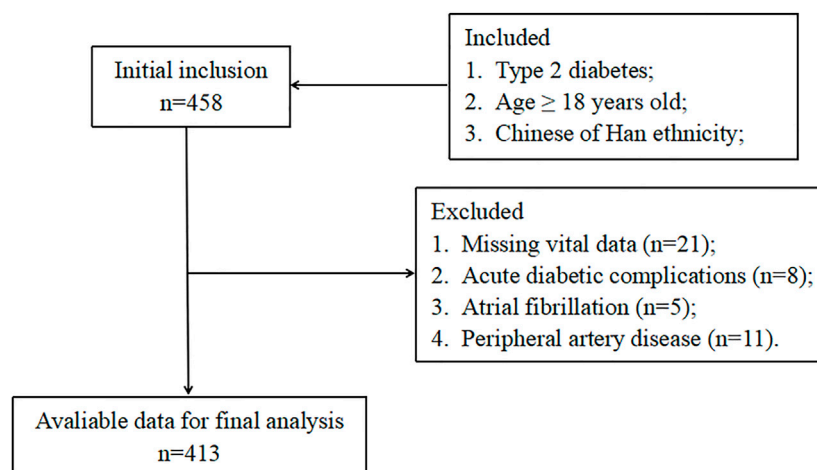


**FIGURE 1**  
The study flowchart.

Spearman's analyses of bivariate correlation were applied to measure the strength of associations between FAR level and other clinical variables. In addition, spearman's bivariate correlation analyses were employed to investigate the associations between the FAR and baPWV and arterial stiffness in the overall population and subgroups of elderly men, non-elderly men, elderly women, and non-elderly women, respectively. To investigate the independent relationships between the FAR level and the baPWV level and the independent relationships between the FAR level and arterial stiffness, multiple linear regression analyses and multivariable logistic regression analyses were constructed. Receiver operating characteristic (ROC) analysis was also carried out to examine the FAR levels' capacity to detect arterial stiffness.

## Results

### Basic characteristics

In total, 413 T2D patients were enrolled in the study. The mean age was  $52.56 \pm 11.53$  years, 60.8% of the participants were male, and 18.6% of the participants had arterial stiffness. The clinical characteristics of the four subgroups are presented in Table 1 according to the FAR quartiles. The proportion of arterial stiffness and baPWV level both significantly increased ( $p < .001$ ) along with the gradual rise in the FAR quartiles. Age, the duration of diabetes, the utilization of acarbose, triglyceride (TG) level, albumin level, fibrinogen level, hemoglobin level, neutrophil percentage, platelet count, and neutrophil/lymphocyte ratio (NLR) level were all significantly different between the four subgroups ( $p < .05$ ). While there were no significant differences in the proportion of males, smoking and drinking status, systolic and diastolic blood pressure, use of additional antihypertensive and antidiabetic treatments, HbA1c level, eGFR level, urinary albumin-to-creatinine ratio (UACR) level, total cholesterol (TC) level, low-density lipoprotein cholesterol (LDL-C) level high-density lipoprotein cholesterol (HDL-C) level, and white blood cells (WBC) count ( $p > .05$ ).

### Relationships between the FAR and clinical parameters in patients with T2D

As shown in Table 2, the FAR had significant positive associations with age, duration of diabetes, UACR level, neutrophil percentage, platelet count, and NLR level ( $r = .226, .161, .115, .245, .165$ , and  $.263$ , respectively;  $p < .001$ ), as well as significant negative associations with eGFR, TG, and hemoglobin level ( $r = -.153, -.127$ , and  $-.318$ , respectively;  $p < .001$ ).

### Relationships between the FAR and baPWV and arterial stiffness in patients with T2D

Table 3 shows that the FAR, baPWV, and arterial stiffness were significantly positively associated in the general population and subgroups of elderly men and non-elderly men ( $p < .01$ ), but were not significantly associated in subgroups of elderly and non-elderly women ( $p > .05$ ). The independent association between the FAR and baPWV in male patients with T2D was further investigated using multiple linear regression models, as shown in Table 4. In the fully adjusted model 3, the lnFAR demonstrated a significant and positive association with the lnbaPWV in male T2D patients ( $\beta = 0.216$ ,  $t = 4.077$ ,  $p < 0.001$ ,  $R^2 = 0.609$ ).

### Association of the FAR with arterial stiffness in male patients with T2D

The multivariable logistic regression analysis of the correlation between FAR and arterial stiffness in male T2D patients is presented in Table 5. In model 0 without any adjustments, the FAR had a significant association with the presence of arterial stiffness [OR (95% CI), 1.039 (1.024–1.054)]. Even in the model with all of the adjustments, there was still an independent association between the FAR and arterial stiffness [OR (95% CI), 1.075 (1.031–1.120)].

TABLE 1 Clinical characteristics of the study participants.

Variables	Q1	Q2	Q3	Q4	<i>p</i> value
FAR (mg/g)	52.25(45.97–55.87)	64.31(62.32–67.01)	76.15(72.99–79.35)	98.40(90.50–117.14)	
FAR (range)	<59.44	59.44–68.96	68.96–83.74	>83.74	
<i>n</i>	103	104	103	103	
Age (years)	49.69 ± 11.12	52.12 ± 11.24	52.47 ± 11.61	55.99 ± 11.43	.001
Male, <i>n</i> (%)	37(35.9)	39(37.5)	39(37.9)	47(45.6)	.484
Diabetic duration (years)	3.0(0–10.0)	5.0(1.0–10.0)	5.0(1.0–10.0)	6.0(1.0–10.0)	.049
BMI (kg/m <sup>2</sup> )	25.77 ± 3.62	26.06 ± 4.38	26.13 ± 3.96	25.16 ± 3.48	.268
SBP (mmHg)	130.0(120.0–141.0)	134.0(125.5–146.5)	135.0(125.0–149.0)	135.0(123.0–150.0)	.112
Smoking status					.654
Never smoking, <i>n</i> (%)	66(64.1)	70(67.3)	64(62.1)	76(73.8)	
Former smoking, <i>n</i> (%)	9(8.7)	6(5.8)	9(8.7)	6(5.8)	
Current smoking, <i>n</i> (%)	28(27.2)	28(26.9)	30(29.1)	21(20.4)	
Drinking status					.274
Never drinking, <i>n</i> (%)	62(60.2)	62(59.6)	63(61.2)	75(72.8)	
Former drinking, <i>n</i> (%)	9(8.7)	5(4.8)	8(7.8)	7(6.8)	
Current drinking, <i>n</i> (%)	32(31.1)	37(35.6)	32(31.1)	21(20.4)	
DBP (mmHg)	83.87 ± 10.91	85.68 ± 9.65	84.94 ± 12.22	83.33 ± 10.33	.399
Antidiabetic treatments					
Insulin treatment, <i>n</i> (%)	17(16.5)	26(25.0)	34(33.0)	25(24.3)	.056
Metformin, <i>n</i> (%)	51(49.5)	48(46.2)	48(46.6)	54(52.4)	.789
Acarbose, <i>n</i> (%)	3(2.9)	6(5.8)	3(2.9)	14(13.6)	.004
Insulin-secretagogues, <i>n</i> (%)	21(20.4)	27(26.0)	30(29.1)	31(30.1)	.385
Insulin-sensitisers, <i>n</i> (%)	9(8.7)	14(13.5)	14(13.6)	7(6.8)	.284
DPP-4 inhibitors, <i>n</i> (%)	6(5.8)	11(10.6)	9(8.7)	6(5.8)	.499
SGLT-2 inhibitors, <i>n</i> (%)	9(8.7)	17(16.3)	11(10.7)	15(14.6)	.330
Antihypertensive treatments					
CCB, <i>n</i> (%)	12(11.7)	24(23.1)	21(20.4)	27(26.2)	.058
ARB, <i>n</i> (%)	18(17.5)	15(14.4)	17(16.5)	23(22.3)	.496
β-blockers, <i>n</i> (%)	5(4.9)	5(4.8)	7(6.8)	5(4.9)	.899
Diuretics, <i>n</i> (%)	5(4.9)	9(8.7)	9(8.7)	9(8.7)	.658
Statins medications, <i>n</i> (%)	3(2.9)	6(5.8)	8(7.8)	5(4.9)	.477
HbA1c (%)	9.70 ± 2.04	9.57 ± 2.26	9.32 ± 2.17	9.82 ± 2.26	.389
UACR (mg/g)	11.30(6.45–30.30)	13.00(7.40–27.15)	16.30(8.70–50.75)	16.10(8.35–33.55)	.061
eGFR (ml/min/1.73m <sup>2</sup> )	108.32 ± 22.27	107.19 ± 23.93	102.47 ± 24.22	99.66 ± 25.93	.081
TG (mmol/L)	1.79(1.05–3.14)	1.77(1.08–3.13)	1.89(1.17–3.02)	1.34(.99–2.21)	.015
TC (mmol/L)	4.39(3.82–5.07)	4.40(3.74–5.24)	4.43(3.79–5.14)	4.13(3.70–5.14)	.528
HDL-C (mmol/L)	1.10(.93–1.28)	1.10(.93–1.30)	1.10(.93–1.27)	1.11(.91–1.36)	.973
LDL-C (mmol/L)	2.73 ± .87	2.86 ± .91	2.85 ± .83	2.80 ± .94	.689
Alb (g/L)	39.34 ± 3.62	38.86 ± 3.32	37.44 ± 3.15	36.15 ± 3.11	<.001
Fg (mg/L)	1990(1770–2200)	2500(2360–2650)	2860(2650–3020)	3610(3320–4100)	<.001
Hb (g/L)	145.18 ± 16.28	142.99 ± 13.56	141.57 ± 14.68	133.38 ± 21.01	<.001
WBC (*10 <sup>9</sup> /L)	6.10(5.10–7.00)	5.90(5.00–7.05)	6.40(4.85–7.45)	6.30(4.73–7.68)	.588
NEU (%)	54.46 ± 8.83	56.97 ± 8.59	57.97 ± 8.94	61.03 ± 10.30	<.001
PLT (*10 <sup>9</sup> /L)	196.00(165.25–237.00)	189.00(157.00–238.50)	201.00(166.50–239.00)	216.00(189.25–267.50)	.001
NLR (%)	1.57(1.24–2.02)	1.79(1.34–2.24)	1.80(1.36–2.45)	2.05(1.56–3.22)	<.001
baPWV (cm/s)	1382.0(1244.0–1548.0)	1489.0(1340.0–1747.0)	1534.5(1294.0–1719.3)	1673.0(1403.0–1865.0)	<.001
Arterial stiffness, <i>n</i> (%)	7(6.8)	15(14.4)	20(19.4)	35(34.0)	<.001

Normally distributed values in the table are given as the mean ± SD, skewed distributed values are given as the median (25% and 75% interquartiles), and categorical variables are given as frequency (percentage).

FAR, fibrinogen/albumin ratio; BMI, body mass index; SBP/DBP, systolic/diastolic blood pressure; PAD, peripheral artery disease; Insulin-secretagogues insulin secretagogues, Insulin-sensitisers insulin sensitizing agents, DPP-4, inhibitors dipeptidyl peptidase-4 inhibitors, sodium-glucose co-transporter-2, inhibitors SGLT-2, inhibitors; CCB, calcium channel blockers; ARB, angiotensin receptor blockers; HbA1c glycosylated hemoglobin A1c; UACR, urinary albumin-to-creatinine ratio; eGFR, estimated glomerular filtration rate; TG, triglyceride; TC, total cholesterol; HDL-C, high-density lipoprotein cholesterol; LDL-C, low-density lipoprotein cholesterol; Alb albumin, Fg fibrinogen, Hb hemoglobin; WBC, white blood cells; NEU, neutrophil percentage; PLT, platelets; NLR, neutrophil/lymphocyte ratio, baPWV, brachial-ankle pulse wave velocity.



**TABLE 2 Relationships between FAR and clinical parameters in patients with T2D.**

Variables	<i>r</i>	<i>p</i> value
Age	.226	<.001
Diabetic duration	.161	.001
BMI	−.074	.135
SBP	.095	.053
DBP	−.031	.534
HbA1c	−.026	.603
UACR	.115	.022
eGFR	−.153	.005
TG	−.127	.010
TC	−.041	.402
HDL-C	.035	.476
LDL-C	−.001	.989
Hb	−.318	<.001
WBC	.024	.637
NEU	.245	<.001
PLT	.165	.001
NLR	.263	<.001

*r* spearman's correlation coefficient.

## The cutoff FAR value to indicate arterial stiffness

In addition, a ROC analysis was conducted to determine the FAR cutoff value that would indicate the presence of arterial stiffness instances in male T2D patients. As depicted in [Figure 2](#), the optimal FAR cutoff value to indicate arterial stiffness was 76.67 mg/g, with a sensitivity of 70.27%, a specificity of 73.84%, and an area under the curve of .783 (95% CI 0.704–.862).

## Discussion

In the present investigation, the association between FAR and arterial stiffness as determined by baPWV in T2D patients was investigated. In comparison to female T2D patients, male T2D

patients had a positive association between the FAR and baPWV and the prevalence of arterial stiffness.

Arterial stiffness can increase cardiac afterload, causing cardiac hypertrophy and left ventricular dysfunction ([Tomiyama and Shiina, 2020](#)), as well as amplifying pulse pressure, reducing coronary perfusion, and causing brain microvascular injury and other target organ damage ([Vlachopoulos et al., 2015](#)). Both of these factors ultimately contribute to a poor prognosis in diabetic and non-diabetic patients. An increase in baPWV of 1 SD was linked to a 1.41-fold rise in the risk of cardiovascular events, according to a meta-analysis of 15 clinical studies ([Sang et al., 2021](#)). In patients with CVD who are controlling for traditional risk factors, improvement of baPWV provides an additional protective impact ([Nakamura et al., 2021](#)). In the current investigation, FAR was found to be independently correlated with arterial stiffness and may thus be significantly associated with cardiovascular prognosis in male T2D patients. The SYNTAX score, derived from the lesion angiographic scoring system, is frequently used to quantify the severity of CVD ([Girasis et al., 2011](#)). Multiple investigations have confirmed the association between FAR and SYNTAX scores in AMI patients ([Erdoğan et al., 2016](#); [Erdoğan et al., 2021](#)). In addition, the relationships between FAR and the severity of coronary arterial calcification, the Gensini score, and the number of diseased coronary arteries were identified ([Duan et al., 2021](#); [Zhu et al., 2022](#)). In a large cohort analysis with a 5-year follow-up, the combination of a high FAR level and diabetes predicted a worse prognosis in patients receiving the percutaneous coronary intervention (PCI) ([Wang et al., 2022](#)). Thus, these findings suggest that FAR may be useful in assessing the risk of CVD as well as determining the severity and predicting the prognosis of CVD in T2D patients.

Arterial stiffness is caused by a combination of variables such as an imbalance in elastin collagen ratio, oxidative stress, chronic inflammation, and so on, and diabetes can accelerate this process ([Lee et al., 2022](#)). Numerous investigations have revealed that arterial stiffness is closely correlated with T2D's essential components, including insulin resistance (IR) ([Lee et al., 2018](#)), glucose fluctuations ([Wakasugi et al., 2021](#)), and chronic hyperglycemia ([Katakami et al., 2020](#)). In turn, arterial stiffness can induce IR ([Chirinos, 2020](#)) and islet damage ([Tian et al., 2022](#)) by damaging capillaries, ultimately increasing glucose metabolism issues. The relationship between the two may be inflammation and hemodynamic alterations ([Sharif et al., 2021](#)).

In a cross-sectional examination of risk factors for diabetic kidney disease (DKD) in T2D patients, FAR was significantly found to be positively associated with neutrophil count and NLR, leading researchers to hypothesize that FAR may be substantially associated with inflammation and consequently DKD ([Wang et al., 2021](#)). Similarly, the present investigation found a significant positive

**TABLE 3 Relationships between the FAR and baPWV, the FAR and arterial stiffness.**

Variables	Total		Male				Female			
			< 60 years		≥ 60 years		< 60 years		≥ 60 years	
	<i>n</i>	413	201		50		112		50	
	<i>R</i>	<i>p</i> value	<i>r</i>	<i>p</i> value	<i>r</i>	<i>p</i> value	<i>R</i>	<i>p</i> value	<i>r</i>	<i>p</i> value
baPWV	.262	<.001	.268	<.001	.435	.002	.057	.548	.050	.731
Arterial stiffness	.266	<.001	.266	<.001	.418	.003	.103	.278	.032	.826

*r* spearman's correlation coefficient.

**TABLE 4** Multiple linear regression models displayed independent associations of the lnFAR with lnbaPWV in male patients with T2D.

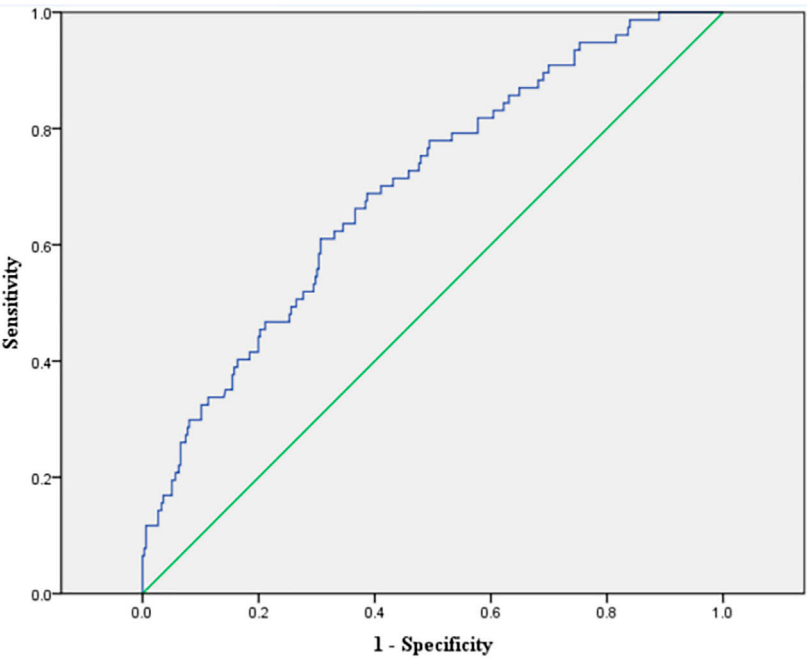
Models	B (95% CI)	$\beta$	<i>t</i>	<i>p</i>	<i>R</i> <sup>2</sup> for model
Model 0	.206(.142–.271)	.370	6.293	<.001	.137
Model 1	.105(.055–.154)	.188	4.188	<.001	.505
Model 2	.118(.059–.176)	.203	3.947	<.001	.546
Model 3	.125(.064–.185)	.216	4.077	<.001	.609

Model 0: unadjusted model.  
Model 1: adjusted for age, diabetic duration, BMI, SBP, DBP.  
Model 2: additionally adjusted for HbA1c, eGFR, lipid profiles.  
Model 3: additionally adjusted for antidiabetic treatments, antihypertensive treatments, statins medications, smoking status, drinking status.

**TABLE 5** Multivariable logistic regression analysis to identify the association of the FAR with arterial stiffness in male patients with T2D.

Models	<i>B</i>	SE	Wald	<i>p</i>	OR	95% CI
Model 0	.038	.007	27.152	<.001	1.039	1.024–1.054
Model 1	.044	.010	17.788	<.001	1.045	1.024–1.066
Model 2	.049	.013	14.367	<.001	1.050	1.024–1.077
Model 3	.072	.021	11.448	.001	1.075	1.031–1.120

Model 0: unadjusted model.  
Model 1: adjusted for age, diabetic duration, BMI, SBP, DBP.  
Model 2: additionally adjusted for HbA1c, eGFR, lipid profiles.  
Model 3: additionally adjusted for antidiabetic treatments, antihypertensive treatments, statins medications, smoking status, drinking status.



ROC analysis to assess the ability of the FAR to indicate arterial stiffness was 0.783 (95% CI 0.704–0.862). Optimal cutoff value of the FAR was 76.67 mg/g to indicate arterial stiffness; Youden index= 0.441, sensitivity= 70.27% and specificity= 73.84%

**FIGURE 2**  
ROC analysis to analyze the ability of the FAR to indicate arterial stiffness in male patients with T2D.

association between FAR and neutrophil percentage and NLR, suggesting that inflammation may function as a link between FAR and arterial stiffness. A higher FAR indicates a lower level of albumin or a higher level of fibrinogen. Hypoalbuminemia is a biomarker for inflammatory load in the body because inflammation can lower the rate of albumin production and increase albumin catabolism (Cesari et al., 2003). Additionally, albumin can prevent inflammation-induced endothelial cell apoptosis by inhibiting cell adhesion molecule expression (Albert et al., 2007). Therefore, the independent relationship between arterial stiffness and FAR may be partially explained by inflammation.

The relationship between FAR and platelet count, a critical component of the coagulation system, was found to be statistically significant and positive in this study. Platelet, the primary cause of coronary thrombosis and atherosclerosis, is an essential target for the management of coronary heart disease (Khodadi, 2020). Albumin has been shown to suppress platelet activation and aggregation, whereas activated platelets can cause coronary artery contraction and worsen myocardial ischemia (Sweetnam et al., 1996). Albumin can also indirectly control platelet aggregation by influencing prostaglandin bioavailability (Garcia-Martinez et al., 2013). In addition, fibrinogen can be converted to water-insoluble fibrin by thrombin, but hypoalbuminemia can block the physiological fibrinolytic system, hence limiting spontaneous thrombus dissolution (De Sain-van der Velden et al., 2000). As a result, FAR may be related to arterial stiffness and reflect changes in the hemodynamic state of T2D patients.

The relationships between arterial stiffness and the FAR in T2D patients were shown to differ by gender in this study. Numerous investigations have conclusively shown that the clinical features and sex-specific processes underlying arterial stiffness in males and females were different (DuPont et al., 2019). In a cross-sectional investigation of T2D patients, there was a higher correlation between arterial stiffness and surrogate indicators of insulin resistance in women than in men (Nakagomi et al., 2020). The findings of the present investigation may be partially supported by these studies.

The following are the study's limitations, which cannot be avoided. First, the limitation of cross-sectional studies prevents the demonstration of a coincidental relationship between FAR and arterial stiffness. Second, due to a lack of data, it was impossible to account for confounding variables, including detailed alcohol and tobacco consumption and daily activity levels. Finally, all of the participants in this study were Chinese, which may restrict the generalizability of the findings.

In conclusion, the FAR level was positively and independently associated with baPWV and arterial stiffness in male T2D patients. When considered in combination with other investigations, FAR has the potential to assist in the better management of cardiovascular problems in patients with T2D, particularly male patients.

## References

- Albert, M. A., Glynn, R. J., Buring, J. E., and Ridker, P. M. (2007). Relation between soluble intercellular adhesion molecule-1, homocysteine, and fibrinogen levels and race/ethnicity in women without cardiovascular disease. *Am. J. Cardiol.* 99, 1246–1251. doi:10.1016/j.amjcard.2006.12.041
- American Diabetes Association (2014). Diagnosis and classification of diabetes mellitus. *Diabetes Care* 37 (1), S81–S90. doi:10.2337/dc14-S081
- Cesari, M., Penninx, B. W., Newman, A. B., Kritchevsky, S. B., Nicklas, B. J., Sutton-Tyrrell, K., et al. (2003). Inflammatory markers and onset of cardiovascular events: Results from the health ABC study. *Circulation* 108, 2317–2322. doi:10.1161/01.CIR.0000097109.90783.FC

## Data availability statement

The raw data supporting the conclusions of this article will be made available by the authors, without undue reservation.

## Ethics statement

The studies involving human participants were reviewed and approved by The medical research ethics committee of Second Affiliated Hospital of Nantong University. The patients/participants provided their written informed consent to participate in this study.

## Author contributions

FX and CC participated in the design of the study, data collection, analysis of the data, and drafting of the manuscript. JJ and XF conceived of the study, participated in its design and revised the manuscript. CL, WL, and XW participated in data collection.

## Funding

The study was supported by the Medical Research Project of Health Commission of Nantong (MSZ21048, MB2020012, JCZ21099, JC22022021, MS2022017, MS2022027) and the Science and Technology Support Program of Nantong (HS2020005, JC2021118).

## Conflict of interest

The authors declare that the research was conducted in the absence of any commercial or financial relationships that could be construed as a potential conflict of interest.

## Publisher's note

All claims expressed in this article are solely those of the authors and do not necessarily represent those of their affiliated organizations, or those of the publisher, the editors and the reviewers. Any product that may be evaluated in this article, or claim that may be made by its manufacturer, is not guaranteed or endorsed by the publisher.

- Chirinos, J. A. (2020). Large artery stiffness and new-onset diabetes. *Circ. Res.* 127, 1499–1501. doi:10.1161/CIRCRESAHA.120.318317

- De Sain-van der Velden, M. G. M., Smolders, H. C., and van Rijn, H. J. M. (2000). Does albumin play a role in fibrinolysis by its inhibition of plasminogen activation? *Proteolysis* 14, 242–246.

- Deveci, B., and Gazi, E. (2021). Relation between globulin, fibrinogen, and albumin with the presence and severity of coronary artery disease. *Angiology* 72, 174–180. doi:10.1177/0003319720959985

- Duan, Z., Luo, C., Fu, B., and Han, D. (2021). Association between fibrinogen-to-albumin ratio and the presence and severity of coronary artery disease in patients with acute coronary syndrome. *BMC Cardiovasc. Disord.* 21, 588. doi:10.1186/s12872-021-02400-z

- DuPont, J. J., Kenney, R. M., Patel, A. R., and Jaffe, I. Z. (2019). Sex differences in mechanisms of arterial stiffness. *Br. J. Pharmacol.* 176, 4208–4225. doi:10.1111/bph.14624
- Erdoğan, G., Arslan, U., Yenercağ, M., Durmuş, G., Tuğrul, S., Şahin, İ., et al. (2016). The relationship between fibrinogen to albumin ratio and severity of coronary artery disease in patients with STEMI. *Am. J. Emerg. Med.* 34, 1037–1042. doi:10.1016/j.ajem.2016.03.003
- Erdoğan, G., Arslan, U., Yenercağ, M., Durmuş, G., Tuğrul, S., and Şahin, İ. (2021). Relationship between the fibrinogen-to-albumin ratio and SYNTAX score in patients with non-ST-elevation myocardial infarction. *Rev. Invest. Clin.* 10, 24875. doi:10.24875/RIC.20000534
- Garcia-Martinez, R., Caraceni, P., Bernardi, M., Gines, P., Arroyo, V., and Jalan, R. (2013). Albumin: Pathophysiologic basis of its role in the treatment of cirrhosis and its complications. *Hepatology* 58, 1836–1846. doi:10.1002/hep.26338
- Geer, E. B., and Shen, W. (2009). Gender differences in insulin resistance, body composition, and energy balance. *Gend. Med.* 6 (1), 60–75. doi:10.1016/j.genm.2009.02.002
- Girasis, C., Garg, S., Räber, L., Sarno, G., Morel, M. A., Garcia-Garcia, H. M., et al. (2011). SYNTAX score and clinical SYNTAX score as predictors of very long-term clinical outcomes in patients undergoing percutaneous coronary interventions: A substudy of SIRolimus-eluting stent compared with paclitAXel-eluting stent for coronary revascularization (SIRTAX) trial. *Eur. Heart J.* 32, 3115–3127. doi:10.1093/eurheartj/ehr369
- Inker, L. A., Schmid, C. H., Tighiouart, H., Eckfeldt, J. H., Feldman, H. I., Greene, T., et al. (2012). Estimating glomerular filtration rate from serum creatinine and cystatin C. *N. Engl. J. Med.* 367, 20–29. doi:10.1056/NEJMoa1114248
- Katakami, N., Omori, K., Taya, N., Arakawa, S., Takahara, M., Matsuo, T. A., et al. (2020). Plasma metabolites associated with arterial stiffness in patients with type 2 diabetes. *Cardiovasc. Diabetol.* 19, 75. doi:10.1186/s12933-020-01057-w
- Khodadi, E. (2020). Platelet function in cardiovascular disease: Activation of molecules and activation by molecules. *Cardiovasc. Toxicol.* 20, 1–10. doi:10.1007/s12012-019-09555-4
- Lee, C. J., Hsieh, Y. J., Lin, Y. L., Wang, C. H., Hsu, B. G., and Tsai, J. P. (2022). Correlation between serum 25-hydroxyvitamin D level and peripheral arterial stiffness in chronic kidney disease stage 3–5 patients. *Nutrients* 14, 2429. doi:10.3390/nu14122429
- Lee, S. B., Ahn, C. W., Lee, B. K., Kang, S., Nam, J. S., You, J. H., et al. (2018). Association between triglyceride glucose index and arterial stiffness in Korean adults. *Cardiovasc. Diabetol.* 17, 41. doi:10.1186/s12933-018-0692-1
- Li, Y., Teng, D., Shi, X., Qin, G., Qin, Y., Quan, H., et al. (2020). Prevalence of diabetes recorded in mainland China using 2018 diagnostic criteria from the American diabetes association: National cross sectional study. *BMJ* 369, m997. doi:10.1136/bmj.m997
- Nakagomi, A., Sunami, Y., Kawasaki, Y., Fujisawa, T., and Kobayashi, Y. (2020). Sex difference in the association between surrogate markers of insulin resistance and arterial stiffness. *J. Diabetes Complicat.* 34, 107442. doi:10.1016/j.jdiacomp.2019.107442
- Nakamura, T., Uematsu, M., Horikoshi, T., Yoshizaki, T., Kobayashi, T., Saito, Y., et al. (2021). Improvement in brachial endothelial vasomotor function and brachial-ankle pulse wave velocity reduces the residual risk for cardiovascular events after optimal medical treatment in patients with coronary artery disease. *J. Atheroscler. Thromb.* 28, 1133–1144. doi:10.5551/jat.57562
- Sang, T., Lv, N., Dang, A., Cheng, N., and Zhang, W. (2021). Brachial-ankle pulse wave velocity and prognosis in patients with atherosclerotic cardiovascular disease: A systematic review and meta-analysis. *Hypertens. Res.* 44, 1175–1185. doi:10.1038/s41440-021-00678-2
- Sharif, S., Van der Graaf, Y., Cramer, M. J., Kapelle, L. J., de Borst, G. J., Visseren, F. L. J., et al. (2021). Low-grade inflammation as a risk factor for cardiovascular events and all-cause mortality in patients with type 2 diabetes. *Cardiovasc. Diabetol.* 20, 220. doi:10.1186/s12933-021-01409-0
- Sheng, C. S., Li, Y., Li, L. H., Huang, Q. F., Zeng, W. F., Kang, Y. Y., et al. (2014). Brachial-ankle pulse wave velocity as a predictor of mortality in elderly Chinese. *Hypertension* 64, 1124–1130. doi:10.1161/HYPERTENSIONAHA.114.04063
- Sörensen, I., Susnik, N., Inhester, T., Degen, J. L., Melk, A., Haller, H., et al. (2011). Fibrinogen, acting as a mitogen for tubulointerstitial fibroblasts, promotes renal fibrosis. *Kidney Int.* 80, 1035–1044. doi:10.1038/ki.2011.214
- Sweetnam, P. M., Thomas, H. F., Yarnell, J. W., Beswick, A. D., Baker, I. A., and Elwood, P. C. (1996). Fibrinogen, viscosity and the 10-year incidence of ischaemic heart disease. *Eur. Heart J.* 17, 1814–1820. doi:10.1093/oxfordjournals.eurheartj.a014797
- Takashima, N., Turin, T. C., Matsui, K., Rumana, N., Nakamura, Y., Kadota, A., et al. (2014). The relationship of brachial-ankle pulse wave velocity to future cardiovascular disease events in the general Japanese population: The takashima study. *J. Hum. Hypertens.* 28, 323–327. doi:10.1038/jhh.2013.103
- Tian, X., Zuo, Y., Chen, S., Zhang, Y., Zhang, X., Xu, Q., et al. (2022). Hypertension, arterial stiffness, and diabetes: A prospective cohort study. *Hypertension* 79, 1487–1496. doi:10.1161/HYPERTENSIONAHA.122.19256
- Tomiya, H., and Shiina, K. (2020). State of the art review: Brachial-ankle PWV. *J. Atheroscler. Thromb.* 27, 621–636. doi:10.5551/jat.RV17041
- Vlachopoulos, C., Xaplanteris, P., Aboyans, V., Brodmann, M., Cifková, R., Cosentino, F., et al. (2015). The role of vascular biomarkers for primary and secondary prevention. A position paper from the European society of cardiology working group on peripheral circulation: Endorsed by the association for research into arterial structure and physiology (artery) society. *Atherosclerosis* 241, 507–532. doi:10.1016/j.atherosclerosis.2015.05.007
- Wakasugi, S., Mita, T., Katakami, N., Okada, Y., Yoshii, H., Osonoi, T., et al. (2021). Associations between continuous glucose monitoring-derived metrics and arterial stiffness in Japanese patients with type 2 diabetes. *Cardiovasc. Diabetol.* 20, 15. doi:10.1186/s12933-020-01194-2
- Wang, K., Xu, W., Zha, B., Shi, J., Wu, G., and Ding, H. (2021). Fibrinogen to albumin ratio as an independent risk factor for type 2 diabetic kidney disease. *Diabetes Metab. Syndr. Obes.* 14, 4557–4567. doi:10.2147/DMSO.S337986
- Wang, P., Yuan, D., Zhang, C., Zhu, P., Jia, S., Song, Y., et al. (2022). High fibrinogen-to-albumin ratio with type 2 diabetes mellitus is associated with poor prognosis in patients undergoing percutaneous coronary intervention: 5-year findings from a large cohort. *Cardiovasc. Diabetol.* 21, 46. doi:10.1186/s12933-022-01477-w
- Wen, J. H., Zhong, Y. Y., Wen, Z. G., Kuang, C. Q., Liao, J. R., Chen, L. H., et al. (2015). Triglyceride to HDL-C ratio and increased arterial stiffness in apparently healthy individuals. *Int. J. Clin. Exp. Med.* 8, 4342–4348.
- Wu, S., Jin, C., Li, S., Zheng, X., Zhang, X., Cui, L., et al. (2019). Aging, arterial stiffness, and blood pressure association in Chinese adults. *Hypertension* 73, 893–899. doi:10.1161/HYPERTENSIONAHA.118.12396
- Yang, F., Wang, G., Wang, Z., Kuang, C. Q., Liao, J. R., Zhu, Z., et al. (2014). Visceral adiposity index may be a surrogate marker for the assessment of the effects of obesity on arterial stiffness. *PLoS One* 9, e104365. doi:10.1371/journal.pone.0104365
- Zhang, R., Xie, J., Yang, R., Li, R., Chong, M., Zhang, X., et al. (2020). Association between ideal cardiovascular health score trajectories and arterial stiffness: The kailuan study. *Hypertens. Res.* 43, 140–147. doi:10.1038/s41440-019-0341-4
- Zhao, Y., Yang, J., Ji, Y., Wang, S., Wang, T., Wang, F., et al. (2019). Usefulness of fibrinogen-to-albumin ratio to predict no-reflow and short-term prognosis in patients with ST-segment elevation myocardial infarction undergoing primary percutaneous coronary intervention. *Heart Vessels* 34, 1600–1607. doi:10.1007/s00380-019-01399-w
- Zheng, Y., Ley, S. H., and Hu, F. B. (2018). Global aetiology and epidemiology of type 2 diabetes mellitus and its complications. *Nat. Rev. Endocrinol.* 14, 88–98. doi:10.1038/nrendo.2017.151
- Zhu, Y., Tao, S., Zhang, D., Xiao, J., Wang, X., Yuan, L., et al. (2022). Association between fibrinogen/albumin ratio and severity of coronary artery calcification in patients with chronic kidney disease: A retrospective study. *PeerJ* 10, e13550. doi:10.7717/peerj.13550



## OPEN ACCESS

## EDITED BY

Min Zhang,  
Faculty of Life Sciences and Medicine,  
King's College London, United Kingdom

## REVIEWED BY

Jens Juul Holst,  
University of Copenhagen, Denmark  
Alison Brewer,  
King's College London, United Kingdom

## \*CORRESPONDENCE

Gang Wang,  
✉ gang\_wang@xjtu.edu.cn

## SPECIALTY SECTION

This article was submitted to  
Cardiovascular and Smooth Muscle  
Pharmacology,  
a section of the journal  
Frontiers in Pharmacology

RECEIVED 16 December 2022

ACCEPTED 01 February 2023

PUBLISHED 14 February 2023

## CITATION

Deng G, Ren J, Li R, Li M, Jin X, Li J, Liu J,  
Gao Y, Zhang J, Wang X and Wang G  
(2023), Systematic investigation of the  
underlying mechanisms of GLP-1  
receptor agonists to prevent myocardial  
infarction in patients with type 2 diabetes  
mellitus using network pharmacology.  
*Front. Pharmacol.* 14:1125753.  
doi: 10.3389/fphar.2023.1125753

## COPYRIGHT

© 2023 Deng, Ren, Li, Li, Jin, Li, Liu, Gao,  
Zhang, Wang and Wang. This is an open-  
access article distributed under the terms  
of the [Creative Commons Attribution  
License \(CC BY\)](#). The use, distribution or  
reproduction in other forums is  
permitted, provided the original author(s)  
and the copyright owner(s) are credited  
and that the original publication in this  
journal is cited, in accordance with  
accepted academic practice. No use,  
distribution or reproduction is permitted  
which does not comply with these terms.

# Systematic investigation of the underlying mechanisms of GLP-1 receptor agonists to prevent myocardial infarction in patients with type 2 diabetes mellitus using network pharmacology

Guorong Deng<sup>1</sup>, Jiajia Ren<sup>1</sup>, Ruohan Li<sup>1</sup>, Minjie Li<sup>2</sup>, Xuting Jin<sup>1</sup>,  
Jiamei Li<sup>1</sup>, Jueheng Liu<sup>1</sup>, Ya Gao<sup>1</sup>, Jingjing Zhang<sup>1</sup>,  
Xiaochuang Wang<sup>1</sup> and Gang Wang<sup>1\*</sup>

<sup>1</sup>Department of Critical Care Medicine, the Second Affiliated Hospital of Xi'an Jiaotong University, Xi'an, China, <sup>2</sup>Department of Cardiology, The Second Affiliated Hospital of Shaanxi University of Traditional Chinese Medicine, Xi'an, China

**Background:** Several clinical trials have demonstrated that glucagon-like peptide-1 (GLP-1) receptor agonists (GLP-1RAs) reduce the incidence of non-fatal myocardial infarction (MI) in patients with type 2 diabetes mellitus (T2DM). However, the underlying mechanism remains unclear. In this study, we applied a network pharmacology method to investigate the mechanisms by which GLP-1RAs reduce MI occurrence in patients with T2DM.

**Methods:** Targets of three GLP-1RAs (liraglutide, semaglutide, and albiglutide), T2DM, and MI were retrieved from online databases. The intersection process and associated targets retrieval were employed to obtain the related targets of GLP-1RAs against T2DM and MI. Gene Ontology (GO) and Kyoto Encyclopedia of Genes and Genes (KEGG) enrichment analyses were performed. The STRING database was used to obtain the protein-protein interaction (PPI) network, and Cytoscape was used to identify core targets, transcription factors, and modules.

**Results:** A total of 198 targets were retrieved for the three drugs and 511 targets for T2DM with MI. Finally, 51 related targets, including 31 intersection targets and 20 associated targets, were predicted to interfere with the progression of T2DM and MI on using GLP-1RAs. The STRING database was used to establish a PPI network comprising 46 nodes and 175 edges. The PPI network was analyzed using Cytoscape, and seven core targets were screened: AGT, TGFB1, STAT3, TIMP1, MMP9, MMP1, and MMP2. The transcription factor MAFB regulates all seven core targets. The cluster analysis generated three modules. The GO analysis for 51 targets indicated that the terms were mainly enriched in the extracellular matrix, angiotensin, platelets, and endopeptidase. The results of KEGG analysis revealed that the 51 targets primarily participated in the renin-angiotensin system, complement and coagulation cascades, hypertrophic cardiomyopathy, and AGE-RAGE signaling pathway in diabetic complications.

**Conclusion:** GLP-1RAs exert multi-dimensional effects on reducing the occurrence of MI in T2DM patients by interfering with targets, biological



processes, and cellular signaling pathways related to atheromatous plaque, myocardial remodeling, and thrombosis.

#### KEYWORDS

GLP-1 receptor agonists, type 2 diabetes mellitus, myocardial infarction, network pharmacology, atheromatous plaque, myocardial remodeling, thrombosis

## Introduction

Over the past four decades, the number of people living with diabetes has increased from 108 million in 1980 to 537 million in 2021, of which the overwhelming majority (over 90%) were diagnosed as type 2 diabetes mellitus (T2DM). In 2021, 6.7 million deaths were caused by diabetes or its complications (International Diabetes Federation, 2022). Among the extensive T2DM-related complications, acute myocardial infarction is a life-threatening and severe complication (Rosenblit, 2019). More than one-third of T2DM patients with myocardial infarction (MI) die within 10 years, and long-term all-cause mortality and cardiovascular mortality are even higher in younger patients than in elderly patients (Singh et al., 2020; Zheng et al., 2021). Numerous studies have shown that strict glycemic control promotes a decrease in non-fatal MI (Rodriguez-Gutierrez et al., 2019). However, intensive controls are followed by severe side effects, such as hypoglycemia; therefore, effective and safe methods for controlling glycemic levels, while simultaneously reducing risk factors for MI, act as necessary interventions in treating patients with T2DM.

Glucagon-like peptide-1 receptor agonists (GLP-1RAs), such as liraglutide and dulaglutide, are widely used to treat patients with T2DM and obesity. They exert beneficial effects, including inhibition of glucagon secretion, delayed gastric emptying, decreased appetite, rare occurrence of hypoglycemia, and controlled weight gain (Helmstadter et al., 2022). In recent years, four clinical trials have shown that dulaglutide (REWIND trial) (Gerstein et al., 2019), albiglutide (HARMONY trial) (Hernandez et al., 2018), semaglutide (SUSTAIN-6 trial) (Marso et al., 2016a), and liraglutide (LEADER trial) (Marso et al., 2016b) have cardiovascular benefits in patients with T2DM, including reducing the occurrence of non-fatal MI. A meta-analysis reported that patients with T2DM benefited from different GLP-1RAs in terms of major adverse cardiac events, all-cause mortality, hospital admission for heart failure, and renal function (Sattar et al., 2021). However, although GLP-1RA therapies are approved and considered safe for treating patients with T2DM, the exerted cardiovascular protection mechanism is still not fully clear. An increasing number of studies have demonstrated that the GLP-1 receptor is expressed in numerous types of cells, including those in the cardiovascular tissues, such as endothelial cells of the left ventricle (GTExPortal, 2021). Theoretically, GLP-1 binds to its receptor, stimulating the adenylyl cyclase pathway, and leading to insulin synthesis and release. As the treatment for T2DM may not fully explain the cardiovascular protective effects of GLP-1RAs, these still must be comprehensively investigated.

Network pharmacology is a big data integration method based on numerous databases and statistical algorithms (Hong et al., 2021). It aims to investigate diseases at the systemic level and

define the interaction between drugs and the body based on the equilibrium theory of biological networks (Zhang, 2016). Chronic diseases are generally caused by a complicated dysfunction of a related regulatory network instead of a single protein or gene (Nogales et al., 2022). Based on an integrated research strategy, the network pharmacology method provides a more efficient and convenient system for determining the relationship between drugs and diseases. In this study, we applied an integrated research strategy to investigate the mechanism of specific GLP-1RAs in T2DM and MI, which may provide a comprehensive interpretation of the cardiovascular protective effect of GLP-1RAs. A flow chart of the study process is shown in Figure 1.

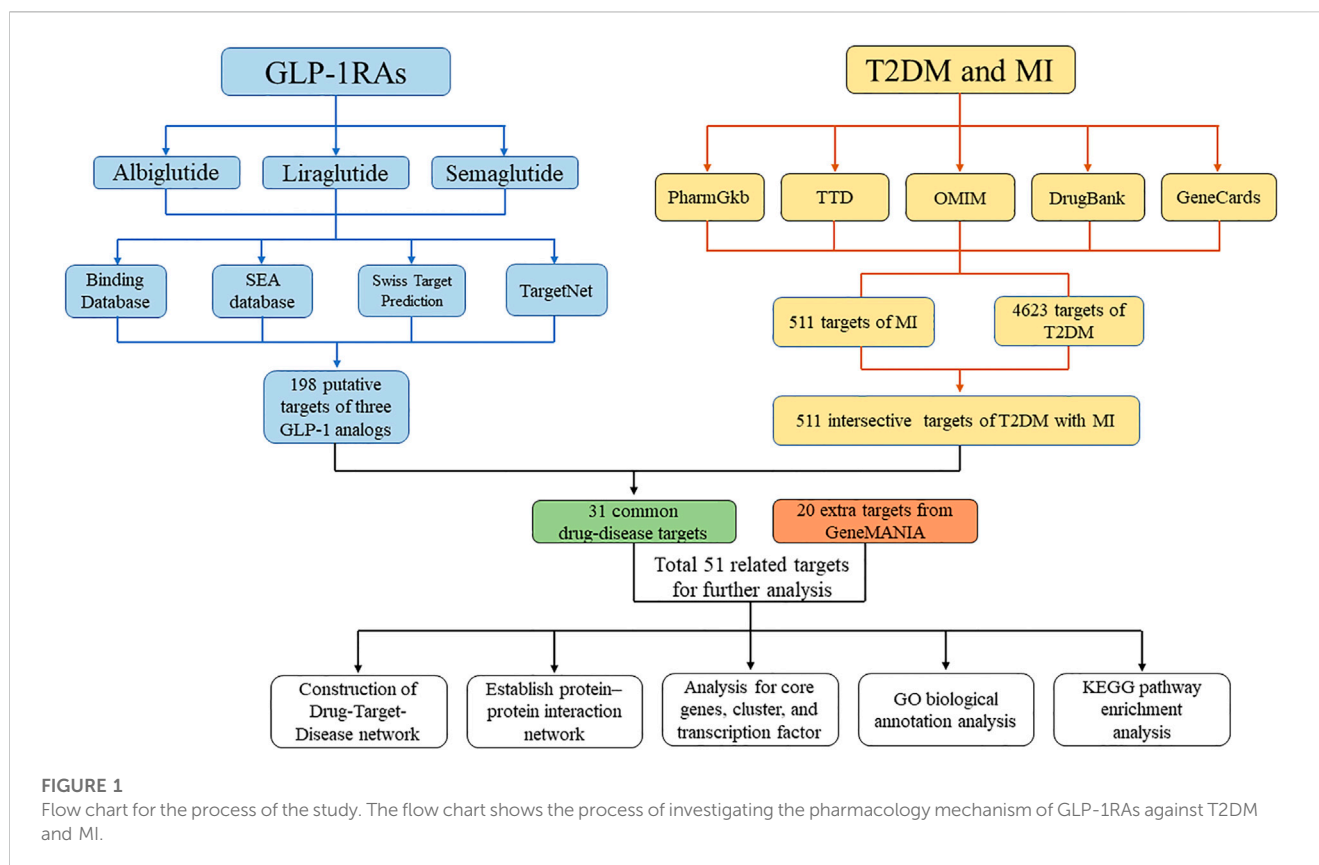
## Materials and methods

### Target prediction for GLP-1 agonists

The chemical structures (mainly in SMILES format) of three GLP-1RAs (liraglutide, semaglutide, and albiglutide) were retrieved from PubChem, an open chemistry database at the National Institutes of Health (<https://pubchem.ncbi.nlm.nih.gov>). As dulaglutide does not have a defined chemical structure, it was excluded from our study. Next, the following four target prediction databases were selected to retrieve targets for the GLP-1RAs: (1) The Binding Database (<http://www.bindingdb.org/bind/ByTargetNames.jsp>), a public and web-accessible database containing 2,096,653 binding data points for 8,185 proteins and over 920,703 drug-like molecules (Gilson et al., 2016); (2) The SEA database (<https://sea.bkslab.org/>), which can be rapidly used to search large compounds and to build cross-target similarity maps (Keiser et al., 2007); (3) The Swiss Target Prediction (<http://www.swisstargetprediction.ch/>) that allows estimating the most probable protein targets of a small molecule (Daina et al., 2019), and (4) the TargetNet (<http://targetnet.scbdd.com/home/index/>), an open web server that can be used to predict the binding of multiple targets for any given molecule across 623 proteins by establishing a high-quality model for each human protein (Yao et al., 2016). All targets from the four databases were further standardized into official gene symbols using Universal Protein Resource (<https://www.uniprot.org/>) (Consortium, 2021) for subsequent analysis.

### Target collection for T2DM and MI

With the keywords “type 2 diabetes,” “type 2 diabetes mellitus,” “myocardial infarction,” “non-fatal myocardial infarction,” “acute myocardial infarction,” “ST-segment elevation myocardial infarction,” and “non-ST-segment elevation myocardial infarction,” the target genes associated with T2DM and MI were



retrieved from the PharmGkb (<https://www.pharmgkb.org/>), TTD (<http://db.idrblab.net/ttd/>), GeneCards (<https://www.genecards.org>), DrugBank (<https://go.drugbank.com/>), and OMIM (<https://www.omim.org>) databases. The PharmGKB database is a pharmacogenomic knowledge resource containing clinical information (Whirl-Carrillo et al., 2021). The TTD database provides information about the known and explored therapeutic protein and nucleic acid targets, the targeted disease, pathway information, and the corresponding drugs directed at each target (Wang et al., 2020). The GeneCards database integrates gene-centric data from more than 150 web sources, including genomic, transcriptomic, proteomic, genetic, clinical, and functional information (Stelzer et al., 2016). The DrugBank database contains information regarding drugs and drug targets (Wishart et al., 2018). The OMIM database is a comprehensive and authoritative compendium of human genes and genetic phenotypes. The five databases provided comprehensive and complementary resources for obtaining targets for the diseases. All T2DM and MI targets from the five databases were transformed into the official gene symbol format.

## Related targets

The targets of GLP-1RAs, T2DM, and MI were uploaded to an online Venn diagram tool (<http://www.bioinformatics.com.cn/static/others/jvenn/example.html>) to obtain a Venn diagram showing the intersection targets of GLP-1RAs against T2DM and MI. Then, the GeneMANIA database was applied to find

extra targets, highly associated with the intersection targets, using a massive set of functional association data (Warde-Farley et al., 2010). Finally, these targets and intersecting targets were integrated into a set of related targets for further analysis.

## Construction of the drug-target-disease network

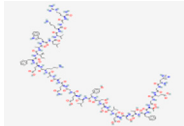
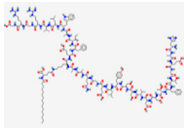
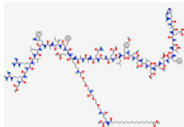
The relationship among the two diseases, three GLP-1RAs, and extra targets was established using Microsoft Excel and then input into Cytoscape (Version 3.8.2) to build and visualize a drug-target-disease network presented by nodes and edges. Nodes represent drugs, diseases, and target genes, whereas edges represent the existing correlations between any two nodes.

## Protein-protein interaction (PPI) network data

The related targets were uploaded to the STRING database (<https://string-db.org/>) and processed in a multiple protein analysis pattern to obtain the PPI network data. The STRING database focuses on researching the interactive relationships between proteins, which helps identify core regulatory genes (Szklarczyk et al., 2019). Some key parameters were also set. For example, the organism was chosen as *Homo sapiens*; the interaction score was selected as high confidence of 0.7, and disconnected nodes



**TABLE 1** Chemical information for three GLP-1RAs from the PubChem database.

Order	Name	PubChem ID	Molecular formula	Molecular weight	2D structure
1	Albiglutide	145994868	C <sub>148</sub> H <sub>224</sub> N <sub>40</sub> O <sub>45</sub>	3283.6	
2	Liraglutide	16134956	C <sub>172</sub> H <sub>265</sub> N <sub>43</sub> O <sub>51</sub>	3751	
3	Semaglutide	56843331	C <sub>187</sub> H <sub>291</sub> N <sub>45</sub> O <sub>59</sub>	4114	

were hidden in the network. Finally, the network data were downloaded in a “TSV” format file for further analysis, and a visualized network image was obtained.

## Gene Ontology (GO) and Kyoto Encyclopedia of genes and genomes (KEGG) enrichment analysis

To further uncover the underlying biological process and involved signaling pathways in related targets, the KEGG pathway and GO enrichment analysis, including biological process (BP), cellular component (CC), and molecular function (MF), were conducted using Enrichr web tools (Kuleshov et al., 2016), and these enrichment results were presented in a scatter plot using the Appyters web application (Clarke et al., 2021). Similar gene sets were clustered in a scatter plot using the Leiden algorithm. According to the *q* value (adjusted *p*-value), the top five GO and KEGG analysis terms were listed and marked in the scatter plots.

## PPI network analysis

The “TSV” file of the PPI network data was input to the Cytoscape software to identify hub targets and clusters using the Cytohubba (Version 0.1) and MCODE (Version 2.0.0) plugins, respectively. The Cytohubba plugin provides 11 methods for exploring virtual nodes in biological networks (Chin et al., 2014). Referring to the method from Shen Jiayu et al., the maximal clique centrality (MCC), edge percolated component (EPC), maximum neighborhood component (MNC), and degree algorithms (Shen et al., 2019) were selected in this study to generate four values for each target, calculate a mean value for each algorithm, and finally select the targets for which the values were simultaneously higher than the mean values of each algorithm as the core targets. The

Iregulon (Version 1.3) plugin was used to identify the direct transcription factor of core targets (Janky et al., 2014). The MCODE plugin can mine protein complexes or functional modules from complex protein networks (Bader and Hogue, 2003). All the processing parameters were set to the default values. Additionally, the most important node in the cluster, SEED node, may be the critical target of each cluster. Next, the targets in each cluster were subjected to KEGG pathway enrichment analysis using the Enrichr web tool.

## Results

### Potential targets of the agonists/diseases and their related targets

We collected the molecular structures of three GLP-1RAs (liraglutide, semaglutide, and albiglutide) from the PubChem database. The detailed information is listed in Table 1. In total, 210 targets were obtained from the Binding Database: 77 were for albiglutide, 77 for liraglutide, and 56 for semaglutide. A total of 370 targets were identified using the SEA database: 155 for albiglutide, 133 for liraglutide, and 82 for semaglutide. The Swiss database was used to obtain 158 potential targets: 62 for albiglutide, 60 for liraglutide, and 36 for semaglutide. From the TargetNet database, 167 targets were obtained: 61 for albiglutide, 56 for liraglutide, and 50 for semaglutide. Finally, 198 targets remained after the integration and elimination of duplicates.

When collecting disease targets, T2DM-related keywords were input into the five databases, and a total of 5004 targets were obtained: 4486 from the GeneCards database, 282 from the OMIM database, 24 from the PharmGkb database, 109 from the TTD database, and 103 from the DrugBank database. Finally, 4623 targets remained after removing repetitions. Parallely, we also retrieved the MI-related targets from the five databases, and 727 targets were identified, including 313 from the GeneCards

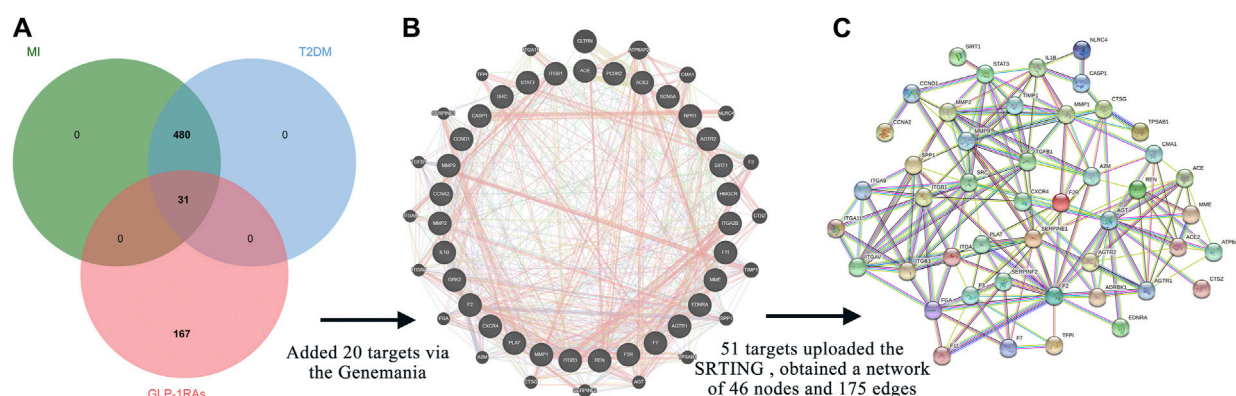


**FIGURE 2**

Intersection targets and associated targets constructed the protein-protein interaction (PPI) network. **(A)** The 31 intersection targets overlap between the targets of GLP-1RAs and the targets of T2DM with MI. **(B)** Twenty targets associated with 31 intersection targets were generated via the GeneMANIA database. **(C)** The 51 related targets constructed a PPI network containing 46 nodes and 175 edges. The interaction score was set at 0.7 (high confidence) and hid disconnected nodes in the network.

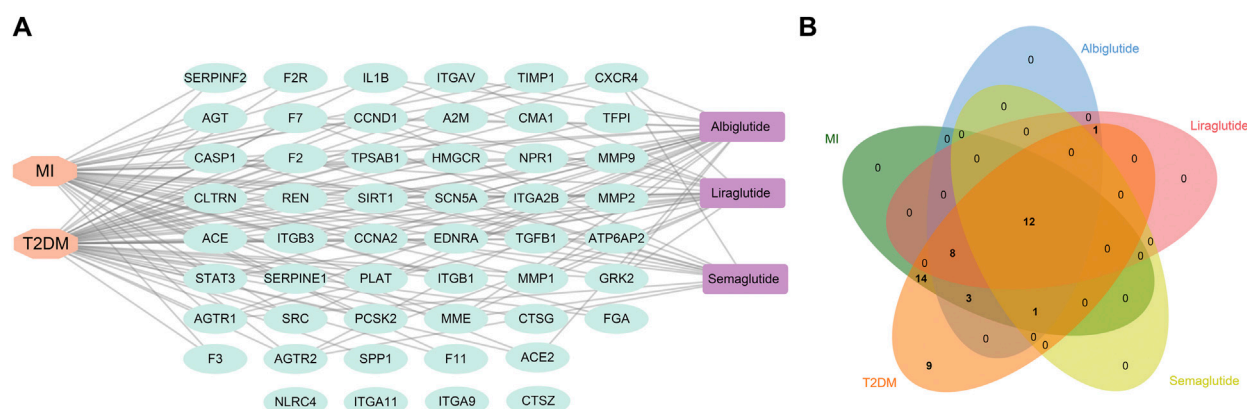


**FIGURE 3**

The construction of a drug-target-disease network. **(A)** Network construction of drug-target-disease composed of three drugs (purple), 102 targets (cyan), and two diseases (orange) via Cytoscape software. **(B)** Venn diagram shows 12 common targets of three drugs against T2DM and MI, and these targets could be regarded as crucial factors mediating the effects of GLP-1RAs on T2DM and MI.

database, 18 from the OMIM database, 121 from the PharmGkb database, 47 from the TTD database, and 133 from the DrugBank database. A total of 511 unique targets were identified after removing duplicates. Interestingly, 511 targets of MI were all covered into targets of T2DM. The online Venn diagram tool generated 31 intersection targets between drugs and diseases (Figure 2A).

The GeneMANIA database provided additional 20 targets (Figure 2B), highly associated with intersection targets. Finally, 51 related targets were identified, indicating potential mechanisms to understand how diabetic patients benefit from the three GLP-1RAs in preventing MI. All 51 related targets were uploaded to the STRING database, and a PPI diagram (Figure 2C) and a TSV format file were obtained. The PPI network included 46 nodes and 175 edges.

## Construction of the drugs-diseases-targets network

The three GLP-1RAs, T2DM and MI, and 51 related targets were input into Cytoscape to construct a drug-disease-target network (Figure 3A). The network contains 56 nodes and 114 edges. We found that T2DM was linked to 47 related targets and MI to 38 targets. Furthermore, 25 connections linked albiglutide to all targets, 21 to liraglutide, and 13 to semaglutide. In contrast, four nodes (NLRC4, ITGA11, ITGA9, and CTSZ) were not associated with any agonists or diseases. Although the three agonists had disparate targets, we intended to explore some shared targets for intervention in the progression of T2DM and MI, and 12 common targets were identified (Figure 3B), namely, AGTR1, AGTR2, CASP1, CCNA2, CCND1, CXCR4, EDNRA, F7, MME, REN,

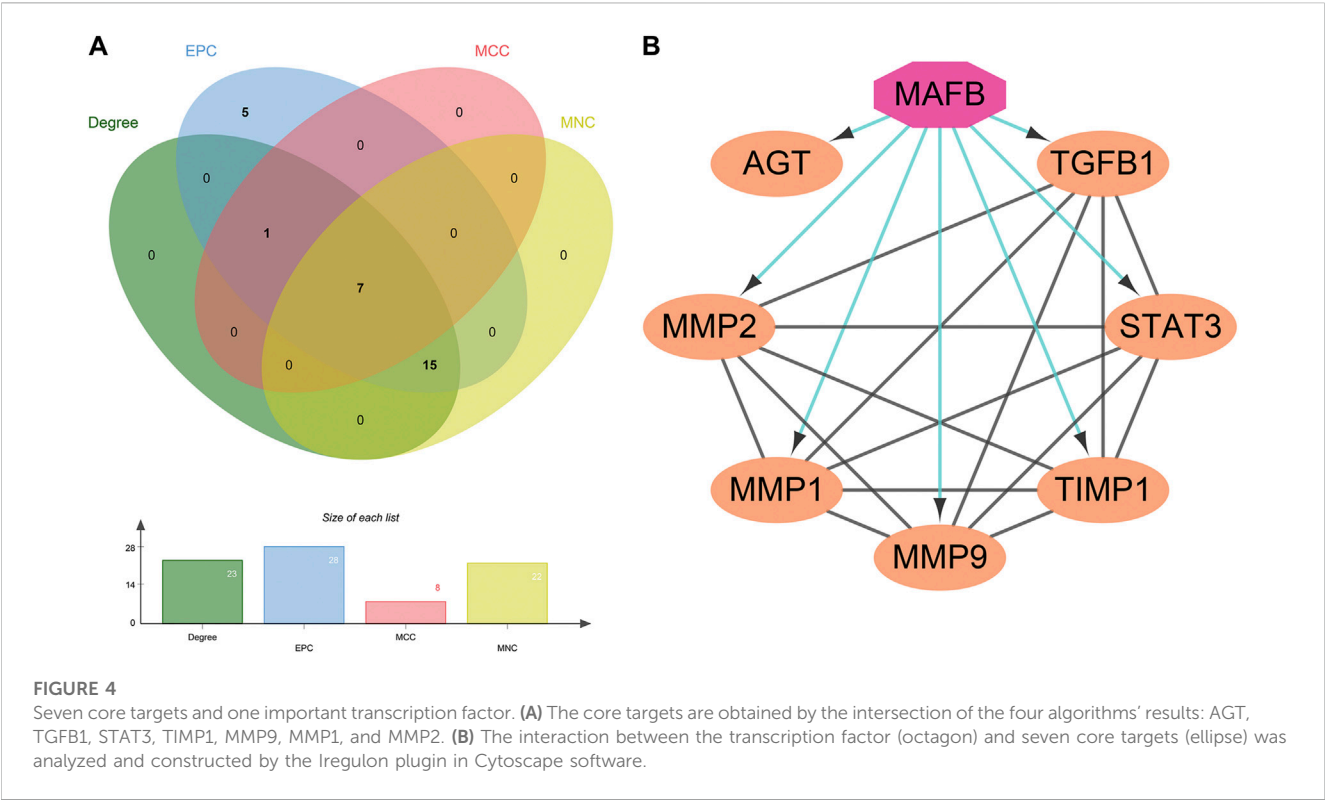


TABLE 2 The top ten transcription factors (ranked by NES) related to six core targets.

Rank	Transcript factor	NES	Targets number	Motifs/Tracks
1	MAFB	7.802	7	11
2	ATF6	7.084	5	10
3	POU3F4	5.922	4	4
4	CBFB	5.803	3	3
5	CEBPA	5.719	4	10
6	FOXO1	5.684	3	8
7	FOXA1	5.561	6	14
8	NKFB1	5.536	4	6
9	SLC18A1	5.516	2	1
10	POU4F3	5.373	3	8

SCN5A, and SIRT1, suggesting that these 12 targets may contribute to the fundamental mechanisms of GLP-1RAs against T2DM and MI.

Analysis of the PPI network of the related targets

The TSV file of the PPI network was loaded into Cytoscape software, and the MMC, MNC, EPC, and Degree algorithms in the “Cytohubba” plugin were used to calculate the core targets. Seven

core targets were identified, including AGT, TGFB1, STAT3, TIMP1, MMP9, MMP1, and MMP2 (Figure 4A), suggesting that they may play a pivotal role in the PPI network of GLP-1RAs interfering with T2DM and MI.

Next, the Iregulon plugin was applied to find the direct transcription factors of seven core targets, and the normalized enrichment score (NES) was calculated and used for ranking purposes (Table 2). The higher the NES value, the better the confidence. The transcription factor MAFB had the highest transcription target number and NES value simultaneously (target number = 7; NES = 7.802) (Figure 4B). The Iregulon

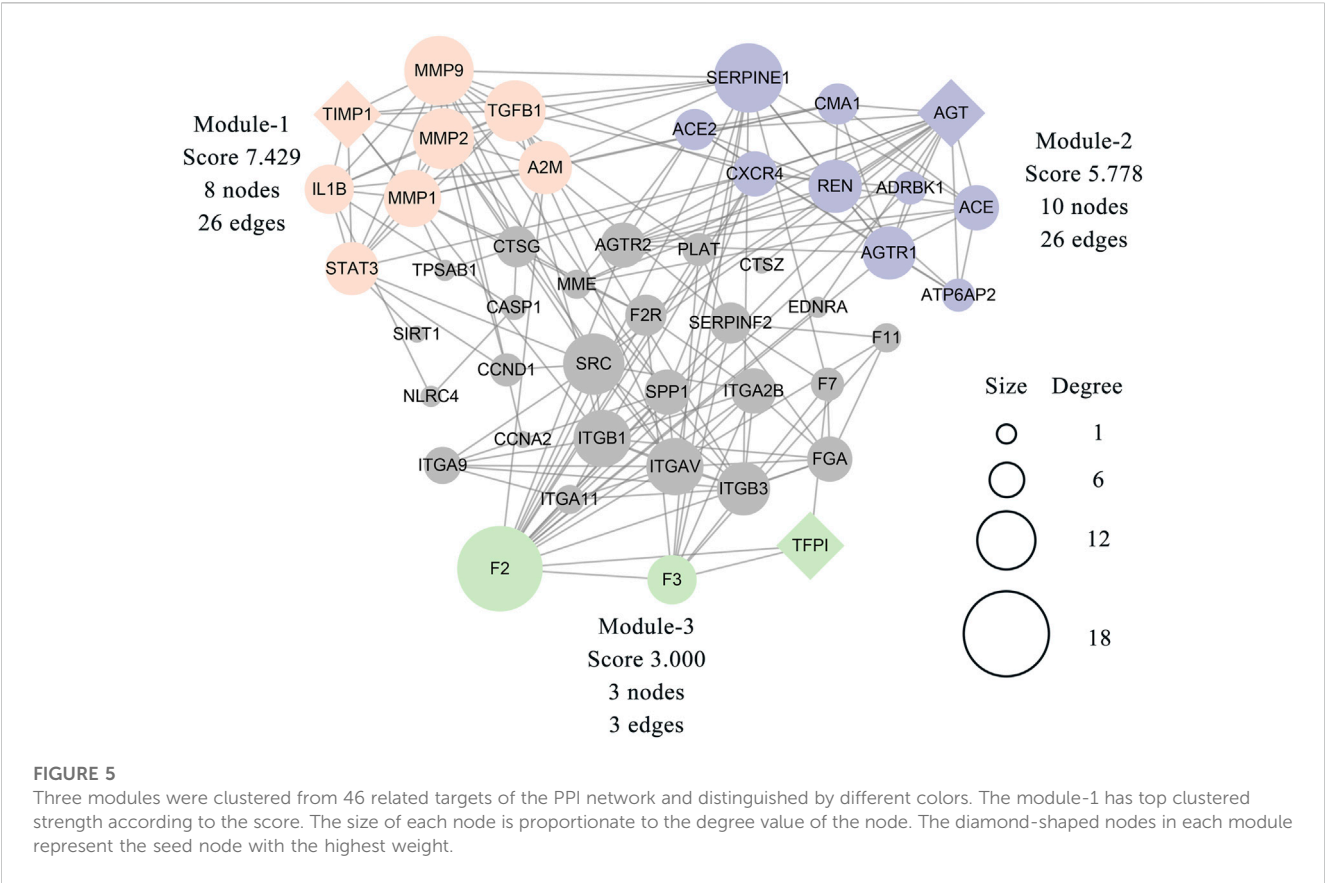


**FIGURE 5** Three modules were clustered from 46 related targets of the PPI network and distinguished by different colors. The module-1 has top clustered strength according to the score. The size of each node is proportionate to the degree value of the node. The diamond-shaped nodes in each module represent the seed node with the highest weight.

**TABLE 3** The top three terms (ranked by Odds Ratio) from KEGG pathway enrichment analysis for each module.

Module	KEGG term	Odds ratio	q value	Genes
1	AGE-RAGE signaling pathway in diabetic complications	207.25	3.57E-06	TGFB1; IL1B; MMP2; STAT3
1	Relaxin signaling pathway	158.94	4.99E-06	TGFB1; MMP1; MMP2; MMP9
1	Bladder cancer	315.06	1.28E-05	MMP1; MMP2; MMP9
2	Renin-angiotensin system	2912.88	4.16E-18	ACE2; ACE; CMA1; ATP6AP2; AGTR1; REN; AGT
2	Renin secretion	204.36	3.22E-07	ACE; CMA1; AGTR1; REN; AGT
2	Diabetic cardiomyopathy	99.96	3.22E-07	ACE; AGTR1; REN; AGT
3	Complement and coagulation cascades	59745.00	6.67E-07	F2; TFPI; F3
3	AGE-RAGE signaling pathway in diabetic complications	100.49	0.044	F3
3	Platelet activation	80.79	0.044	F2

plugin detects transcription factors using more than one thousand ChIP-Seq tracks, providing highly credible results. Therefore, we suggest that MAFB may positively contribute to the beneficial effect of GLP-1RAs in reducing MI in T2DM patients.

The MCODE plugin was then used to predict the modules in the PPI network. The targets were clustered into three modules. Each module represents a densely connected region of the molecular interaction network (Bader and Hogue, 2003). Detailed

characteristics of the modules are shown in Figure 5. Moreover, three seed nodes, TIMP1, AGT, and TFPI (marked by a rhombic shape), had the highest weights in the respective modules. KEGG analysis was performed using the Enrichr web tool. The three top-ranked terms in each module were the AGE-RAGE signaling pathway in diabetic complications (module 1), the renin-angiotensin system (RAS) (module 2), and complement and coagulation cascades (module 3). KEGG results are presented in Table 3.



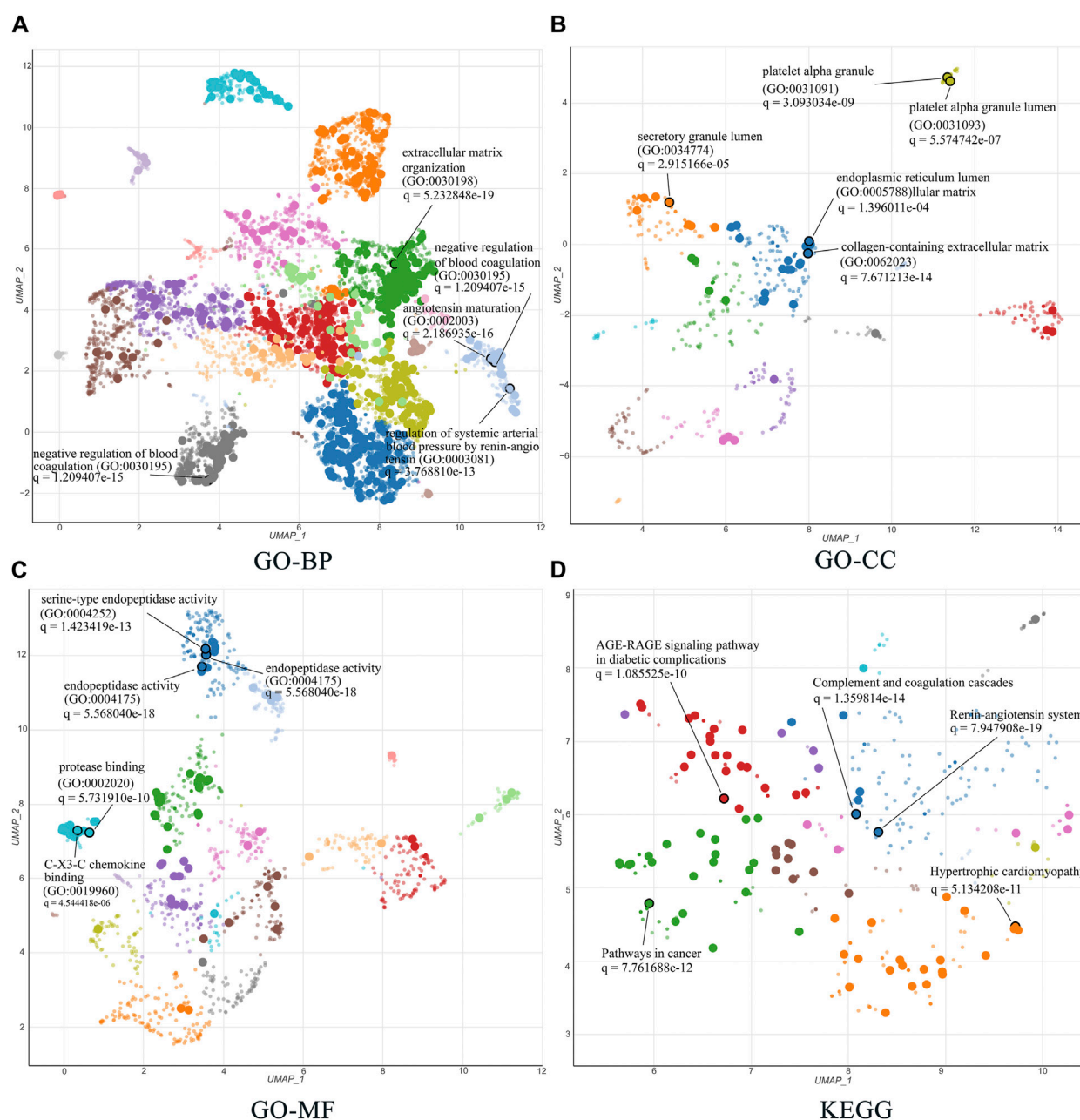


FIGURE 6

GO and KEGG enrichment analysis of 51 related targets via the Enrichr database. (A–C) Biological processes, cellular components, and molecular functions in GO biological annotation analysis. (D) KEGG pathway enrichment analysis entries. All results show the top five items according to the q value. The lower the q value, the higher the credibility.

## Global GO and KEGG enrichment analysis

The 51 related targets were uploaded to Enrichr for KEGG and GO enrichment analyses, and the top five terms ranked by q-value were selected for display. For the GO enrichment analysis, we identified the top five terms from BP, CC, and MF. The results are shown in detail in Figures 6A–C. First, in BP analysis, the top three terms were extracellular matrix (ECM) organization, angiotensin maturation, and regulation of angiotensin levels in the blood. The

top three terms for CC were collagen-containing ECM, platelet-alpha granules, and platelet-alpha granule lumen. In the MF analysis, the top three terms were endopeptidase activity, serine-type endopeptidase activity, and serine-type peptidase activity.

The top five terms for global KEGG enrichment analysis are shown in Figure 6D. The detailed terms were RAS, complement and coagulation cascades, pathways in cancer, hypertrophic cardiomyopathy, and the AGE-RAGE signaling pathway in diabetic complications.

## Discussion

Complications related to diabetes result in 1.5 million deaths per year, and cardiovascular events are the primary cause of death (Collaborators, 2018). Several trials have demonstrated that GLP-1RAs protect diabetic patients from the occurrence of MI, but the underlying mechanism remains unclear. The present study provides novel and systematic explanations for how GLP-1RAs decrease the occurrence of MI in T2DM patients. We applied network pharmacology to predict 51 related targets between GLP-1RAs and diseases and filtered out seven core targets: AGT, TGF $\beta$ 1, STAT3, TIMP1, MMP9, MMP1, and MMP2. MAFB is an essential transcription factor that regulates the expression of all seven core targets. The GO enrichment terms mainly involved angiotensin, ECM, and platelets. For KEGG enrichment analysis, the related targets were principally enriched in RAS, complement and coagulation cascades, and the AGE-RAGE signaling pathway in diabetic complications.

Researchers have proposed various hypotheses to elucidate the therapeutic mechanism of GLP-1RAs in cardiovascular diseases. Many studies have consistently reported that several GLP-1RAs exert inhibitory effects on plaque formation, development, and rupture (Tashiro et al., 2014; Sudo et al., 2017; Wu et al., 2019; Li et al., 2020). However, evidence is insufficient to comprehensively explain the signaling pathways involved in the prophylactic effects of GLP-1RAs on MI. Our results are aligned with previous studies and hypotheses while also unveiling novel perspectives. After applying the CytoHubba plugin using a multi-algorithm, we identified seven core targets. Four targets (MMP1, MMP2, MMP9, and TIMP1) are associated with metalloproteinases. MMP1, MMP2, and MMP9 participate in ECM proteolysis, whereas TIMP1 acts as a metalloproteinase inhibitor that inhibits the function of MMP 1, MMP2, and MMP9 (Moore et al., 2012). The dynamic balance between MMPs and TIMP1 maintains myocardial ECM stability. Several reports have demonstrated that diabetes disrupts the balance of MMPs/TIMPs in the serum and related tissues (Li et al., 2013; Bastos et al., 2017; Zhou et al., 2021), which may significantly enhance the activities of MMPs and pathological remodeling of the vessel wall (Wang and Khalil, 2018), subsequently resulting in obstruction and ischemia. Several reports have shown that GLP-1, exenatide, and semaglutide reduce MMP expression (such as MMP1, MMP2, MMP9, and MMP13), which maintains intact fibrous caps and protects atheromatous plaque from rupture (Burgmaier et al., 2013; Garczorcz et al., 2018; Rakipovski et al., 2018). GLP-1RAs may contribute to the reduction of atherosclerotic plaque instability and cardiac ECM degradation by maintaining the balance between MMPs and TIMPs.

The other three core targets identified were AGT, STAT3, and TGF $\beta$ 1. AGT-encoding angiotensinogen is an essential component of the RAS and participates in the regulation of blood pressure, body fluids, and electrolyte balance. Angiotensinogen undergoes two cleavages to form angiotensin II (Ang II), which has well-known adverse effects on the myocardium. A recent study showed that the mRNA expression of GLP-1R was considerably associated with the components of the renin-angiotensin-aldosterone system (RAAS) detected in epicardial and pericardial fat in patients with severe coronary artery disease (Haberka et al., 2021). However, the interactive regulation between GLP-1R and the RAAS is still

unclear. TGF $\beta$ 1 mediates Ang II-induced myocardial fibrosis (Frangogiannis, 2019). Limited data have shown an inconsistent relationship between GLP-1RAs and TGF $\beta$ 1. Long-acting semaglutide decreased hepatic TGF $\beta$ 1 expression (McLean et al., 2021), whereas exenatide and liraglutide did not reduce TGF $\beta$ 1 levels in adipose tissue (Pastel et al., 2016; Pastel et al., 2017). Although GLP-1 has a beneficial effect on myocardial ECM remodeling (Robinson et al., 2015), the relationship between GLP-1RAs and TGF $\beta$ 1 in the heart is unclear and requires further investigation.

STAT3 responds to cytokines and growth factors. Shiraishi et al. demonstrated that GLP-1 induces macrophage transformation into the M2 phenotype, contributing to the beneficial effects of GLP-1 against diabetes (Shiraishi et al., 2012). A later study also provided consistent evidence that in the process of myocardial repair, STAT3 activation was a prerequisite for macrophage transformation to the reparative M2 phenotype (Shirakawa et al., 2018). Thus, the changes induced by GLP-1RAs contribute to a reduction in the size and instability of atherosclerotic plaques (Vinué et al., 2017), which could, to some extent, explain the lower MI mortality and incidence in patients using GLP-1RA.

The Iregulon plugin used in this study showed that the transcription factor MAFB may regulate all seven core targets, suggesting that it exerts crucial effects on GLP-1RAs by interfering with T2DM and MI. In patients with T2DM, MAFB expression is significantly reduced (Guo et al., 2013). In contrast, overexpressed MAFB can upregulate some cell cycle regulators and subsequently promote human  $\beta$  cell proliferation (Lu et al., 2012). Many previous studies have considered MAFA to be a characteristic of human  $\beta$ -cell function, whereas this view is increasingly being challenged (Velazco-Cruz et al., 2019). Recently, it was suggested that MAFB could be regarded as an essential regulator of the human  $\beta$ -cell signature (Russell et al., 2020). However, only a few studies have tried to reveal the potential relationship between GLP-1 and MAFB. A recent study showed that exenatide (9-39) accelerated the transdifferentiation from  $\alpha$  cells to  $\beta$  cells by reducing MAFB expression in  $\alpha$  cells (Zhang et al., 2019). Therefore, the relationship between GLP-1 and MAFB in  $\beta$ -cells warrants further investigation.

The MCODE plugin provides a practical clustering algorithm to identify the potential functional modules behind these targets. Three modules were obtained in this study and were subsequently subjected to KEGG analysis. The enrichment results mainly focused on the AGE-RAGE signaling pathway, RAS, and complement and coagulation cascades. These biological processes have been demonstrated to have a significant pathogenic relationship with T2DM and MI (Beckman et al., 2002; Husain et al., 2015; Yamagishi, 2019). Some researchers have provided evidence regarding the association between GLP-1RAs and the abovementioned results. GLP-1RAs, such as liraglutide and exenatide, attenuate RAGE expression in several cell types, especially under diabetic conditions (Zhang et al., 2016; Zhang et al., 2017; Zhang et al., 2020), suggesting that the downregulation of RAGE represents a potential mechanism of GLP-1RAs against T2DM. In module two, RAS was a significant KEGG-enriched item. GLP-1RAs play a competitive role in regulating RAS by inhibiting renin synthesis and increasing the inactive form of renin in blood circulation (Puglisi et al., 2021). The

final module included three coagulation-related targets. To date, there is rare information on the direct influence of GLP-1RAs on the processes of coagulation cascades. Furthermore, hyperglycemia facilitates coagulation activation and invalidation of fibrinolytic activity in diabetic patients (Sechterberger et al., 2015). Thus, we hypothesize that the effect of GLP-1RAs on blood coagulation is mediated primarily through controlling blood glucose levels.

Several GLP-1RAs trials have demonstrated that these agonists reduce cardiovascular risk factors, including glycated hemoglobin (HbA1c) values, systolic blood pressure, and body weight (Marso et al., 2016a; Marso et al., 2016b; Hernandez et al., 2018). The median duration of these trials ranged from 1.6 to 3.8 years. Cumulative beneficial changes induced by GLP-1RAs contributed to a decrease in MI prevalence. However, the exact mechanisms underlying the contribution of GLP-1RAs remain unclear, as no cardiac tissue was detected in the trials. The GO and KEGG analyses showed that the enrichment terms mainly focused on ECM, coagulation, RAS, and endopeptidase. As most matrix metalloproteinases are elastase-type endopeptidases, mainly MMP2 and MMP9 (Shapiro, 1998), the dynamic balance of MMPs/TIMPs maintains the stabilization of the ECM; however, diabetes disturbs this balance and causes atherosclerotic plaque disruption, myocardial fibrosis, and remodeling. Four of the seven core targets were involved in this balance, and AGT and TGFB1 directly influenced fibrosis and remodeling. These pathological processes considerably induce cardiac death in diabetic cardiomyopathy and acute MI. Therefore, our results suggest that GLP-1RAs play a crucial role in regulating plaque stability, myocardial fibrosis, and remodeling. Other significant enrichment sets included coagulation, complement, and platelets. The burden of thrombus formation induced by coagulation and the complement system in the coronary artery mainly determines the MI area and clinical outcomes (Sianos et al., 2007; Sianos et al., 2010). Thus, inhibition of the coagulation cascades is an effective measure when plaque ruptures occur. To a certain extent, the related targets and enrichment terms involved in coagulation and complement provide a plausible mechanistic explanation for the fact that some GLP-1RAs reduce non-fatal MI in patients with T2DM.

## Conclusion

Our study provides a comprehensive investigation and analysis of the multi-dimensional effects of GLP-1RAs on preventing MI in patients with T2DM, which may be mainly mediated by interfering

with specific targets, biological processes, and cellular signaling pathways related to atheromatous plaque, myocardial remodeling, and thrombosis. However, this study has some limitations as it lacks a series of experiments to prove the proposed hypothesis. Accordingly, further experiments and multi-omics studies are warranted to understand the comprehensive mechanism of GLP-1RAs.

## Data availability statement

The original contributions presented in the study are included in the article/supplementary material, further inquiries can be directed to the corresponding author.

## Author contributions

GW, XW, and GD generated the conception of the study; GD and JR analyzed the data and wrote the manuscript; XJ, ML, and RL helped to revise and improve the manuscript; JL, YG, and JZ, assisted in retrieving for databases.

## Funding

This article was supported by the Young Talent Support Program of Shaanxi Province University and The National Key Research and Development Program of China (2018YFC1705905).

## Conflict of interest

The authors declare that the research was conducted in the absence of any commercial or financial relationships that could be construed as a potential conflict of interest.

## Publisher's note

All claims expressed in this article are solely those of the authors and do not necessarily represent those of their affiliated organizations, or those of the publisher, the editors and the reviewers. Any product that may be evaluated in this article, or claim that may be made by its manufacturer, is not guaranteed or endorsed by the publisher.

## References

- Bader, G. D., and Hogue, C. W. (2003). An automated method for finding molecular complexes in large protein interaction networks. *BMC Bioinforma.* 4, 2. doi:10.1186/1471-2105-4-2
- Bastos, M. F., Tucci, M. A., de Siqueira, A., de Faveri, M., Figueiredo, L. C., Vallim, P. C., et al. (2017). Diabetes may affect the expression of matrix metalloproteinases and their inhibitors more than smoking in chronic periodontitis. *J. Periodontol. Res.* 52 (2), 292–299. doi:10.1111/jre.12394
- Beckman, J. A., Creager, M. A., and Libby, P. (2002). Diabetes and atherosclerosis: Epidemiology, pathophysiology, and management. *Jama* 287 (19), 2570–2581. doi:10.1001/jama.287.19.2570
- Burgmaier, M., Liberman, A., Möllmann, J., Kahles, F., Reith, S., Leberer, C., et al. (2013). Glucagon-like peptide-1 (GLP-1) and its split products GLP-1(9-37) and GLP-1(28-37) stabilize atherosclerotic lesions in apoe<sup>-/-</sup> mice. *Atherosclerosis* 231 (2), 427–435. doi:10.1016/j.atherosclerosis.2013.08.033
- Chin, C. H., Chen, S. H., Wu, H. H., Ho, C. W., Ko, M. T., and Lin, C. Y. (2014). cytoHubba: identifying hub objects and sub-networks from complex interactome. *BMC Syst. Biol.* 8 (4), S11. doi:10.1186/1752-0509-8-S4-S11
- Clarke, D. J. B., Jeon, M., Stein, D. J., Moiseyev, N., Kropiwnicki, E., Dai, C., et al. (2021). Appyters: Turning jupyter notebooks into data-driven web apps. *Patterns (N Y)* 2 (3), 100213. doi:10.1016/j.patter.2021.100213



- Collaborators, G. D. a. I. I. a. P. (2018). Global, regional, and national incidence, prevalence, and years lived with disability for 354 diseases and injuries for 195 countries and territories, 1990–2017: A systematic analysis for the global burden of disease study 2017. *Lancet* 392 (10159), 1789–1858. doi:10.1016/S0140-6736(18)32279-7
- Consortium, U. (2021). UniProt: The universal protein knowledgebase in 2021. *Nucleic Acids Res.* 49 (D1), D480–d489. doi:10.1093/nar/gkaa1100
- Daina, A., Michielin, O., and Zoete, V. (2019). SwissTargetPrediction: Updated data and new features for efficient prediction of protein targets of small molecules. *Nucleic Acids Res.* 47 (W1), W357–w364. doi:10.1093/nar/gkz382
- Frangogiannis, N. G. (2019). Cardiac fibrosis: Cell biological mechanisms, molecular pathways and therapeutic opportunities. *Mol. Asp. Med.* 65, 70–99. doi:10.1016/j.mam.2018.07.001
- Garczorz, W., Gallego-Colon, E., Kosowska, A., Klych-Ratuszny, A., Woźniak, M., Marcol, W., et al. (2018). Exenatide exhibits anti-inflammatory properties and modulates endothelial response to tumor necrosis factor  $\alpha$ -mediated activation. *Cardiovasc. Ther.* 36 (2), e12317. doi:10.1111/1755-5922.12317
- Gerstein, H. C., Colhoun, H. M., Dagenais, G. R., Diaz, R., Lakshmanan, M., Pais, P., et al. (2019). Dulaglutide and renal outcomes in type 2 diabetes: An exploratory analysis of the REWIND randomised, placebo-controlled trial. *Lancet* 394 (10193), 131–138. doi:10.1016/S0140-6736(19)31150-X
- Gilson, M. K., Liu, T., Baitaluk, M., Nicola, G., Hwang, L., and Chong, J. (2016). BindingDB in 2015: A public database for medicinal chemistry, computational chemistry and systems pharmacology. *Nucleic Acids Res.* 44 (D1), D1045–D1053. doi:10.1093/nar/gkv1072
- GTEXPortal (2021). Transcripts per million (TPM) of the GLP1R gene [Online]. Available: <https://gtexportal.org/home/gene/GLP1R> (Accessed).
- Guo, S., Dai, C., Guo, M., Taylor, B., Harmon, J. S., Sander, M., et al. (2013). Inactivation of specific  $\beta$  cell transcription factors in type 2 diabetes. *J. Clin. Invest* 123 (8), 3305–3316. doi:10.1172/jci65390
- Haberka, M., Siniarski, A., Gajos, G., Machnik, G., Kowalówka, A., Deja, M., et al. (2021). Epicardial, pericardial fat and glucagon-like peptide-1 and -2 receptors expression in stable patients with multivessel coronary artery disease: An association with the renin-angiotensin-aldosterone system. *Pol. Arch. Intern. Med.* 131 (3), 233–240. doi:10.20452/pamw.15797
- Helmstadter, J., Keppeler, K., Kuster, L., Munzel, T., Daiber, A., and Steven, S. (2022). Glucagon-like peptide-1 (GLP-1) receptor agonists and their cardiovascular benefits-The role of the GLP-1 receptor. *Br. J. Pharmacol.* 179 (4), 659–676. doi:10.1111/bph.15462
- Hernandez, A. F., Green, J. B., Janmohamed, S., D'Agostino, R. B., Sr., Granger, C. B., et al. (2018). Albiglutide and cardiovascular outcomes in patients with type 2 diabetes and cardiovascular disease (harmony outcomes): A double-blind, randomised placebo-controlled trial. *Lancet* 392 (10157), 1519–1529. doi:10.1016/S0140-6736(18)32261-X
- Hong, Z., Zhang, T., Zhang, Y., Xie, Z., Lu, Y., Yao, Y., et al. (2021). Reveals of candidate active ingredients in Justicia and its anti-thrombotic action of mechanism based on network pharmacology approach and experimental validation. *Sci. Rep.* 11 (1), 17187. doi:10.1038/s41598-021-96683-z
- Husain, K., Hernandez, W., Ansari, R. A., and Ferder, L. (2015). Inflammation, oxidative stress and renin angiotensin system in atherosclerosis. *World J. Biol. Chem.* 6 (3), 209–217. doi:10.4331/wjbc.v6.i3.209
- International Diabetes Federation (2022). *IDF diabetes atlas*. 10th ed [Online]. Brussels, Belgium. 2021Available: <https://www.diabetesatlas.org/> (Accessed).
- Janky, R., Verfaillie, A., Imrichova, H., Van de Sande, B., Standaert, L., Christiaens, V., et al. (2014). iRegulon: from a gene list to a gene regulatory network using large motif and track collections. *PLoS Comput. Biol.* 10 (7), e1003731. doi:10.1371/journal.pcbi.1003731
- Keiser, M. J., Roth, B. L., Armbruster, B. N., Ernsberger, P., Irwin, J. J., and Shoichet, B. K. (2007). Relating protein pharmacology by ligand chemistry. *Nat. Biotechnol.* 25 (2), 197–206. doi:10.1038/nbt1284
- Kuleshov, M. V., Jones, M. R., Rouillard, A. D., Fernandez, N. F., Duan, Q., Wang, Z., et al. (2016). Enrichr: A comprehensive gene set enrichment analysis web server 2016 update. *Nucleic Acids Res.* 44 (W1), W90–W97. doi:10.1093/nar/gkw377
- Li, Q., Tuo, X., Li, B., Deng, Z., Qiu, Y., and Xie, H. (2020). Semaglutide attenuates excessive exercise-induced myocardial injury through inhibiting oxidative stress and inflammation in rats. *Life Sci.* 250, 117531. doi:10.1016/j.lfs.2020.117531
- Li, Z., Guo, S., Yao, F., Zhang, Y., and Li, T. (2013). Increased ratio of serum matrix metalloproteinase-9 against TIMP-1 predicts poor wound healing in diabetic foot ulcers. *J. Diabetes Complicat.* 27 (4), 380–382. doi:10.1016/j.jdiacomp.2012.12.007
- Lu, J., Hamze, Z., Bonnavion, R., Herath, N., Pouponnot, C., Assade, F., et al. (2012). Reexpression of oncoprotein MafB in proliferative  $\beta$ -cells and Men1 insulinomas in mouse. *Oncogene* 31 (31), 3647–3654. doi:10.1038/ncr.2011.538
- Marso, S. P., Bain, S. C., Consoli, A., Eliaschewitz, F. G., Jodar, E., Leiter, L. A., et al. (2016a). Semaglutide and cardiovascular outcomes in patients with type 2 diabetes. *N. Engl. J. Med.* 375 (19), 1834–1844. doi:10.1056/NEJMoa1607141
- Marso, S. P., Daniels, G. H., Brown-Frandsen, K., Kristensen, P., Mann, J. F., Nauck, M. A., et al. (2016b). Liraglutide and cardiovascular outcomes in type 2 diabetes. *N. Engl. J. Med.* 375 (4), 311–322. doi:10.1056/NEJMoa1603827
- McLean, B. A., Wong, C. K., Kaur, K. D., Seeley, R. J., and Drucker, D. J. (2021). Differential importance of endothelial and hematopoietic cell GLP-1Rs for cardiometabolic versus hepatic actions of semaglutide. *JCI Insight* 6 (22), e153732. doi:10.1172/jci.insight.153732
- Moore, L., Fan, D., Basu, R., Kandam, V., and Kassiri, Z. (2012). Tissue inhibitor of metalloproteinases (TIMPs) in heart failure. *Heart Fail Rev.* 17 (4-5), 693–706. doi:10.1007/s10741-011-9266-y
- Nogales, C., Mamdouh, Z. M., List, M., Kiel, C., Casas, A. I., and Schmidt, H. (2022). Network pharmacology: Curing causal mechanisms instead of treating symptoms. *Trends Pharmacol. Sci.* 43 (2), 136–150. doi:10.1016/j.tips.2021.11.004
- Pastel, E., Joshi, S., Knight, B., Liversedge, N., Ward, R., and Kos, K. (2016). Effects of Exendin-4 on human adipose tissue inflammation and ECM remodelling. *Nutr. Diabetes* 6 (12), e235. doi:10.1038/nutd.2016.44
- Pastel, E., McCulloch, L. J., Ward, R., Joshi, S., Gooding, K. M., Shore, A. C., et al. (2017). GLP-1 analogue-induced weight loss does not improve obesity-induced AT dysfunction. *Clin. Sci. (Lond)* 131 (5), 343–353. doi:10.1042/cs20160803
- Puglisi, S., Rossini, A., Poli, R., Dughera, F., Pia, A., Terzolo, M., et al. (2021). Effects of SGLT2 inhibitors and GLP-1 receptor agonists on renin-angiotensin-aldosterone system. *Front. Endocrinol. (Lausanne)* 12, 738848. doi:10.3389/fendo.2021.738848
- Rakipovski, G., Rolin, B., Nohr, J., Klewe, I., Frederiksen, K. S., Augustin, R., et al. (2018). The GLP-1 analogs liraglutide and semaglutide reduce atherosclerosis in ApoE(-/-) and LDLr(-/-) mice by a mechanism that includes inflammatory pathways. *JACC Basic Transl. Sci.* 3 (6), 844–857. doi:10.1016/j.jacbs.2018.09.004
- Robinson, E., Cassidy, R. S., Tate, M., Zhao, Y., Lockhart, S., Calderwood, D., et al. (2015). Exendin-4 protects against post-myocardial infarction remodelling via specific actions on inflammation and the extracellular matrix. *Basic Res. Cardiol.* 110 (2), 20. doi:10.1007/s00395-015-0476-7
- Rodriguez-Gutierrez, R., Gonzalez-Gonzalez, J. G., Zuñiga-Hernandez, J. A., and McCoy, R. G. (2019). Benefits and harms of intensive glycemic control in patients with type 2 diabetes. *Bmj* 367, l5887. doi:10.1136/bmj.l5887
- Rosenblit, P. D. (2019). Extreme atherosclerotic cardiovascular disease (ASCVD) risk recognition. *Curr. Diab Rep.* 19 (8), 61. doi:10.1007/s11892-019-1178-6
- Russell, R., Carneese, P. P., Hennings, T. G., Walker, E. M., Russ, H. A., Liu, J. S., et al. (2020). Loss of the transcription factor MAFB limits  $\beta$ -cell derivation from human PSCs. *Nat. Commun.* 11 (1), 2742. doi:10.1038/s41467-020-16550-9
- Sattar, N., Lee, M. M. Y., Kristensen, S. L., Branch, K. R. H., Del Prato, S., Khurmi, N. S., et al. (2021). Cardiovascular, mortality, and kidney outcomes with GLP-1 receptor agonists in patients with type 2 diabetes: A systematic review and meta-analysis of randomised trials. *Lancet Diabetes Endocrinol.* 9 (10), 653–662. doi:10.1016/S2213-8587(21)00203-5
- Sechterberger, M. K., Hermanides, J., Poolman, R. W., Kal, J. E., Meijers, J. C., Hoekstra, J. B., et al. (2015). Lowering blood glucose during hip surgery does not influence coagulation activation. *BBA Clin.* 3, 227–232. doi:10.1016/j.bbaci.2015.03.001
- Shapiro, S. D. (1998). Matrix metalloproteinase degradation of extracellular matrix: Biological consequences. *Curr. Opin. Cell Biol.* 10 (5), 602–608. doi:10.1016/S0955-0674(98)80035-5
- Shen, J., Yu, S., Sun, X., Yin, M., Fei, J., and Zhou, J. (2019). Identification of key biomarkers associated with development and prognosis in patients with ovarian carcinoma: Evidence from bioinformatic analysis. *J. Ovarian Res.* 12 (1), 110. doi:10.1186/s13048-019-0578-1
- Shiraishi, D., Fujiwara, Y., Komohara, Y., Mizuta, H., and Takeya, M. (2012). Glucagon-like peptide-1 (GLP-1) induces M2 polarization of human macrophages via STAT3 activation. *Biochem. Biophys. Res. Commun.* 425 (2), 304–308. doi:10.1016/j.bbrc.2012.07.086
- Shirakawa, K., Endo, J., Kataoka, M., Katsumata, Y., Yoshida, N., Yamamoto, T., et al. (2018). IL (Interleukin)-10-STAT3-Galectin-3 Axis is essential for osteopontin-producing reparative macrophage polarization after myocardial infarction. *Circulation* 138 (18), 2021–2035. doi:10.1161/circulationaha.118.035047
- Sianos, G., Papafakis, M. I., Daemen, J., Vaina, S., van Mieghem, C. A., van Domburg, R. T., et al. (2007). Angiographic stent thrombosis after routine use of drug-eluting stents in ST-segment elevation myocardial infarction: The importance of thrombus burden. *J. Am. Coll. Cardiol.* 50 (7), 573–583. doi:10.1016/j.jacc.2007.04.059
- Sianos, G., Papafakis, M. I., and Serruys, P. W. (2010). Angiographic thrombus burden classification in patients with ST-segment elevation myocardial infarction treated with percutaneous coronary intervention. *J. Invasive Cardiol.* 22 (10), 6B–14B.
- Singh, A., Gupta, A., DeFilippis, E. M., Qamar, A., Biery, D. W., Almarzooq, Z., et al. (2020). Cardiovascular mortality after type 1 and type 2 myocardial infarction in Young adults. *J. Am. Coll. Cardiol.* 75 (9), 1003–1013. doi:10.1016/j.jacc.2019.12.052
- Stelzer, G., Rosen, N., Plaschkes, I., Zimmerman, S., Twik, M., Fishilevich, S., et al. (2016). The GeneCards suite: From gene data mining to disease genome sequence analyses. *Curr. Protoc. Bioinforma.* 54, 131–3031. doi:10.1002/cpbi.5

- Sudo, M., Li, Y., Hiro, T., Takayama, T., Mitsumata, M., Shiomi, M., et al. (2017). Inhibition of plaque progression and promotion of plaque stability by glucagon-like peptide-1 receptor agonist: Serial *in vivo* findings from iMap-IVUS in Watanabe heritable hyperlipidemic rabbits. *Atherosclerosis* 265, 283–291. doi:10.1016/j.atherosclerosis.2017.06.920
- Szklarczyk, D., Gable, A. L., Lyon, D., Junge, A., Wyder, S., Huerta-Cepas, J., et al. (2019). STRING v11: Protein-protein association networks with increased coverage, supporting functional discovery in genome-wide experimental datasets. *Nucleic Acids Res.* 47 (D1), D607–D613. doi:10.1093/nar/gky1131
- Tashiro, Y., Sato, K., Watanabe, T., Nohtomi, K., Terasaki, M., Nagashima, M., et al. (2014). A glucagon-like peptide-1 analog liraglutide suppresses macrophage foam cell formation and atherosclerosis. *Peptides* 54, 19–26. doi:10.1016/j.peptides.2013.12.015
- Velazco-Cruz, L., Song, J., Maxwell, K. G., Goedegebuure, M. M., Augsornworawat, P., Hogrebe, N. J., et al. (2019). Acquisition of dynamic function in human stem cell-derived  $\beta$  cells. *Stem Cell Rep.* 12 (2), 351–365. doi:10.1016/j.stemcr.2018.12.012
- Vinué, Á., Navarro, J., Herrero-Cervera, A., García-Cubas, M., Andrés-Blasco, I., Martínez-Hervás, S., et al. (2017). The GLP-1 analogue lixisenatide decreases atherosclerosis in insulin-resistant mice by modulating macrophage phenotype. *Diabetologia* 60 (9), 1801–1812. doi:10.1007/s00125-017-4330-3
- Wang, X., and Khalil, R. A. (2018). Matrix metalloproteinases, vascular remodeling, and vascular disease. *Adv. Pharmacol.* 81, 241–330. doi:10.1016/bs.apha.2017.08.002
- Wang, Y., Zhang, S., Li, F., Zhou, Y., Zhang, Y., Wang, Z., et al. (2020). Therapeutic target database 2020: Enriched resource for facilitating research and early development of targeted therapeutics. *Nucleic Acids Res.* 48 (D1), D1031–D1041. doi:10.1093/nar/gkz981
- Warde-Farley, D., Donaldson, S. L., Comes, O., Zuberi, K., Badrawi, R., Chao, P., et al. (2010). The GeneMANIA prediction server: Biological network integration for gene prioritization and predicting gene function. *Nucleic Acids Res.* 38, W214–W220. Web Server issue). doi:10.1093/nar/gkq537
- Whirl-Carrillo, M., Huddart, R., Gong, L., Sangkuhl, K., Thorn, C. F., Whaley, R., et al. (2021). An evidence-based framework for evaluating pharmacogenomics knowledge for personalized medicine. *Clin. Pharmacol. Ther.* 110 (3), 563–572. doi:10.1002/cpt.2350
- Wishart, D. S., Feunang, Y. D., Guo, A. C., Lo, E. J., Marcu, A., Grant, J. R., et al. (2018). DrugBank 5.0: A major update to the DrugBank database for 2018. *Nucleic Acids Res.* 46 (D1), D1074–d1082. doi:10.1093/nar/gkx1037
- Wu, Y. C., Wang, W. T., Lee, S. S., Kuo, Y. R., Wang, Y. C., Yen, S. J., et al. (2019). Glucagon-like peptide-1 receptor agonist attenuates autophagy to ameliorate pulmonary arterial hypertension through Drp1/NOX- and atg-5/atg-7/beclin-1/lc3 $\beta$  pathways. *Int. J. Mol. Sci.* 20 (14), 3435. doi:10.3390/ijms20143435
- Yamagishi, S. I. (2019). Role of advanced glycation endproduct (AGE)-Receptor for advanced glycation endproduct (RAGE) Axis in cardiovascular disease and its therapeutic intervention. *Circ. J.* 83 (9), 1822–1828. doi:10.1253/circj.CJ-19-0618
- Yao, Z. J., Dong, J., Che, Y. J., Zhu, M. F., Wen, M., Wang, N. N., et al. (2016). TargetNet: A web service for predicting potential drug-target interaction profiling via multi-target SAR models. *J. Comput. Aided Mol. Des.* 30 (5), 413–424. doi:10.1007/s10822-016-9915-2
- Zhang, H., Chu, Y., Zheng, H., Wang, J., Song, B., and Sun, Y. (2020). Liraglutide improved the cognitive function of diabetic mice via the receptor of advanced glycation end products down-regulation. *Aging (Albany NY)* 13 (1), 525–536. doi:10.18632/aging.202162
- Zhang, S. S., Wu, Z., Zhang, Z., Xiong, Z. Y., Chen, H., and Huang, Q. B. (2017). Glucagon-like peptide-1 inhibits the receptor for advanced glycation endproducts to prevent podocyte apoptosis induced by advanced oxidative protein products. *Biochem. Biophys. Res. Commun.* 482 (4), 1413–1419. doi:10.1016/j.bbrc.2016.12.050
- Zhang, W. (2016). Network pharmacology further description. *Netw. Pharmacol.* 1 (1), 1–14.
- Zhang, Z., Hu, Y., Xu, N., Zhou, W., Yang, L., Chen, R., et al. (2019). A new way for beta cell neogenesis: Transdifferentiation from alpha cells induced by glucagon-like peptide 1. *J. Diabetes Res.* 2019, 2583047. doi:10.1155/2019/2583047
- Zhang, Z., Yang, L., Lei, L., Chen, R., Chen, H., and Zhang, H. (2016). Glucagon-like peptide-1 attenuates advanced oxidation protein product-mediated damage in islet microvascular endothelial cells partly through the RAGE pathway. *Int. J. Mol. Med.* 38 (4), 1161–1169. doi:10.3892/ijmm.2016.2711
- Zheng, Y., Lang, Y., Qi, Z., Gao, W., Hu, X., and Li, T. (2021). PIK3R1, SPNB2, and CRYAB as potential biomarkers for patients with diabetes and developing acute myocardial infarction. *Int. J. Endocrinol.* 2021, 2267736. doi:10.1155/2021/2267736
- Zhou, P., Yang, C., Zhang, S., Ke, Z. X., Chen, D. X., Li, Y. Q., et al. (2021). The imbalance of MMP-2/TIMP-2 and MMP-9/TIMP-1 contributes to collagen deposition disorder in diabetic non-injured skin. *Front. Endocrinol. (Lausanne)* 12, 734485. doi:10.3389/fendo.2021.734485

## Glossary

**AGE** advanced glycosylation end products

**AGT** angiotensinogen

**AGTR1/2** angiotensin II receptor type 1/2

**AMI** acute myocardial infarction

**Ang II** angiotensin II

**BP** biological process

**CASP1** caspase 1

**CC** cellular component

**CCNA2** cyclin A2

**CCND1** cyclin D1

**ChIP-seq** chromatin immunoprecipitation-sequence

**CTSZ** cathepsin Z

**CXCR4** C-X-C motif chemokine receptor 4

**ECM** extracellular matrix

**EDNRA** endothelin receptor type A

**EPC** edge percolated component

**F7** coagulation factor VII

**GLP-1** glucagon-like peptide-1

**GLP-1RAs** GLP-1 receptor agonists

**GO** gene ontology

**ITGA9/11** integrin subunit alpha 9/11

**KEGG** Kyoto encyclopedia of genes and genes

**MAFA** MAF BZIP transcription factor A

**MAFB** MAF BZIP transcription factor B

**MCC** maximal clique centrality

**MCODE** molecular complex detection

**MF** molecular function

**MI** myocardial infarction

**MME** membrane metalloendopeptidase

**MMP1/2/9** matrix metalloproteinase 1/2/9

**MNC** maximum neighborhood component

**NES** normalized enrichment score

**NF-κB** nuclear factor kappa B subunit 1

**NLRC4** NLR family CARD domain containing 4

**OMIM** online mendelian inheritance in man

**ox-LDL** oxidized low density lipoprotein

**PharmGKB** pharmacogenetics and pharmacogenomics knowledge base

**PPI** protein-protein interaction

**RAAS** renin-angiotensin-aldosterone system

**RAGE** receptor for advanced glycosylation end products

**RAS** renin-angiotensin system

**REN** renin

**SCN5A** sodium voltage-gated channel alpha subunit 5

**SIRT1** sirtuin 1

**SMILES** simplified molecular input line entry system

**STAT3** signal transducer and activator of transcription 3

**T2DM** type 2 diabetes mellitus

**TFPI** tissue factor pathway inhibitor

**TGFB1** transforming growth factor beta 1

**TIMP1/2/3** tissue inhibitor of metalloproteinases 1/2/3

**TSV** tab separated values

**TTD** therapeutic target database.



## OPEN ACCESS

## EDITED BY

Xianwei Wang,  
Xinxiang Medical University, China

## REVIEWED BY

Iana Orlova,  
Lomonosov Moscow State University,  
Russia  
Kenes Erimbetov,  
Moscow Technological University, Russia

## \*CORRESPONDENCE

Alexey Moskalev,  
✉ amoskalev@list.ru

## SPECIALTY SECTION

This article was submitted to  
Cardiovascular and Smooth Muscle  
Pharmacology, a section of the journal  
Frontiers in Pharmacology

RECEIVED 24 January 2023

ACCEPTED 21 February 2023

PUBLISHED 02 March 2023

## CITATION

Maganova F, Voevoda M, Popov V and  
Moskalev A (2023), A prospective  
randomized comparative placebo-  
controlled double-blind study in two  
groups to assess the effect of the use of  
biologically active additives with Siberian  
fir terpenes for the biological age of  
a person.

*Front. Pharmacol.* 14:1150504.

doi: 10.3389/fphar.2023.1150504

## COPYRIGHT

© 2023 Maganova, Voevoda, Popov and  
Moskalev. This is an open-access article  
distributed under the terms of the  
[Creative Commons Attribution License](https://creativecommons.org/licenses/by/4.0/)  
(CC BY). The use, distribution or  
reproduction in other forums is  
permitted, provided the original author(s)  
and the copyright owner(s) are credited  
and that the original publication in this  
journal is cited, in accordance with  
accepted academic practice. No use,  
distribution or reproduction is permitted  
which does not comply with these terms.

# A prospective randomized comparative placebo-controlled double-blind study in two groups to assess the effect of the use of biologically active additives with Siberian fir terpenes for the biological age of a person

Faniya Maganova <sup>1</sup>, Mikhail Voevoda <sup>2</sup>, Vladimir Popov <sup>3,4</sup>  
and Alexey Moskalev <sup>5,6\*</sup>

<sup>1</sup>Initium-Pharm LLC, Moscow, Russia, <sup>2</sup>Federal Research Center of Fundamental and Transnational Medicine, Moscow, Russia, <sup>3</sup>Department of Internal Medicine with a Pharmacy Course of the Medical Institute of Continuing Education, Federal State Budgetary Educational Institution of Higher Education Russian Biotechnological University, Moscow, Russia, <sup>4</sup>Department of Biochemistry and Pharmacology at Medical Institute of Tambov State University Named After G.R. Derzhavin, Tambov, Russia, <sup>5</sup>Laboratory of Genetics and Epigenetics of Aging, Russian Clinical and Research Center of Gerontology, Pirogov Russian National Research Medical University, Moscow, Russia, <sup>6</sup>Institute of Biogerontology, Lobachevsky State University of Nizhny Novgorod, Nizhny Novgorod, Russia

A prospective randomized comparative placebo-controlled double-blind study was carried out based on Arterial Indices model of biological age. The study involved 60 men and women aged 40–65 years that were randomly divided into two equal groups of 30 people: the main group and the control one. The study participants from the main group received a dietary supplement containing Siberian fir terpenes, limonene, alpha-linolenic acid, and vitamin E—1 capsule 3 times a day for 90 days. Patients in the comparison group received a placebo according to a similar scheme. Anthropometric and biochemical characteristics of patients from both groups have not undergone any significant changes. According to ultrasound examination of the carotid arteries, we observed a statistically significant decrease in the minimum thickness of the intima-media complex (by 45%). The maximum carotid artery stenosis on the right or left and the expansion index in patients of both groups did not change significantly during treatment. According to the results of applanation tonometry, it was revealed that when taking the studied dietary supplement, the pulse wave velocity significantly decreased compared to the initial one (by 10%). Accordingly, the Arterial Indices biological age decreased by 2.5 years compared to the baseline level in patients of the main group and did not change in patients from the comparison group. Supplementation of fir terpenes in middle-aged patients of both sexes reduces the biological age reflecting the condition of the arteries.

## KEYWORDS

terpenes, dietary supplement, artery stiffness, pulse wave velocity, carotid intima-media thickness, biological age, ultrasound, applanation tonometry

## Introduction

The concept of biological age appeared because of the awareness of the unevenness of aging (Moskalev, 2019). It is obvious that the intensity of aging is related to heredity, environmental conditions in the place of residence, the level of medical care and the lifestyle of the person. Therefore, with the same chronological age in different people, the degree of deterioration of the whole body, as well as individual organs and systems, is different. The consequences of age-related processes are also expressed to varying degrees—violations of the most important vital functions, narrowing of the range of adaptation, resilience, stress-resistance, development of disease states. We can assume that the difference between chronological and biological age reflects the intensity of aging and the risks of age-related diseases.

Considering the conventionality of the concept of biological age, researchers have made numerous attempts to establish a set of measurable criteria of aging. For various models of biological age, empirical clinical parameters (biochemical and functional), aging-based molecular measurements, or big omics data (methylome, transcriptome, proteome, metabolome, metagenome) are currently used (Moskalev, 2020).

An original method for determining the biological age has been proposed, based on the determination of sex-specific Arterial Indices model (Fedintsev et al., 2017). The method allows the use of widely used medical equipment in hospitals and clinics without performing molecular or cellular tests. Arterial indices are determined non-invasively by combining four functional indicators of cardiovascular health from the results of carotid duplex scanning and applanation tonometry.

Cardiovascular aging is characterized by a complex of pathophysiological changes affecting both the myocardium and blood vessel walls at the structural, cellular, molecular, and functional levels. As it is known, cardiovascular diseases are the main component of age-related mortality. Aging is associated with functional changes in blood vessels, including stiffening of the arteries, which is the main cause of hypertension. Moreover, a study in a recent publication has shown that arterial aging correlates better with chronological age than with the accompanying changes in blood biochemical parameters (Fedintsev et al., 2017). Carotid intima-media thickness (cIMT) is an established surrogate marker of atherosclerosis. This parameter is also associated with metabolic syndrome, insulin sensitivity and other age-related functional disorders.

The aim of this study was to investigate the effect of Siberian fir terpenes diet supplement in healthy middle-aged people. The impact of the study dietary supplement was assessed by the following primary

endpoints—biological age determined by ultrasound and applanation tonometry (B4/B1) in healthy middle-aged subjects (Figure 1).

## Materials and methods

### Characteristics of patients participating in the study

A prospective, randomized, comparative, placebo-controlled, double-blind study was conducted based on N.I. cc, a separate structural subdivision of the Russian Gerontological Research and Clinical Center.

The study was conducted in accordance with the requirements of the Russian Federation National Standard “Good Clinical Practice” GOST R 53279–2005, the World Medical Association Declaration of Helsinki Ethical Principles for Medical Research Involving Human Subjects and ICH E6 Good Clinical Practice (GCP) rules and approved by the ethical committee of the Pirogov Russian State Medical University on 12/30/2020.

The study involved 60 men and women aged 40–65 years who signed an informed consent form.

The exclusion criteria were:

- The presence of any of the diseases or conditions: diabetes mellitus; body mass index (BMI)  $\leq 25$  or  $\geq 38$  kg/m<sup>2</sup>; arterial hypertension of the second or third degree; acute coronary syndrome or acute cerebrovascular accident or transient ischemic attack or revascularization interventions on coronary or brachiocephalic arteries in the anamnesis; atrial fibrillation; angina; chronic heart failure; GFR  $\leq 59$  ml/min/1.73 m<sup>2</sup>; increased activity of AST or ALT serum more than 2.5 times from the upper limit of the norm; chronic hepatitis or cirrhosis of the liver of any etiology; oncological disease of any localization at present or in the anamnesis.
- Current or previously conducted regular drug therapy, including all dietary supplements, antidiabetic drugs, statins, NSAIDs, RAAS blockers in less than 14 days or 5 half-lives.
- Hypersensitivity to the test product and/or its component in the anamnesis.
- Simultaneous participation in another clinical trial.
- Pregnancy, breastfeeding.
- A history of alcohol and/or drug addiction.

After the examination, the patients were randomly divided into two equal groups of 30 people: the main and the comparison group. Table 1 shows the anthropometric and biochemical

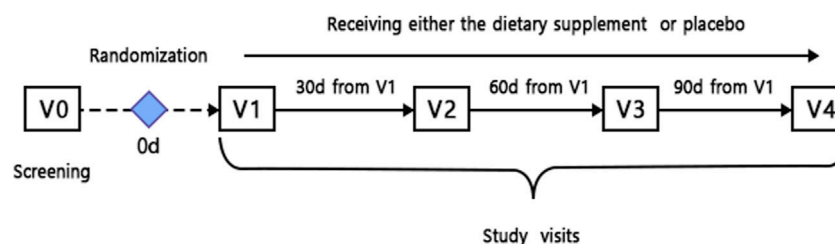


FIGURE 1  
Schematic visit schedule.

**TABLE 1** Anthropometric and biochemical characteristics of patients from both groups.

Indicator	Comparison group	Main group	Reference values
Demographic and anthropometric characteristics			
Gender: men, number of persons women, number of persons	2	8	
	28	22	
Age, years	45.5	51.0	
	42.2–51.0	45.5–57.5	
Body mass index, kg/m <sup>2</sup>	31.2	30.1	18.5–25—norm
	28.1–34.0	28.6–31.8	25–30—overweight over 30 - obesity
Heart rate, beats per min	72.5	74.0	
	65.5–75.0	69.5–80.0	
Systolic blood pressure, mmHg	129	129	
	125–134	122–134	
Diastolic blood pressure, mmHg	82	82	
	76–90	77–90	
Markers of carbohydrate metabolism and insulin resistance			
Glycated hemoglobin, %	5.50	5.50	4.27–6.07
	5.35–5.70	5.40–5.65	
Fasting venous blood glucose, mmol/L	5.22	5.36	4.1–5.9
	5.08–5.39	5.12–5.55	
Insulin, mkU/ml	8.29	9.21	2.1–27
	5.68–12.17	5.75–13.45	
Markers of blood lipid profile			
Triglycerides, mmol/L	1.02	1.14	0.68–6
	0.82–1.57	0.90–2.08	
Cholesterol—HDL, mmol/L	1.58	1.60	< 3.3
	1.51–1.82	1.34–1.88	
Cholesterol—LDL, mmol/L	3.66	3.71	1.81–4.04
	3.14–4.33	3.21–4.60	
Markers of endothelial dysfunction			
The Willebrand Factor, %	140	115.0	70–150
	114–159	83.5–154.0	
Homocysteine, mmol/L	9.15	9.7	<20
	7.64–11.0	9.0–11.25	

Note: The data in the table are presented in the form of median and interquartile ranges.

characteristics of patients from both groups. Individual data collected in the [Supplementary Table S1](#).

Study participants from the main group received the dietary supplement “CardioOrganic®” 1 capsule 3 times a day, 20 min before meals for 90 days.

Patients in the comparison group according to a similar scheme received a placebo, which was a capsule of the same shape, color, and size as the study product, following a similar scheme.

## Medications used

Dietary supplement Vitaterpen brand “CardioOrganic®” produced by Korolevpharm LLC, contains biologically active substances of natural origin in an amount not exceeding the upper permissible level of consumption. One capsule (600 mg) contains at least: 20 mg of Siberian fir terpenes, 1.7 mg of limonene, 250 mg of omega-3 PUFA (alpha-linolenic acid),



6.5 mg of vitamin E. The quantitative composition of the placebo; 1 capsule (600 mg) contains at least: 592.5 mg - linseed oil, 7.5 mg—of vitamin E.

## Defined parameters

Primary endpoints of the clinical study—estimated indicators of biological age:

1. Biological age determined by ultrasound and applanation tonometry (B4/B1)
2. Biological age determined from the results of a blood test (B4/B1)

Secondary endpoints—additional indicators (blood):

1. Score of the quality of life according to the SF-36 questionnaire (B4/B1)
2. Interleukin-6 (B4/B1)
3. C-reactive protein (B4/B1)
4. TNF- $\alpha$  (B4/B1)
5. Ferritin (B4/B1)
6. Lipid peroxidation (B4/B1)
7. Insulin (B4/B1)
8. Willebrand factor (B4/B1)
9. Homocysteine (B4/B1)
10. Omega-3 index (B4/B1)
11. Unsaturated fatty acids (B4/B1)
12. Insulin-like growth factor IGF-1, (somatomedin C) (B4/B1)
13. Platelet aggregation with ADP (B4/B1)

In the dynamics of observation, a physical examination of patients, a biochemical blood test, Doppler ultrasound of the carotid arteries and applanation tonometry were performed; the frequency of adverse events and adverse reactions was noted, the value of biological age was calculated.

The pulse wave velocity was measured using the SphygmoCor device (AtCor Medical, Australia). The applanation tonometer is sequentially superimposed on the proximal (carotid) and, with a short interval, on the distal (femoral) artery, while an ECG is simultaneously recorded. The pulse wave velocity is calculated using the time of passage of the wave between the registration points, determined using the R wave on the ECG.

Duplex examination of the carotid arteries was performed using (Ultrasound Diagnostic Medical System, Vivid E9, Israel).

Biological age was calculated according to the formulas for women and men (Fedintsev et al., 2017).

Female Arterial Index

$$\text{AGEW} = -59.92 + 48.87 \cdot \text{CIMmin} + 2.4 \cdot \text{AIx} + 32.41 \cdot \log(\text{PWV}) + 0.64 \cdot \text{STENmax} - 0.95 \cdot \text{AIx} \cdot \log(\text{PWV}) - 0.7 \cdot \text{CIMmin} \cdot \text{STENmax}$$

Male Arterial Index:

$$\text{AGEM} = -0.86 + 46.68 \cdot \text{CIMmin} + 0.17 \cdot \text{STENmax} + 6.18 \cdot \log(\text{PWV}).$$

Where:

$\text{CIM}_{\text{min}}$ —minimal thickness of the intima-media complex, in the left or right carotid,  $\text{AIx}$ —Augmentation Index (the degree of pressure rise in the artery after the return of the reflected wave; the difference of the dicrotic wave and the anacrotic, divided by the

central pulse pressure),  $\text{PWV}$ —pulse wave velocity,  $\text{STEN}_{\text{max}}$ —Maximal of two stenosis values, on the left or on the right.

## Statistical processing

Statistical processing of the results was carried out using the STATISTICA v.12 program. To assess the statistical significance of the differences obtained, non-parametric criteria were used: Mann-Whitney for independent and Wilcoxon for dependent samples. The data in the table are presented in the form of median and interquartile ranges. The level of statistical significance was taken to correspond to  $p \leq 0.05$ .

## Results

There were no cases of clinically significant abnormalities in the physical examination at any visit in any group. The average values of blood biochemical parameters in both groups did not differ at the beginning and at the end of the study.

According to the ultrasound examination of the carotid arteries in patients of the main group a statistically significant decrease in the minimum value of the thickness of the intima-media complex on the right or left from the initial was noted. No such changes were observed in the placebo group (Table 2).

A decrease in this parameter indicates favorable changes in the vascular wall, accompanied by an increase in the lumen of the carotid arteries and, accordingly, an improvement in the blood supply to the brain.

The maximum stenosis of the carotid artery, on the right or left in patients of both groups did not change statistically significantly during the treatment.

According to the results of applanation tonometry, it was revealed that while taking the studied dietary supplement, the pulse wave velocity decreased statistically significantly from the initial (Table 2).

There were no statistically significant changes in the placebo group. The decrease in pulse wave velocity reflects a decrease in arterial stiffness (a characteristic age-related change) and normalization of the reflected wave return velocity. These positive changes ultimately led to a decrease in the excess load on the left ventricle and an increase in perfusion pressure in the coronary arteries.

Table 3 shows the values of the biological age calculated from the data of the ultrasound of the carotid arteries and applanation tonometry.

It decreased compared to the baseline in patients of the main group and did not change in patients from the comparison group.

## Discussion

Currently, there is a growing interest in biomarkers of biological age. Biological age is understood as a synthetic index consisting of one marker or a combination of several biological markers, which by itself or in combination with functional markers not only correlates with chronological age, but is also able to identify people “younger”



**TABLE 2 Results of ultrasound of carotid arteries and applanation tonometry.**

Indicator	Comparison group		Main group	
	Before taking a placebo	After 90 days of taking a placebo	Before taking dietary supplements	After 90 days of taking dietary supplements
Minimum value of the thickness of the intima-media complex on the right or left (cIMT), mm	0.71	0.73	0.72	0.70 **
	0.66–0.80	0.65–0.80	0.68–0.81	0.64–0.73
Maximum carotid artery stenosis, right or left (STENmax), %	0	0	25.0	20
	0.0–25.0	0.0–20.0	0.00–25.0	0.00–25
Augmentation Index (AIx), %	27.0	28	29.0	27
	19.25–33.50	24.0–33.0	22.50–36.00	24.0–32.75
Pulse wave velocity, m/s	10.20	9.10	10.50	9.50*
	8.93–10.57	8.10–10.10	9.25–12.45	8.70–10.75

1. The data in the table are presented in the form of median and interquartile ranges.

2. The differences are statistically significant compared to the beginning of the study:

\*\* -  $p < 0.001$ ; \* -  $p < 0.01$  (non-parametric criteria Wilcoxon for dependent samples).

**TABLE 3 Biological age (years), calculated according to the data of the ultrasound of the carotid arteries and applanation tonometry.**

Comparison group		Main group	
Before taking a placebo	After 90 days of taking a placebo	Before taking dietary supplements	After 90 days of taking dietary supplements
54.7	55.6	57.6	55.0**
50.5–61.2	50.6–61.0	50.5–61.6	48.7–59.4

1. The data in the table are presented in the form of median and interquartile ranges.

2. The differences are statistically significant compared to the beginning of the study:

\*\* -  $p < 0.001$  (nonparametric criteria Wilcoxon for dependent samples).

or “older” than their chronological age in the same demographic group cohorts (Franceschi et al., 2018).

Carotid intima-media thickness (cIMT) is an established surrogate marker of atherosclerosis (Carpenter et al., 2016). This parameter is also associated with metabolic syndrome, insulin sensitivity and other age-related functional disorders (Lee et al., 2014; Roussel et al., 2016). It has been shown that the thickness of intima-media reliably predicts the progression of Alzheimer’s disease in general (Wang et al., 2016) and cognitive decline associated with Alzheimer’s disease, in particular (Buratti et al., 2015). In addition, revascularization improves cognitive functions, suggesting that the relationship between carotid artery stenosis and cognitive decline may be causal (Lal et al., 2011; Ortega et al., 2014). In addition, cIMT is largely associated with cardiovascular and overall mortality (Murakami et al., 2005).

Another predictor of cardiovascular diseases, the Augmentation index (AIx), is associated with the risk of symptomatic cardiovascular disease (Nurnberger et al., 2002). The pulse wave velocity in the aorta is a reliable predictor of future cardiovascular events and mortality from all causes—an increase in PWV in the aorta by 1 m/s corresponds to the risk adjusted for age, gender and risk factors for 14%, 15% and 15% of the total number of cardiovascular events, cardiovascular mortality, and mortality from all causes, respectively (Vlachopoulos et al., 2010). Thus, the aging of the arteries can be considered as a key factor in the overall aging process.

As a measure of biological age in this study we applied Artery Indices (Fedintsev et al., 2017). While creating this model, more than 80 hematological and functional health parameters were studied in a well-characterized cohort of patients for 2 years. Machine learning methods were applied to them, and the greatest predictive power was found for markers of arterial stiffness and artery wall thickness, which were combined into the Artery Indices model. Arterial Indices were determined by combining four functional indicators of cardiovascular health from the results of carotid duplex scanning and applanation tonometry. The advantage of this model is the non-invasiveness of measurements. The Artery Index was significantly higher in people with hypertension and type 2 diabetes than in healthy people that validates it as a biological age predictor (Fedintsev et al., 2017).

It is assumed that the improvement and introduction of personalized non-drug interventions, including diet and exercise, are more likely to lead to a healthy aging of the population than new or repurposed drugs (Guerville et al., 2020). In addition, food supplements could help to improve certain parameters of a person’s quality of life: physical, mental, emotional, or social functioning.

It should be noted that the patients aged 40–60 years, whom we accepted into the study, were relatively healthy and did not need pharmacotherapy. However, it is known that atherosclerotic lesions and vascular stiffness at this age are already quite pronounced. Taking food additives with a high safety profile can help improve

endothelial function and reduce biological age. This strategy can prolong the patient's health and prevent the need for pharmacotherapy, which, despite its effectiveness, is often associated with undesirable drug reactions, individual intolerance, etc.

The dietary supplement contains a combination of terpenes of fir. It was revealed that in normal fibroblasts, terpenes induced genes for stress response, autophagy, apoptosis regulation, and tissue regeneration. The restoration of the expression level of some longevity genes after fir extract treatment was shown in senescent cells (Kudryavtseva et al., 2016). In subsequent preclinical studies on human fibroblasts, have shown that a substance containing fir terpenes exhibits antioxidant activity, induces autophagy, and affects aging-associated molecular pathways in the transcriptome and proteome (Kudryavtseva et al., 2016; Lipatova et al., 2021). Terpenoids exhibit many properties of potential geroprotectors that can effectively influence the mechanisms of aging and age-related diseases (Proshkina et al., 2020), including blood vessel endothelial dysfunction.

In patients taking supplement for 3 months, there was a decrease in the minimum thickness of the intima-media complex on the right or left side, which was a manifestation of favorable changes in the vascular wall an increase in the lumen of the carotid arteries and, accordingly, an increase in the improvement of blood supply to the brain.

The decrease in pulse wave velocity in patients of the main group after a 3-month course of taking food additive reflects a decrease in arterial stiffness (a characteristic age-related change) and normalization of the rate of return of the reflected wave, which ultimately leads to a decrease in excessive load on the left ventricle and an increase in perfusion pressure in the coronary arteries.

In this work, the assessment of biological age and the effect of dietary supplements on it was carried out exclusively according to the parameters of the cardiovascular system. Therefore, it is natural that the positive effect obtained because of taking supplement was expressed in a decrease in biological age.

As mentioned above food additive contains polyunsaturated omega-3 fatty acids, vitamin E, limonene, Siberian fir terpenes, and placebo capsules contain flaxseed oil, which also contains unsaturated omega-3, 6 and 9 fatty acids and vitamin E. One would expect that patients in the placebo group would also experience positive effects, but we did not find statistically significant changes in the indicators characterizing the state of the vascular bed.

This suggests that the positive effect of terpenes on the stiffness of the vascular wall has been revealed.

A similar example is the European RISTOMED project, a multicenter open randomized study of the effect of a diet designed to meet the recommended daily requirement for nutrients, vitamins, and minerals in accordance with various cultural traditions, separately or with three nutraceuticals, including d-limonene, on inflammatory and metabolic markers. In healthy middle-aged people. It has been shown that the addition of d-limonene in the context of this dietary intervention can have a beneficial effect on the middle-aged, limiting the negative effects of chronic inflammation and improving the parameters of insulin resistance (Ostan et al., 2016).

In addition, it is likely that Siberian fir terpenes supplement, as well as any dietary additive, is characterized by a weak or moderate

cumulative effect without a pronounced effect on laboratory and/or functional parameters of the body, which, in turn, characterizes the safety of food additives well. Siberian fir terpenes supplement has demonstrated a high safety profile. At the same time, additional research is needed to understand the detailed mechanisms of action of the composition of the substances that make up a supplement.

Thus, according to the instrumental method of examination (ultrasound examination and applanation tonometry), it was proved that taking the studied dietary supplement helps to improve blood supply to the brain. At the same time, it does not affect laboratory parameters, which confirms the safety of dietary supplements. The positive effect of the investigated dietary supplement on the condition of blood vessels was ultimately expressed in a statistically significant decrease in biological age, estimated by Artery Indexes model.

## Data availability statement

The original contributions presented in the study are included in the article/[Supplementary Material](#), further inquiries can be directed to the corresponding author.

## Ethics statement

The studies involving human participants were reviewed and approved by Ethical committee of the Pirogov Russian State Medical University, Moscow, Russia. The patients/participants provided their written informed consent to participate in this study.

## Author contributions

FM, MV, VP, and AM planned a clinical trial protocol; VP performed the collection and processing of experimental data; FM, MV, VP, and AM discussed the results and wrote the manuscript.

## Funding

This study received funding from Initium-Pharm LLC. The funder was involved in the study design, the writing of this article or the decision to submit it for publication.

## Conflict of interest

FM is founder of Initium-Pharm, owing the brand cardioOrganicR.

The remaining authors declare that the research was conducted in the absence of any commercial or financial relationships that could be construed as a potential conflict of interest.

## Publisher's note

All claims expressed in this article are solely those of the authors and do not necessarily represent those of their

affiliated organizations, or those of the publisher, the editors and the reviewers. Any product that may be evaluated in this article, or claim that may be made by its manufacturer, is not guaranteed or endorsed by the publisher.

## References

- Buratti, L., Balestrini, S., Altamura, C., Viticchi, G., Falsetti, L., Luzzi, S., et al. (2015). Markers for the risk of progression from mild cognitive impairment to Alzheimer's disease. *J. Alzheimers Dis.* 45 (3), 883–890. doi:10.3233/JAD-143135
- Carpenter, M., Sinclair, H., and Kunadian, V. (2016). Carotid intima media thickness and its utility as a predictor of cardiovascular disease: A review of evidence. *Cardiol. Rev.* 24 (2), 70–75. doi:10.1097/CRD.000000000000077
- Fedintsev, A., Kashtanova, D., Tkacheva, O., Strazhesko, I., Kudryavtseva, A., Baranova, A., et al. (2017). Markers of arterial health could serve as accurate non-invasive predictors of human biological and chronological age. *Aging (Albany NY)* 9 (4), 1280–1292. doi:10.18632/aging.101227
- Franceschi, C., Garagnani, P., Morsiani, C., Conte, M., Santoro, A., Grignolio, A., et al. (2018). The continuum of aging and age-related diseases: Common mechanisms but different rates. *Front. Med. (Lausanne)* 5, 61. doi:10.3389/fmed.2018.00061
- Guerville, F., De Souto Barreto, P., Ader, I., Andrieu, S., Casteilla, L., Dray, C., et al. (2020). Revisiting the hallmarks of aging to identify markers of biological age. *J. Prev. Alzheimers Dis.* 7 (1), 56–64. doi:10.14283/jpad.2019.50
- Kudryavtseva, A., Krasnov, G., Lipatova, A., Alekseev, B., Maganova, F., Shaposhnikov, M., et al. (2016). Effects of Abies sibirica terpenes on cancer- and aging-associated pathways in human cells. *Oncotarget* 7 (50), 83744–83754. doi:10.18632/oncotarget.13467
- Lal, B. K., Younes, M., Cruz, G., Kapadia, I., Jamil, Z., and Pappas, P. J. (2011). Cognitive changes after surgery vs stenting for carotid artery stenosis. *J. Vasc. Surg.* 54 (3), 691–698. doi:10.1016/j.jvs.2011.03.253
- Lee, Y. H., Shin, M. H., Kweon, S. S., Nam, H. S., Park, K. S., Choi, J. S., et al. (2014). Normative and mean carotid intima-media thickness values according to metabolic syndrome in Koreans: The namwon study. *Atherosclerosis* 234 (1), 230–236. doi:10.1016/j.atherosclerosis.2014.02.023
- Lipatova, A., Krasnov, G., Vorobyov, P., Melnikov, P., Alekseeva, O., Vershinina, Y., et al. (2021). Effects of Siberian fir terpenes extract Abisil on antioxidant activity, autophagy, transcriptome and proteome of human fibroblasts. *Aging (Albany NY)* 13 (16), 20050–20080. doi:10.18632/aging.203448
- Moskalev, A. (2019). *Biomarkers of human aging*. Springer International Publishing: Imprint: Springer.
- Moskalev, A. (2020). The challenges of estimating biological age. *Elife* 9, e54969. doi:10.7554/eLife.54969
- Murakami, S., Otsuka, K., Hotta, N., Yamanaka, G., Kubo, Y., Matsuoka, O., et al. (2005). Common carotid intima-media thickness is predictive of all-cause and cardiovascular mortality in elderly community-dwelling people: Longitudinal Investigation for the Longevity and Aging in Hokkaido County (LILAC) study. *Biomed. Pharmacother.* 1 (1), S49–S53. doi:10.1016/s0753-3322(05)80010-1
- Nurnberger, J., Keflioglu-Scheiber, A., Opazo Saez, A. M., Wenzel, R. R., Philipp, T., and Schafers, R. F. (2002). Augmentation index is associated with cardiovascular risk. *J. Hypertens.* 20 (12), 2407–2414. doi:10.1097/00004872-200212000-00020
- Ortega, G., Alvarez, B., Quintana, M., Yugueros, X., Alvarez-Sabin, J., and Matas, M. (2014). Asymptomatic carotid stenosis and cognitive improvement using transcervical stenting with protective flow reversal technique. *Eur. J. Vasc. Endovasc. Surg.* 47 (6), 585–592. doi:10.1016/j.ejvs.2014.02.022
- Ostan, R., Bene, M. C., Spazzafumo, L., Pinto, A., Donini, L. M., Pryn, F., et al. (2016). Impact of diet and nutraceutical supplementation on inflammation in elderly people. Results from the RISTOMED study, an open-label randomized control trial. *Clin. Nutr.* 35 (4), 812–818. doi:10.1016/j.clnu.2015.06.010
- Proshkina, E., Plyusnin, S., Babak, T., Lashmanova, E., Maganova, F., Koval, L., et al. (2020). Terpenoids as potential geroprotectors. *Antioxidants (Basel)* 9 (6), 529. doi:10.3390/antiox9060529
- Roussel, R., Natali, A., Balkau, B., Hojlund, K., Sanchez, G., Nolan, J. J., et al. (2016). Beta-cell function is associated with carotid intima-media thickness independently of insulin resistance in healthy individuals. *J. Hypertens.* 34 (4), 685–691. doi:10.1097/HJH.0000000000000842
- Vlachopoulos, C., Aznaouridis, K., and Stefanadis, C. (2010). Prediction of cardiovascular events and all-cause mortality with arterial stiffness: A systematic review and meta-analysis. *J. Am. Coll. Cardiol.* 55 (13), 1318–1327. doi:10.1016/j.jacc.2009.10.061
- Wang, T., Mei, B., and Zhang, J. (2016). Atherosclerotic carotid stenosis and cognitive function. *Clin. Neurol. Neurosurg.* 146, 64–70. doi:10.1016/j.clineuro.2016.03.027

## Supplementary material

The Supplementary Material for this article can be found online at: <https://www.frontiersin.org/articles/10.3389/fphar.2023.1150504/full#supplementary-material>



## OPEN ACCESS

## EDITED BY

Xianwei Wang,  
Xinxiang Medical University, China

## REVIEWED BY

Evangelia Zvintzou,  
University of Patras, Greece  
Juan Badimon,  
Icahn School of Medicine at Mount Sinai,  
United States

## \*CORRESPONDENCE

Youlu Shen,  
✉ 2568656114@qq.com  
Yuhong Li,  
✉ 641297625@qq.com

## SPECIALTY SECTION

This article was submitted to  
Cardiovascular and Smooth Muscle  
Pharmacology,  
a section of the journal  
Frontiers in Pharmacology

RECEIVED 15 February 2023

ACCEPTED 14 March 2023

PUBLISHED 27 March 2023

## CITATION

Chai B, Shen Y, Li Y and Wang X (2023),  
Meta-analysis and trial sequential analysis  
of ezetimibe for coronary atherosclerotic  
plaque compositions.  
*Front. Pharmacol.* 14:1166762.  
doi: 10.3389/fphar.2023.1166762

## COPYRIGHT

© 2023 Chai, Shen, Li and Wang. This is an  
open-access article distributed under the  
terms of the [Creative Commons  
Attribution License \(CC BY\)](#). The use,  
distribution or reproduction in other  
forums is permitted, provided the original  
author(s) and the copyright owner(s) are  
credited and that the original publication  
in this journal is cited, in accordance with  
accepted academic practice. No use,  
distribution or reproduction is permitted  
which does not comply with these terms.

# Meta-analysis and trial sequential analysis of ezetimibe for coronary atherosclerotic plaque compositions

Bofeng Chai<sup>1</sup>, Youlu Shen<sup>2\*</sup>, Yuhong Li<sup>2\*</sup> and Xiaoyu Wang<sup>3</sup>

<sup>1</sup>Graduate School of Qinghai University, Xining, China, <sup>2</sup>Affiliated Hospital of Qinghai University, Xining, China, <sup>3</sup>The Third People's Hospital of Tianshui, Tianshui, China

**Background:** Lipid aggregation, inflammatory cell infiltration, fibrous cap formation, and disruption are the major causes of atherosclerotic cardiovascular disease (ASCVD) and the pathologic features of atherosclerotic plaques. Although ezetimibe's role in decreasing blood lipids is widely known, there are insufficient data to determine which part of the drug has an effect on atherosclerotic plaque compositions.

**Objective:** The study aimed to systematically evaluate the efficacy of ezetimibe for coronary atherosclerotic plaque compositions.

**Methods:** Two researchers independently searched the PubMed, Embase, Cochrane Library, and Web of Science databases for randomized controlled trials (RCTs) on the efficacy of ezetimibe for coronary atherosclerotic plaques from inception until 22 January 2023. The meta-analysis and trial sequential analysis (TSA) were performed using Stata 14.0 and TSA 0.9.5.10 Beta software, respectively.

**Results:** Four RCTs were finally included this study, which comprised 349 coronary artery disease patients. Meta-analysis findings showed that, compared with the control group, intervention measures could effectively reduce the fibro-fatty plaque (FFP) volume [WMD = -2.90, 95% CI (-4.79 and -1.00), and  $p = 0.003 < 0.05$ ]; there were no significant difference in the reduction of fibrous plaque (FP) volume [WMD = -4.92, 95% CI (-11.57 and 1.74), and  $p = 0.15 > 0.05$ ], necrotic core (NC) volume [WMD = -2.26, 95% CI (-6.99 and 2.46), and  $p = 0.35 > 0.05$ ], and change dense calcification (change DC) volume [WMD = -0.07, 95% CI (-0.34 and 0.20), and  $p = 0.62 > 0.05$ ] between the treatment group and the control group. TSA findings showed more studies are still required to confirm the efficacy of ezetimibe for FP and NC in the future.

**Conclusion:** Compared to the control group, ezetimibe significantly decreased FFP, but it had no statistically significant difference on FP, NC, or change DC. According to TSA, further research will be required to confirm the efficacy of ezetimibe for FP and NC in the future.

## KEYWORDS

ezetimibe, coronary atherosclerotic plaques, compositions, meta-analysis, trial sequential analysis

# 1 Introduction

Lipid aggregation, inflammatory cell infiltration, fibrous cap formation, and disruption are the major causes of atherosclerotic cardiovascular disease (ASCVD) and the pathological features of atherosclerotic plaques (Falk et al., 2013; Dawson et al., 2022). The cholesterol absorption inhibitor, ezetimibe, in combination with statins has been shown to significantly reduce low-density lipoprotein cholesterol (LDL-C) levels and improve outcomes in acute coronary syndromes in a large sample, double-blind, randomized controlled trial (Cannon et al., 2015). As compared to statin treatment alone, ezetimibe and statin combination significantly decreased coronary plaque volume, according to Ueda et al. (2017).

Although ezetimibe's role in decreasing blood lipids is widely known and it is recommended in clinical guidelines (Grundy et al., 2019; Mach et al., 2020), there are insufficient data to determine which part of the drug has an effect on atherosclerotic plaque compositions. Multiple investigations on the efficacy of ezetimibe on coronary atherosclerotic plaque compositions have been conducted, although the findings are not entirely consistent. In order to give information for therapeutic practices, the aim of this study was to systematically evaluate the efficacy of ezetimibe for coronary atherosclerotic plaque compositions.

# 2 Materials and methods

The Preferred Reporting Items for Systematic Reviews and Meta-Analysis (PRISMA) criteria (Page et al., 2021) were followed for performing this meta-analysis, which was registered in the International Prospective Register of Systematic Reviews.

## 2.1 Inclusion and exclusion criteria

Inclusion criteria were as follows: 1) study type: RCTs in English language; 2) patients: patients who meet the diagnostic criteria for all types of coronary atherosclerotic heart disease and underwent intravascular ultrasound (IVUS) examinations, regardless of disease duration and severity, gender, age, and region; 3) intervention measures: the treatment group was treated with ezetimibe combined with statin or ezetimibe monotherapy, while the control group was treated with placebo, statin monotherapy, or blank control; and 4) endpoints: ① fibro-fatty plaque volume (FFP, mm<sup>3</sup>), ② fibrous plaque volume (FP, mm<sup>3</sup>), ③ necrotic core volume (NC, mm<sup>3</sup>), and ④ change dense calcification volume (change DC, mm<sup>3</sup>). Endpoints should be measured and calculated according to *American College of Cardiology Clinical Expert Consensus Document on Standards for Acquisition, Measurement and Reporting of Intravascular Ultrasound Studies* (Mintz, 2001).

Exclusion criteria were as follows: 1) patients with other types of coronary artery disease, structural heart disease, heart failure, cardiomyopathy, connective tissue disease, and other influencing factors; 2) repeated literature; 3) errors or incomplete study data;

and 4) case reports, conference reports, experts' experience, animal experiments, and reviews.

## 2.2 Literature search strategy, data extraction, and quality evaluation

Two investigators separately searched the PubMed, Embase, Cochrane Library, and the Web of Science databases from inception until 22 January 2023. The terms searched included "Coronary Vessels," "Coronary Artery," "Plaque, Atherosclerotic," "Atherosclerotic Plaques," "Ezetimibe," and "randomized controlled trial." The detailed search strategy is shown in [Supplementary Material S1](#).

Two investigators conducted literature screening and full-text reading and then extracted the information required for this study independently.

According to the RCT risk of the bias assessment tool in the Cochrane Handbook for Systematic Reviews, two researchers assessed the methodological quality of the included literature from seven aspects: sequence generation, allocation concealment, blinding of participants and personnel, blinding of the outcome assessment, incomplete outcome data, selective outcome reporting, and other sources of bias. Each aspect was rated as "low risk," "unclear risk," or "high risk" based on the tool.

## 2.3 Statistical analysis

Statistical analysis was performed using Stata 14.0 (Stata Corporation, College Station, TX, USA) software. Continuous variables were analyzed using the weighted mean difference (WMD) as the pooled statistic, which described the 95% confidence interval (CI). Heterogeneity size was evaluated by the  $I^2$  value and  $p$ -value; if the inter-study statistical heterogeneity was less ( $I^2 \leq 50\%$  or  $p \geq 0.1$ ), the fixed-effect model was used; if the inter-study heterogeneity was significant ( $I^2 > 50\%$  or  $p < 0.1$ ), the random effect model was used. To check if there was publication bias, Egger's test was used and a funnel plot was generated.  $p < 0.05$  was considered statistically significant for the pooled effect. Finally, the TSA 0.9.5.10 Beta software was used to perform TSA analysis on the associated results.

# 3 Results

## 3.1 Search results, basic characteristics, and quality evaluation results of the included literature

A total of 194 relevant literature reports were obtained in the initial screening, after excluding the repeated literature, meta-analyses, reviews, animal tests, no RCTs, or no match research contents, and four RCTs were finally included (Tomas et al., 2012; Jung et al., 2016; Mikkel et al., 2017; Kiyoshi et al., 2018), which comprised 349 patients; the literature screening processes are shown in [Figure 1](#).



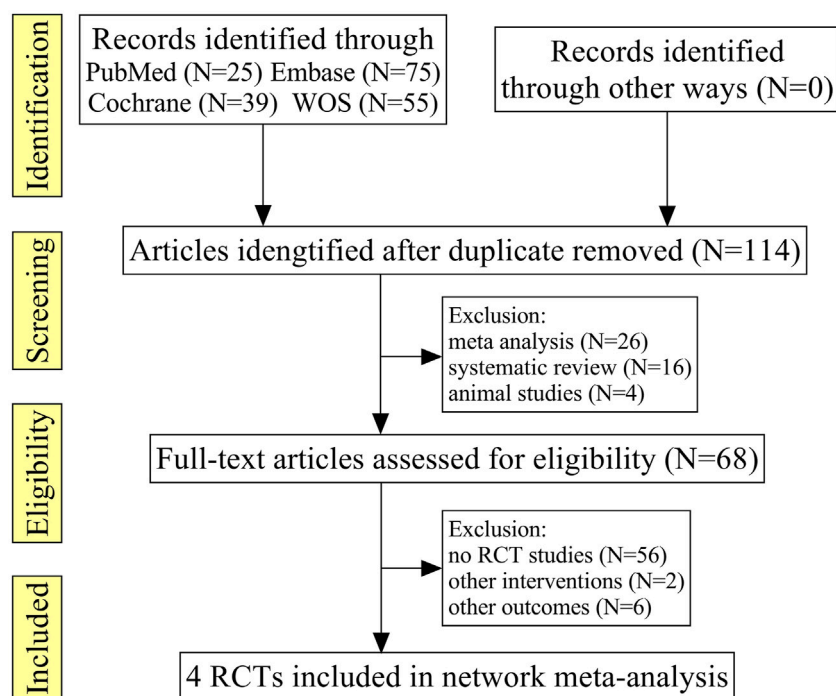


**FIGURE 1**  
PRISMA flowchart with details of the literature search and study selection.

**TABLE 1** Basic information for the included studies.

Number	Study (year)	Region/ country	Sample size	Male/ female	Age	Intervention		Duration	Endpoint
			T/C	T; C	T/C	T (mg/d)	C (mg/d)		
1	Kiyoshi H (2018)	Japan multicenter	50/53	41/9; 41/12	63 ± 10/63 ± 12	EZ (10) + PI (2)	PI (2)	10 months	①②④
2	Mikkel H (2016)	Denmark	43/44	39/4; 36/8	55.3 ± 11.0/ 57.2 ± 9.1	EZ (10) + AT (80)	PL (10) + AT (80)	12 months	①②③④
3	Jung-H L (2016)	Korea	34/36	27/7; 27/9	60.9 ± 10.9/ 59.3 ± 10.7	EZ (10) + SI (40)	PR (20)	03 months	①②③④
4	Tomas K (2012)	Czech	42/47	33/9; 31/16	63.5 ± 9.3/ 65.1 ± 10.6	EZ (10) + AT (80)	AT (10)	12 months	①②③④

T, treatment group; C, control group; EZ, ezetimibe; PI, pitavastatin; AT, atorvastatin; PL, placebo; SI, simvastatin; PR, pravastatin. Endpoints: ① fibro-fatty plaque (FFP, mm<sup>3</sup>); ② fibrous plaque (FP, mm<sup>3</sup>); ③ necrotic core (NC, mm<sup>3</sup>); ④ change dense calcification (change DC, mm<sup>3</sup>).

A multi-center research study was among the included research studies, which were primarily from Europe and Asia. The duration ranged from 3 to 12 months, and three of the studies were followed up for more than 10 months; the other basic characteristics are shown in Table 1.

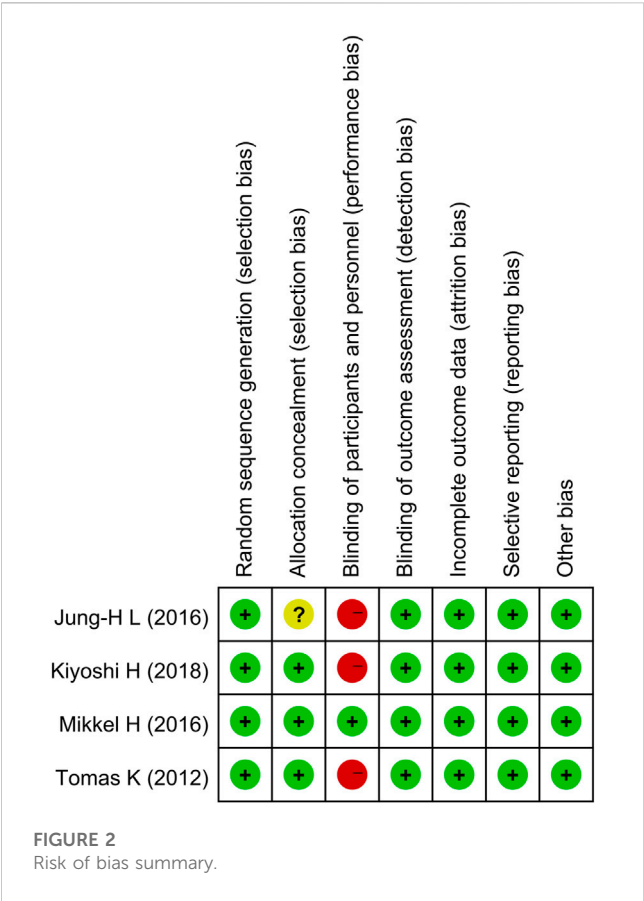
All four studies successfully described the random sequence generation method; however, one research's allocation concealment was not well explained. Three studies successfully completed single blinding of the outcome assessment, while one study successfully completed the double-blinded study. The data on all studies were complete. All studies specifically described the interventions and

outcome measures, as shown in Figure 2; Supplementary Material S2.

## 3.2 Meta-analysis

### 3.2.1 Fibro-fatty plaque (FFP) volume

All research studies reported the efficacy of FFP, involving a total of 349 patients. There was no heterogeneity among the studies ( $I^2 = 0\%$ ,  $p = 0.94$ ). Fixed-effects model analysis was carried out, and the result showed that compared with the control group, treatment



group intervention measures could effectively reduce FFP, and there was a statistically significant difference [WMD = -2.90, 95% CI (-4.79 and -1.00), and  $p = 0.003$ ], as shown in in [Figure 3](#).

3.2.2 Fibrous (FP) plaque volume

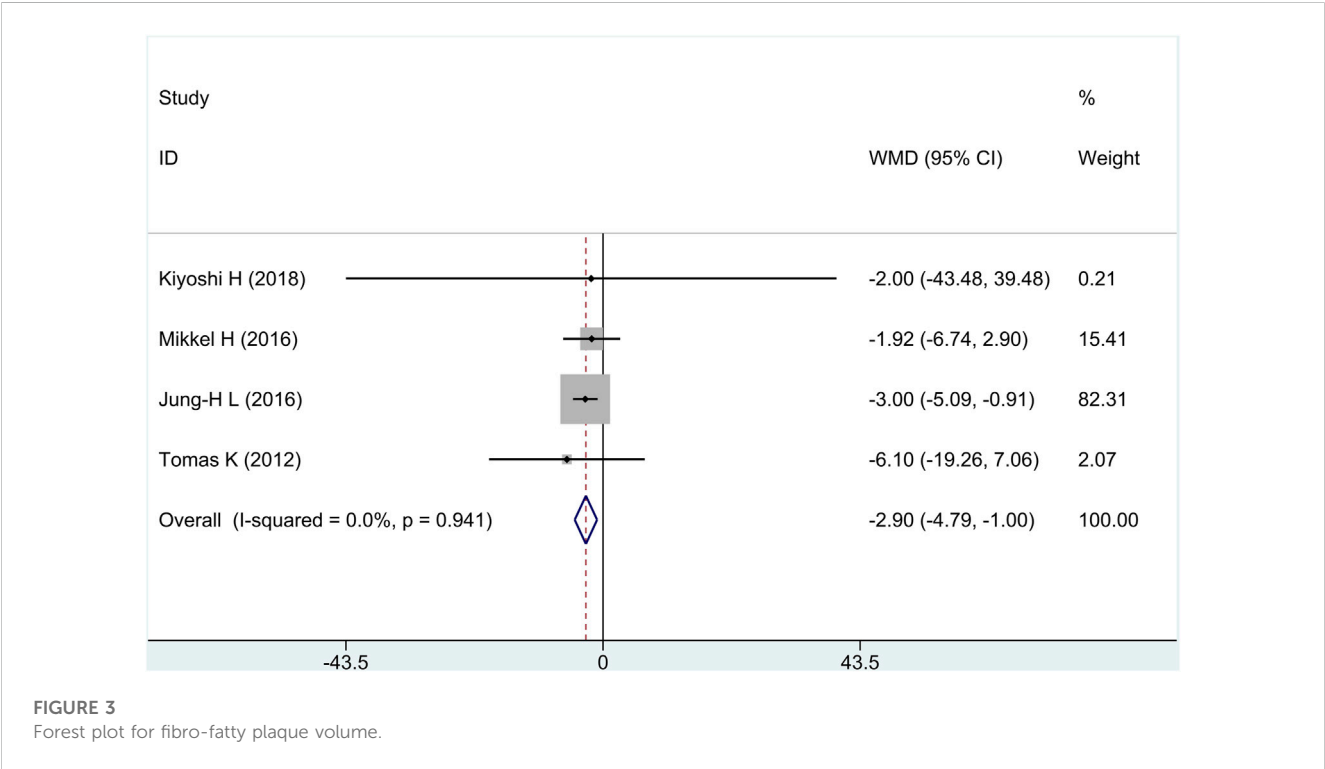
All research studies reported the efficacy of FP, involving a total of 349 patients. There was no heterogeneity among the studies ( $I^2 = 0\%$ ,  $p = 0.87$ ); fixed-effects model analysis was carried out, and the result showed that there was no significant difference in the reduction of FP between the treatment group and the control group [WMD = -4.92, 95% CI (-11.57 and 1.74), and  $p = 0.15$ ], as shown in [Figure 4](#).

3.2.3 Necrotic core (NC) volume

Three of the four research studies reported the efficacy of NC, involving a total of 246 patients. There was no heterogeneity among the studies ( $I^2 = 0\%$ ,  $p = 0.42$ ); fixed-effects model analysis was carried out, and the result showed that there was no significant difference in the reduction of NC between the treatment group and the control group [WMD = -2.26, 95% CI (-6.99 and 2.46), and  $p = 0.35$ ], as shown in [Figure 5](#).

3.2.4 Change dense calcification (change DC) volume

All research studies reported the efficacy of change DC, involving a total of 349 patients. There was no heterogeneity among the studies ( $I^2 = 0\%$ ,  $p = 0.63$ ); fixed-effects model analysis was carried out, and the result showed that there was no significant difference in the reduction of change DC between the treatment group and the control group [WMD = -0.07, 95% CI (-0.34 and 0.20), and  $p = 0.62$ ], as shown in [Figure 6](#).



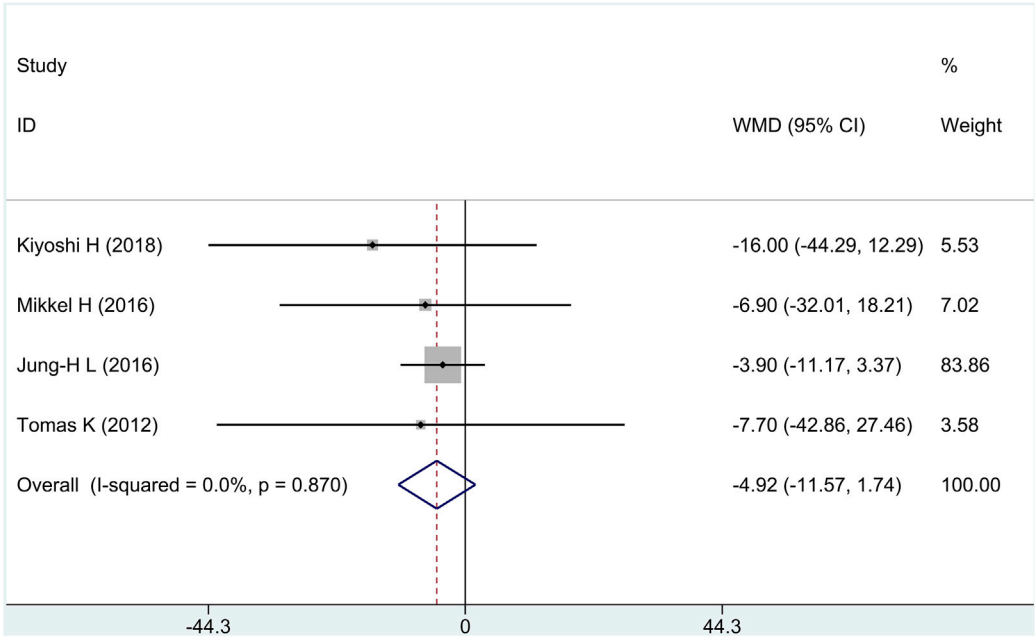


**FIGURE 4**  
Forest plot for fibrous plaque volume.

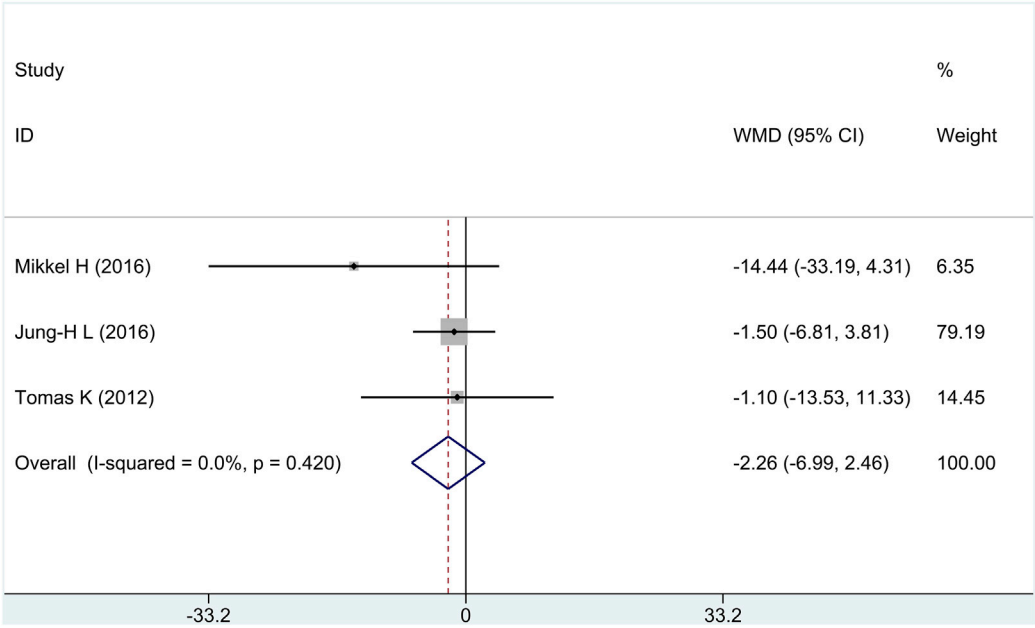


**FIGURE 5**  
Forest plot for necrotic core volume.

### 3.3 Subgroup analysis

We conducted subgroup analyses using patients' continents as the covariable since Asian and European patients had different genetic variables. The result showed that compared with the

control group, treatment group intervention measures could effectively reduce FFP in Asian patients; there was a statistically significant difference [WMD = -3.00, 95% CI (-5.08 and -0.91), and  $p = 0.005$ ], but there was no statistically significant difference [WMD = -2.41, 95% CI (-6.94, 2.11), and  $p = 0.296$ ] in European

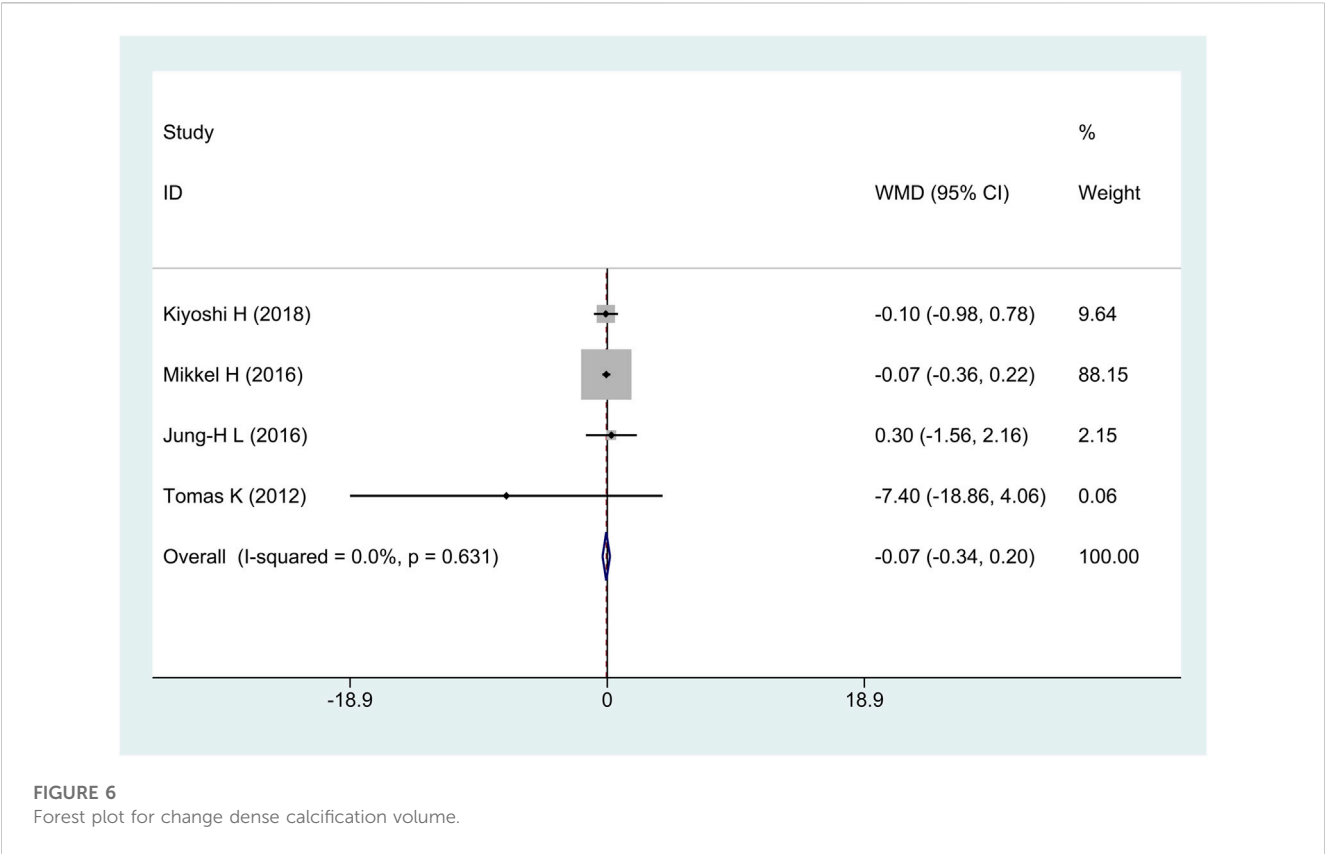


**FIGURE 6**  
Forest plot for change dense calcification volume.

**TABLE 2 Results of subgroup analysis.**

Endpoint	Asia/Europe	Number of studies	Heterogeneity		Effect model	Meta-analysis result		
			I <sup>2</sup> value (%)	p-value		WMD (95%CI)	Z-value	p-value
①	Asia	2	0.00	= 0.96	Fixed	-3.00 (-5.08, -0.91)	2.82	= 0.005
	Europe	2	0.00	= 0.56	Fixed	-2.41 (-6.94, 2.11)	1.05	= 0.296
②	Asia	2	0.00	= 0.42	Fixed	-4.65 (-11.69, 2.39)	1.29	= 0.196
	Europe	2	0.00	= 0.97	Fixed	-7.17 (-27.61, 13.27)	0.69	= 0.492
③	Asia	1	—	—	—	—	—	—
	Europe	2	26.0	= 0.25	Fixed	-5.17 (-15.53, 5.19)	0.98	= 0.328
④	Asia	2	0.00	= 0.70	Fixed	-0.03 (-0.82, 0.77)	0.07	= 0.947
	Europe	2	36.3	= 0.21	Fixed	-0.07 (-0.37, 0.22)	0.50	= 0.615

Endpoints: ① fibro-fatty plaque (FFP, mm<sup>3</sup>); ② fibrous plaque (FP, mm<sup>3</sup>); ③ necrotic core (NC, mm<sup>3</sup>); ④ change dense calcification (change DC, mm<sup>3</sup>). WMD, weighted mean difference.

patients. Between the treatment group and the control group, there was no statistically significant difference in the reduction of FP, NC, and change DC in Asian or European patients, as shown in Table 2.

### 3.4 Publication bias

Publication bias was performed for FP and NC. The findings demonstrated that Egger’s test results were  $p = 0.20 > 0.05$  and  $p =$

$0.47 > 0.05$ , respectively, and funnel plots were used, as shown in Figures 7A, B, indicating the little possibility of publication bias.

### 3.5 Trial sequential analysis

TSA were performed for FP and NC. The parameters were set as follows: boundary type was two-side, Type 1 Error  $\alpha = 5\%$ , Type 2 Error  $\beta = 20\%$ , and statistical power  $1-\beta = 80\%$ ; the information axis

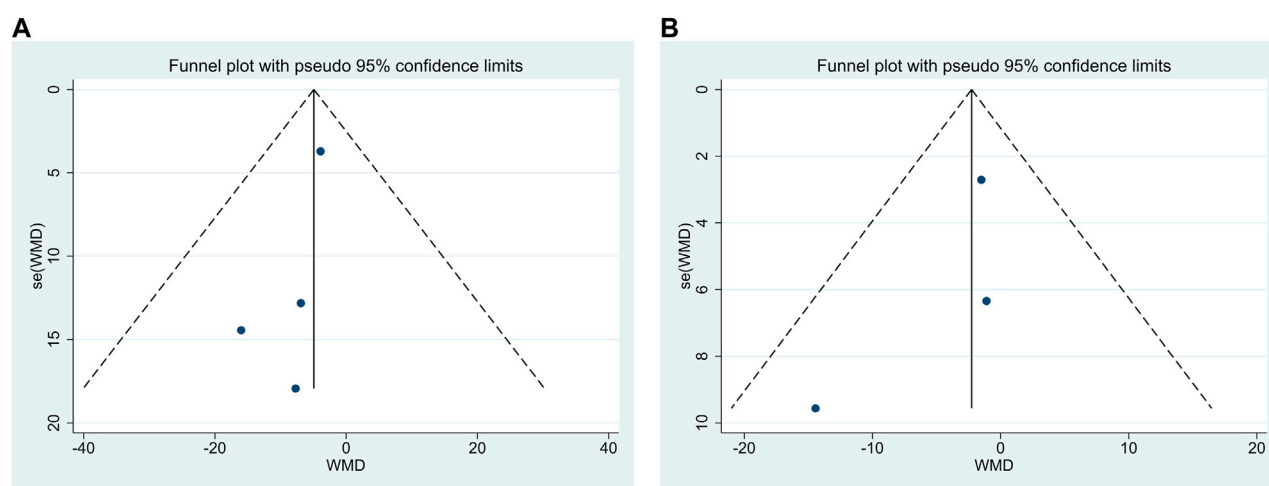


**FIGURE 7**  
Funnel plots for fibrous plaque volume (A) and necrotic core volume (B).

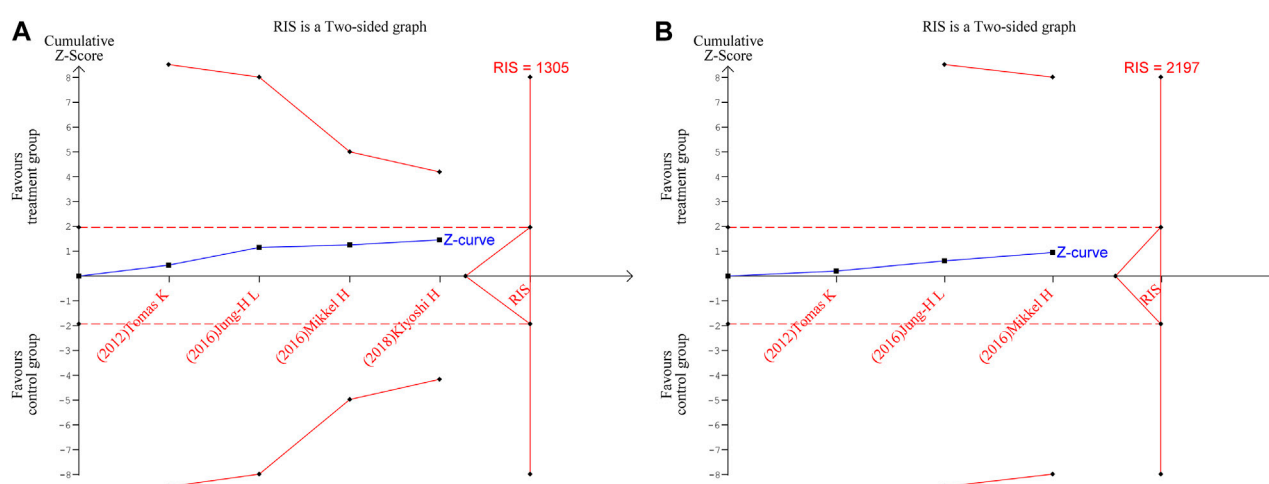


**FIGURE 8**  
Trial sequential analysis for fibrous plaque volume (A) and necrotic core volume (B).

was a sample size. The findings revealed that neither of the Z-curves crosses the traditional boundary values nor the TSA boundary values, and the accumulated information fell short of the required information size (RIS). Therefore, there was no statistically significant difference between the treatment group and the control group in terms of efficacy, and more studies are still required to confirm the efficacy in the future, as shown in Figures 8A, B.

## 4 Discussion

Since the endpoints were not published in the original publication as a mean  $\pm$  standard deviation (mean  $\pm$  SD), we converted data using the approach described by Luo et al. (2018). In terms of patients, acute coronary syndrome was studied in three

trials, and stable angina, in one trial. According to the meta-analysis, patient differences did not cause heterogeneity among studies; compared to the control group, ezetimibe significantly decreased FFP, but it had no statistically significant difference on FP, NC, and change DC. FP and NC did not show any statistically significant differences between the treatment group and the control group, according to TSA, and further research will be required to confirm the efficacy in the future.

According to previous studies, the volume of the compositions in coronary atherosclerotic plaques can be impacted by statins. For example, statins increased FP and decreased FFP, but no change in NC was seen (Nasu et al., 2009). Ezetimibe inhibits the absorption of cholesterol from the intestine by blocking the Niemann–Pick-like 1 receptor. The findings of our meta-analyses demonstrated that ezetimibe combined with statins reduced FFP more significantly



than statins alone; however, due to the limited sample size of the included trials, our study was inconclusive in terms of FP and NC, and TSA showed that further research is required. One of the included studies analyzed the whole investigated segment, and it is possible to infer that the changes in the worst segment are different from those in less affected parts of the vessel (Tomas et al., 2012). One study showed that in patients with ACS, additional reductions in LDL-C levels were associated with a reduction in cardiovascular events after ezetimibe combined with statin therapy compared with statins alone (Cannon et al., 2015). According to Newby (2005), both human and animal atherosclerotic plaques have higher levels of matrix metalloproteinase-9 (MMP-9), which can make plaque rupture more likely, resulting in thrombosis. According to Wang et al. (2016) findings, ezetimibe decreased the level of MMP-9. Additional research studies have demonstrated that a local high cholesterol concentration in foam cells can result in cholesterol crystal formation and localized inflammation (Duewell et al., 2010), inducing foam cell apoptosis and final formation of a lipid-rich necrotic core (Geng et al., 2003), while ezetimibe can reduce cholesterol crystal accumulation and plaque inflammation (Kataoka et al., 2015). These provide the basis for suggesting that ezetimibe may increase cardiovascular events due to plaque rupture and increase plaque stability.

According to Hong et al. (2009), statins had no significant effect on DC. The common occurrence of calcification in arteries, which mostly happens in the latter stages of atherosclerosis and has been linked to arterial degeneration and various metabolic diseases, has been thought of as a passive process (Otsuka et al., 2014; Jeevarethinam et al., 2017; Yahagi et al., 2017). According to a recent research study by Cho et al. (2018), both passive and active calcification processes are involved. We are unaware of any studies that demonstrate the ability of ezetimibe to inhibit both passive and active calcification processes, which may account for the lack of a statistically significant difference between the treatment group and the control group in terms of the change dense calcification volume. A study of 101 patients with coronary heart disease (CHD) by the Second Affiliated Hospital of Kunming Medical University (Qi et al., 2021) showed that the smaller the curvature and shallower the depth of dense calcification, the more prone they were to instability and rupture; curvature and depth are independent predictors of plaque rupture in patients with CHD. Future research studies on the effectiveness of ezetimibe on the curvature and depth of dense calcification might be carried out even though this study demonstrated that treatment measures in the treatment group and the control group had no statistical significance in the change dense calcification volume.

Lipid-lowering treatment is a first-line therapy for ACS; all of the included trials showed that the treatment and control groups can decrease total cholesterol (TC) and low-density lipoprotein (LDL) (Tomas et al., 2012; Jung et al., 2016; Mikkil et al., 2017; Kiyoshi et al., 2018), while only one study reported that the treatment group can increase high-density lipoprotein (HDL) (Kiyoshi et al., 2018).

## 5 Innovations and limitations

**Innovations:** As is known, this study is the first meta-analysis and trial sequential analysis to evaluate the efficacy of ezetimibe

on the volume of each coronary atherosclerotic plaque composition.

**Limitations:** Patients with acute coronary syndrome and stable angina made up the majority of the study population, and the pathophysiological mechanisms of the former and the latter were not completely consistent. There may have been some deviation in data conversion because the data from several studies were not presented as the mean  $\pm$  SD. Statins and their dose of four RCTs were different. A few inconclusive results show up as results of the limited sample size and the overall amount of literature; more high-quality randomized controlled trials can be conducted in the future.

## 6 Conclusion

This meta-analysis demonstrated that, compared to the control group, ezetimibe significantly decreased FFP, but it had no statistically significant difference on FP and NC; trial sequential analysis also showed that the meta-analysis results were inconclusive, and further research will be required to confirm the efficacy in the future. This meta-analysis showed that, compared to the control group, ezetimibe also had no statistically significant difference on change DC.

## Author contributions

BC and YS searched the literature, performed the statistical analysis, and wrote the manuscript. BC and XW extracted data. YS and YL revised the manuscript. All authors contributed to the article and approved the submitted version.

## Conflict of interest

The authors declare that the research was conducted in the absence of any commercial or financial relationships that could be construed as a potential conflict of interest.

## Publisher's note

All claims expressed in this article are solely those of the authors and do not necessarily represent those of their affiliated organizations, or those of the publisher, the editors, and the reviewers. Any product that may be evaluated in this article, or claim that may be made by its manufacturer, is not guaranteed or endorsed by the publisher.

## Supplementary material

The Supplementary Material for this article can be found online at: <https://www.frontiersin.org/articles/10.3389/fphar.2023.1166762/full#supplementary-material>

## References

- Cannon, C. P., Blazing, M. A., Giugliano, R. P., McCagg, A., White, J. A., Theroux, P., et al. (2015). Ezetimibe added to statin therapy after acute coronary syndromes. *N. Engl. J. Med.* 372, 2387–2397. doi:10.1056/NEJMoa1410489
- Cho, K. I., Sakuma, I., Sohn, I. S., Jo, S. H., and Koh, K. K. (2018). Inflammatory and metabolic mechanisms underlying the calcific aortic valve disease. *Atherosclerosis* 277, 60–65. doi:10.1016/j.atherosclerosis.2018.08.029
- Dawson, L. P., Lum, M., Nerleker, N., Nicholls, S. J., and Layland, J. (2022). Coronary atherosclerotic plaque regression: Jacc state-of-the-art review. *J. Am. Coll. Cardiol.* 79, 66–82. doi:10.1016/j.jacc.2021.10.035
- Duewell, P., Kono, H., Rayner, K. J., Sirois, C. M., Vladimer, G., Bauernfeind, F. G., et al. (2010). Nlrp3 inflammasomes are required for atherogenesis and activated by cholesterol crystals. *Nature* 464, 1357–1361. doi:10.1038/nature08938
- Falk, E., Nakano, M., Bentzon, J. F., Finn, A. V., and Virmani, R. (2013). Update on acute coronary syndromes: The pathologists' view. *Eur. Heart J.* 34, 719–728. doi:10.1093/eurheartj/ehs411
- Geng, Y. J., Phillips, J. E., Mason, R. P., and Casscells, S. W. (2003). Cholesterol crystallization and macrophage apoptosis: Implication for atherosclerotic plaque instability and rupture. *Biochem. Pharmacol.* 66, 1485–1492. doi:10.1016/s0006-2952(03)00502-1
- Grundey, S. M., Stone, N. J., Bailey, A. L., Beam, C., Birtcher, K. K., Blumenthal, R. S., et al. (2019). 2018 AHA/ACC/AACVPR/AAPA/ABC/ACPM/ADA/AGS/APhA/ASPC/NLA/PCNA guideline on the management of blood cholesterol: A report of the American college of cardiology/American heart association task force on clinical practice guidelines. *Circulation* 139, e1082–e1143. doi:10.1161/CIR.0000000000000625
- Hong, M. K., Park, D. W., Lee, C. W., Lee, S. W., Kim, Y. H., Kang, D. H., et al. (2009). Effects of statin treatments on coronary plaques assessed by volumetric virtual histology intravascular ultrasound analysis. *Jacc Cardiovasc Interv.* 2, 679–688. doi:10.1016/j.jcin.2009.03.015
- Jeevarethinam, A., Venuraju, S., Dumo, A., Ruano, S., Mehta, V. S., Rosenthal, M., et al. (2017). Relationship between carotid atherosclerosis and coronary artery calcification in asymptomatic diabetic patients: A prospective multicenter study. *Clin. Cardiol.* 40, 752–758. doi:10.1002/clc.22727
- Jung, -H. L., Shin, D. H., Kim, B. K., Ko, Y. G., Choi, D., Jang, Y., et al. (2016). Early effects of intensive lipid-lowering treatment on plaque characteristics assessed by virtual histology intravascular ultrasound. *Yonsei Med. J.* 57, 1087–1094. doi:10.3349/ymj.2016.57.5.1087
- Kataoka, Y., Puri, R., Hammadah, M., Duggal, B., Uno, K., Kapadia, S. R., et al. (2015). Cholesterol crystals associate with coronary plaque vulnerability *in vivo*. *J. Am. Coll. Cardiol.* 65, 630–632. doi:10.1016/j.jacc.2014.11.039
- Kiyoshi, H., Sonoda, S., Kawasaki, M., Otsuji, Y., Murohara, T., Ishii, H., et al. (2018). Effects of ezetimibe-statin combination therapy on coronary atherosclerosis in acute coronary syndrome. *Circ. J.* 82, 757–766. doi:10.1253/circj.CJ-17-0598
- Luo, D., Wan, X., Liu, J., and Tong, T. (2018). Optimally estimating the sample mean from the sample size, median, mid-range, and/or mid-quartile range. *Stat. Methods Med. Res.* 27, 1785–1805. doi:10.1177/0962280216669183
- Mach, F., Baigent, C., Catapano, A. L., Koskinas, K. C., Casula, M., Badimon, L., et al. (2020). 2019 esc/eas guidelines for the management of dyslipidaemias: Lipid modification to reduce cardiovascular risk. *Eur. Heart J.* 41, 111–188. doi:10.1093/eurheartj/ehz455
- Mikkel, H., Hansen, H. S., Thayssen, P., Antonsen, L., Junker, A., Veien, K., et al. (2017). Influence of ezetimibe in addition to high-dose atorvastatin therapy on plaque composition in patients with st-segment elevation myocardial infarction assessed by serial: Intravascular ultrasound with imap: The octivus trial. *Cardiovasc. Revasc. Med.* 18, 110–117. doi:10.1016/j.carrev.2016.11.010
- Mintz, G. (2001). American college of cardiology clinical expert consensus document on standards for acquisition, measurement and reporting of intravascular ultrasound studies (ivus). A report of the American college of cardiology task force on clinical expert consensus documents developed in collaboration with the European society of cardiology endorsed by the society of cardiac angiography and interventions. *Eur. J. Echocardiogr.* 2, 299–313. doi:10.1053/euje.2001.0133
- Nasu, K., Tsuchikane, E., Katoh, O., Tanaka, N., Kimura, M., Ehara, M., et al. (2009). Effect of fluvastatin on progression of coronary atherosclerotic plaque evaluated by virtual histology intravascular ultrasound. *Jacc Cardiovasc Interv.* 2, 689–696. doi:10.1016/j.jcin.2009.04.016
- Newby, A. C. (2005). Dual role of matrix metalloproteinases (matrixins) in intimal thickening and atherosclerotic plaque rupture. *Physiol. Rev.* 85, 1–31. doi:10.1152/physrev.00048.2003
- Otsuka, F., Sakakura, K., Yahagi, K., Joner, M., and Virmani, R. (2014). Has our understanding of calcification in human coronary atherosclerosis progressed? *Arterioscler. Thromb. Vasc. Biol.* 34, 724–736. doi:10.1161/ATVBAHA.113.302642
- Page, M. J., McKenzie, J. E., Bossuyt, P. M., Boutron, I., Hoffmann, T. C., Mulrow, C. D., et al. (2021). The prisma 2020 statement: An updated guideline for reporting systematic reviews. *Syst. Rev.* 10, 89. doi:10.1186/s13643-021-01626-4
- Qi, Z., Jikun, D., Fan, Y., Zhi, L., Hua, G., and Lin, S. (2021). Relationship between spotty calcification and plaque stability in patients with coronary heart disease: an optical coherence tomography study. *J. Clin. Cardiol.* 37, 1117–1120. doi:10.13201/j.issn.1001-1439.2021.12.010
- Tomas, K., Mintz, G. S., Skalicka, H., Kral, A., Horak, J., Skulec, R., et al. (2012). Virtual histology evaluation of atherosclerosis regression during atorvastatin and ezetimibe administration: Heaven study. *Circ. J.* 76, 176–183. doi:10.1253/circj.cj-11-0730
- Ueda, Y., Hiro, T., Hirayama, A., Komatsu, S., Matsuoka, H., Takayama, T., et al. (2017). Effect of ezetimibe on stabilization and regression of intracoronary plaque - the zipangu study. *Circ. J.* 81, 1611–1619. doi:10.1253/circj.CJ-17-0193
- Wang, X., Zhao, X., Li, L., Yao, H., Jiang, Y., and Zhang, J. (2016). Effects of combination of ezetimibe and rosuvastatin on coronary artery plaque in patients with coronary heart disease. *Heart Lung Circ.* 25, 459–465. doi:10.1016/j.hlc.2015.10.012
- Yahagi, K., Kolodgie, F. D., Lutter, C., Mori, H., Romero, M. E., Finn, A. V., et al. (2017). Pathology of human coronary and carotid artery atherosclerosis and vascular calcification in diabetes mellitus. *Arterioscler. Thromb. Vasc. Biol.* 37, 191–204. doi:10.1161/ATVBAHA.116.306256



## OPEN ACCESS

## EDITED BY

Xianwei Wang,  
Xinxiang Medical University, China

## REVIEWED BY

Sho Torii,  
Tokai University Isehara Hospital, Japan  
Anargyros Moulas,  
University of Thessaly, Greece  
Zhong Chen,  
Shanghai Jiao Tong University, China

## \*CORRESPONDENCE

Zhenjiang Liu,  
✉ zhenjliu@csu.edu.cn

RECEIVED 06 February 2023

ACCEPTED 20 April 2023

PUBLISHED 17 May 2023

## CITATION

Teng S, Zhu Z, Li Y, Hu X, Fang Z, Liu Z and Zhou S (2023). A novel glycyrrhizin acid-coated stent reduces neointimal formation in a rabbit iliac artery model. *Front. Pharmacol.* 14:1159779. doi: 10.3389/fphar.2023.1159779

## COPYRIGHT

© 2023 Teng, Zhu, Li, Hu, Fang, Liu and Zhou. This is an open-access article distributed under the terms of the [Creative Commons Attribution License \(CC BY\)](https://creativecommons.org/licenses/by/4.0/). The use, distribution or reproduction in other forums is permitted, provided the original author(s) and the copyright owner(s) are credited and that the original publication in this journal is cited, in accordance with accepted academic practice. No use, distribution or reproduction is permitted which does not comply with these terms.

# A novel glycyrrhizin acid-coated stent reduces neointimal formation in a rabbit iliac artery model

Shuai Teng<sup>1</sup>, Zhaowei Zhu<sup>1</sup>, Yang Li<sup>2</sup>, Xinqun Hu<sup>1</sup>, Zhenfei Fang<sup>1</sup>, Zhenjiang Liu<sup>1\*</sup> and Shenghua Zhou<sup>1</sup>

<sup>1</sup>Department of Cardiovascular Medicine, the Second Xiangya Hospital, Central South University, Changsha, Hunan, China, <sup>2</sup>Department of Vascular Surgery, Xiamen Cardiovascular Hospital, Xiamen University, Xiamen, Fujian, China

**Introduction:** Most drug-eluting stents (DESs) inhibit intimal hyperplasia but impair re-endothelialization. This study aimed to evaluate *in vivo* strut coverage and neointimal growth in a new glycyrrhizin acid (GA)-eluting stent.

**Methods:** New Zealand White rabbits ( $n = 20$ ) with atherosclerotic plaques were randomly divided into three groups based on implanted iliac artery stents: bare-metal stents (BMSs), rapamycin-eluting stents, and GA-eluting stents. After the *in vivo* intravascular ultrasound (IVUS) assessment at 28 days, the vessels were harvested for scanning electron microscopy (SEM) and histology. After 4 weeks of follow-up, the stent and external elastic lamina (EEL) areas were compared among the groups.

**Results:** The rapamycin- or GA-eluting stents significantly reduced the neointimal area compared with BMSs, though GA-eluting stents had the lowest reduction. There were more uncovered struts for rapamycin-eluting stents than those for GA-eluting stents and bare-metal stents. The endothelial nitric oxide synthase (eNOS) expression in GA-eluting stents was much higher than that in BMSs and rapamycin-eluting stents, even though the endothelial coverage between struts was equivalent between BMSs and GA-eluting stents. Moreover, GA-eluting stents markedly promoted re-endothelialization and improved arterial healing compared to rapamycin-eluting stents in a rabbit atherosclerotic model.

**Conclusion:** In conclusion, the novel GA-coated stent used in this study inhibited intimal hyperplasia and promoted re-endothelialization.

## KEYWORDS

drug-eluting stents, glycyrrhizin acid, intimal hyperplasia, eNOS, re-endothelialization

## 1 Introduction

Coronary artery disease is the most prevalent type of heart disease and the primary cause of mortality in developed and developing countries (Sanchis-Gomar et al., 2016). The increasing use of percutaneous coronary interventions (PCIs) or stents has improved the prognosis of patients with coronary artery disease and acute coronary syndrome (Dudek et al., 2019).

After years of investigation, two important pathological processes have been identified after stent deployment: intimal hyperplasia and re-endothelialization, which are mainly driven by smooth muscles and endothelial cells, respectively (Van Belle et al., 1997). Since

smooth muscle cell proliferation is triggered by sterile inflammation and foreign body reactions, intimal hyperplasia clinically leads to lumen loss or in-stent restenosis (Van Belle et al., 1997; Chaabane et al., 2013). However, re-endothelialization is the process of covering the surface of a stent with endothelial cells, thus protecting it from thrombus formation. Restenosis and stent thrombosis are associated with adverse clinical outcomes after stent application (Lu et al., 2016).

Although the application of drug-eluting stents (DESs) has greatly reduced the rate of restenosis compared to bare-metal stents (BMSs), the rate of restenosis remains high (Giustino et al., 2022). Drugs that elute off-current DESs, including sirolimus, paclitaxel, everolimus, and zotarolimus, have strong antiproliferative effects but lack cellular specificity, resulting in delayed re-endothelialization and endothelial dysfunction, which is linked to stent thrombosis (Xu et al., 2022). Owing to inadequate endothelial healing, late stent-associated thrombosis may develop following DES implantation, despite the regular use of extended dual antiplatelet therapy (Finn et al., 2007).

Even in advanced generations, most DESs are not designed with a focus on resolving re-endothelialization and endothelial dysfunction. Our previous study indicated that glycyrrhizin acid (GA) could protect against endothelium-dependent relaxation in an animal model of diabetes (Zhu et al., 2020a) and attenuate neointimal formation by inhibiting HMGB1 in a rabbit vascular injury model (Zhu et al., 2020b). Therefore, this study aimed to investigate the anti-restenotic and anti-inflammatory properties of GA-eluting stents in a rabbit model of atherosclerosis using intravascular ultrasound (IVUS) after stent implantation.

## 2 Materials and methods

### 2.1 Induction and identification of atherosclerosis

All animal experiments were approved by the Animal Care and Use Committee of Central South University. A total of 20 adult male New Zealand White rabbits (3 months old, 3.0–3.5 kg) were purchased from the Shanghai Animal Administration Center (Shanghai, China). For the first 4 weeks of the trial, all rabbits were fed with a high-cholesterol diet (purified rabbit chow supplemented with 1% cholesterol and 6% peanut oil; SLACCAS, Shanghai, China), followed by a low-cholesterol diet (0.025%) for the remaining time (i.e., 4 weeks after stent implantation).

Oil Red O staining was performed to detect vascular atherosclerosis. Vascular sections were rinsed with 60% isopropanol (5 min), stained with 0.5% Oil Red O/60% (20°C, 10 min), destained for 2 min, and thoroughly washed with distilled water. The images were acquired using a microscope (ZEISS).

### 2.2 Construction of the DESs

GA-eluting stents were prepared by coating a cobalt–chromium alloy stent (APT Medical Company, China) with a monolithic matrix of polyvinylidene fluoride-co-hexafluoropropylene and a GA base. The GA-eluting stents were 15 mm long and 2.50 mm in diameter, with a strut thickness of 88  $\mu$ m and a polymer layer

thickness of 5–20  $\mu$ m on the wire. Polyvinylidene fluoride-co-hexafluoropropylene and GA were sequentially dissolved and mixed in acetone to form a coating polymer, and the stents were coated using ultrasonic spraying equipment. Subsequently, the stent underwent a 10-min air-drying process to eliminate acetone completely. Each coated stent contained 100  $\mu$ g of GA. The integrity and homogeneity of the coated stents were evaluated using a stereomicroscope under white light before and after balloon catheter inflation. This polymer coating does not crack or flake during stent expansion and has been used in other DESs (Kamberi et al., 2018). After the stent was attached to the angioplasty balloon, it was sanitized using the ethylene oxide gas method and aseptically enclosed.

The kinetics of GA elution from polymer-coated scaffolds that had undergone sterilization were assessed *in vitro*. The GA-eluting stent was immersed in phosphate-buffered saline (pH 7.4) in an Eppendorf tube and shaken in a horizontal shaker at 50 rpm, at 37°C. The stents were removed at a set time, a certain amount of acetonitrile was added to the tube and left to stratify, and the supernatant was collected, filtered, and tested by UV spectroscopy at 258 nm. During *in vitro* elution of GA-eluting stents, the GA-eluting stents released 60% of its total GA amount by day 1 and 88% by day 13 (Supplementary Figure S1). Moreover, bare-metal stents (APT Medical Company, China) of the same size and commercially available rapamycin-eluting stents (Partner durable-polymer SES; Lepu Medical Technology, China) were used.

### 2.3 Stent placement, harvest, and preparation

General anesthesia (sodium pentobarbital; 100 mg/kg IV) was administered to the rabbits. A median neck incision was made, and a 5F vascular sheath was placed in the left carotid artery. After the administration of heparin (100 IU/kg), aortography and bilateral iliac angiography were performed. The rabbits ( $n = 20$ ) were randomly divided into three groups as follows: bare-metal stents (BMS group,  $n = 6$ ), rapamycin-eluting stents (rapamycin group,  $n = 6$ ), and GA-eluting stents (GA group,  $n = 8$ ). The operators were unaware of the group assignments, and the stents looked similar. A balloon-to-artery ratio of approximately 1.2:1 was achieved by manually crimping each stent onto a 2.5-mm angioplasty balloon before deploying it in the proximal bilateral iliac artery with 8-atm balloon inflation for 30 s. Aspirin (40 mg) was administered orally to the rabbits 2 days before surgery and thereafter (Nakazawa et al., 2016). Euthanasia was performed 4 weeks after stent deployment, followed by harvesting. The same type of stent was implanted in both iliac arteries of the rabbits, one for scanning electron microscopy (SEM) and the other for histological and immunostaining analyses.

### 2.4 SEM and morphometric analyses

The luminal surfaces of the stented iliac arteries were exposed by longitudinally severing them in half. Frontal SEM images of half of the stent were taken at low power ( $\times 15$  magnification) to evaluate neointimal development throughout the luminal stent surface visually. The percentage of endothelial coverage was visually evaluated after the images were gradually enlarged ( $\times 600$ ).



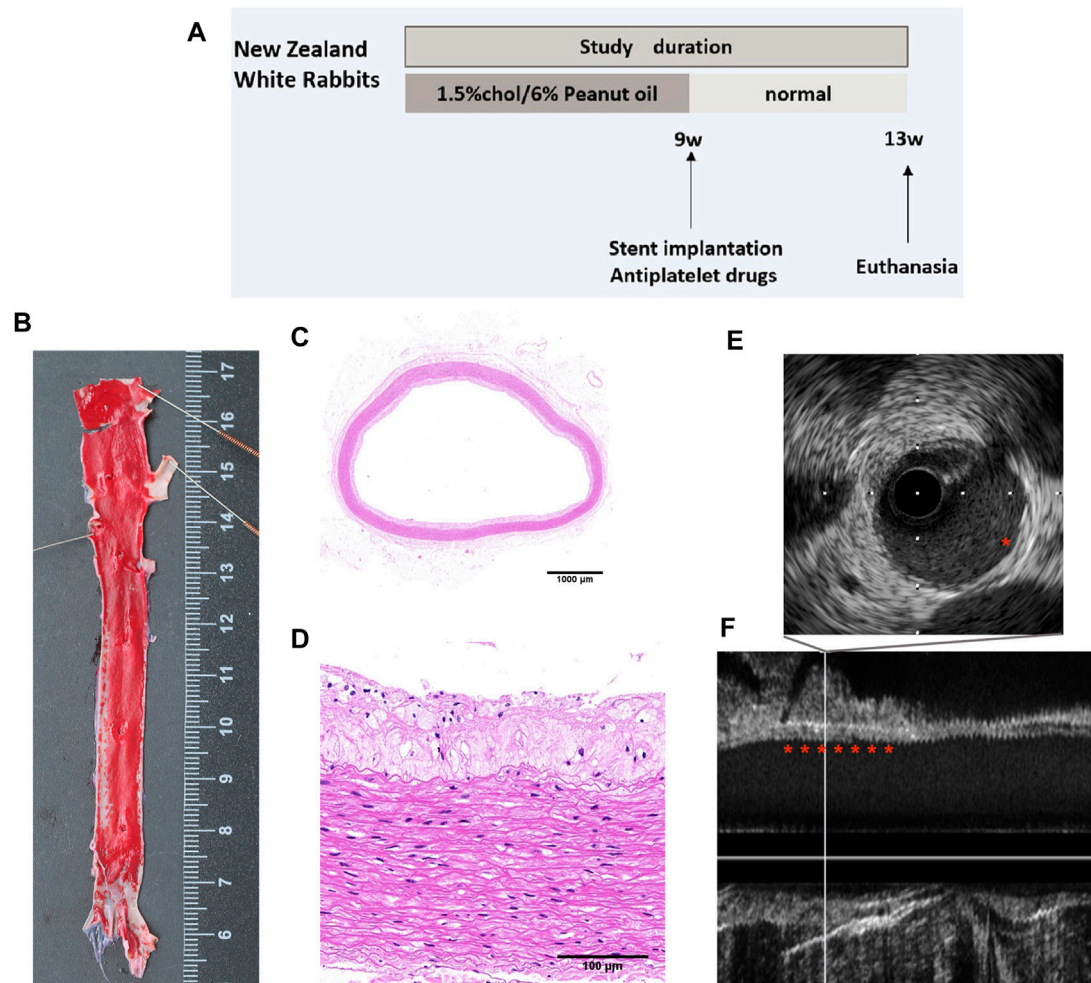


FIGURE 1

Atherosclerosis model of rabbits. (A) Study flow for the induction of atherosclerosis in rabbits. (B) Oil Red O staining of the iliofemoral artery. Representative cross-sectional images of H&E-stained iliofemoral arteries at (C) low- (x1) and (D) higher-power (x20) magnifications. (E) Cross-sectional images and (F) longitudinal view of IVUS images showing the atherosclerotic aorta.

## 2.5 Histological analysis of neointimal hyperplasia

The stented sections were stained with hematoxylin and eosin. The external elastic lamina (EEL; mm<sup>2</sup>), internal elastic lamina (IEL; mm<sup>2</sup>), and lumen area (LA; mm<sup>2</sup>) were measured using an imaging analysis system (Imagine-Pro Plus). Moreover, the following formulas were used to calculate the neointimal area (NA; mm<sup>2</sup>) and percentage of stenosis:  $NA = (IEL \rightarrow LA)$  and percentage stenosis (%) =  $[(IEL \rightarrow LA)/IEL \times 100]$ .

## 2.6 Endothelial nitric oxide synthase immunostaining

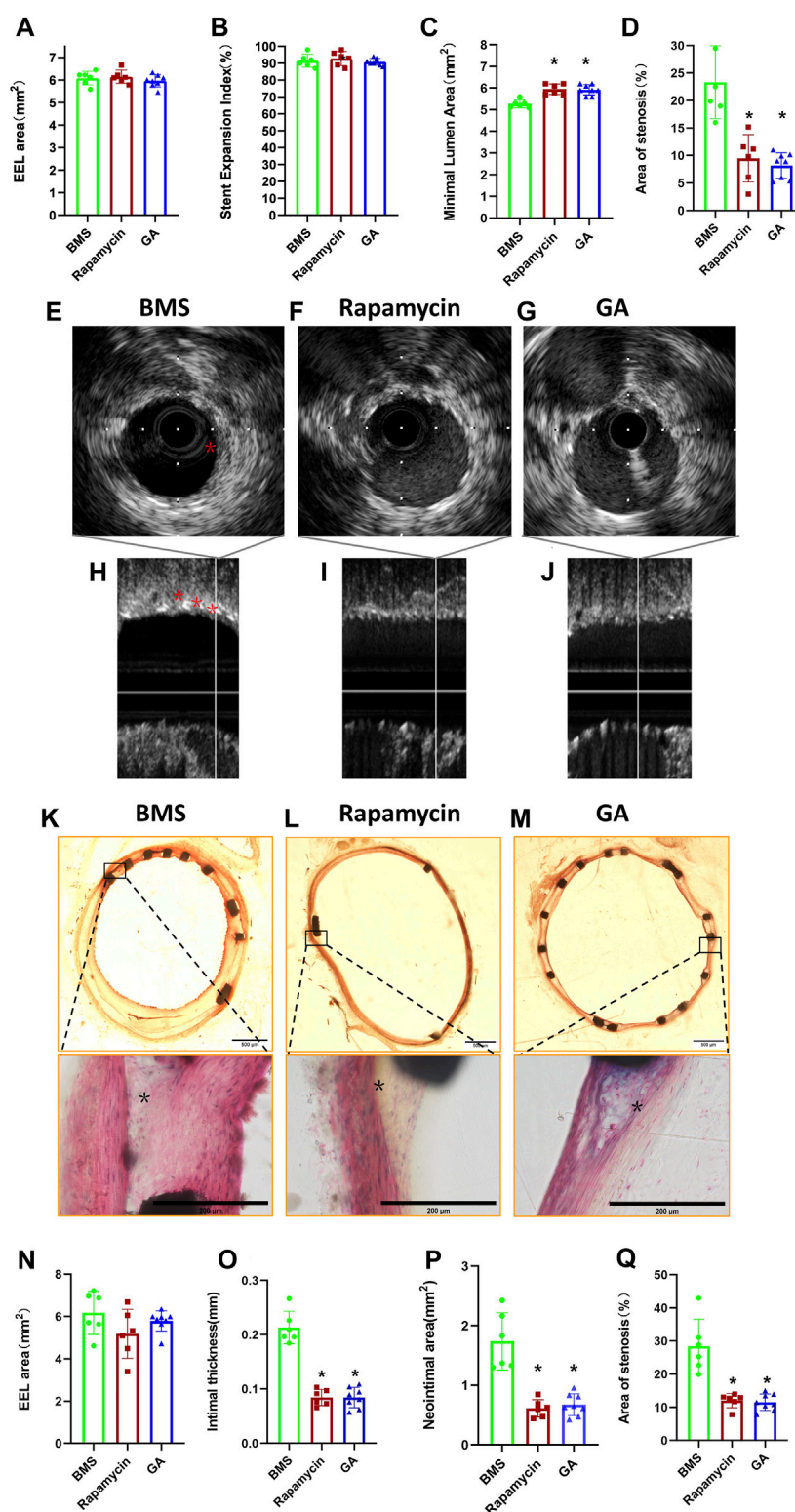
The longitudinally dissected half of the stent was dissected under a low-power (x10 magnification) microscope to separate the hyperplastic endothelium covering the stent struts. The dissected stent was fixed, paraffin-embedded, and sliced into sections (5 μm thick). After overnight incubation with eNOS antibody markers (1:100; BD

Biosciences, CA, United States), the paraffin-embedded slides were incubated with the secondary antibody donkey anti-mouse Alexa Fluor 488 (1:150 dilution; Invitrogen Corp., Carlsbad, California). The nuclei were counterstained with DAPI. The images were captured using an IX73 fluorescence microscope (Olympus, Tokyo, Japan).

## 2.7 In vivo evaluation by IVUS after 28 days

IVUS was conducted as described previously (Cui et al., 2017). We used a 40-MHz 2.9 Fr sheath-based catheter (Atlantis, SR Pro, Boston Scientific) and IVUS (iLAB™ Ultrasound Imaging System, Boston Scientific, Natick, MA, United States). The IVUS catheter was positioned 10 mm distal to the stent, and imaging was subsequently performed back to a point 10 mm proximal to the treated section using an automated transducer pullback at 0.5 mm/s. The scaffold area, minimal lumen area, intrascaffold neointimal area, and vessel area (area in the vessel's EEL) were measured. The stent



**FIGURE 2**

IVUS and histological analyses of restenosis of BMSs, rapamycin-eluting stents, and GA-eluting stents post 28 days of implantation. (A) EEL area, (B) stent expansion index, (C) minimum lumen area, and (D) stenosis area for BMSs, rapamycin-eluting stents, and GA-eluting stents evaluated by IVUS.  $n = 6-8$ . \*  $p < 0.05$  vs. BMSs. Cross-sectional images and longitudinal views of IVUS images of the representative cases of BMSs (E, H), rapamycin-eluting stents (F, I), and GA-eluting stents (J, G) (\* atherosclerotic plaques). Representative cross-sectional images of low- (x2) and high-magnification (x40) hematoxylin-eosin staining of BMSs (K), rapamycin-eluting stents (L), and GA-eluting stents (M) in atherosclerotic rabbit iliofemoral arteries (\* atherosclerotic plaques). (N) EEL area, (O) intimal thickness, (P) neointimal area, and (Q) area of stenosis assessed by histological analysis.

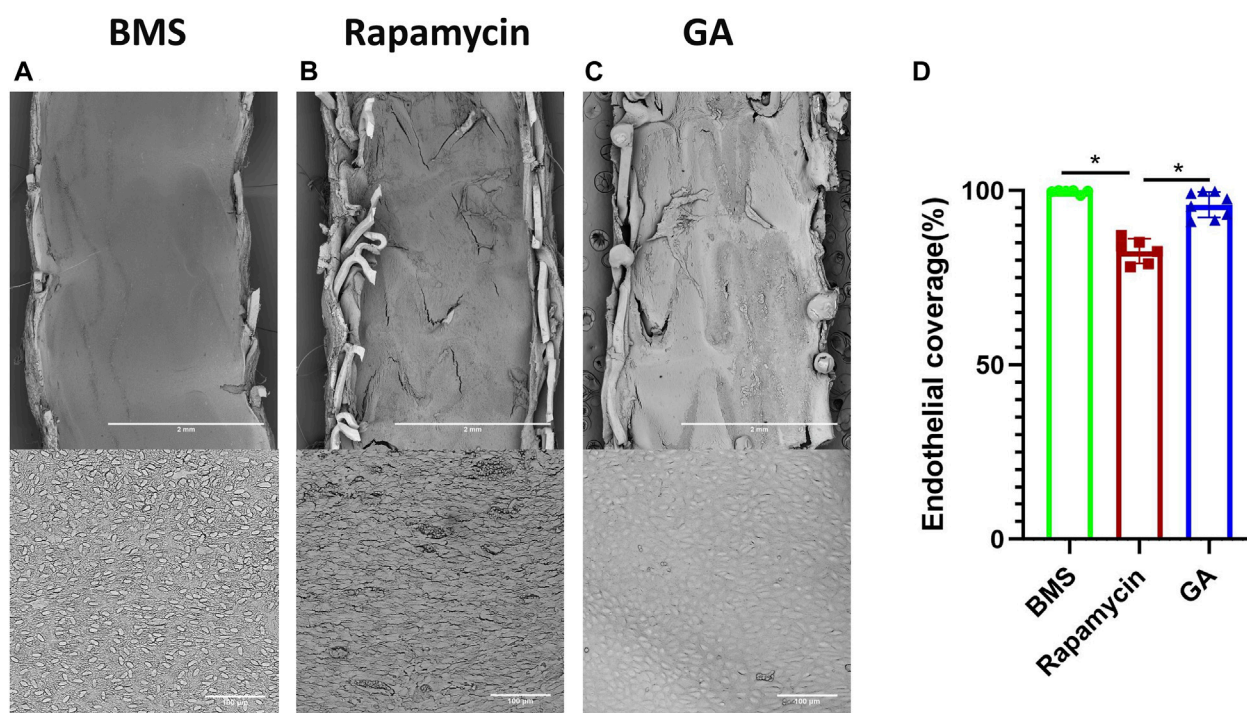


**FIGURE 3**

SEM and quantitative analysis of 28-day rabbit iliac artery stent implants. (A–C) Representative SEM images of 28-day BMSs and comparator DESs implanted in the atherosclerotic rabbit iliofemoral artery (at  $\times 15$  magnification), whereas the corresponding higher-power images ( $\times 600$  magnification) from each stent are shown underneath. (D) Quantitative analysis of endothelial coverage of different stents.  $n = 6-8$ . \*  $p < 0.05$ .

expansion index and percentage of lumen area stenosis were calculated according to the following formulas: stent expansion index =  $([\text{actual lumen area}/\text{ideal lumen area}] \times 100)$  and percentage of lumen area stenosis =  $([\text{mean lumen intrascaffold area} \rightarrow \text{the lumen area}]/\text{mean lumen intrascaffold area} \times 100)$ .

## 2.8 Statistical analyses

All results are expressed as means  $\pm$  standard error. Statistical analyses were performed using Student's *t*-test or analysis of variance (ANOVA)/Dunnett's *t*-test of variance. All analyses were performed using GraphPad Prism 8.0 (GraphPad Software Inc., San Diego, CA, United States of America), and a *p*-value  $< 0.05$  (two-sided) was considered to be significant.

## 3 Results

### 3.1 Confirmation of atherosclerosis of the artery

Figure 1A shows a schematic representation of the experimental setup. Oil Red O staining was performed to confirm the success of the rabbit atherosclerosis model. Following Oil Red O staining, atherosclerotic lesions were grossly observed in the aortas of rabbits (Figure 1B). The lesions were sporadically present throughout the iliac

artery, as confirmed by hematoxylin and eosin staining of the aorta cross section (Figures 1C, D). Additionally, *in vivo* IVUS showed a mild plaque burden throughout the iliac artery (Figures 1E, F).

### 3.2 Morphometric measurements and histological observations

To clarify the extent of restenosis in different stents, we first examined iliac stents using IVUS before animal euthanasia. As shown in Figure 2, there were no significant differences in the EEL area (Figure 2A) and stent expansion index (Figure 2B) among groups ( $6.09 \pm 0.31 \text{ mm}^2$  and  $91.5\% \pm 3.8\%$  for the BMS group,  $6.15 \pm 0.29 \text{ mm}^2$  and  $92.8\% \pm 4.2\%$  for the rapamycin group, and  $5.97 \pm 0.27 \text{ mm}^2$  and  $90.9\% \pm 2.0\%$  for the GA group;  $p > 0.05$ ). However, the results showed that the minimal lumen area of rapamycin-eluting stent and GA-eluting stent groups was significantly larger than that of the bare-metal stent group ( $5.95 \pm 0.24 \text{ mm}^2$  vs.  $5.27 \pm 0.18 \text{ mm}^2$ ;  $5.93 \pm 0.24 \text{ mm}^2$  vs.  $5.27 \pm 0.18 \text{ mm}^2$ , respectively;  $p < 0.05$ ) (Figure 2C). In addition, the mean stenosis of rapamycin-eluting stent and GA-eluting stent groups was also significantly lesser than that of the bare-metal stent group ( $12.0\% \pm 2.2\%$  vs.  $28.5\% \pm 8.2\%$ ;  $11.5\% \pm 2.5\%$  vs.  $28.5\% \pm 8.2\%$ , respectively;  $p < 0.05$ ) (Figure 2D). There were no differences in the minimal lumen area or mean stenosis between the rapamycin- and GA-eluting stent groups.

Consistent with the IVUS results, histological observations showed that there were no significant differences in the EEL area (Figure 2N) among groups ( $6.51 \pm 0.47 \text{ mm}^2$ ,  $6.39 \pm 0.27 \text{ mm}^2$ , and  $6.22 \pm 0.35 \text{ mm}^2$ ,

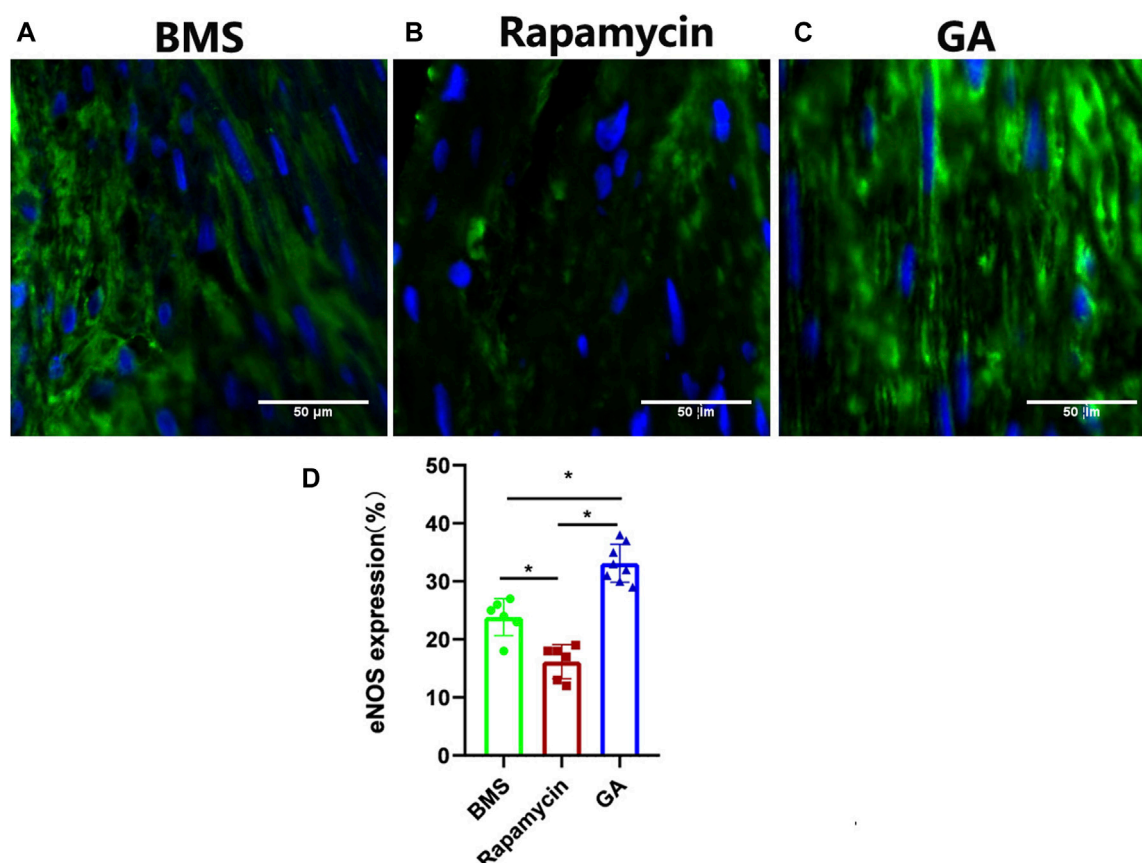


**FIGURE 4**

Representative images of eNOS immunofluorescence staining of 28-day stents implanted in the iliofemoral arteries of atherosclerotic rabbits. (A) BMSs, (B) rapamycin-eluting stents, and (C) GA-eluting stents. Images of eNOS showing reduced staining in comparator DESs relative to BMSs (green channel, eNOS; blue channel, nuclear counterstain magnification  $\times 200$ ). (D) Statistical analysis of eNOS expression in different stents.  $n = 6-8$ . \*  $p < 0.05$ .

respectively;  $p > 0.05$ ). Both GA- and rapamycin-eluting stents reduced neointimal thickness compared with bare-metal stents (Figure 2Q;  $p < 0.05$ ). Most importantly, compared with the bare-metal stent group, there was less lumen stenosis of rapamycin-eluting stent ( $12.02\% \pm 2.2\%$  vs.  $28.5\% \pm 8.2\%$ , respectively;  $p < 0.05$ ) and GA-eluting stent groups ( $11.5\% \pm 2.5\%$  vs.  $28.5\% \pm 8.2\%$ , respectively;  $p < 0.05$ ) (Figure 2Q). There were no significant differences between the rapamycin- and GA-eluting stent groups. Moreover, the neointimal area was greater in the GA-eluting stent and rapamycin-eluting stent groups than in the bare-metal stent group ( $1.87 \pm 0.59 \text{ mm}^2$  vs.  $0.51 \pm 0.09 \text{ mm}^2$ ;  $1.87 \pm 0.59 \text{ mm}^2$  vs.  $0.53 \pm 0.08 \text{ mm}^2$ , respectively;  $p < 0.05$ ) (Figure 2P).

### 3.3 Endothelial coverage by *en face* SEM after 28 days

To verify the endothelialization of each stent type, we examined the samples using SEM. As shown in Figure 3, the representative SEM images of the implanted stents after 28 days were obtained. The estimated endothelial coverage of the luminal surface was 96% for GA-eluting stents, 99% for BMSs, and 83% for rapamycin-eluting stents, indicating that a few rapamycin-eluting stents showed evidence of delayed healing, exhibiting occasionally uncovered

struts ( $p < 0.05$ ). The GA-eluting stents showed good healing, which was comparable to that of BMSs ( $p > 0.05$ ).

### 3.4 Expression of eNOS in BMSs and comparator DESs

To confirm the endothelialization of different groups, and based on our previous work showing that GA could restore eNOS expression, we tested eNOS expression in the neointima of different stents. As shown in Figure 4, eNOS expression was significantly lower in the rapamycin-eluting stent than in BMSs and GA-eluting stents (BMSs,  $24\% \pm 3\%$ ; rapamycin-eluting stents,  $16\% \pm 3\%$ ; and GA-eluting stents,  $33\% \pm 3\%$ ;  $p < 0.05$ ) (Figure 4D). In addition, eNOS expression was higher in the GA-eluting stent group than in the bare-metal stent group ( $p < 0.05$ ). These results indicated that GA could restore or promote the healing ability of endothelial cells after stenting.

## 4 Discussion

This study investigated the efficacy and safety of a novel drug-eluting stent in a rabbit model of atherosclerosis. The



results showed that GA-eluting stents were more attractive and beneficial for endothelial cells, promoting re-endothelialization in the injured artery. Moreover, this novel stent has a similar effect in inhibiting intimal hyperplasia to the rapamycin-eluting stent, which has been broadly applied in the clinic.

Coronary artery stents have been developed for over 40 years, ranging from bare-metal stents to DESs designed to inhibit smooth muscle cell proliferation and intimal hyperplasia. Currently, DESs are the most popular stents used in PCI. Consequently, restenosis, mainly caused by intimal hyperplasia, reduced from 20%–30% in the BMS era to approximately 5%–10% in the DES era (Waksman and Steinvil, 2016; Shlofmitz et al., 2019). Bioabsorbable stents have recently emerged as a novel advancement in this area; however, negative results have been reported in clinical trials (Jabara et al., 2009; Hoare et al., 2019).

The eluting drugs were developed from paclitaxel and sirolimus (rapamycin) for first-generation DESs to zotarolimus and everolimus for second-generation DESs. Paclitaxel is a diterpenoid derivative that exerts an antineoplastic effect by interfering with microtubule activity (Zhu and Chen, 2019). It prevents the migration and proliferation of vascular smooth muscle cells stimulated by growth factors, thereby preventing neointimal formation (Sollott et al., 1995). Sirolimus and everolimus are immunosuppressants that are used post-transplantation to prevent organ transplant rejection; they both inhibit mammalian rapamycin, thereby blocking protein synthesis and cell cycle progression (Granata et al., 2016). Although the drugs eluting on the scaffold differ in structure and target proteins, they generally have the same effect of inhibiting cell proliferation and a relative lack of cell specificity.

Although intimal hyperplasia is the most crucial pathological process after stenting, re-endothelialization is a critical protective process against thrombosis in stents. However, few studies have investigated the role of endothelialization after PCI, and eluting medicine that focuses on promoting endothelialization has also been omitted. Animal and human studies have indicated that inflammation is pivotal in linking vascular injury to neointimal growth or restenosis. Anti-inflammatory therapy provides an alternative strategy for inhibiting intimal hyperplasia after stenting. GA is a pentacyclic triterpenoid glycoside that occurs naturally in substantial amounts in licorice root extract (Li et al., 2019). GA, an inhibitor of HMGB1, reduces endothelium-dependent relaxation impairment by upregulating eNOS expression in an animal model of diabetes (Zhu et al., 2020a; Zhou et al., 2021), and it attenuates neointimal formation in a rat model of iliac artery balloon injury (Zhu et al., 2020b). A previous study reported that the introduction of NO into rapamycin-eluting stents alleviated incomplete re-endothelialization (Chen et al., 2022). In this study, GA was applied to the eluting stent to inhibit intimal hyperplasia and promote re-endothelialization. A good balance between intimal hyperplasia and re-endothelialization was achieved.

Researchers are exploring new treatment options that inhibit neointimal formation while promoting stent endothelialization. Recent research studies have focused on developing polymer-free stents to prevent inflammatory responses to polymers (Worthley

et al., 2017). Applying anti-CD34 on the surface of DESs promotes rapid re-endothelialization by capturing circulating endothelial progenitor cells (Nakazawa et al., 2010). Although this stent has a more rapid endothelial coverage, it has a higher risk of intimal hyperplasia. The SORT OUT X trial results with a 12-month follow-up showed that the CD34 antibody-covered sirolimus-eluting stent had a higher incidence of target lesion revascularization than the sirolimus-eluting stent (Jakobsen et al., 2021). In patients with acute coronary syndrome, there was no significant difference in stent endothelial coverage between CD34 antibody-covered sirolimus-eluting stents and everolimus-eluting stents at 60 days, as analyzed via optical coherence tomography (Jaguszewski et al., 2017). In contrast, CD31-mimetic stents preferentially promote the adherence of endothelial cells rather than smooth muscle cells or blood components (Diaz-Rodriguez et al., 2021). Stents with an endothelial-mimetic coating significantly inhibit acute thrombosis and accelerate re-endothelialization (Zhang et al., 2022). Even biodegradable vascular grafts that are 3D-printed and laden with dipyridamole have been created to achieve rapid re-endothelialization (Domínguez-Robles et al., 2021).

The novel GA-coated stent used in this study inhibited intimal hyperplasia and promoted re-endothelialization. Based on previous studies, the underlying mechanism could be attributed to HMGB1 inhibition and the promotion effect. Additionally, endothelial coverage was greater in the GA-eluting stents than in the rapamycin-eluting stents.

## 4.1 Limitations

This study had some limitations. First, although accelerated re-endothelialization was observed in the new DES, the process was not monitored at different time points. Hence, we could not record information on when the new DES completed re-endothelialization. Second, the sample size was small. Finally, although this study confirmed the effect of the novel stents, the specific mechanism remains unclear, and further studies are needed.

## Data availability statement

The original contributions presented in the study are included in the article/Supplementary Material; further inquiries can be directed to the corresponding author.

## Ethics statement

The animal study was reviewed and approved by the Animal Care and Use Committee of Central South University.

## Author contributions

ST performed animal experiments and data analysis and approved the article. ZZ and YL reviewed and approved the

article. XH, ZF, and SZ contributed to and discussed the research strategy and data interpretation and reviewed and approved the article. ZL conceived and supervised the project, designed the experiments, and took responsibility for the integrity of the data and accuracy of the data analysis.

## Funding

This work was supported in part by the National Natural Science Foundation of China (NSFC) (projects 81600248 (to ZZ), 81870258, and 82150006 (to SZ)).

## Acknowledgments

The authors are grateful to Min Xie for the careful guidance and technical assistance in the construction of DESs in this experiment. The authors would like to thank Editage ([www.editage.cn](http://www.editage.cn)) for English language editing.

## References

- Chaabane, C., Otsuka, F., Virmani, R., and Bochaton-Piallat, M.-L. (2013). Biological responses in stented arteries. *Cardiovasc Res.* 99 (2), 353–363. doi:10.1093/cvr/cvt115
- Chen, S.-Y., Wang, J., Jia, F., Shen, Z.-D., Zhang, W.-B., Wang, Y.-X., et al. (2022). Bioinspired No release coating enhances endothelial cells and inhibits smooth muscle cells. *J. Mater Chem. B* 10 (14), 2454–2462. doi:10.1039/d1tb01828k
- Cui, H.-K., Li, F.-B., Guo, Y.-C., Zhao, Y.-L., Yan, R.-F., Wang, W., et al. (2017). Intermediate analysis of magnesium alloy covered stent for a lateral aneurysm model in the rabbit common carotid artery. *Eur. Radiol.* 27 (9), 3694–3702. doi:10.1007/s00330-016-4715-6
- Diaz-Rodriguez, S., Rasser, C., Mesnier, J., Chevallier, P., Gallet, R., Choqueux, C., et al. (2021). Coronary stent Cd31-mimetic coating favours endothelialization and reduces local inflammation and neointimal development *in vivo*. *Eur. Heart J.* 42 (18), 1760–1769. doi:10.1093/eurheartj/ehab027
- Dominguez-Robles, J., Shen, T., Cornelius, V. A., Corduas, F., Mancuso, E., Donnelly, R. F., et al. (2021). Development of drug loaded cardiovascular prosthesis for thrombosis prevention using 3d printing. *Mater Sci. Eng. C Mater Biol. Appl.* 129, 112375. doi:10.1016/j.msec.2021.112375
- Dudek, D., Dziewierz, A., Stone, G., and Wijns, W. (2019). The year in Cardiology 2018: Coronary interventions. *Eur. Heart J.* 40 (2), 195–203. doi:10.1093/eurheartj/ehy882
- Finn, A. V., Joner, M., Nakazawa, G., Kolodgie, F., Newell, J., John, M. C., et al. (2007). Pathological correlates of late drug-eluting stent thrombosis: Strut coverage as a marker of endothelialization. *Circulation* 115 (18), 2435–2441. doi:10.1161/CIRCULATIONAHA.107.693739
- Giustino, G., Colombo, A., Camaj, A., Yasumura, K., Mehran, R., Stone, G. W., et al. (2022). Coronary in-stent restenosis: Jacc state-of-the-art review. *J. Am. Coll. Cardiol.* 80 (4), 348–372. doi:10.1016/j.jacc.2022.05.017
- Granata, S., Dalla Gassa, A., Carraro, A., Brunelli, M., Stallone, G., Lupo, A., et al. (2016). Sirolimus and everolimus pathway: Reviewing candidate genes influencing their intracellular effects. *Int. J. Mol. Sci.* 17 (5), 735. doi:10.3390/ijms17050735
- Hoare, D., Bussooa, A., Neale, S., Mirzai, N., and Mercer, J. (2019). The future of cardiovascular stents: Bioresorbable and integrated biosensor Technology. *Adv. Sci. (Weinheim)* 6 (20), 1900856. doi:10.1002/advs.201900856
- Jabara, R., Pendyala, L., Geva, S., Chen, J., Chronos, N., and Robinson, K. (2009). Novel fully bioabsorbable salicylate-based sirolimus-eluting stent. *EuroIntervention* 5 (Suppl. 1), F58–F64. doi:10.4244/EIJV5IFA10
- Jaguszewski, M., Aloysius, R., Wang, W., Bezerra, H. G., Hill, J., De Winter, R. J., et al. (2017). The remedee-oct study: An evaluation of the bioengineered combo dual-therapy Cd34 antibody-covered sirolimus-eluting coronary stent compared with a cobalt-chromium everolimus-eluting stent in patients with acute coronary syndromes: Insights from optical coherence tomography imaging analysis. *JACC Cardiovasc Interv.* 10 (5), 489–499. doi:10.1016/j.jcin.2016.11.040
- Jakobsen, L., Christiansen, E. H., Freeman, P., Kahlert, J., Veien, K., Maeng, M., et al. (2021). Randomized clinical comparison of the dual-therapy Cd34 antibody-covered sirolimus-eluting combo stent with the sirolimus-eluting orsiro stent in patients treated with percutaneous coronary intervention: The sort out X trial. *Circulation* 143 (22), 2155–2165. doi:10.1161/CIRCULATIONAHA.120.052766
- Kamberi, M., Pinson, D., Pacetti, S., Perkins, L. E. L., Hossainy, S., Mori, H., et al. (2018). Evaluation of chemical stability of polymers of xience everolimus-eluting coronary stents *in vivo* by pyrolysis-gas chromatography/mass spectrometry. *J. Biomed. Mater Res. B Appl. Biomater.* 106 (5), 1721–1729. doi:10.1002/jbm.b.33979
- Li, X., Sun, R., and Liu, R. (2019). Natural products in licorice for the therapy of liver diseases: Progress and future opportunities. *Pharmacol. Res.* 144, 210–226. doi:10.1016/j.phrs.2019.04.025
- Lu, R., Tang, F., Zhang, Y., Zhu, X., Zhu, S., Wang, G., et al. (2016). Comparison of drug-eluting and bare metal stents in patients with chronic kidney disease: An updated systematic review and meta-analysis. *J. Am. Heart Assoc.* 5 (11), e003990. doi:10.1161/JAHA.116.003990
- Nakazawa, G., Granada, J. F., Alviar, C. L., Tellez, A., Kaluza, G. L., Guilhemier, M. Y., et al. (2010). Anti-Cd34 antibodies immobilized on the surface of sirolimus-eluting stents enhance stent endothelialization. *JACC Cardiovasc Interv.* 3 (1), 68–75. doi:10.1016/j.jcin.2009.09.015
- Nakazawa, G., Torii, S., Ijichi, T., Nagamatsu, H., Ohno, Y., Kurata, F., et al. (2016). Comparison of vascular responses following new-generation biodegradable and durable polymer-based drug-eluting stent implantation in an atherosclerotic rabbit iliac artery model. *J. Am. Heart Assoc.* 5 (10), e003803. doi:10.1161/JAHA.116.003803
- Sanchis-Gomar, F., Perez-Quilis, C., Leischik, R., and Lucia, A. (2016). Epidemiology of coronary heart disease and acute coronary syndrome. *Ann. Transl. Med.* 4 (13), 256. doi:10.21037/atm.2016.06.33
- Shlofmitz, E., Iantorno, M., and Waksman, R. (2019). Restenosis of drug-eluting stents: A new classification system based on disease mechanism to guide treatment and state-of-the-art review. *Circ. Cardiovasc Interv.* 12 (8), e007023. doi:10.1161/CIRCINTERVENTIONS.118.007023
- Sollott, S. J., Cheng, L., Pauly, R. R., Jenkins, G. M., Monticone, R. E., Kuzuya, M., et al. (1995). Taxol inhibits neointimal smooth muscle cell accumulation after angioplasty in the rat. *J. Clin. Invest.* 95 (4), 1869–1876. doi:10.1172/JCI117867
- Van Belle, E., Tio, F. O., Couffignal, T., Maillard, L., Passeri, J., and Isner, J. M. (1997). Stent endothelialization. Time course, impact of local catheter delivery, feasibility of recombinant protein administration, and response to cytokine expedition. *Circulation* 95 (2), 438–448. doi:10.1161/01.cir.95.2.438
- Waksman, R., and Steinvil, A. (2016). In-stent restenosis? The raiders of the magic remedy. *Circ. Cardiovasc Interv.* 9 (7), e004150. doi:10.1161/CIRCINTERVENTIONS.116.004150

## Conflict of interest

The authors declare that the research was conducted in the absence of any commercial or financial relationships that could be construed as a potential conflict of interest.

## Publisher's note

All claims expressed in this article are solely those of the authors and do not necessarily represent those of their affiliated organizations, or those of the publisher, the editors, and the reviewers. Any product that may be evaluated in this article, or claim that may be made by its manufacturer, is not guaranteed or endorsed by the publisher.

## Supplementary material

The Supplementary Material for this article can be found online at: <https://www.frontiersin.org/articles/10.3389/fphar.2023.1159779/full#supplementary-material>



- Worthley, S. G., Abizaid, A., Kirtane, A. J., Simon, D. I., Windecker, S., Brar, S., et al. (2017). First-in-Human evaluation of a novel polymer-free drug-filled stent: Angiographic, ivus, oct, and clinical outcomes from the revelation study. *JACC Cardiovasc Interv.* 10 (2), 147–156. doi:10.1016/j.jcin.2016.10.020
- Xu, W., Sasaki, M., and Niidome, T. (2022). Sirolimus release from biodegradable polymers for coronary stent application: A review. *Pharmaceutics* 14 (3), 492. doi:10.3390/pharmaceutics14030492
- Zhang, B., Qin, Y., and Wang, Y. (2022). A nitric oxide-eluting and redv peptide-conjugated coating promotes vascular healing. *Biomaterials* 284, 121478. doi:10.1016/j.biomaterials.2022.121478
- Zhou, Q., Tu, T., Tai, S., Tang, L., Yang, H., and Zhu, Z. (2021). Endothelial specific deletion of Hmgb1 increases blood pressure and retards ischemia recovery through enos and ros pathway in mice. *Redox Biol.* 41, 101890. doi:10.1016/j.redox.2021.101890
- Zhu, L., and Chen, L. (2019). Progress in research on paclitaxel and tumor immunotherapy. *Cell Mol. Biol. Lett.* 24, 40. doi:10.1186/s11658-019-0164-y
- Zhu, Z., Guo, Y., Li, X., Teng, S., Peng, X., Zou, P., et al. (2020). Glycyrrhizic acid attenuates balloon-induced vascular injury through inactivation of rage signaling pathways. *Cardiovasc. Innovations Appl.* 4 (2), 11. doi:10.15212/cvia.2019.0577
- Zhu, Z., Peng, X., Li, X., Tu, T., Yang, H., Teng, S., et al. (2020). Hmgb1 impairs endothelium-dependent relaxation in diabetes through tlr4/enos pathway. *FASEB J.* 34 (6), 8641–8652. doi:10.1096/fj.202000242R



## OPEN ACCESS

## EDITED BY

Xianwei Wang,  
Xinxiang Medical University, China

## REVIEWED BY

Alexander N. Shikov,  
Saint-Petersburg State Chemical  
Pharmaceutical Academy, Russia  
Hai-Gang Zhang,  
Army Medical University, China

## \*CORRESPONDENCE

Jing Li,  
✉ lijingfighting@163.com

<sup>†</sup>These authors have contributed equally  
to this work

RECEIVED 12 February 2023

ACCEPTED 22 May 2023

PUBLISHED 30 May 2023

## CITATION

Wang S, Bai J, Che Y, Qu W and Li J  
(2023), Fucoidan inhibits apoptosis and  
improves cardiac remodeling by  
inhibiting p53 transcriptional activation  
through USP22/Sirt 1.  
*Front. Pharmacol.* 14:1164333.  
doi: 10.3389/fphar.2023.1164333

## COPYRIGHT

© 2023 Wang, Bai, Che, Qu and Li. This is  
an open-access article distributed under  
the terms of the [Creative Commons  
Attribution License \(CC BY\)](#). The use,  
distribution or reproduction in other  
forums is permitted, provided the original  
author(s) and the copyright owner(s) are  
credited and that the original publication  
in this journal is cited, in accordance with  
accepted academic practice. No use,  
distribution or reproduction is permitted  
which does not comply with these terms.

# Fucoidan inhibits apoptosis and improves cardiac remodeling by inhibiting p53 transcriptional activation through USP22/Sirt 1

Shuai Wang<sup>1†</sup>, Jie Bai<sup>2†</sup>, Yilin Che<sup>3</sup>, Weikun Qu<sup>4</sup> and Jing Li<sup>5\*</sup>

<sup>1</sup>Second Affiliated Hospital of Dalian Medical University, Dalian, China, <sup>2</sup>School of Public Health, Dalian Medical University, Dalian, China, <sup>3</sup>The 1st Department of Thoracic Medical Oncology, Second Affiliated Hospital of Dalian Medical University, Dalian, China, <sup>4</sup>Department of OPO Office, Second Affiliated Hospital of Dalian Medical University, Dalian, China, <sup>5</sup>Department of Cardiology, Institute of Heart and Vascular Diseases, Second Affiliated Hospital of Dalian Medical University, Dalian, China

**Background:** Humans with hypertensive heart disease are more likely to experience heart failure, arrhythmia, myocardial infarction, and sudden death, and it is crucial to treat this condition. Fucoidan (FO) is a natural substance derived from marine algae that has antioxidant and immunomodulatory activities. FO has also been shown to regulate apoptosis. However, whether FO can protect against cardiac hypertrophy is unknown.

**Methods:** We investigated the effect of FO in hypertrophic models *in vivo* and *in vitro*. C57BL/6 mice were given an oral gavage of FO (300 mg/kg/day) or PBS (internal control) the day before surgery, followed by a 14-day infusion of Ang II or saline. AC-16 cells were treated with si-USP22 for 4 h and then treated with Ang II (100 nM) for 24 h. Systolic blood pressure (SBP) was recorded, echocardiography was used to assess cardiac function, and pathological changes in heart tissues were assessed by histological staining. Apoptosis levels were detected by TUNEL assays. The mRNA level of genes was assessed by qPCR. Protein expression was detected by immunoblotting.

**Results:** Our data showed that USP22 expression was lowered in Ang II-infused animals and cells, which could promote cardiac dysfunction and remodeling. However, treatment with FO significantly upregulated the expression of USP22 and reduced the incidence of cardiac hypertrophy, fibrosis, inflammation, and oxidative responses. Additionally, FO treatment lowered p53 expression and apoptosis while increasing Sirt 1 and Bcl-2 expression.

**Conclusion:** By reducing the level of Ang II-induced apoptosis through the regulation of USP22/Sirt 1 expression, FO treatment might improve cardiac function. According to this study, FO might be potential targeted approach for treating heart failure.

## KEYWORDS

USP22, fucoidan, cardiac remodeling, Sirt 1, apoptosis

## Introduction

Diastolic dysfunction (CHF-D) and left ventricular hypertrophy (LVH) are crucial indicators of hypertensive heart disease (Slivnick and Lampert, 2019). Because individuals with hypertensive heart disease are more likely to experience heart failure, arrhythmia, myocardial infarction, and sudden death, it is crucial to cure this condition. Anti-hypertensive therapy aims to lower blood pressure (BP) and stop the pathophysiological processes that cause LVH and CHF-D that are not dependent on blood pressure (Diamond and Phillips, 2005; Shimizu I and Minamino, 2016). The renin-angiotensin system (RAS) controls salt intake, vasoconstriction, potassium excretion, blood pressure, and other physiological processes (Lev-Ran and Porta, 2005). The main RAS effector molecule is angiotensin II (Ang II). This factor raises blood pressure, influences the renal tubules to retain sodium and water, and increases the release of aldosterone from the adrenal glands. Ang II is a powerful vasoconstrictor that also has proliferative, inflammatory, and fibrotic effects (Benigni et al., 2010). Angiotensinogen type 1 receptors (AT1Rs), which are widely distributed in all organs, including the heart and vascular system, mediate the majority of the known physiological activities of Ang II. Thus, inhibiting AT1R-mediated activation of signaling is critical for blocking hypertensive heart disease.

By attaching or removing ubiquitins to substrate proteins, ubiquitination and deubiquitination are critical posttranslational modifications of metabolic enzymes that control their breakdown, delocalization, and activation in cells (Eletr ZM and Wilkinson KD, 2014). Cardiovascular diseases are more likely to develop when ubiquitination and deubiquitination are dysregulated, which is directly connected to lipid metabolism in cells (Gu et al., 2022). Deubiquitinating enzymes (DUBs) have a critical role in cardiovascular illnesses such as cardiac hypertrophy, myocardial infarction, atrial fibrillation, and heart failure, according to recent research (Komander D., 2010; Komander D and Rape M., 2012; Kliza and Husnjak, 2020). USP22, a member of the ubiquitin-specific protease (USP) subfamily of DUBs, has been linked to both human and mouse malignancies and placental development in mice (Melo-Cardenas J et al., 2016). According to a recent study, USP22 may prevent cardiac ischemia–reperfusion damage by preventing cardiomyocyte death (Ma S et al., 2020). The nicotinamide adenine dinucleotide (NAD)-dependent protein deacetylase sirtuin-1 (Sirt 1) is specifically deubiquitinated by USP22, and this deubiquitination leads to the stabilization of the Sirt1-repressed tumor protein p53, affecting transcriptional and proapoptotic activities (Lin Z et al., 2012). Sirt1 was shown to contribute to myocardial ischemia and reperfusion damage, as well as vascular endothelial dysfunction, safeguarding mitochondrial function, inhibiting oxidative stress, and relieving the inflammatory response (Luo G et al., 2019). Therefore, the goal of this study was to determine whether USP22 and Sirt 1 were involved in the molecular processes underlying the control of apoptosis in Ang II-induced cardiac remodeling.

Fucoidan (FO) is a fucose-enriched sulfated polysaccharide that is mostly produced by brown algae and has been extensively used as a dietary supplement and health food because of its many positive effects, including anti-inflammatory, anticancer, and antidiabetic effects (Li and Ye, 2008; Zhang SM et al., 2015; Fitton HJ et al., 2019). An FO preparation called ‘Haikun Shenxi capsules’ was approved in

China in 2003, and its clinical use as a treatment for chronic renal failure has been described (Fitton HJ et al., 2019). This preparation has been shown to alleviate diabetes-induced kidney fibrosis by increasing the levels of USP22 and inducing deubiquitination of the Sirt1 protein through overexpression (Yu et al., 2020). However, the molecular processes underlying the functions of USP22 and Sirt1 in Ang II-induced ventricular hypertrophy are unknown.

In this study, we used FO as a protective agent to investigate its effects on USP22/Sirt 1 in Ang II-induced cardiac hypertrophy and aimed to highlight a novel targeted approach to treat heart failure.

## Materials and methods

### Antibodies and chemicals

Fucoidan (FO) was obtained from Med Chem Express (HY-132179), the average molecular weight is 220–300 kDa, polysaccharide, content of this fucan is approx (20%–23%), sulphate approx (24%–30%). Anti-USP22 (1:800, ab195289) and calcineurin A (CaNA, 1:800, ab71149) primary antibodies were from Abcam; anti-Sirt 1 (1:800, WL02995) and anti-transforming growth factor-beta 1 (TGF- $\beta$ 1) (1:800, WL02998) were from Wanleibio; anti-CD68 (1:600, bs-1432R) and anti-NADPH-Oxidase 4 (NOX4) (1:600, bs-1091R) were from Bioss Antibodies; anti-p53 (1:1000, #2524) and anti-Bcl-2 (1:500, #3498) were from Cell Signaling Technology; and anti-GAPDH (1:2000, AP0063) and anti- $\beta$ -tubulin (1:2000, AP0064) were from BIOWORLD. Wheat germ agglutinin (WGA) was purchased from Vector Laboratories. Dihydroethidium (DHE) was purchased from BIOFOUNT. The TUNEL Apoptosis Detection Kit (Cat# 40308) was purchased from YEASEN.

### Animal study

Four groups of forty wild-type (WT) C57BL/6 male mice (8 weeks old) were used. Using osmotic mini-pumps (Alzet Model 1007D or 1002, DURECT), the mice were infused for 7 or 14 days with normal saline or Ang II (1,000 ng/kg/min, Aladdin) (Bai et al., 2022). The mice were given an oral gavage of FO (300 mg/kg/day) or PBS (internal control) the day before surgery, followed by a 14-day infusion of Ang II or saline (Yu et al., 2020). All mice received an intraperitoneal injection of 2.5% tribromoethanol (0.02 mL/g, Sigma–Aldrich) to induce anesthesia after receiving therapy for 14 days. The hearts were removed and used for future research.

The animal experimental procedures were approved by the Animal Experimental Ethics Committee of Dalian Medical University, and extensive efforts were made to minimize the distress of the included animals.

### Monitoring of blood pressure and cardiac function

The blood pressure of mice in each group was measured by a noninvasive blood pressure automatic measurement system (BP-

**TABLE 1** The details of primers used in RT-qPCR.

Gene	Forward primer (5'-3')	Reverse primer (5'-3')
USP22	CATGACCCCTTTCATGGCCT	GATGTTCTGGTGACGGGTGT
ANF	CACAGATCTGATGGATTCAAGA	CCTCATCTTCTACCGGCATC
BNP	GAAGGTGCTGTCCAGATGA	CCAGCAGCTGCATCTTGAAT
Collagen I	GAGTACTGGATCGACCCCTAACCA	GACGGCTGAGTAGGGAACACA
Collagen III	TCCCCTGGAATCTGTGAATC	TGAGTCGAATTGGGGAGAAT
NOX2	ACCGGGTTTATGATATTCCACCT	GATTTGCACAGACTGGCAAGA
NOX4	CAGATGTTGGGGCTAGGATTG	GAGTGTTCCGGCACATGGGTA
IL-1 $\beta$	TGCCACCTTTTGACAGTGATG	TGATGTGCTGCTGCGAGATT
IL-6	TGATGGATGCTACCAAACTGGA	TGTGACTCCAGCTTATCTCTTGG
GAPDH	GGTTGTCTCTGCGACTTCA	GGTGGTCCAGGGTTTCTTACTC

300A, Chengdu Taimeng Software Co., Ltd.). Mice in each group were weighed and anesthetized with 1.5% isoflurane. Cardiac function was monitored using a 70 MHz probe (Vevo 3,100 System, FUJIFILM).

## Histopathology and immunohistochemical analysis

Myocardial tissue was fixed with 4% paraformaldehyde, embedded in paraffin or optimal cutting temperature compound (OCT) and sectioned (5  $\mu$ m). Cardiac tissue sections were immersed in hematoxylin for 3 min, stained with eosin for 5 min, and then sealed with neutral gel. Masson staining was used to observe myocardial fibrosis. Cardiomyocyte (CM) hypertrophy was detected by WGA staining, and reactive oxygen species (ROS) levels were detected by DHE staining. Four fields were randomly selected in the stained sections and observed microscopically.

For immunohistochemical staining, heart tissue sections were incubated with an anti-CD68 antibodies (1:200), and then development was performed with DAB as previously described (Bai et al., 2022).

## Cell culture and treatment

AC-16 cells were cultured in DMEM/F12 with 10% FBS and 1% penicillin/streptomycin. The cells were starved for 2 h, treated with si-USP22 and si-control for 4 h, and then treated with Ang II (100 nM) or saline for 24 h. Similarly, cells were starved for 2 h, treated with FO (60  $\mu$ g/mL) for 4 h, and then treated with Ang II (100 nM) or saline for 24 h (Zhang et al., 2015).

## Heart tissue and cell RNA extraction and RT-qPCR detection

Using TRIzol reagent, we isolated total RNA from cardiac tissue and cells (Invitrogen). Using superscript II, the first strand of cDNA

was produced from total RNA (2  $\mu$ g) (Invitrogen). Real-time quantitative PCR was used to identify the mRNA levels of USP22, Atrial natriuretic factor (ANF), brain natriuretic peptide (BNP), collagen I, collagen III, Interleukin-1 $\beta$  (IL-1 $\beta$ ), Interleukin-6 (IL-6), NADPH-Oxidase 2 (NOX2) and NOX4. These data were normalized to GAPDH. Sango Biotech provided the primers. Table 1 shows the primer details.

## Western blotting

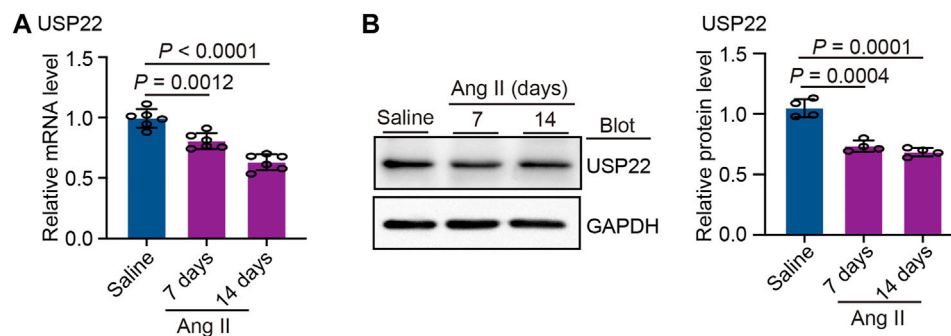
A total protein extraction kit (BC3711, Solarbio) was used to extract the total protein from cardiac tissue and cells, and a BCA kit from Thermo Scientific was used to quantify the protein concentrations. Equal amounts of protein (25  $\mu$ g) were placed on a PVDF membrane after being separated by 10% or 12% SDS-PAGE. The membrane was incubated with the binding antibody (Thermo Scientific) overnight at 4 °C. With the aid of the ECL Light Chemiluminescence Kit, the bands were discovered (Epizyme Biomedical Technology). We used  $\beta$ -tubulin and GAPDH as internal controls.

## TUNEL assay

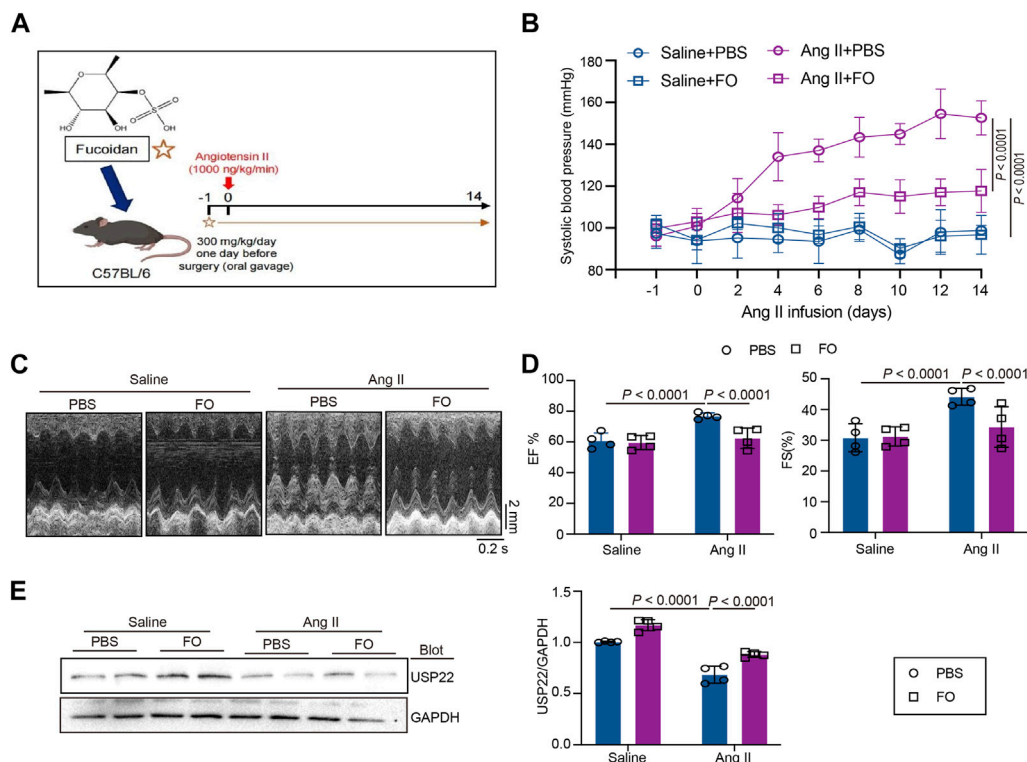
The TUNEL apoptosis detection kit was used to detect apoptosis in frozen cardiac tissue sections and cells after they had been dried at room temperature for 30 min, fixed with 4% paraformaldehyde, and washed with PBS solution. In the stained sections, four fields of view were chosen at random for microscopic examination.

## Statistical analysis

Statistical analysis of the data was performed with GraphPad Prism 9.0. First, a normalcy test was conducted. Student's t-test or one-way ANOVA was used as necessary if all groups satisfied the requirements for normality and the intergroup variances were equal. If the aforementioned requirements were not met, the nonparametric Mann-Whitney *U* test was used. The threshold for significant differences was *p* < 0.05. The results are shown as the mean  $\pm$  SD.

**FIGURE 1**

Ang II reduced the expression of USP22. The WT C57BL/6 mice were infused with Ang II (1,000 ng/kg/min) or saline for 7 or 14 days. **(A)** The mRNA expression of USP22 in heart at day 7 and 14 of Ang II infusion ( $n = 6$  per group); **(B)** Western blot analysis of USP22 protein in hearts (left) and quantification of protein bands (right,  $n = 4$ ).

**FIGURE 2**

FO treatment increased cardiac function and decreased SBP by upregulating the expression of USP22. The WT C57BL/6 mice were treated with Fucoidan (FO) (300 mg/kg/day) 1 day before surgery, and then the mice were infused with Ang II (1,000 ng/kg/min) or saline for 14 days. **(A)** The structure of FO and a protocol of administration of FO in Ang II-induced model of cardiac remodeling. **(B)** The systolic blood pressure (SBP) was measured 1 day before surgery signed as -1 day and then every 2 days after Ang II infusion ( $n = 6$ ); **(C)** M-mode echocardiography of LV chamber at 14 days ( $n = 4$ ); **(D)** Measurement of EF% and FS% ( $n = 6$ ); **(E)** Western blot analysis of USP22 protein in hearts (left), and quantification of protein bands (right,  $n = 4$ ).

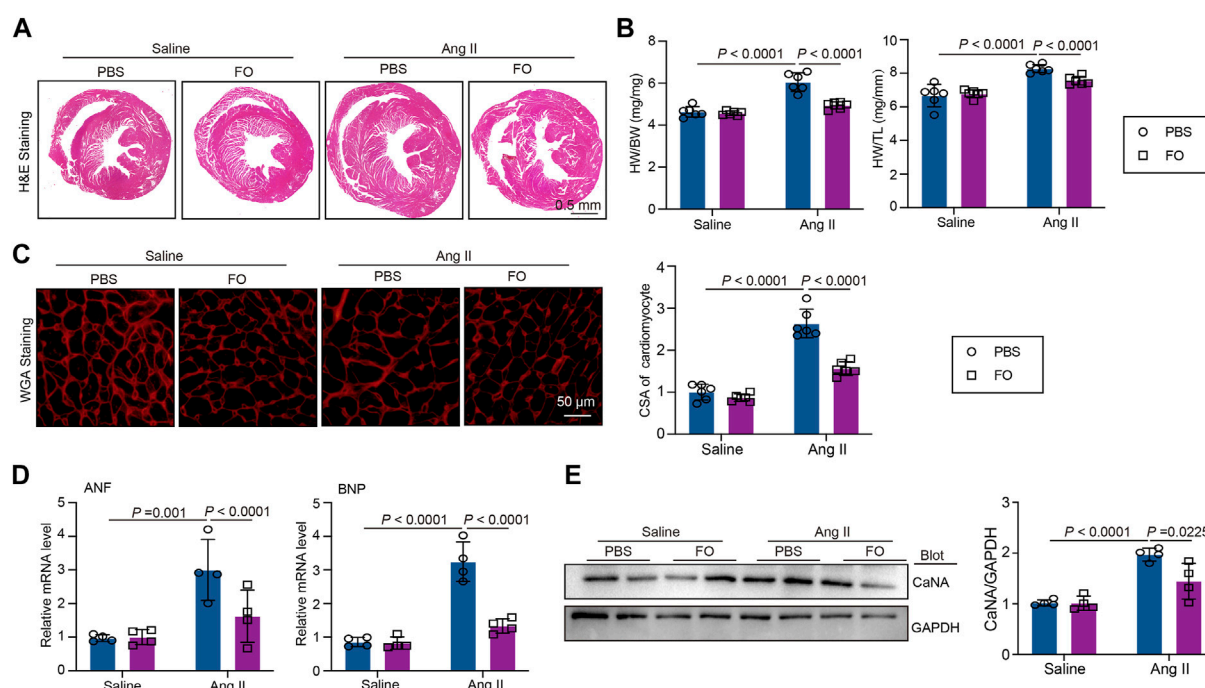
## Results

### USP22 expression was downregulated by Ang II

We initially measured the levels of USP22 in the heart 7 and 14 days after Ang II infusion to better understand the role of

USP22 in Ang II-induced cardiac remodeling. The levels of USP22 mRNA dramatically decreased after 7 and 14 days of Ang II infusion, as shown in Figure 1A. Western blot analysis revealed that following Ang II infusion, USP22 expression was downregulated (Figure 1B). Therefore, the incidence of Ang II-induced cardiac remodeling may be significantly influenced by the reduced expression of USP22.



**FIGURE 3**

FO treatment improves Ang II-induced cardiac hypertrophy. The WT C57BL/6 mice were treated with Fucoidan (FO) (300 mg/kg/day) 1 day before surgery, and then the mice were infused with Ang II (1,000 ng/kg/min) or saline for 14 days. **(A)** H & E staining of heart sections in each group ( $n = 4$ ); **(B)** The ratio of heart weight to body weight (HW/BW) and heart weight to tibial length (HW/TL,  $n = 6$ ); **(C)** WGA staining of heart sections in each group (left,  $n = 6$ ), the quantitation of CSA of cardiomyocyte (right,  $n = 6$ ); **(D)** The mRNA level of ANF and BNP in heart sections of each group ( $n = 4$ ); **(E)** Western blot analysis of CaNA protein expression in hearts (left), and quantification of protein bands (right,  $n = 4$ ).

## USP22 improves Ang II-Induced Hypertension and cardiac insufficiency

The mice were given an oral gavage of FO (300 mg/kg/day) the day before surgery and then received an Ang II infusion for 14 days (Figure 2A). Systolic blood pressure (SBP) was measured in each group, as shown in Figure 2B, and the results revealed that Ang II infusion significantly increased SBP, while FO treatment significantly lowered Ang II-induced high SBP in comparison to the Ang II + PBS group. The echocardiography results demonstrated that FO greatly reduced Ang II-induced cardiac dysfunction by raising the levels of ejection fraction (EF%) and fractional shortening (FS%) (Figures 2C, D). We next examined USP22 expression, and the results showed that after receiving FO, animals given Ang II had increased USP22 protein expression (Figure 2E). These findings suggested that FO therapy could increase USP22 expression, which might reduce SBP and cardiac dysfunction.

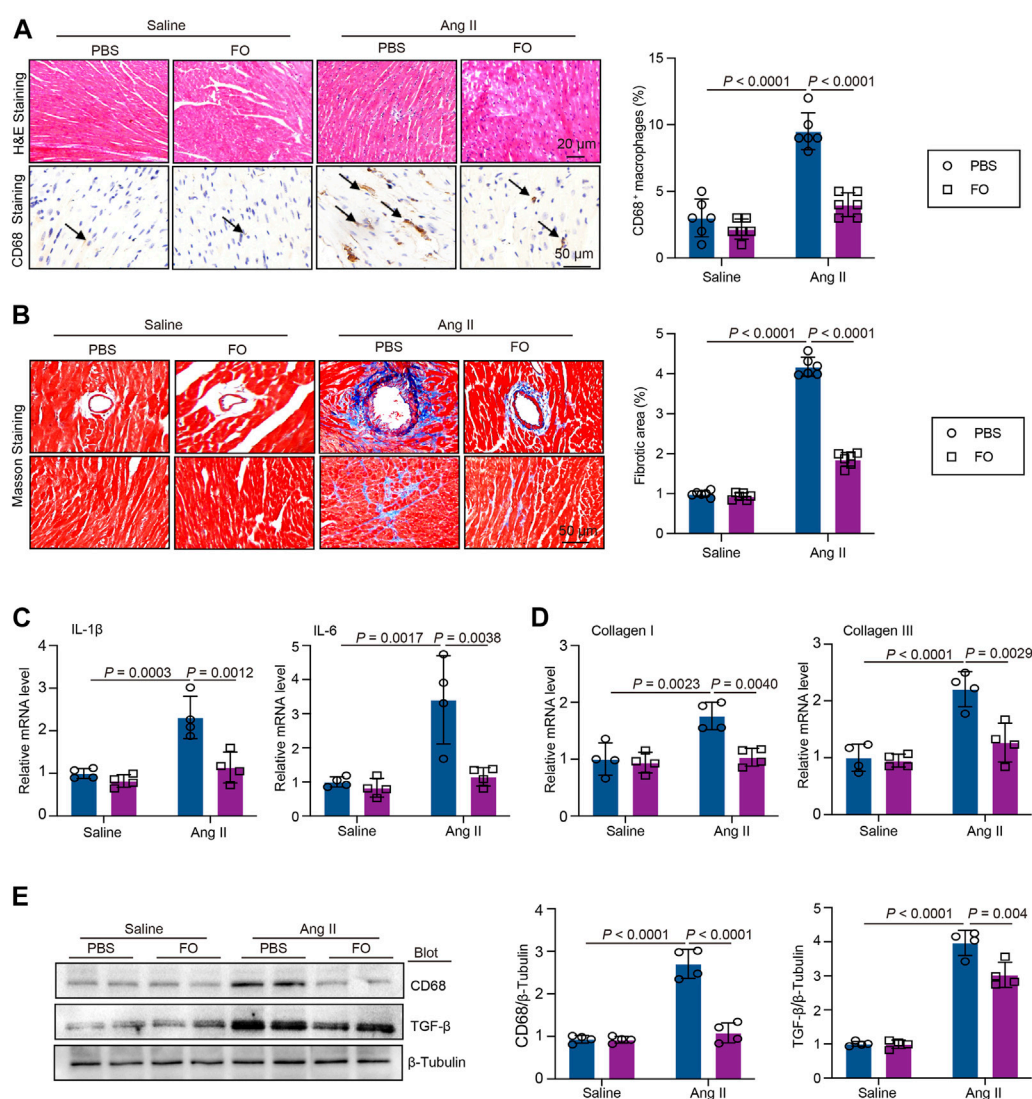
## USP22 inhibits cardiac hypertrophic in Ang II-infused hearts

The role of USP22 in Ang II-induced cardiac hypertrophy and the oxidative response was then investigated. Left ventricular thickness, heart weight/body weight (HW/BW), and heart weight/tibia length (HW/TL) were significantly increased

2 weeks after Ang II infusion, and FO therapy could reduce these effects (Figures 3A, B). Additionally, we used WGA staining to show how the cross-sectional areas of the myocytes changed in each group. The findings demonstrated that FO therapy reduced myocyte size in comparison to that in the Ang II + PBS group (Figure 3C). In Ang II-infused animals, the expression of hypertrophic markers ANF and BNP was reduced after FO therapy (Figure 3D). Similarly, in Ang II-infused mice, FO reduced the production of CaNA protein, which are involved in the hypertrophic signaling cascade (Figure 3E).

## Addition of USP22 reduces Ang II-induced cardiac inflammation and fibrosis

We administered FO to mice to increase USP22 expression to confirm the involvement of USP22 in Ang II-induced inflammatory damage and cardiac fibrosis. The results showed that after FO treatment, inflammatory CD68<sup>+</sup> cells in Ang II-infused hearts significantly decreased (Figure 4A). In the majority of cardiac disorders, myocardial fibrosis is a histological marker of structural change. An increase in USP22 in Ang II-infused mice reduced collagen deposition, as shown by Masson staining (Figure 4B). The mRNA levels of IL-1 $\beta$ , IL-6, collagen I, and collagen III were next examined, and we discovered that FO dramatically reduced the expression of inflammatory and fibrosis

**FIGURE 4**

FO treatment decreased Ang II-induced cardiac inflammatory cell and collagen deposition. The WT C57BL/6 mice were treated with Fucoidan (FO) (300 mg/kg/day) 1 day before surgery, and then the mice were infused with Ang II (1,000 ng/kg/min) or saline for 14 days. **(A)** H & E and CD68 immunohistochemical staining of heart sections in each group (left,  $n = 4$ ), the quantification of CD68 positive macrophages (right,  $n = 6$ ); **(B)** Masson staining of heart sections in each group ( $n = 6$ ), the quantification of fibrotic area in each heart section ( $n = 6$ ); **(C)** The mRNA level of IL-1 $\beta$  and IL-6 in heart sections of each group ( $n = 4$ ); **(D)** The mRNA level of collagen I and collagen III in heart sections of each group ( $n = 4$ ); **(E)** Western blot analysis of CD68 and TGF- $\beta$  protein expression in hearts (left), and quantification of protein bands (right,  $n = 4$ ).

markers in mice that had received Ang II (Figures 4C, D). Additionally, Ang II increased the expression of CD68 and TGF- $\beta$ 1 relative to saline infusion, which was also inhibited in mice treated with FO (Figure 4E).

USP22 Protects Against Ang II-induced Oxidative Reactions, and Apoptosis Through the Sirt1/p53 Axis.

DHE staining demonstrated that FO therapy could reduce the oxidative response in animals that had received Ang II (Figure 5A). In Ang II-infused animals, the expression of oxidative marker NOX2 and NOX4 (Figure 5B). Similarly, in Ang II-infused mice, FO reduced the production of NOX4 protein which are involved in oxidative signaling cascade (Figure 5C). The TUNEL assay results demonstrated

that Ang II infusion increased the incidence of apoptosis compared to that in animals that received saline infusions, and the effect was alleviated by FO (Figure 5D). The expression of Sirt1, p53, and Bcl-2 was then measured. In contrast to saline-infused mice, Ang II-infused mice exhibited increased expression of p53 and decreased expression of Sirt1 and Bcl-2, but FO therapy attenuated these responses (Figure 5E). These findings indicated that Sirt1 deubiquitination by USP22 overexpression could prevent p53 transcriptional activation, although this work had significant limitations. Future research will need to confirm the link between USP22 and Sirt1 and their impact on p53 in basic myocardial cells.

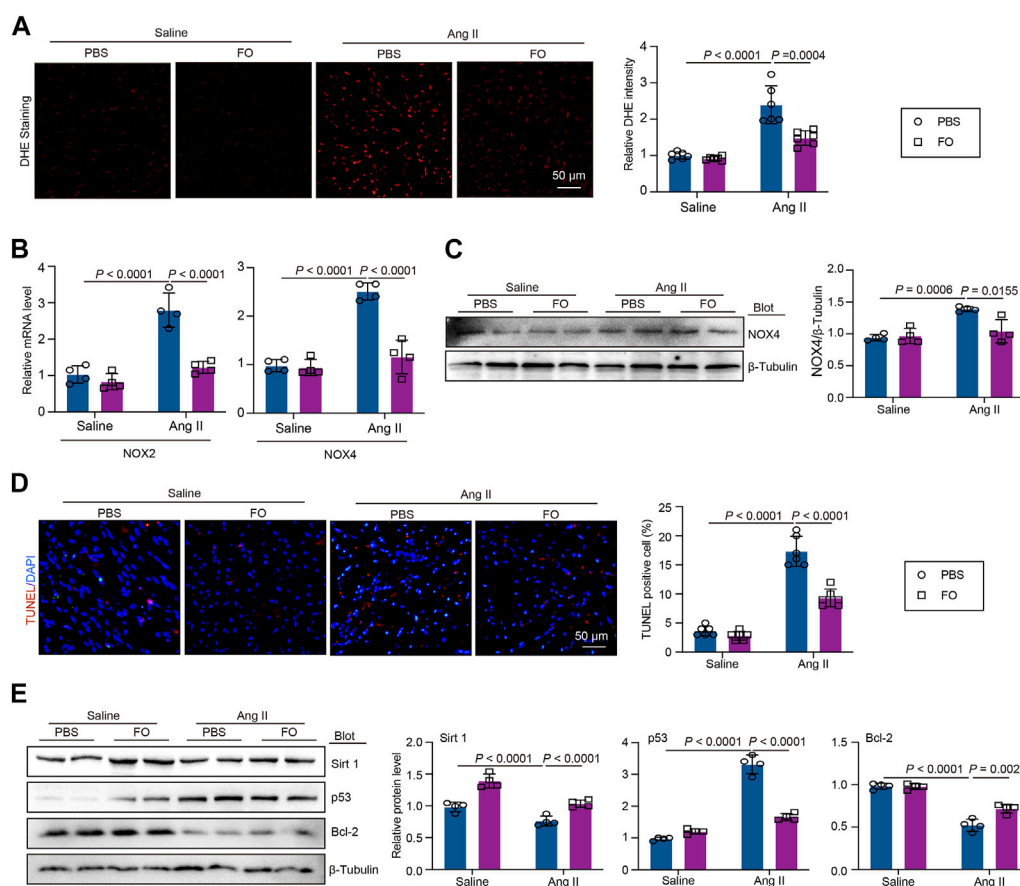


FIGURE 5

FO treatment reduced Ang II-induced cardiac oxidative stress and apoptosis by regulating the expression of Sirt1 and p53. The WT C57BL/6 mice were treated with Fucoidan (FO) (300 mg/kg/day) 1 day before surgery, and then the mice were infused with Ang II (1,000 ng/kg/min) or saline for 14 days. (A) DHE staining of cardiac sections in each group (left,  $n = 6$ ), the quantification of DHE intensity (right,  $n = 6$ ); (B) The mRNA level of NOX2 and NOX4 in heart sections of each group ( $n = 4$ ); (C) Western blot analysis of NOX4 protein expression (left), and quantification of protein bands (right,  $n = 4$ ). (D) TUNEL staining of cardiac sections in each group (left,  $n = 4$ ), the quantification of TUNEL positive cell (right,  $n = 6$ ); (E) Western blot analysis of Sirt1, p53 and Bcl-2 protein expression in hearts (left), and quantification of protein bands (right,  $n = 4$ ).

## The decrease in USP22 aggravated Ang II-induced apoptosis, and FO rescued this effect

To further investigate the role of USP22 and the protective effect of FO, we treated AC-16 cells with si-USP22 and si-control. We found that after treatment with Ang II, the expression of Sirt1 was significantly decreased, and the addition of si-USP22 aggravated the decrease in Sirt1 expression induced by Ang II (Figure 6A). In contrast, the expression of p53 was increased by Ang II infusion, and si-USP22 treatment further increased the expression of p53 (Figure 6A). Next, we treated the cells with FO (60  $\mu$ g/mL). The TUNEL assay showed that Ang II infusion increased apoptosis in AC-16 cells and that FO treatment obviously protected against this reaction (Figure 6B). Furthermore, we detected the expression of USP22, Sirt1 and p53, and the results showed that Ang II infusion decreased the expression of USP22 and Sirt1 and increased the expression of p53 compared with the saline group (Figure 6C). FO treatment rescued the decrease in USP22 and Sirt1 and the increase in p53 induced by Ang II infusion (Figure 6C). These results

suggested that the lack of USP22 could induce apoptosis in Ang II-treated cells and that FO treatment could protect against this reaction.

## Discussion

In the current study, we show that the overexpression of USP22 induced by treatment with FO greatly improved Ang II-induced cardiac dysfunction, heart hypertrophy, inflammation, and fibrosis (Figures 1–4). Additionally, by deubiquitinating Sirt1, the increased expression of USP22 decreased the frequency of p53-dependent apoptosis and oxidative response (Figures 5, 6). Therefore, as indicated in the working model shown in Figure 7, our findings suggest that FO is a targeted approach to treat heart failure, but more clinical trials are required to establish its clinical use and verify its safety.

An increase in cardiac myocyte size without cell division is a characteristic of cardiac hypertrophy. This condition is believed to be an adaptive reaction to increased cardiac afterload-induced wall

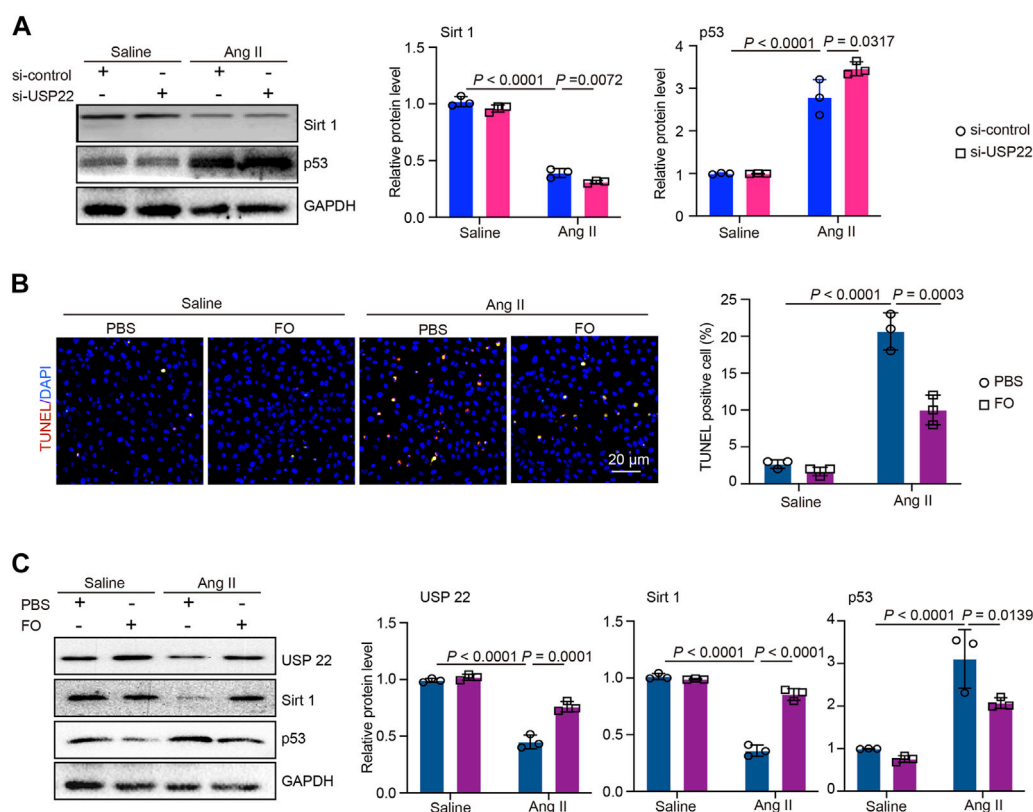


FIGURE 6

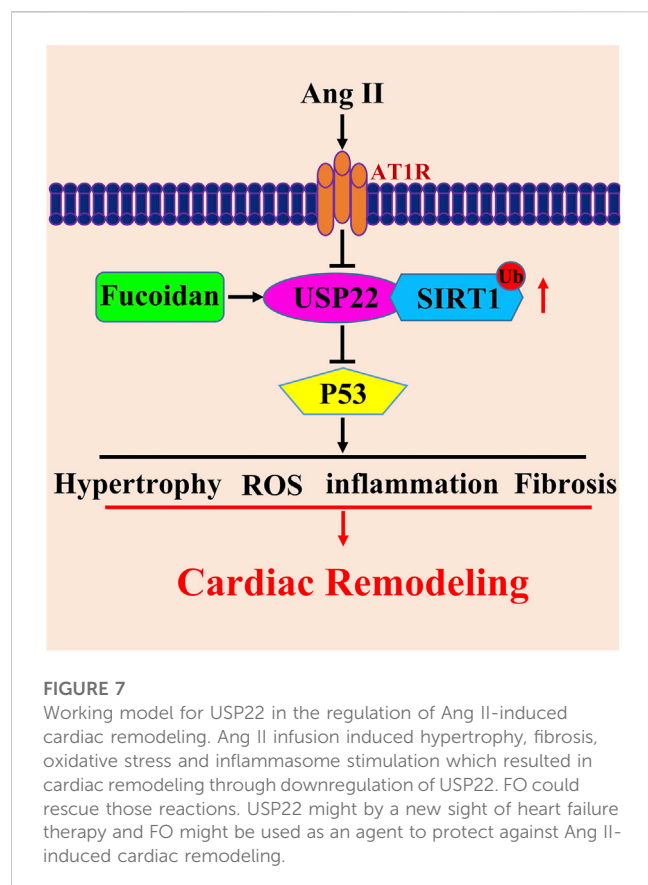
si-USP22 aggravated Ang II-induced apoptosis in AC-16 cells and FO could protect against this effect. AC-16 cells were starved for 2 h and then treated with si-USP22 and si-control for 4 h, and then treated with Ang II (100 nM) or saline for 24 h. Similarly, the cells were starved for 2 h and then treated with FO (60  $\mu$ g/mL) for 4 h, and then treated with Ang II (100 nM) or saline for 24 h. (A) Western blot analysis of Sirt1 and p53 protein expression in cells (left), and quantification of protein bands (right,  $n = 3$ ); (B) TUNEL staining of cells in each group (left,  $n = 3$ ), the quantification of TUNEL positive cell (right,  $n = 3$ ); (C) Western blot analysis of USP 22, Sirt1 and p53 protein expression in cells (left), and quantification of protein bands (right,  $n = 3$ ).

stress (Zhu et al., 2019). One of the major factors contributing to morbidity and mortality in elderly individuals is cardiac insufficiency, and the etiology of this condition is frequently linked to myocardial remodeling caused by myocardial hypertrophy (Shimizu and Minamino, 2016). The myocardium is impacted by Ang II, which also encourages the development of hypertension. Heart failure and abnormal hypertrophy can result from Ang II exposure. There is evidence that some cell types, such as cardiomyocytes, cardiac fibroblasts, kidney cells, and neurons, are negatively impacted by high intracellular Ang II levels (Zhou et al., 2016). These effects are linked to organ damage, cardiac hypertrophy and fibrosis, conduction problems, and inflammation. They include the promotion of hypertrophy, apoptosis, oxidative stress, and the production of TGF- $\beta$  and nuclear factor kappa-B (NF- $\kappa$ B) (Benigni et al., 2010). Our earlier research revealed that the ubiquitin-proteasome system is crucial for controlling protein quality and the prevalence of ventricular fibrillation (Li et al., 2018; Li et al., 2019). Ubiquitin-specific processing proteases (USPs), which are also known as ubiquitin-binding proteins in yeast, are the largest subfamily of deubiquitinases. USP22 is one of these proteins (UBP). From yeast to vertebrates, USP22 is remarkably conserved (Melo-Cardenas et al., 2016). USP22 can stabilize the Sirt 1 protein,

which inhibits p53 transcriptional activity and causes cell death, because Sirt1 is polyubiquitinated and targeted for proteasomal degradation. Indeed, abolishing Sirt1 ubiquitination by replacing the ubiquitin-conjugating lysine residues with arginines prolongs Sirt1 half-life. USP22 removes polyubiquitination of Sirt1 to control its protein stability and functions. Therefore, USP22 is a positive regulator of Sirt1. (Lin et al., 2012). Recent research has shown that USP22 protects against myocardial ischemia-reperfusion injury (Ma et al., 2020), but it is still unknown how USP22 affects Ang II-induced cardiac remodeling and hypertrophy. In the current study, we found that an increase in USP22 could ameliorate Ang II-induced cardiac dysfunction and remodeling.

Marine algae contain large amounts of non-starch polysaccharides that cannot be digested completely by the human digestive system and which therefore have potential as new sources of dietary fiber, prebiotics or other functional ingredients (Kim KT et al., 2014). As with plant fiber from other sources, seaweed fiber is interesting because its consumption has been associated with a significant reduction of chronic diseases such as diabetes, obesity, blood pressure, and so on (Ou et al., 2001; Maki et al., 2007). Soluble fiber can slow down digestion and absorption of nutrients by increasing viscosity and might thereby decrease blood sugar and





cholesterol (Kim KT et al., 2014). In this context, FO, a bioactive polysaccharide found in brown algae, appears promising. Marine algae have been considered as a source of enzyme inhibitors. Similar to plant extracts, algal extracts may be considered for this purpose because they contain some polyphenolic compounds, such as bromophenols (Liu et al., 2011) and phlorotannins, which are inhibitors of  $\alpha$ -glucosidase. Additionally, polysaccharides isolated from algae have become attractive in the biomedical area because of their numerous bioactivities. Studies have found that FO was an efficient inhibitor of  $\alpha$ -amylase and  $\alpha$ -glucosidase (Kim KT et al., 2014). The structural changes, molecular weight and concentrations of FO may result in the seasonal variation of  $\alpha$ -amylase and  $\alpha$ -glucosidase inhibitory activity by FO. Additionally, the structure of FO varies depending on the alga source and could impact the enzyme activity (Kim KT et al., 2014; Pozharitskaya ON et al., 2020). The pharmacokinetics and tissue distribution of this agent are crucial in understanding its biological activity. The microdetermination of fucoidan distribution is one of the key problems in pharmacokinetic studies. Studies have shown that after oral administration, serum levels of FO were increased at 6 h and 9 h (Pozharitskaya ON et al., 2018). The recently described observations of the clinical efficacy of orally administered FO for chronic renal failure indicate probable systemic uptake in humans (Tokita Y et al., 2010). Systemic uptake after oral delivery indicates the potential for additional clinical applications in the future, perhaps including the control of thrombosis. FO's distinctive biological structure is thought to

be the cause of its exceptional biological function. Antioxidant, antitumor, anticoagulant, antithrombotic, immunomodulatory, antiviral, and anti-inflammatory processes are some of the traditional biological processes associated with FO (Luthuli et al., 2019). According to recent research, FO could decrease neutrophil and macrophage accumulation, the level of inflammatory cytokines and lung fibrosis (Yu HH et al., 2018). Furthermore, another study showed that FO could increase the expression and activity of the Sirt 1 protein by upregulating the expression of USP22 (Yu et al., 2020). On the other hand, by downregulating USP22, the RAS system can reduce Sirt 1 protein expression (Wang et al., 2021). In our study, after treatment with FO, the expression of USP22 was markedly increased, and the increase in USP22 increased the activity of Sirt1 and decreased myocardial cell death. FO also reduced macrophage accumulation, oxidative stress and fibrosis in Ang II-induced hypertrophic cardiac remodeling. This approach provides a potential targeted strategy to treat heart failure.

However, our research still has many limitations. We used a single dose of FO treatment, and ubiquitinated Sirt1 expression after USP22 knockdown needs to be examined. We will study more details of FO in our future research.

## Data availability statement

The original contributions presented in the study are included in the article/Supplementary Materials, further inquiries can be directed to the corresponding author.

## Ethics statement

The animal study was reviewed and approved by the Animal Experimental Ethics Committee of Dalian Medical University, and extensive efforts were made to minimize the distress of the included animals.

## Author contributions

SW and JB carried out blood pressure and Heart function of each mice and the histopathology and immunohistochemical analysis in Ang II-infused cardiac remodeling models; YC provided the pharmaceuticals of fucoidan and the protocol of FO, and carried out Western blot analysis, RNA extraction and RT-qPCR experiments; WQ carried out the Western blot analysis, RNA extraction and RT-qPCR experiments; JL wrote the article, revised the manuscript, and approved the unpublished version. All authors contributed to the article and approved the submitted version.

## Funding

The work was funded by funds from the Natural Science Foundation of Liaoning Provincial (2021-BS-208) and the National Natural Science Foundation of China (81900223 to JL; 82103667 to YC).



## Conflict of interest

The authors declare that the research was conducted in the absence of any commercial or financial relationships that could be construed as a potential conflict of interest.

## Publisher's note

All claims expressed in this article are solely those of the authors and do not necessarily represent those of their affiliated

organizations, or those of the publisher, the editors and the reviewers. Any product that may be evaluated in this article, or claim that may be made by its manufacturer, is not guaranteed or endorsed by the publisher.

## Supplementary material

The Supplementary Material for this article can be found online at: <https://www.frontiersin.org/articles/10.3389/fphar.2023.1164333/full#supplementary-material>

## References

- Bai, J., Yin, L., Yu, W. J., Zhang, Y. L., Lin, Q. Y., and Li, H. H. (2022). Angiotensin II induces cardiac edema and hypertrophic remodeling through lymphatic-dependent mechanisms. *Oxid. Med. Cell Longev.* 2022, 5044046. doi:10.1155/2022/5044046
- Benigni, A., Cassis, P., and Remuzzi, G. (2010). Angiotensin II revisited: New roles in inflammation, immunology and aging. *EMBO Mol. Med.* 2 (7), 247–257. doi:10.1002/emmm.201000080
- Diamond, J. A., and Phillips, R. A. (2005). Hypertensive heart disease. *Hypertens. Res.* 28 (3), 191–202. doi:10.1291/hypres.28.191
- Eletr, Z. M., and Wilkinson, K. D. (2014). Regulation of proteolysis by human deubiquitinating enzymes. *Biochim. Biophys. Acta* 1843 (1), 114–128. doi:10.1016/j.bbamer.2013.06.027
- Fitton, H. J., Stringer, D. S., Park, A. Y., and Karpinić, S. N. (2019). Therapies from fucoidan: New developments. *Mar. Drugs* 17 (10), 571. doi:10.3390/md17100571
- Gu, Y. H., Ren, K. W., Wang, Y., Wang, S. H., Yu, X. H., Xu, L. W., et al. (2022). Administration of USP7 inhibitor P22077 inhibited cardiac hypertrophy and remodeling in Ang II-induced hypertensive mice. *Front. Pharmacol.* 13, 1021361. doi:10.3389/fphar.2022.1021361
- Kim, K. T., Rioux, L. E., and Turgeon, S. L. (2014). Alpha-amylase and alpha-glucosidase inhibition is differentially modulated by fucoidan obtained from *Fucus vesiculosus* and *Ascophyllum nodosum*. *Phytochemistry* 98, 27–33. doi:10.1016/j.phytochem.2013.12.003
- Kliza, K., and Husnjak, K. (2020). Resolving the complexity of ubiquitin networks. *Front. Mol. Biosci.* 7, 21. doi:10.3389/fmolb.2020.00021
- Komander, D. (2010). Mechanism, specificity and structure of the deubiquitinases. *Subcell. Biochem.* 54, 69–87. doi:10.1007/978-1-4419-6676-6\_6
- Komander, D., and Rape, M. (2012). The ubiquitin code. *Annu. Rev. Biochem.* 81, 203–229. doi:10.1146/annurev-biochem-060310-170328
- Lev-Ran, A., and Porta, M. (2005). Salt and hypertension: A phylogenetic perspective. *Diabetes Metab. Res. Rev.* 21 (2), 118–131. doi:10.1002/dmrr.539
- Li, J., Wang, S., Bai, J., Yang, X. L., Zhang, Y. L., Che, Y. L., et al. (2018). Novel role for the immunoproteasome subunit PSMB10 in angiotensin II-induced atrial fibrillation in mice. *Hypertension* 71 (5), 866–876. doi:10.1161/HYPERTENSIONAHA.117.10390
- Li, J., Wang, S., Zhang, Y. L., Bai, J., Lin, Q. Y., Liu, R. S., et al. (2019). Immunoproteasome subunit  $\beta 5i$  promotes Ang II (angiotensin II)-induced atrial fibrillation by targeting ATRAP (Ang II type I receptor-associated protein) degradation in mice. *Hypertension* 73 (1), 92–101. doi:10.1161/HYPERTENSIONAHA.118.11813
- Li, W., and Ye, Y. (2008). Polyubiquitin chains: Functions, structures, and mechanisms. *Cell Mol. Life Sci.* 65 (15), 2397–2406. doi:10.1007/s00018-008-8090-6
- Lin, Z., Yang, H., Kong, Q., Li, J., Lee, S. M., Gao, B., et al. (2012). USP22 antagonizes p53 transcriptional activation by deubiquitinating Sirt1 to suppress cell apoptosis and is required for mouse embryonic development. *Mol. Cell* 46 (4), 484–494. doi:10.1016/j.molcel.2012.03.024
- Liu, M., Hansen, P. E., and Lin, X. (2011). Bromophenols in marine algae and their bioactivities. *Mar. Drugs* 9 (7), 1273–1292. doi:10.3390/md9071273
- Luo, G., Jian, Z., Zhu, Y., Chen, B., Ma, R., et al. (2019). Sirt1 promotes autophagy and inhibits apoptosis to protect cardiomyocytes from hypoxic stress. *Int. J. Mol. Med.* 43 (5), 2033–2043. doi:10.3892/ijmm.2019.4125
- Luthuli, S., Wu, S., Cheng, Y., Zheng, X., Wu, M., and Tong, H. (2019). Therapeutic effects of fucoidan: A review on recent studies. *Mar. Drugs* 17 (9), 487. doi:10.3390/md17090487
- Ma, S., Sun, L., Wu, W., Wu, J., Sun, Z., and Ren, J. (2020). USP22 protects against myocardial ischemia-reperfusion injury via the SIRT1-p53/slc7a11-dependent inhibition of ferroptosis-induced cardiomyocyte death. *Front. Physiol.* 11, 551318. doi:10.3389/fphys.2020.551318
- Maki, K. C., Galant, R., Samuel, P., Tesser, J., Witchger, M. S., Ribaya-Mercado, J. D., et al. (2007). Effects of consuming foods containing oat beta-glucan on blood pressure, carbohydrate metabolism and biomarkers of oxidative stress in men and women with elevated blood pressure. *Eur. J. Clin. Nutr.* 61 (6), 786–795. doi:10.1038/sj.ejcn.1602562
- Melo-Cardenas, J., Zhang, Y., Zhang, D. D., and Fang, D. (2016). Ubiquitin-specific peptidase 22 functions and its involvement in disease. *Oncotarget* 7 (28), 44848–44856. doi:10.18632/oncotarget.8602
- Ou, S., Kwok, K., Li, Y., and Fu, L. (2001). *In vitro* study of possible role of dietary fiber in lowering postprandial serum glucose. *J. Agric. Food Chem.* 49 (2), 1026–1029. doi:10.1021/jf000574n
- Pozharitskaya, O. N., Obluchinskaya, E. D., and Shikov, A. N. (2020). Mechanisms of bioactivities of fucoidan from the Brown seaweed *Fucus vesiculosus* L. Of the barents sea. *Mar. Drugs* 18 (5), 275. doi:10.3390/md18050275
- Pozharitskaya, O. N., Shikov, A. N., Faustova, N. M., Obluchinskaya, E. D., Kosman, V. M., Vuorela, H., et al. (2018). Pharmacokinetic and tissue distribution of fucoidan from *Fucus vesiculosus* after oral administration to rats. *Mar. Drugs* 16 (4), 132. doi:10.3390/md16040132
- Shimizu, I., and Minamino, T. (2016). Physiological and pathological cardiac hypertrophy. *J. Mol. Cell Cardiol.* 97, 245–262. doi:10.1016/j.jmcc.2016.06.001
- Slivnick, J., and Lampert, B. C. (2019). Hypertension and heart failure. *Heart Fail Clin.* 15 (4), 531–541. doi:10.1016/j.hfc.2019.06.007
- Tokita, Y., Nakajima, K., Mochida, H., Iha, M., and Nagamine, T. (2010). Development of a fucoidan-specific antibody and measurement of fucoidan in serum and urine by sandwich ELISA. *Biosci. Biotechnol. Biochem.* 74 (2), 350–357. doi:10.1271/bbb.90705
- Wang, W., Wang, L., Yang, M., Wu, C., Lan, R., et al. (2021). Circ-SIRT1 inhibits cardiac hypertrophy via activating SIRT1 to promote autophagy. *Cell Death Dis.* 12 (11), 1069. doi:10.1038/s41419-021-04059-y
- Yu, H. H., Chengchuan Ko, E., Chang, C. L., Yuan, K. S., Wu, A. T. H., Shan, Y. S., et al. (2018). Fucoidan inhibits radiation-induced pneumonitis and lung fibrosis by reducing inflammatory cytokine expression in lung tissues. *Mar. Drugs* 16 (10), 392. doi:10.3390/md16100392
- Yu, W. C., Huang, R. Y., and Chou, T. C. (2020). Oligo-fucoidan improves diabetes-induced renal fibrosis via activation of sirt-1, GLP-1R, and Nrf2/HO-1: An *in vitro* and *in vivo* study. *Nutrients* 12 (10), 3068. doi:10.3390/nu12103068
- Zhang, S. M., Xie, Z. P., Xu, M. L., and Shi, L. F. (2015). Cardioprotective effects of fucoidan against hypoxia-induced apoptosis in H9c2 cardiomyoblast cells. *Pharm. Biol.* 53 (9), 1352–1357. doi:10.3109/13880209.2014.982298
- Zhou, L., Ma, B., and Han, X. (2016). The role of autophagy in angiotensin II-induced pathological cardiac hypertrophy. *J. Mol. Endocrinol.* 57 (4), R143–R152. doi:10.1530/JME-16-0086



## OPEN ACCESS

## EDITED BY

Min Zhang,  
King's College London, United Kingdom

## REVIEWED BY

Guang Li,  
Southwest Medical University, China  
Jun Yu,  
Temple University, United States

## \*CORRESPONDENCE

Miao Wang,  
✉ miao.wang@pumc.edu.cn

RECEIVED 24 April 2023

ACCEPTED 22 June 2023

PUBLISHED 04 July 2023

## CITATION

Peng Z, Chen H and Wang M (2023),  
Identification of the biological processes,  
immune cell landscape, and hub genes  
shared by acute anaphylaxis and ST-  
segment elevation myocardial infarction.  
*Front. Pharmacol.* 14:1211332.  
doi: 10.3389/fphar.2023.1211332

## COPYRIGHT

© 2023 Peng, Chen and Wang. This is an  
open-access article distributed under the  
terms of the [Creative Commons  
Attribution License \(CC BY\)](#). The use,  
distribution or reproduction in other  
forums is permitted, provided the original  
author(s) and the copyright owner(s) are  
credited and that the original publication  
in this journal is cited, in accordance with  
accepted academic practice. No use,  
distribution or reproduction is permitted  
which does not comply with these terms.

# Identification of the biological processes, immune cell landscape, and hub genes shared by acute anaphylaxis and ST-segment elevation myocardial infarction

Zekun Peng<sup>1</sup>, Hong Chen<sup>1</sup> and Miao Wang<sup>1,2\*</sup>

<sup>1</sup>State Key Laboratory of Cardiovascular Disease, Fuwai Hospital, National Center for Cardiovascular Diseases, Chinese Academy of Medical Sciences and Peking Union Medical College, Beijing, China,

<sup>2</sup>Clinical Pharmacology Center, Fuwai Hospital, National Center for Cardiovascular Diseases, Chinese Academy of Medical Sciences and Peking Union Medical College, Beijing, China

**Background:** Patients with anaphylaxis are at risk for ST-segment elevation myocardial infarction (STEMI). However, the pathological links between anaphylaxis and STEMI remain unclear. Here, we aimed to explore shared biological processes, immune effector cells, and hub genes of anaphylaxis and STEMI.

**Methods:** Gene expression data for anaphylactic (GSE69063) and STEMI (GSE60993) patients with corresponding healthy controls were pooled from the Gene Expression Omnibus database. Differential expression analysis, enrichment analysis, and CIBERSORT were used to reveal transcriptomic signatures and immune infiltration profiles of anaphylaxis and STEMI, respectively. Based on common differentially expressed genes (DEGs), Gene Ontology analysis, cytoHubba algorithms, and correlation analyses were performed to identify biological processes, hub genes, and hub gene-related immune cells shared by anaphylaxis and STEMI. The robustness of hub genes was assessed in external anaphylactic (GSE47655) and STEMI (GSE61144) datasets. Furthermore, a murine model of anaphylaxis complicated STEMI was established to verify hub gene expressions. The logistic regression analysis was used to evaluate the diagnostic efficiency of hub genes.

**Results:** 265 anaphylaxis-related DEGs were identified, which were associated with immune-inflammatory responses. 237 STEMI-related DEGs were screened, which were involved in innate immune response and myeloid leukocyte activation. M0 macrophages and dendritic cells were markedly higher in both anaphylactic and STEMI samples compared with healthy controls, while CD4<sup>+</sup> naïve T cells and CD8<sup>+</sup> T cells were significantly lower. Enrichment analysis of 33 common DEGs illustrated shared biological processes of anaphylaxis and STEMI, including cytokine-mediated signaling pathway, response to reactive oxygen species, and positive regulation of defense response. Six hub genes were identified, and their expression levels were positively correlated with M0 macrophage abundance and negatively correlated with CD4<sup>+</sup> naïve T cell abundance. In external anaphylactic and STEMI samples, five hub genes (IL1R2, FOS, MMP9, DUSP1, CLEC4D) were confirmed to be markedly upregulated. Moreover,

experimentally induced anaphylactic mice developed impaired heart function featuring STEMI and significantly increased expression of the five hub genes. DUSP1 and CLEC4D were screened as blood diagnostic biomarkers of anaphylaxis and STEMI based on the logistic regression analysis.

**Conclusion:** Anaphylaxis and STEMI share the biological processes of inflammation and defense responses. Macrophages, dendritic cells, CD8<sup>+</sup> T cells, and CD4<sup>+</sup> naïve T cells constitute an immune cell population that acts in both anaphylaxis and STEMI. Hub genes (DUSP1 and CLEC4D) identified here provide candidate genes for diagnosis, prognosis, and therapeutic targeting of STEMI in anaphylactic patients.

#### KEYWORDS

anaphylaxis, STEMI, immune response, inflammation, hub gene

## 1 Introduction

Anaphylaxis is a severe hypersensitivity reaction that occurs rapidly after allergen irritation (medications, foods, insect venom) to sensitized individuals. It typically manifests with severe pathophysiological symptoms, such as respiratory distress, angioedema, and myocardial depression (LoVerde et al., 2018; Cardona et al., 2020). The prevalence of anaphylaxis among U.S. residents is estimated at 1.6%–5.1% (Wood et al., 2014), and the mortality rate for hospitalized patients is 0.5%–1% (Turner et al., 2020). In most cases, anaphylaxis is initiated by the allergen-IgE/IgG complex-induced activation of immune effector cells, followed by the release of inflammatory mediators that cause vascular hyperpermeability, bronchoconstriction, and airway edema (Finkelman et al., 2016; LoVerde et al., 2018).

Anaphylactic reactions may trigger adverse cardiovascular events (Abdelghany et al., 2017), such as ST-segment elevation myocardial infarction (STEMI) (Engheta et al., 2021), a severe form of heart attack with high mortality rate. A nationwide epidemiological study in the United States reported that among 235,420 patients hospitalized for allergy, hypersensitivity, or anaphylaxis, 0.2% of patients experienced STEMI (Desai et al., 2019). Acute STEMI following anaphylaxis is associated with allergic mediators-induced coronary spasms, plaque erosion/rupture, or stent thrombosis (Li et al., 2018; Sakaue et al., 2020; Yamamoto et al., 2022). Inflammatory responses elicited by mast cell-released vasoactive substances appears to be involved in this process and aggravate myocardial injury (Galli and Tsai, 2012; Abdelghany et al., 2017; Li et al., 2018; Yamamoto et al., 2022). Clinically, anaphylaxis complicated with STEMI is one of the most serious emergencies without effective predictors and medications. Due to severe cardiac ischemia and output depression, anaphylaxis-related STEMI might eventually progress to cardiovascular collapse and cause a fatal outcome. However, key molecules and immune cell subsets that drive the development of this complication have not been fully characterized.

Transcriptomic analysis has become an emerging approach for uncovering the complex pathophysiological processes in anaphylaxis and STEMI (Rung and Brazma, 2013; Xu and Yang, 2021; Rijavec et al., 2022). The common biological processes and signal transduction pathways of anaphylaxis and STEMI might indicate the underlying mechanisms for the coexistence of these two diseases. In particular, due to the ease of access and preservation of peripheral blood samples, in-depth analysis of gene expression

profiles and screening hub genes in diseased specimens may allow identification of the whole blood gene signature shared by anaphylaxis and STEMI, facilitating precise diagnosis, prediction and drug discovery for anaphylaxis complicated STEMI.

Herein, we analyzed whole blood transcriptomic datasets of anaphylaxis and STEMI patients and identified the pathological processes, immune effector cell subsets, and hub genes associated with both anaphylaxis and STEMI, and we also established a mouse model of anaphylaxis complicated with STEMI and further validated the hub genes. The genomic signatures identified here may provide novel insights into the pathogenesis of anaphylaxis-related STEMI.

## 2 Materials and methods

### 2.1 Microarray data collection

The microarray data of anaphylactic patients, STEMI patients, and corresponding healthy controls were pooled from the public GEO database (<https://www.ncbi.nlm.nih.gov/geo/>). Datasets that satisfied the following inclusion criteria were selected: (1) gene expression profiles were based on human specimens; (2) all samples were obtained from peripheral blood; (3) the datasets included disease cases and healthy controls. GSE69063 (anaphylaxis) and GSE60993 (STEMI) datasets that meet the above criteria were used in the present study. GSE69063 contains 17 anaphylactic patients and 10 healthy controls whose blood specimens were collected 1 h after arriving at the emergency department. GSE60993 dataset consists of 7 STEMI patients and 7 healthy individuals, and peripheral blood from STEMI patients was obtained within 4 h after the attack of chest pain. Details of these datasets were summarized in [Supplementary Table S1](#).

### 2.2 DEG screening

DEGs between case and control groups were screened by GEO2R (an official web application in NCBI that helps analyze GEO data, [www.ncbi.nlm.nih.gov/geo/ge2r](http://www.ncbi.nlm.nih.gov/geo/ge2r)) (Barrett et al., 2013), with screening criteria set as  $|\log_{2}(\text{fold change})| > 1$  and adjusted  $p$ -value  $< 0.05$ . Probe sets without corresponding gene symbols were removed and genes with multiple probe sets were averaged. The volcano map was drawn with ggplot2 R package (<https://ggplot2.tidyverse.org>). TBtools software was applied to draw heatmaps to

visualize the differential gene expression profiles between case and control groups (Chen et al., 2020).

## 2.3 Enrichment analysis of DEGs

Gene Ontology (GO) enrichment analysis and Kyoto Encyclopedia of Genes and Genomes (KEGG) pathway analysis were performed with the clusterProfiler package (Yu et al., 2012). The top 20 terms of biological process (BP) and top 5 KEGG terms were visualized with bubble charts by ggplot2 R package.

## 2.4 Analysis of immune cell distribution

The composition and distribution of immune cells in anaphylactic samples (GSE69063), STEMI samples (GSE60993), and normal samples were evaluated by CIBERSORTx (<https://cibersortx.stanford.edu/>) (Newman et al., 2015), which is based on a set of feature gene expression data from 22 cell subtypes (LM22 dataset). The fraction of these cell populations in diseased and healthy groups were compared using the ggpubr R package (Wilcoxon test) (<https://CRAN.R-project.org/package=ggpubr>).

## 2.5 Protein-protein interaction network construction and hub gene identification

STRING database was applied to predict PPI (<https://cn.string-db.org/>) (Franceschini et al., 2013) and a combined score >0.4 was considered statistically significant. Cytoscape software (Shannon et al., 2003) was used to visualize PPI networks. DEGs in the intersection of six algorithms (DMNC, Stress, MCC, Degree, Closeness, and Radiality) were determined as hub genes. The co-expression and co-localization network of hub genes was constructed and visualized by GeneMANIA (<http://www.genemania.org/>) (Warde-Farley et al., 2010).

## 2.6 Verification of hub gene expression in GSE47655 and GSE61144

Hub gene expression was confirmed in the GSE47655 (anaphylaxis) and GSE61144 (STEMI) datasets. GSE47655 contains 6 anaphylactic patients and 6 healthy controls. GSE60993 dataset consists of 7 STEMI patients and 10 healthy subjects. All samples from GSE47655 and GSE61144 were obtained from peripheral blood. Details of these datasets were shown in [Supplementary Table S1](#). The differences in mRNA expression of hub genes between the diseased and healthy groups were compared using Student's *t*-test and visualized using the ggplot2 package.

## 2.7 Correlation analysis

Pearson's correlation analysis between the expression of hub genes and the abundance of immune effector cells was carried out to further explore the immunomodulatory mechanisms.

## 2.8 Prediction of transcription factor and drug-hub gene interaction

TRRUST (<https://www.grnpedia.org/trrust/>) (Han et al., 2018), a database that provides transcription factor-target regulatory relationships, was applied to predict transcription factors that regulate hub gene expression. The expression levels of transcription factors predicted by TRRUST were confirmed in GSE69063 (anaphylaxis) and GSE60993 (STEMI), and the differences between diseased and healthy groups were compared using *t*-test. ChEA3 (ChIP-X Enrichment Analysis, version 3) platform provides transcription factor enrichment analysis and integrates RNA-seq data from GTEx, TCGA, and ARCHS4, as well as CHIP-seq data from ENCODE and ReMap (Keenan et al., 2019). The hub gene list was submitted to ChEA3, and transcription factors common to those predicted by TRRUST were identified. Based on the MeanRank method, transcription factors were ranked according to their composite scores. DGIdb (Drug-gene interaction database, <http://www.dgldb.org>) was utilized to predict the drug-hub gene interaction (Freshour et al., 2021).

## 2.9 Murine model

C57BL/6 mice were obtained from the Charles River Laboratories (Beijing, China). The murine model used in this study was based on an active systemic anaphylaxis model described previously (Jonsson et al., 2011) with modifications. Six-week-old female mice were sensitized subcutaneously on day 0 with bovine serum albumin (BSA, 50 µg per mouse, Sigma-Aldrich, United States) in complete Freund adjuvant (CFA, Sigma-Aldrich, United States) and boosted on day 7 and day 14 with 50 µg BSA in incomplete Freund adjuvant (IFA, Sigma-Aldrich, United States). One week after the last sensitization, mice were intravenously injected with 15 µg BSA to elicit systemic anaphylaxis. After BSA challenge, the temperature was monitored every 10 min with a rectal thermometer (TH212, China), and the severity of anaphylaxis was scored every 10 min on a scale of 0–4 based on the grading system described previously (Cloutier et al., 2018), score 0: normal; score 1: slow motions; score 2: impaired mobility, still reacting to touch; score 3: immobilized and do not react to touch; score 4: death.

## 2.10 Electrocardiogram recording

When fully anesthetized with inhalant isoflurane (RWD, China), mice were immobilized in a supine position with electrodes implanted subcutaneously in the limbs. The Animal Bio Amp device (ADInstruments, Australia) and LabChart software were used to acquire and record the lead II ECGs of naïve and model mice.

## 2.11 Heart function assessment

One day prior to ultrasound, hair around the chest wall was carefully removed using depilatory cream (Nair, United States).

Gene	Forward sequence (5'-3')	Reverse sequence (5'-3')
IL1R2	TCCGGGTCAAAGGAACAACC	CCCAGAAACACTTTGCACGG
FOS	TACTACCATTCCCCAGCCGA	GCTGTCACCGTGGGGATAAA
MMP9	TAGATCATTCCAGCGTGCCG	GCCTTGGGTCAGGCTTAGAG
DUSP1	ATCGTGCCCAACGCTGAA	GAAAACGCTTCATATCCTCCTTGG
CLEC4D	ACTGATCCCTTGCGTCTTCG	CGGATGCACGTTACTCTCGT
CREM	TGGAAACAGTTGAATCACAGCA	ATCTTGGGAATACCAGGCACA
SRF	GGCCGCGTGAAGATCAAGAT	CACATGGCCTGTCTCACTGG
STAT6	CTCTGTGGGGCCTAATTTCCTCA	CATCTGAACCGACCAGGAAGT
STAT3	CAATACCATTGACCTGCCGAT	GAGCGACTCAAAGTGCCTT
SP1	GCCGCTTTTCTCAGACTC	TTGGGTGACTCAATTCTGCTG
$\beta$ -Actin	TTACTGCTCTGGCTCCTAGC	CAGCTCAGTAACAGTCCGC

Mice were anesthetized by inhalant isoflurane (RWD, China), at a concentration of 1.5%. When fully anesthetized, the mouse was positioned on the warm imaging platform ventral side up, and the medical ultrasonic gel was applied to the limb leads to generate ECG. Vevo2100 System (Visual Sonics, Canada) was used to record the transthoracic echocardiograms of naïve and model mice. The MS550D transducer was placed on the left sternal edge to obtain a parasternal short axis (PSAX) view. Left ventricular ejection fraction (EF) and fractional shortening (FS) were acquired from PSAX M-mode scans at the mid-papillary muscle level. Echocardiographic data were analyzed offline using Vevo Lab software and all measurements were averaged from 3 cardiac cycles.

## 2.12 Quantitative real-time polymerase Chain reaction

Total RNA was extracted from the peripheral blood of naïve mice and model mice using TRIzol reagent (Invitrogen, United States). PrimeScript™ RT Master Mix (TaKaRa, Japan) was utilized to convert the equivalent amount (500 ng) of total RNA into cDNA. The relative mRNA expression of target genes was quantified with the SYBR master mix (Yeast, China). All samples were normalized to the housekeeping gene  $\beta$ -Actin. Details of primers are listed as follows.

## 2.13 Logistic regression analysis

SPSS version 23.0 (SPSS Inc., Chicago, IL, United States) was used to perform univariate logistic analysis and construct multivariate logistic regression model with the expression profiles of hub genes as the continuous prediction variable and the physical condition (disease or not) as the categorical response variable. Statistically significant variables ( $p < 0.05$ ) were included in the multivariate logistic regression model using the backward LR method for variable selection. ROC curves were plotted and the

AUC value was calculated to evaluate the diagnostic efficiency of hub genes.

## 2.14 Statistics.

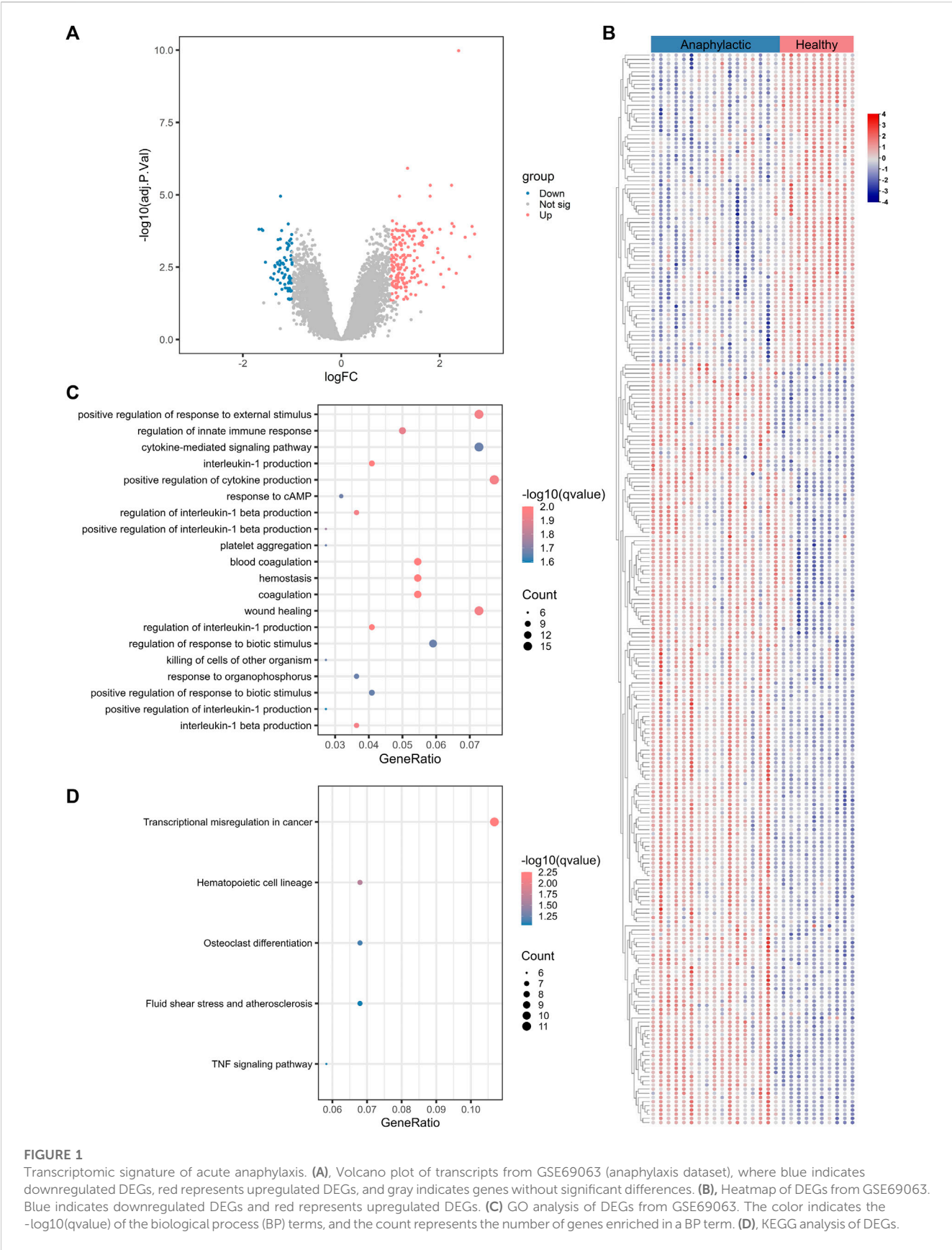
Statistical analysis was performed using R language (R Foundation for Statistical Computing, Vienna, Austria) and GraphPad Prism 8.0 software (GraphPad Software, San Diego, CA, United States). Data were evaluated for normal distribution using Shapiro-Wilk tests. If data were normally distributed and with similar variances, two-tailed Student's *t*-test (parametric) was used to compare the differences between two groups. For normally distributed data with unequal variances, unpaired *t*-test with Welch's correction was performed. For abnormally distributed data with unequal variances, Kolmogorov-Smirnov test (nonparametric) was used to determine differences between two groups. Pearson's correlation test was used to analyze the correlation between the expression of hub genes and the abundance of immune effector cells. Quantitative data are shown as mean  $\pm$  SEM. \* $p < 0.05$ , \*\* $p < 0.01$ , \*\*\* $p < 0.001$  were considered statistically significant.

## 3 Results

### 3.1 Transcriptomic signatures of acute anaphylaxis

The workflow of this study was shown in [Supplementary Figure S1](#). To characterize the gene expression profile of acute anaphylaxis, we compared mRNA expression in whole blood between anaphylactic patients and healthy subjects. Venous blood was collected at 1 hour after patients' arriving at the emergency department. A total of 265 genes were differentially expressed in the anaphylactic patients, among which 188 were upregulated and 77 were downregulated ([Figure 1A](#)). The heatmap revealed high heterogeneity of gene expression between anaphylactic patients and healthy controls ([Figure 1B](#)). To explore the pathogenesis of anaphylaxis, we





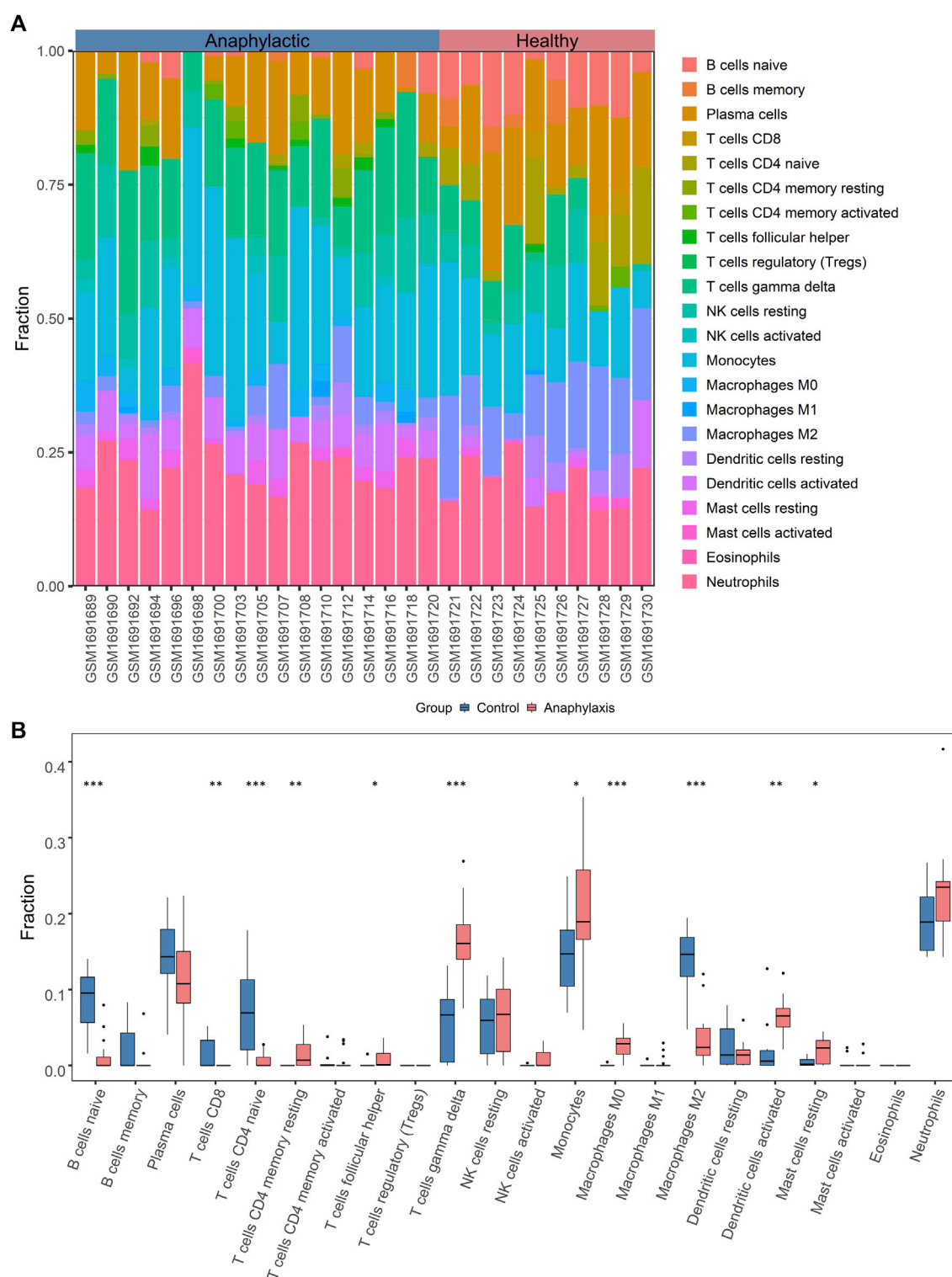
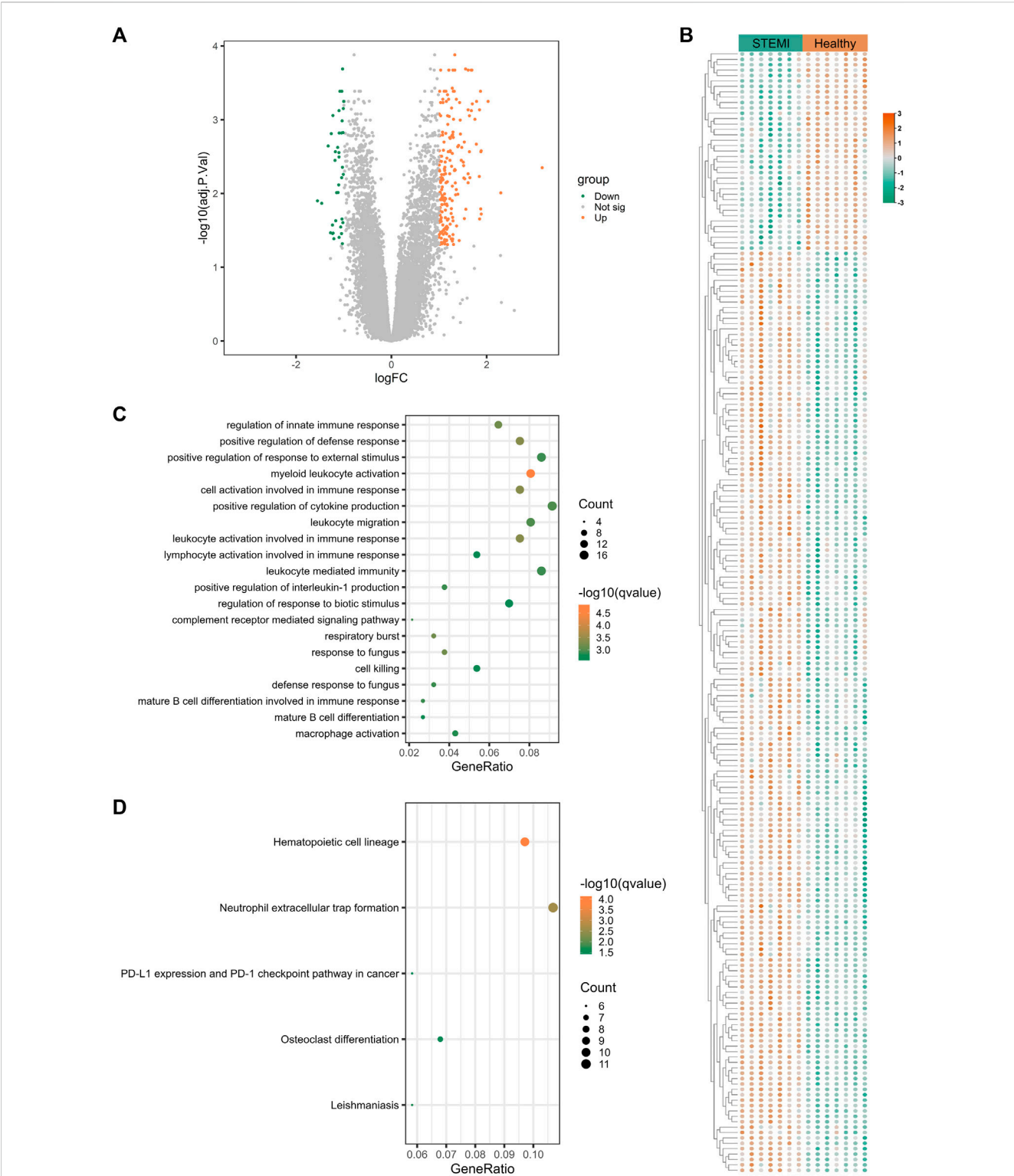


FIGURE 2

Immune cell characterization of acute anaphylaxis. (A), Histogram of the distribution of 22 immune cell subtypes in GSE69063 (anaphylaxis dataset). (B), Boxplot of the fraction of 22 immune cell subtypes in control and anaphylactic specimens.

performed GO and KEGG analysis, and profiling of biological processes and signaling pathways revealed the complex pathology of anaphylaxis. This disease was featured by marked activation of

immune-inflammatory responses, including positive regulation of response to external stimulus, regulation of innate immune response, cytokine-mediated signaling pathways, and positive



**FIGURE 3** Transcriptomic signature of STEMI. **(A)**, Volcano plot of transcripts from GSE60993 (STEMI dataset), where green indicates downregulated DEGs, orange represents upregulated DEGs, and gray indicates genes without significant differences. **(B)**, Heatmap of DEGs from GSE60993. Green indicates downregulated DEGs and orange represents upregulated DEGs. **(C)** GO enrichment analysis of DEGs from GSE60993. The color indicates  $-\log_{10}(\text{qvalue})$  of the BP terms, and the count represents the number of genes enriched in a BP term. **(D)**, KEGG analysis of DEGs from GSE60993.

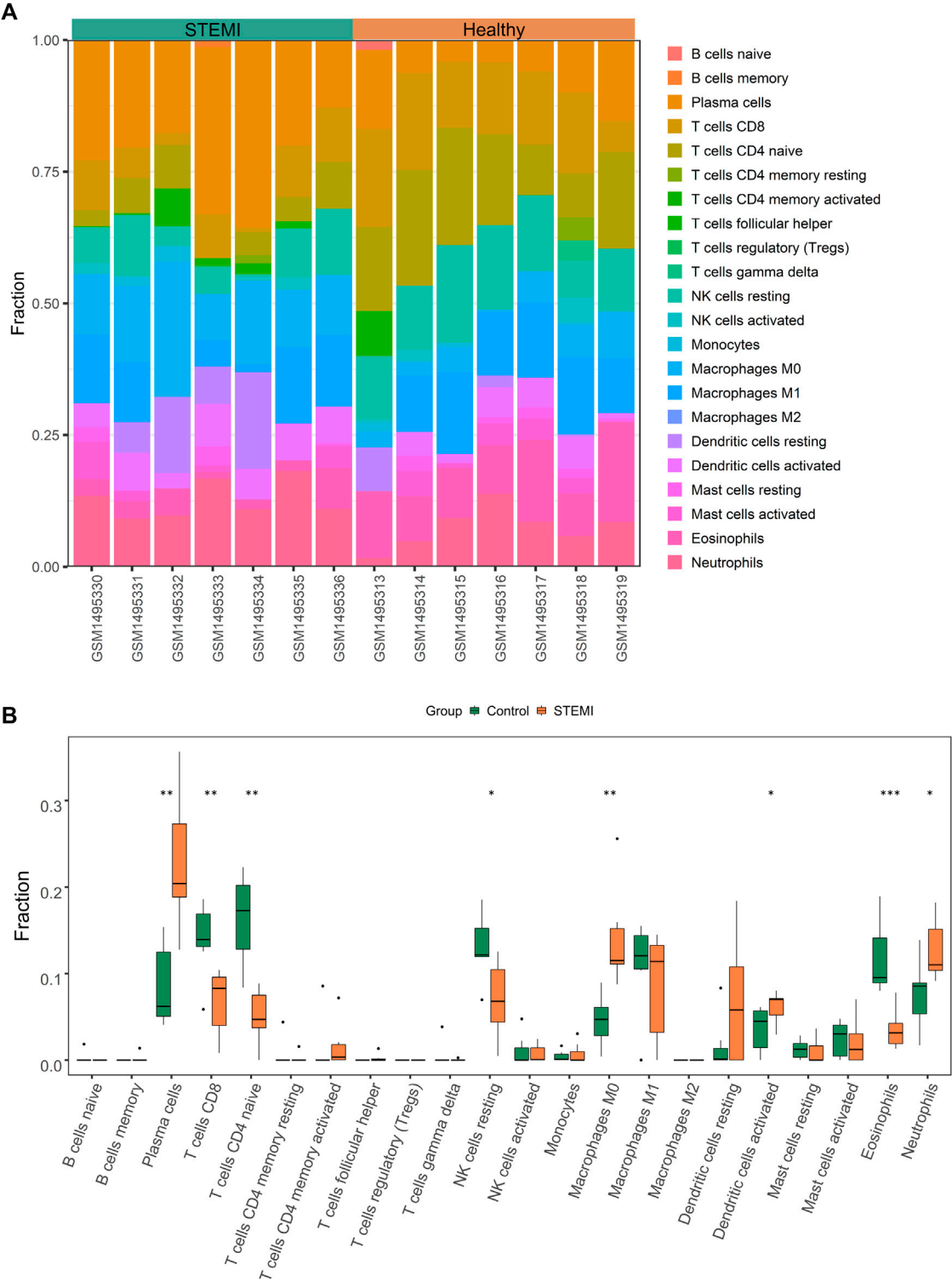


**FIGURE 4** Immune cell characterization of STEMI. **(A)**, Histogram of the composition and distribution of 22 immune cell subtypes in GSE60993 (STEMI dataset). **(B)**, Boxplot of the fraction of 22 immune cell subtypes in control and STEMI specimens.

regulation of cytokine production, especially interleukin-1 (Figure 1C). In addition, the blood coagulation cascade, platelet aggregation, hemostasis, and wound healing actively participated in

the development of anaphylaxis (Figure 1C). KEGG results illustrated that anaphylaxis-related DEGs were associated with transcriptional misregulation and hematopoietic cell lineage (Figure 1D).



### 3.2 Leukocyte composition of acute anaphylaxis

Since anaphylaxis was characterized by marked activation of immune-inflammatory responses, the CIBERSORT deconvolution algorithm was applied to further explore the details of immune cells involved in acute anaphylaxis. As shown in Figure 2A, a wide heterogeneity of immune cell distribution was observed in anaphylactic patients compared to healthy subjects. Among the 22 immune cell subtypes, CD4<sup>+</sup> memory T cells (resting), follicular helper T cells, and M0 macrophages were distributed only in anaphylactic samples but not in controls. Compared to the controls, anaphylactic specimens showed significantly increased levels of T cells gamma delta, monocytes, dendritic cells (activated) and mast cells (resting) and markedly decreased proportions of naïve B cells, CD8<sup>+</sup> T cells, CD4<sup>+</sup> naïve T cells, and M2 macrophages (Figure 2B).

### 3.3 Transcriptomic signatures of STEMI

To uncover the gene expression profiles of STEMI, we compared the mRNA expression in whole blood between STEMI patients and healthy subjects. A total of 237 STEMI-related DEGs were screened, including 199 upregulated and 38 downregulated genes, and these DEGs were visualized with the volcano plot and heatmap (Figures 3A,B). STEMI-related DEGs were primarily involved in the biological processes of innate immune response regulation, positive regulation of defense response, and positive regulation of response to external stimulus, indicating immune defense responses were essential in STEMI. Notably, myeloid leukocyte activation, positive regulation of cytokine production, leukocyte migration, and leukocyte-mediated immunity were critically involved in the development of STEMI (Figure 3C). KEGG analysis revealed that STEMI-related DEGs were associated with hematopoietic cell lineage, neutrophil extracellular trap formation, PD-L1 expression and PD-1 checkpoint pathway (Figure 3D).

### 3.4 Leukocyte composition of STEMI

As highlighted above, myeloid leukocyte activation and leukocyte-mediated immunity were essential in STEMI. To further elucidate components of immune cells key to STEMI pathology, we used CIBERSORTx to profile the composition and distribution of immune cell subtypes in STEMI and normal samples. As shown in Figure 4A, there were marked differences in the distribution of immune cells between these two groups. STEMI samples were featured by increased levels of plasma cells, M0 macrophages, dendritic cells (activated), and neutrophils, and by decreased infiltration of CD8<sup>+</sup> T cells, CD4<sup>+</sup> naïve T cells, NK cells (resting), and eosinophils (Figure 4B).

### 3.5 Identification of hub genes shared by anaphylaxis and STEMI

By extracting DEGs that were shared by anaphylaxis and STEMI, 33 common DEGs were identified (Figure 5A). The PPI network of these common DEGs contained 33 nodes and 24 edges, revealing

complex interactions among these molecules (Figure 5B). These common DEGs were enriched in the secretory granules, and their molecular functions include immune receptor activity, pattern recognition receptor activity, and cytokine receptor activity (Figure 5C), suggesting immune-inflammatory regulation is essential in both anaphylaxis and STEMI. Enrichment analysis of these common DEGs demonstrated that the shared biological processes of anaphylaxis and STEMI included cytokine-mediated signaling pathway, response to reactive oxygen species, positive regulation of defense response, regulation of immune effector process, and positive regulation of NF-kappa B transcription factor activity (Figure 5C). Taking the intersection of six algorithms (DMNC, Stress, MCC, Degree, Closeness, Radiality) in cytoHubba (Figure 5D), we found 6 hub genes shared by anaphylaxis and STEMI: IL1R2, S100A12, FOS, MMP9, DUSP1, and CLEC4D (Figure 5E). The description and major functions of hub genes are listed in Supplementary Table S2. These hub genes constituted an interactive network with a co-expression rate of 96.23% and a co-localization rate of 3.77% (Figure 5F). The prominent functions of hub genes included positive regulation of defense response, response to cadmium ion, cell chemotaxis, regulation of inflammatory response, regulation of apoptotic signaling pathway, and positive regulation of DNA-binding transcription factor activity (Figure 5F).

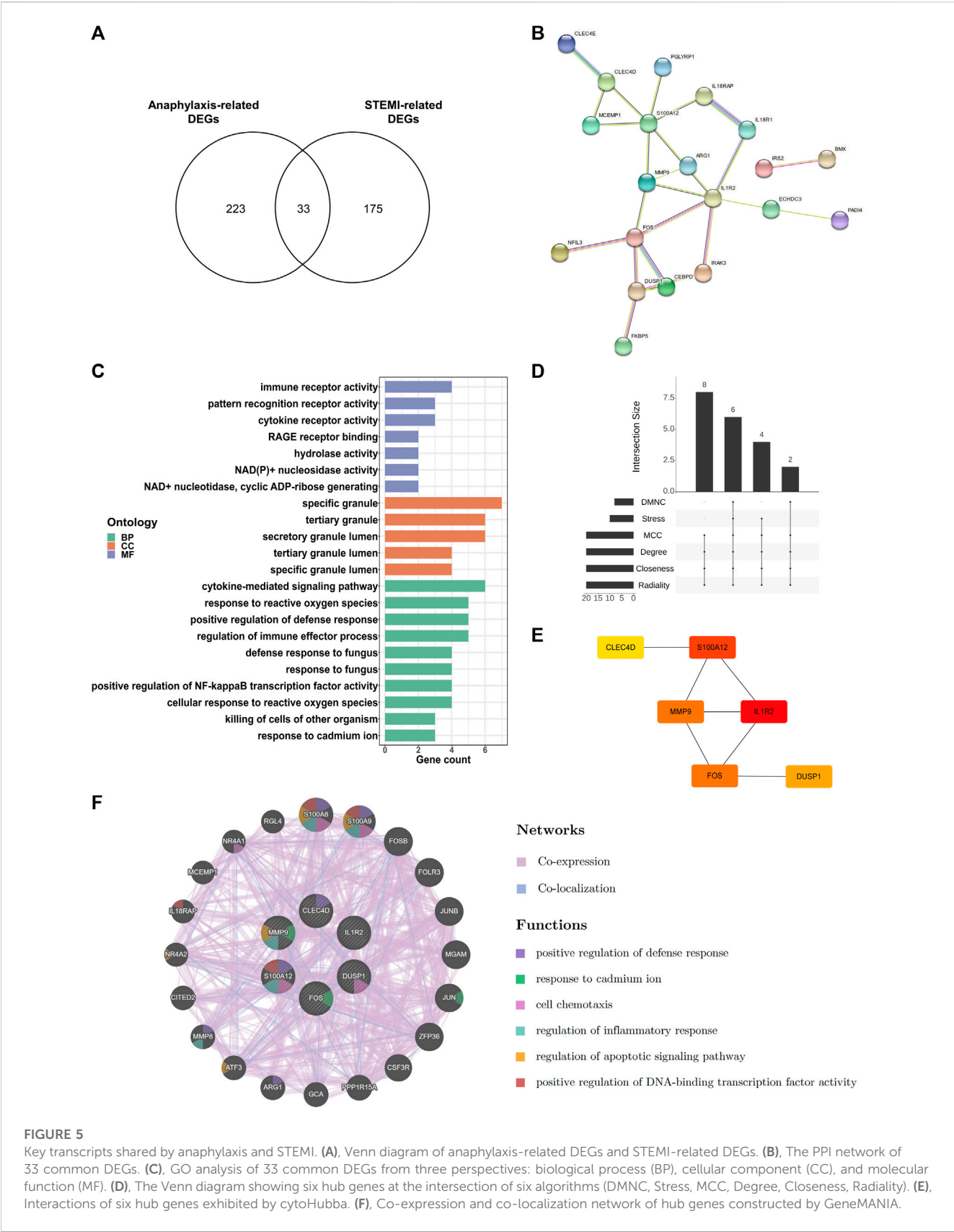
### 3.6 Correlation analysis between hub genes and immune cells

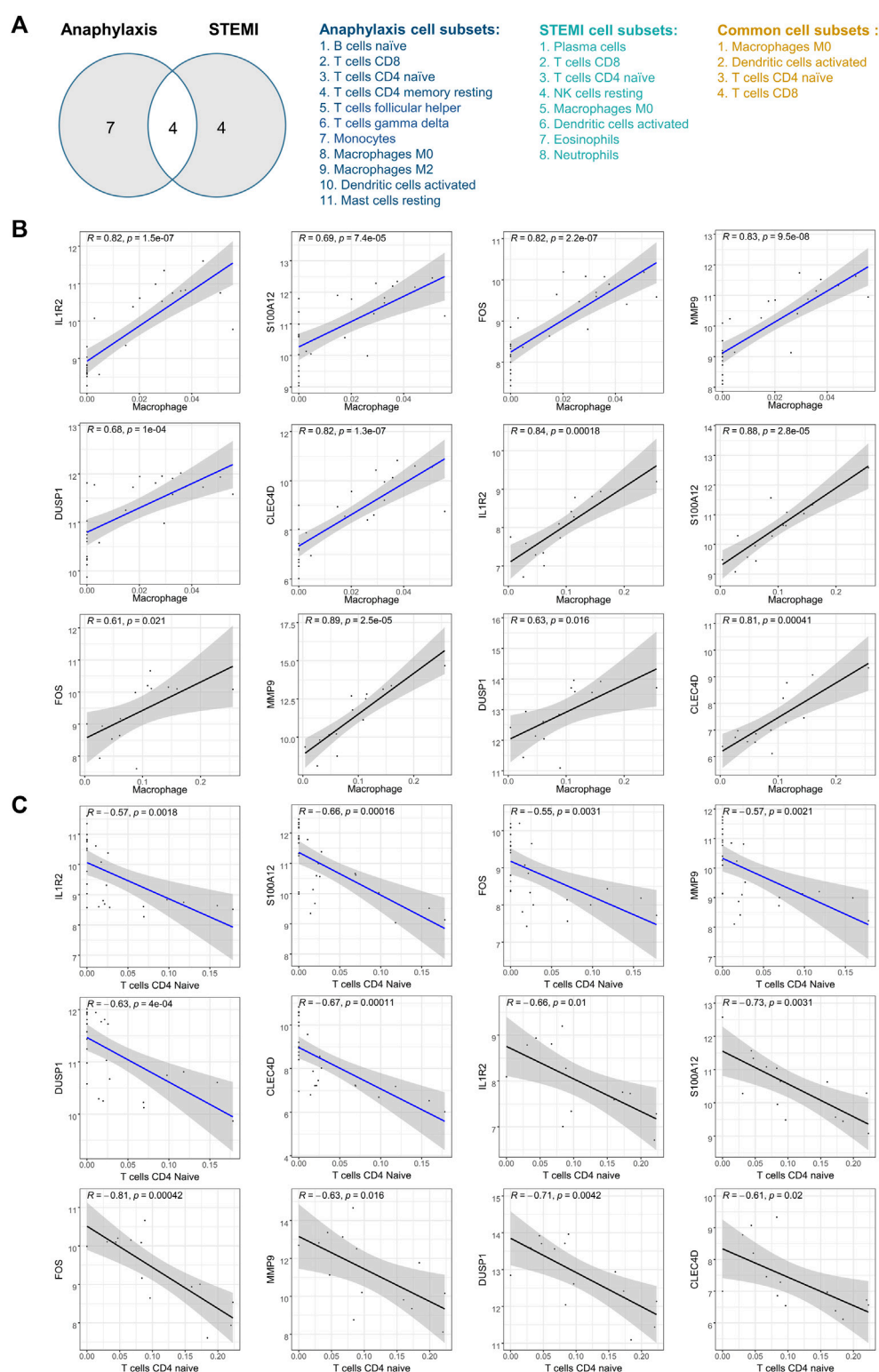
After taking the intersection and excluding the immune cells with opposite infiltration trends in anaphylactic and STEMI groups, M0 macrophages, activated dendritic cells, CD4<sup>+</sup> naïve T cells, and CD8<sup>+</sup> T cells were identified as immune effector cells associated with both anaphylaxis and STEMI (Figure 6A). To further investigate the association of hub genes and these immune cell subtypes, Pearson's correlation analysis was performed on the expression levels of hub genes and the abundance of immune cells in both anaphylactic and STEMI samples. The results illustrated that all hub genes were positively correlated with M0 macrophage ( $R > 0$ ,  $p < 0.05$ ), while negatively correlated ( $R < 0$ ,  $p < 0.05$ ) with CD4<sup>+</sup> naïve T cells (Figures 6B,C). FOS showed a significant positive correlation with activated dendritic cells, and CLEC4D had a significant negative correlation with CD8<sup>+</sup> T cells (Supplementary Figure S2A, B).

### 3.7 Verification of hub gene expression in external cohorts

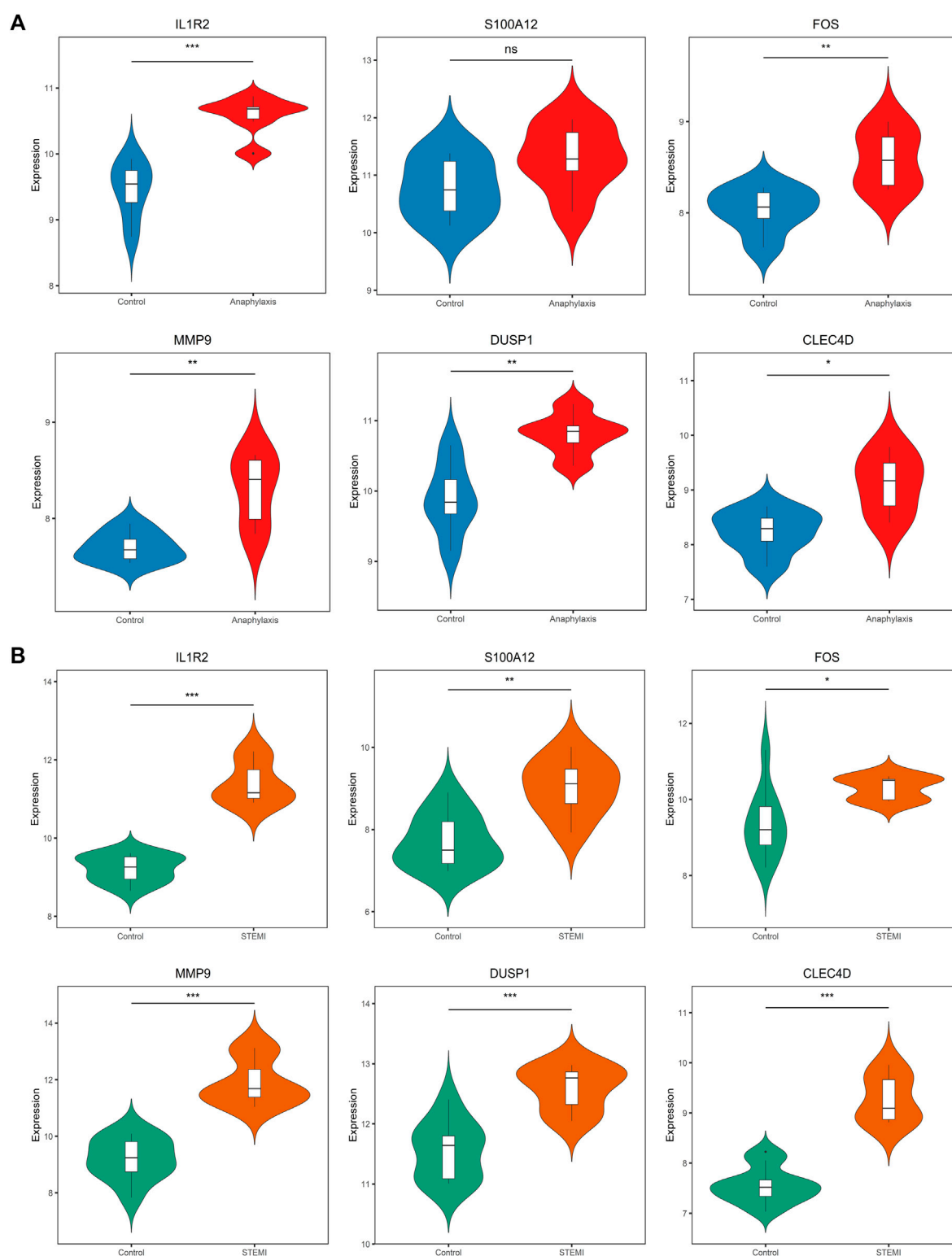
To assess the robustness of hub genes identified above, we analyzed their gene expression in external human microarray datasets (GSE47655 for anaphylaxis and GSE61144 for STEMI) (Supplementary Table S1). Compared with healthy controls, 5 hub genes (IL1R2, FOS, MMP9, DUSP1, CLEC4D) were significantly upregulated in anaphylactic samples, while S100A12 showed no statistical difference (Figure 7A). In STEMI samples, the expression of all hub genes (IL1R2, S100A12, FOS, MMP9, DUSP1, CLEC4D) was markedly higher than that of controls (Figure 7B).





**FIGURE 6**

Pearson's correlation analysis between hub genes and immune effector cells. **(A)**, Venn diagram of anaphylaxis-related cell subsets and STEMI-related cell subsets. **(B)**, Scatter diagrams of the correlations between hub gene expression and M0 macrophage abundance in anaphylactic samples (blue) and STEMI samples (black). **(C)**, Scatter diagrams of the correlations between hub gene expression and CD4<sup>+</sup> naïve T cell abundance in anaphylactic samples (blue) and STEMI samples (black).  $R > 0$  indicates positively correlated and  $R < 0$  indicates negatively correlated.  $p < 0.05$  was considered statistically significant.

**FIGURE 7**

Validation of hub gene expression in GSE47655 (anaphylaxis) and GSE61144 (STEMI) datasets. **(A)**, Validation of hub gene expression (IL1R2, S100A12, FOS, MMP9, DUSP1, CLEC4D) in GSE47655 (anaphylaxis dataset). **(B)**, Validation of hub gene expression (IL1R2, S100A12, FOS, MMP9, DUSP1, CLEC4D) in GSE61144 (STEMI dataset).

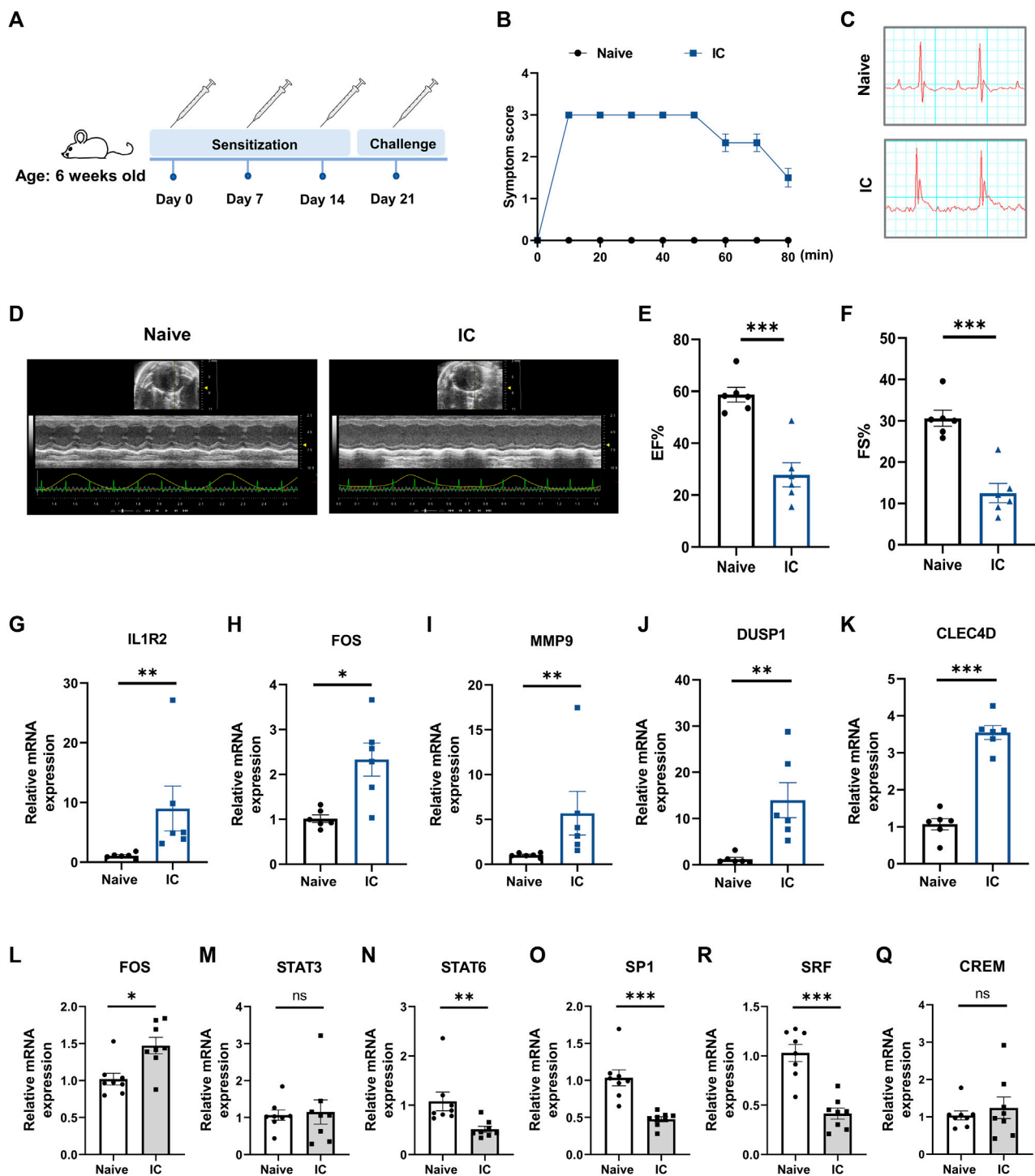


FIGURE 8

Verification of hub gene expression in a murine model of anaphylaxis complicated with STEMI. (A), Schematic diagram of the experimental protocol for establishing the murine model. 6-week-old female mice were subcutaneously sensitized on day 0 with 50  $\mu$ g BSA in CFA and boosted subcutaneously on day 7 and day 14 with 50  $\mu$ g BSA in IFA. On day 21, mice were intravenously injected with 15  $\mu$ g BSA to induce systemic anaphylaxis. After the BSA challenge, the anaphylactic mice showed acute and transient ST-segment elevations on electrocardiograms. (B), Severity of anaphylactic response was scored on a scale of 0–4 ( $n = 6$  per group). Score 0: normal; score 1: slow motions; score 2: impaired mobility, still reacting to touch; score 3: immobilized and does not react to touch; score 4: death. (C), Representative electrocardiograms of naive mice and model mice. (D) through (F), Heart function was measured with echocardiography 10 min after BSA challenge. Representative echocardiogram (D), ejection fraction (EF%) (E), and fractional shortening (FS%) (F) of naive mice and model mice ( $n = 6$  per group). (G) through (K), qRT-PCR analysis of IL1R2 (G), FOS (H), MMP9 (I), DUSP1 (J), and CLEC4D (K) in peripheral whole blood ( $n = 6$  per group). (L) through (Q), qRT-PCR analysis of FOS (L), STAT3 (M), STAT6 (N), SP1 (O), SRF (P), and CREM (Q) in peripheral whole blood ( $n = 8$  per group). Naive indicates untreated control mice. IC indicates BSA-treated model mice. \* $p < 0.05$ , \*\* $p < 0.01$ , \*\*\* $p < 0.001$ . Statistical analysis: unpaired Student's *t*-test (E, F, K, P), Kolmogorov-Smirnov test (G, I, J, N, O), Unpaired *t*-test with Welch's correction (H), Mann-Whitney test (L).

**TABLE 1** Potential drug-hub gene interaction predicted by DGIdb database.

Gene	Potential drug	Interaction score	Drug class	Drug indication
IL1R2	ANAKINRA	7.73	IL1R antagonist	Rheumatoid arthritis
FOS	BACLOFEN	1.24	Muscle relaxant	Multiple sclerosis
MMP9	ANDECALIXIMAB	10.30	MMP9 antibody	Gastric cancer
DUSP1	ALBUTEROL	6.87	$\beta$ 2 adrenergic agonist	Acute asthma
CLEC4D	N/A	N/A	N/A	N/A

**Abbreviations:** DGIdb, drug-gene interaction database; IL1R, interleukin-1, receptor; CGRP, calcitonin gene-related peptide; FOS, Fos proto-oncogene; MMP9, matrix metalloproteinase 9; DUSP1, dual specificity phosphatase 1; CLEC4D, C-type lectin domain family 4 member D.

### 3.8 Validation of hub gene expression in a murine model of acute anaphylaxis

To further verify the findings from human microarray data, the expression levels of five hub genes (IL1R2, FOS, MMP9, DUSP1, CLEC4D) were measured in an experimentally induced murine model of acute anaphylaxis by qRT-PCR analysis. Systemic anaphylaxis was induced by intravenously injected with BSA in mice sensitized with the same antigen (Figure 8A). 10 min after the BSA challenge, mice showed obvious symptoms of anaphylaxis, including impaired mobility, lethargy, and unresponsiveness (Figure 8B). Compared with naïve mice, the anaphylactic mice exhibited ST-segment elevations on electrocardiograms (Figure 8C) and showed markedly impaired heart function (Figures 8D–F) as reflected by decreases in ejection fraction (EF;  $58.68\% \pm 2.87\%$  versus  $27.84\% \pm 4.67\%$ ) and fractional shortening (FS;  $30.62\% \pm 1.95\%$  versus  $12.53\% \pm 2.33\%$ ). qRT-PCR analysis of peripheral blood extracts demonstrated that the levels of IL1R2, FOS, MMP9, DUSP1, and CLEC4D in the anaphylactic mice with STEMI were significantly upregulated (Figures 8G–K), which was consistent with the human microarray results. Taken together, these results indicated that the hub genes we screened were of high reliability.

### 3.9 Prediction of transcription factor and candidate druggable hub genes

TRRUST database was applied to explore key upstream regulators for hub genes. Signal transducer and activator of transcription 3 (STAT3), cAMP-responsive element modulator (CREM), signal transducer and activator of transcription 6 (STAT6), Sp1 transcription factor (SP1), Fos proto-oncogene (FOS), serum response factor (SRF), and histone deacetylase 1 (HDAC1) were identified as transcription factors that modulated hub gene expression (Supplementary Figure S3A). The details of these transcription factors are summarized in Supplementary Table S3. With further analysis, we found that CREM and FOS were highly expressed in anaphylactic samples, while 3 transcription factors (SRF, STAT6, SP1) were significantly downregulated (Supplementary Figures S3B–H). In STEMI samples, 3 transcription factors (FOS, STAT3, SP1) were markedly upregulated, while HDAC1 was significantly downregulated (Supplementary Figures S3I–O). Moreover, ChEA3 platform was used to validate the findings from TRRUST and further rank the transcription factors according to their MeanRank

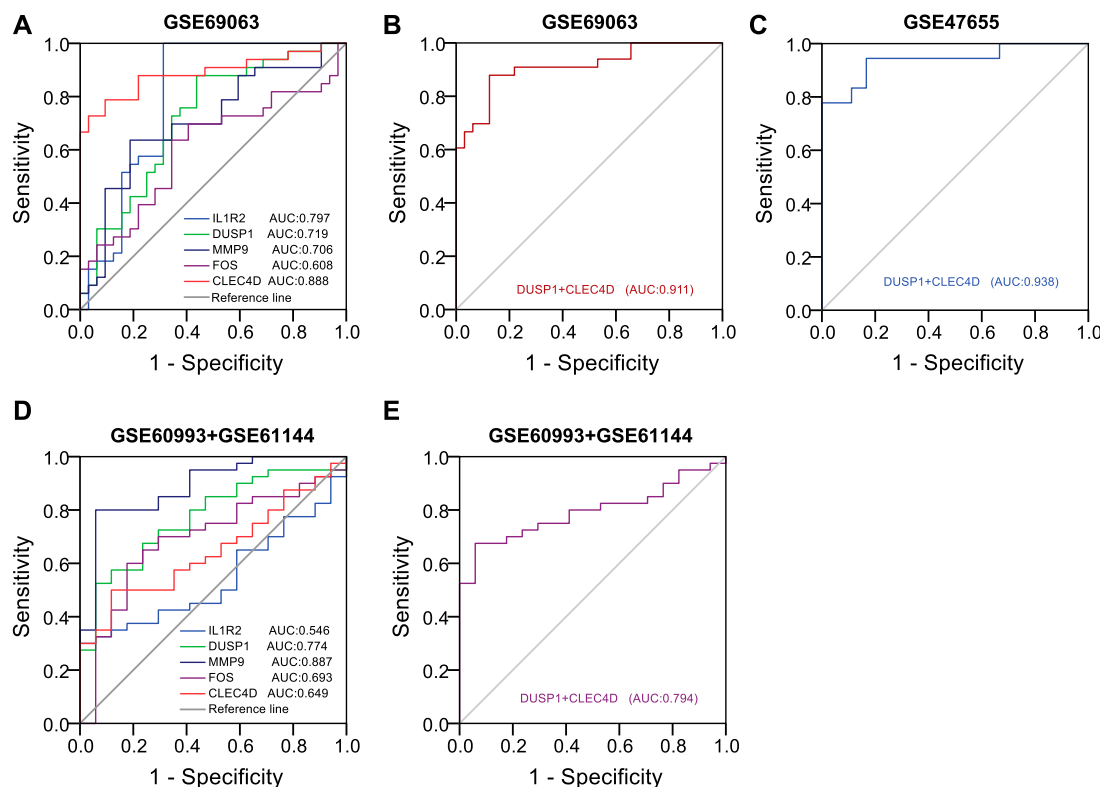
composite scores. STAT3, CREM, STAT6, SP1, FOS, and SRF were identified as transcription factors of hub genes that common to those predicted by TRRUST, ranking as: FOS, STAT3, STAT6, SP1, SRF, and CREM (Supplementary Table S4). qRT-PCR analysis of peripheral blood extracts showed significantly increased expression of FOS, and markedly decreased expression of STAT6, SP1, and SRF in the murine model of anaphylaxis complicated STEMI (Figures 8L–Q), suggesting the important regulatory role of these transcription factors in anaphylaxis induced myocardial damage.

The candidate druggable hub genes were predicted via the DGIdb database. As listed in Table 1, IL1R2, FOS, MMP9, and DUSP1 showed interactions with approved drugs, suggesting the potential targeting and regulatory effects of approved drugs on these hub genes.

### 3.10 Identification of diagnostic efficiency of hub genes on anaphylaxis and STEMI

To predict the occurrence of anaphylaxis and STEMI, univariate logistic analysis followed by multivariate logistic regression analysis was applied to construct the diagnostic model, and receiver operating characteristic (ROC) curves were used to evaluate the diagnostic efficiency of hub genes. Univariate logistic analysis of hub genes in anaphylactic dataset GSE69063 revealed that IL1R2 ( $p < 0.001$ , AUC = 0.797, 95% CI 0.679–0.916), DUSP1 ( $p = 0.002$ , AUC = 0.719, 95% CI 0.593–0.844), MMP9 ( $p = 0.003$ , AUC = 0.706, 95% CI 0.577–0.835), and CLEC4D ( $p < 0.001$ , AUC = 0.888, 95% CI 0.803–0.974) were significantly correlated with anaphylaxis as continuous variables (Figure 9A). All statistically significant variables were then included in the multivariate logistic regression model using the backward LR method for variable selection. The results showed DUSP1 ( $p = 0.028$ ) and CLEC4D ( $p = 0.001$ ) were selected as significant variables and used to construct diagnostic model. The regression equation of logit (P) =  $-33.355 + 2.9 \times \text{DUSP1} + 2.294 \times \text{CLEC4D}$  was established and the accuracy of this logistic model was evaluated by ROC curves. AUC values in GSE69063 and another independent anaphylactic dataset GSE47655 were 0.911 (95% CI, 0.840–0.982) and 0.938 (95% CI, 0.857–1.000), respectively (Figures 9B,C), suggesting this model was of high diagnostic efficacy in distinguishing anaphylactic patients from healthy individuals. As anaphylaxis and STEMI shared common hub genes, the diagnostic efficiency of hub genes was further evaluated in STEMI datasets. Univariate logistic analysis of hub genes in STEMI dataset GSE60993 and GSE61144 revealed that DUSP1 ( $p = 0.001$ ,



**FIGURE 9**

Identification of diagnostic efficiency of hub genes based on logistic regression models. (A), Receiver operating characteristic (ROC) curves of five hub genes in the anaphylactic dataset (GSE69063). (B), ROC curves of DUSP1+CLEC4D in the anaphylactic dataset (GSE69063). (C), Validation of the diagnostic efficiency of DUSP1+CLEC4D in the independent anaphylactic dataset (GSE47655). (D), ROC curves of five hub genes in the STEMI datasets (GSE60993 and GSE61144). (E), Validation of the diagnostic efficiency of DUSP1+CLEC4D in the STEMI datasets (GSE60993 and GSE61144).

AUC = 0.774, 95% CI 0.649–0.898), MMP9 ( $p < 0.001$ , AUC = 0.887, 95% CI 0.794–0.980), and CLEC4D ( $p = 0.03$ , AUC = 0.649, 95% CI 0.507–0.790) were significantly correlated with STEMI (Figure 9D). Next, the efficiency of the established diagnostic model was validated in the STEMI datasets (GSE60993 and GSE61144) based on the expression profiles of DUSP1 and CLEC4D. As shown in Figure 9E, the AUC values in STEMI datasets exceeded 0.7, indicating this model also had good accuracy in discriminating STEMI. Taken together, these results suggested that two hub genes, DUSP1 and CLEC4D, held a promise for the diagnosis of anaphylaxis complicated STEMI as blood diagnostic biomarkers.

## 4 Discussion

STEMI following anaphylaxis is an underdiagnosed but potentially fatal disease (Roumeliotis et al., 2021). The pathogenesis of anaphylaxis complicated STEMI remains poorly understood and the early diagnosis and treatment have not been fully established. The present study demonstrates the pivotal role of inflammation and defense responses in anaphylaxis and STEMI, uncovers five hub genes (IL1R2, FOS, MMP9, DUSP1, CLEC4D) closely correlated with immune effector cells of anaphylaxis and STEMI, and identifies two effective diagnostic markers (DUSP1 and CLEC4D), which deepens our understanding of the pathogenesis of

anaphylaxis complicated with STEMI and provides potential blood diagnostic biomarkers and therapeutic targets for this complication.

In anaphylactic patients with pre-existing atherosclerosis, STEMI is associated with allergic factors-triggered atheromatous plaque erosion or stent thrombosis, which culminates in coronary occlusion and myocardial damage (Sakaue et al., 2020; Engheta et al., 2021; Yamamoto et al., 2022). While in patients with angiographically normal coronary arteries and no risk factors for coronary artery disease, prolonged coronary spasm appears to be the leading cause of acute STEMI following anaphylaxis (Goto et al., 2016; Li et al., 2018). Mast cells, distributed around coronary arteries and plaques, have been proposed to be implicated in anaphylaxis complicated with STEMI (Marone et al., 2014; Li et al., 2018; Yamamoto et al., 2022). Upon activation, mast cells secrete inflammatory mediators such as histamine (Galli and Tsai, 2012; Galli et al., 2020), which regulates coronary artery tone and vascular permeability, thus affecting hemodynamic stress and coronary blood flow (Matsuyama et al., 1990; Kounis and Zavras, 1991; Mikelis et al., 2015). In this study, we observed specific immune cell subsets, including macrophages, dendritic cells, CD8<sup>+</sup> T cells, and CD4<sup>+</sup> naïve T cells, which act in both anaphylaxis and STEMI (Figure 6A).

Macrophages express FcγR, and IgG/FcγR/macrophage pathway is implicated in the initiation of the immune-inflammatory cascade upon IgG-allergen immune complex stimulation (Beutier et al., 2017). Depletion of macrophages significantly attenuated both IgG2a- and

IgG2b-mediated passive systemic anaphylaxis in mice (Beutier et al., 2017). During anaphylaxis, crosslinking of macrophage FcγR activates macrophages to release platelet-activating factor, an endogenous phospholipid mediator that may contribute to anaphylaxis-related STEMI by inducing platelet aggregation, endothelial dysfunction, inflammatory cell adhesion, and vascular hyperpermeability (Gill et al., 2015). Dendritic cells play essential roles in allergy sensitization, CD4<sup>+</sup> naïve T cell activation, and T cell differentiation (Ruiter and Shreffler, 2012). Following uptake of exogenous allergens, dendritic cells integrate signals derived from exogenous allergens and present processed allergen to CD4<sup>+</sup> naïve T cells through the peptide-MHC II-TCR and co-stimulatory signaling, leading to allergen-specific activation and expansion of CD4<sup>+</sup> naïve T cells. Communication between dendritic cells and CD4<sup>+</sup> T cells during allergen presentation further elicits Th2-type allergic responses, triggering the release of type 2 cytokines, IgE production, and accumulation of mast cells (Ruiter and Shreffler, 2012; Walker and McKenzie, 2018). Once re-exposure to allergen, allergen-IgE complex induced crosslinking of FcεR receptors rapidly triggers mast cell activation and secretion of allergic chemicals (e.g., histamine and tryptase) that initiate immediate clinical symptoms (Galli and Tsai, 2012; Galli et al., 2020). Taken together, the above results and reported studies strongly suggest that anaphylaxis is a systemic inflammatory disease with extensive involvement of immune cells (increases in macrophage, activation of dendritic cells, differentiation of T cells, degranulation of mast cells). The episodes of STEMI secondary to anaphylaxis might be elicited by inflammatory factors-mediated direct stimulation to coronary intima or indirect hemodynamic change-triggered myocardial injury.

IL1R2, FOS, MMP9, DUSP1, and CLEC4D were screened and identified as hub genes shared by anaphylaxis and STEMI (Figures 5D,E). IL1R2 is expressed by monocytes/macrophages, T cells, and other immune cells (Boraschi et al., 2018). It has been reported that plasma levels of IL1R2 are profoundly increased in patients with STEMI and IL1R2 levels correlate independently with the adverse remodeling of left ventricle after STEMI, indicating the pivotal role of IL1R2 in myocardial injury and infarct healing (Orrem et al., 2018). Moreover, IL1R2 showed significantly increased expression in the whole blood of peanut-allergic subjects (Watson et al., 2017). FOS has been implicated in the regulation of degranulation capacity and inflammatory responses in FcεR-activated mast cells (Lee et al., 2004). Inhibition of FOS expression by T-5224 attenuates IgE-mediated anaphylaxis (Wang et al., 2021). MMP9 is mainly involved in leukocyte migration and proteolysis. The levels of MMP9 are markedly increased in post-myocardial infarction patients, and high MMP9 is an independent predictor of 2-year adverse cardiovascular events (Webb et al., 2006; Kelly et al., 2008; Somuncu et al., 2020). DUSP1 regulates the MAPK signaling pathway via dephosphorylating threonine and tyrosine (Liu et al., 2007). Jana V. Maier et al. demonstrated that DUSP1-deficient mice showed high susceptibility to passive anaphylaxis (Maier et al., 2007). CLEC4D is a calcium-dependent pattern-recognition receptor that interacts with FcγR and forms a receptor complex. Binding of pathogens to this complex induces phosphorylation of ITAM, which facilitates activation of CARD9 and NF kappa B, consequently triggering antigen-presenting cell maturation and T cell differentiation (Miyake et al., 2013; Zhu et al., 2013). As shown in Figure 5F, these hub genes were primarily involved in the regulation of defense response, cell chemotaxis, and inflammatory response and shared a complex co-expression and co-localization

network. Besides, these hub genes were closely correlated with macrophages and CD4<sup>+</sup> naïve T cells (Figure 6), and the crosstalk between hub genes and special immune effector cell subsets potentially regulates the ongoing immune-inflammatory responses during anaphylaxis and STEMI.

Based on TRRUST and ChEA3 database, FOS, STAT3, STAT6, SP1, SRF, and CREM were identified as the upstream regulators for hub genes. Further qRT-PCR results from the murine model validated that FOS, STAT6, SP1, and SRF were key transcription factors that highly involved in anaphylaxis complicated STEMI. STAT6 is a member of the signal transducer and activator of transcription family. STAT6-deficient mice lack Th2-type allergic responses and cannot undergo class switching to produce IgE against allergens (Shimoda et al., 1996), and STAT6 gain-of-function variant exacerbates allergic inflammation (Takeuchi et al., 2023). Clinical studies indicate that two STAT6 gene variants, rs324015 and rs1059513, are significantly associated with food allergy and more severe allergic symptoms (van Ginkel et al., 2018). Moreover, STAT 6 is activated in post-infarction hearts (El-Adawi et al., 2003), in hypertrophied hearts (Mascareno et al., 1998), and in the heart subjected to ischemia/reperfusion (Mascareno et al., 2001). Disruption of STAT6 signal promotes cardiac fibrosis and impairs cardiac contractility (Hikoso et al., 2004; Zhang et al., 2020). These studies indicate that STAT6 is involved in the pathophysiology of both allergy and cardiac dysfunction. SRF, serum response factor, is a pivotal factor that not only regulates the expression of FOS, but also interacts with transcription factor SP1 (Deshpande et al., 2022). Precise regulation of SRF expression is critical for cardiac signal transduction, myocardial contractility and cytoskeletal remodeling, and transcription dysregulation of SRF leads to adverse cardiac remodeling and ultimately heart failure, suggesting the vital role played by SRF in cardiac development and disease (Li et al., 2020; Deshpande et al., 2022). FOS, STAT6, SP1, and SRF identified in our study might represent a transcriptional regulatory signature of anaphylaxis with STEMI predisposition.

Currently, many cases of anaphylaxis-related STEMI are underdiagnosed or misdiagnosed due to lack of effective detection biomarkers. The hub genes identified here constitute a whole blood gene signature shared by anaphylaxis and STEMI, and based on the logistic regression model, DUSP1 and CLEC4D are identified as blood diagnostic markers with high diagnostic efficacy, which hold a promise for diagnostic assessment of anaphylaxis complicated STEMI in clinical practice. Moreover, treatment guidelines for anaphylaxis complicated with STEMI have not been fully established. Injectable epinephrine (adrenaline) is now used as the first-line therapy for anaphylaxis (Muraro et al., 2022), yet its use in patients with allergic angina may bring adverse effects, such as ventricular arrhythmias and worsening myocardial ischemia. Meanwhile, medications used to treat STEMI, such as angiotensin-converting enzyme inhibitors and β-blockers potentially aggravate anaphylaxis (Lieberman and Simons, 2015). The adverse effects of these medications might hamper the effective management of this clinical emergency, thus novel therapeutic medications for anaphylaxis complicated STEMI are in urgent need (Lieberman and Simons, 2015). In this study, we identified four approved drugs that have the potential to be repurposed against hub genes involved in anaphylaxis complicated STEMI, including anakinra, baclofen, andecaliximab, and albuterol targeting IL1R2, FOS, MMP9, and DUSP1, respectively. Anakinra is a recombinant IL-1R antagonist

approved for the treatment of COVID-19 related pneumonia and rheumatoid arthritis. A cohort study evaluating the clinical effectiveness of anakinra in patients with COVID-19 showed that anakinra had a favorable improvement in respiratory insufficiency and hyperinflammation (Cavalli et al., 2021), two pathological processes that also have pivotal roles in anaphylaxis. Besides, in the VCUART trial, administration of anakinra to patients with STEMI for 14 days significantly decreased the incidence of new-onset heart failure and heart failure hospitalization compared with placebo (Abbate et al., 2013; Abbate et al., 2020), supporting the benefits of IL-1 blockade with anakinra in slowing STEMI progression. DGIdb identified baclofen as an FDA-approved drug that potentially target FOS. Baclofen, a skeletal muscle relaxant that acts on the spinal cord nerves to reduce spasms, is commonly used in patients with multiple sclerosis. The application of baclofen in anaphylaxis and STEMI is rarely reported and deserves further study. Andecaliximab, a recombinant IgG4 monoclonal antibody targeting MMP9, is under development for the treatment different types of diseases, such as rheumatoid arthritis, Crohn's disease, and non-small cell lung cancer (Gossage et al., 2018; Schreiber et al., 2018). Due to the critical role of MMP9 in STEMI and anaphylaxis, andecaliximab might be a promising strategy to curtail anaphylaxis complicated STEMI. According to DGIdb results, DUSP1 has a good interaction with albuterol, a  $\beta_2$  adrenergic agonist that relaxes muscles in the airways. Presently, albuterol is used as a second-line drug to relieve wheezing during anaphylaxis attacks (Irani and Akl, 2015). Moreover, in a randomized controlled trial, albuterol improved pulmonary vascular reserve and enhanced cardiac output reserve in patients with HFpEF (Reddy et al., 2019), showing its cardiovascular benefits. Collectively, these repurposed drug candidates provide a window of opportunity for the development of much-needed drugs for anaphylaxis complicated STEMI.

There are some limitations in the present study. First, the biological functions of immune cell subsets and hub genes shared by anaphylaxis and STEMI require further *in-vivo* and *in-vitro* experimental verification. Second, public microarray datasets for anaphylactic studies are limited, and the sample size in this study is relatively small.

## 5 Conclusion

By comprehensively profiling the peripheral whole blood transcriptome of anaphylactic and STEMI individuals, we identified the biological processes, special immune effector cell subsets, and hub genes shared by anaphylaxis and STEMI, laying down a foundation for further our mechanistic understanding of anaphylaxis complicated with STEMI. Hub genes identified here (IL1R2, FOS, MMP9, DUSP1, and CLEC4D) represent a whole blood gene signature of anaphylaxis with STEMI predisposition and provide candidate diagnostic and therapeutic targets for follow-up studies.

## Data availability statement

The original contributions presented in the study are included in the article/**Supplementary Material**, further inquiries can be directed to the corresponding author.

## Ethics statement

The animal study was reviewed and approved by the Institutional Animal Care and Use Committee, Fuwai Hospital, National Center for Cardiovascular Diseases, China. No human studies are presented in this article.

## Author contributions

ZP analyzed the microarray data, performed the experiments, and wrote the manuscript. HC proposed suggestions and revised the manuscript. MW conceived and supervised the study. All authors contributed to the article and approved the submitted version.

## Funding

This work was supported by the National Key Research and Development Program of China [2020YFC2008000], the National Natural Science Foundation of China [92149305], Chinese Academy of Medical Sciences (CAMS) Innovation Fund for Medical Sciences [2021-I2M-1-016, 2016-I2M-1-003, 2017-I2M-1-008], and research funds from Fuwai Hospital (2022-GSP-GG-8), CAMS.

## Acknowledgments

We thank the authors who uploaded and shared the GEO microarray data.

## Conflict of interest

The authors declare that the research was conducted in the absence of any commercial or financial relationships that could be construed as a potential conflict of interest.

## Publisher's note

All claims expressed in this article are solely those of the authors and do not necessarily represent those of their affiliated organizations, or those of the publisher, the editors and the reviewers. Any product that may be evaluated in this article, or claim that may be made by its manufacturer, is not guaranteed or endorsed by the publisher.

## Supplementary material

The Supplementary Material for this article can be found online at: <https://www.frontiersin.org/articles/10.3389/fphar.2023.1211332/full#supplementary-material>

## References

- Abbate, A., Trankle, C. R., Buckley, L. F., Lipinski, M. J., Appleton, D., Kadariya, D., et al. (2020). Interleukin-1 blockade inhibits the acute inflammatory response in patients with ST-segment-elevation myocardial infarction. *J. Am. Heart Assoc.* 9 (5), e014941. doi:10.1161/JAHA.119.014941
- Abbate, A., Van Tassel, B. W., Biondi-Zoccai, G., Kontos, M. C., Grizzard, J. D., Spillman, D. W., et al. (2013). Effects of interleukin-1 blockade with anakinra on adverse cardiac remodeling and heart failure after acute myocardial infarction [from the Virginia Commonwealth University-Anakinra Remodeling Trial (2) (VCU-ART2) pilot study]. *Am. J. Cardiol.* 111 (10), 1394–1400. doi:10.1016/j.amjcard.2013.01.287
- Abdelghany, M., Subedi, R., Shah, S., and Kozman, H. (2017). Kounis syndrome: A review article on epidemiology, diagnostic findings, management and complications of allergic acute coronary syndrome. *Int. J. Cardiol.* 232, 1–4. doi:10.1016/j.ijcard.2017.01.124
- Barrett, T., Wilhite, S. E., Ledoux, P., Evangelista, C., Kim, I. F., Tomashevsky, M., et al. (2013). NCBI GEO: Archive for functional genomics data sets--update. *Nucleic Acids Res.* 41, D991–D995. doi:10.1093/nar/gks1193
- Beutier, H., Gillis, C. M., Iannascoli, B., Godon, O., England, P., Sibillano, R., et al. (2017). IgG subclasses determine pathways of anaphylaxis in mice. *J. Allergy Clin. Immunol.* 139 (1), 269–280.e7. doi:10.1016/j.jaci.2016.03.028
- Borascchi, D., Italiani, P., Weil, S., and Martin, M. U. (2018). The family of the interleukin-1 receptors. *Immunol. Rev.* 281 (1), 197–232. doi:10.1111/imr.12606
- Cardona, V., Ansotegui, I. J., Ebisawa, M., El-Gamal, Y., Fernandez Rivas, M., Fineman, S., et al. (2020). World allergy organization anaphylaxis guidance 2020. *World Allergy Organ J.* 13 (10), 100472. doi:10.1016/j.waojou.2020.100472
- Cavalli, G., Larcher, A., Tomelleri, A., Campochiaro, C., Della-Torre, E., De Luca, G., et al. (2021). Interleukin-1 and interleukin-6 inhibition compared with standard management in patients with COVID-19 and hyperinflammation: A cohort study. *Lancet Rheumatol.* 3 (4), e253–e261. doi:10.1016/S2665-9913(21)00012-6
- Chen, C., Chen, H., Zhang, Y., Thomas, H. R., Frank, M. H., He, Y., et al. (2020). TBtools: An integrative toolkit developed for interactive analyses of big biological data. *Mol. Plant* 13 (8), 1194–1202. doi:10.1016/j.molp.2020.06.009
- Cloutier, N., Allaes, I., Marcoux, G., Machlus, K. R., Mailhot, B., Zufferey, A., et al. (2018). Platelets release pathogenic serotonin and return to circulation after immune complex-mediated sequestration. *Proc. Natl. Acad. Sci. U. S. A.* 115 (7), E1550–E1559. doi:10.1073/pnas.1720553115
- Desai, R., Parekh, T., Patel, U., Fong, H. K., Samani, S., Patel, C., et al. (2019). Epidemiology of acute coronary syndrome co-existent with allergic/hypersensitivity/anaphylactic reactions (Kounis syndrome) in the United States: A nationwide inpatient analysis. *Int. J. Cardiol.* 292, 35–38. doi:10.1016/j.ijcard.2019.06.002
- Deshpande, A., Shetty, P. M. V., Frey, N., and Rangrez, A. Y. (2022). Srf: A seriously responsible factor in cardiac development and disease. *J. Biomed. Sci.* 29 (1), 38. doi:10.1186/s12929-022-00820-3
- El-Adawi, H., Deng, L., Tramontano, A., Smith, S., Mascareno, E., Ganguly, K., et al. (2003). The functional role of the JAK-STAT pathway in post-infarction remodeling. *Cardiovasc Res.* 57 (1), 129–138. doi:10.1016/s0008-6363(02)00614-4
- Engheta, M., Urbanczyk, J., Fidone, E., Escobedo, Y., and Mixon, T. (2021). Kounis syndrome presenting as ST elevation acute myocardial infarction. *Proc. (Bayl Univ. Med. Cent.* 34 (4), 500–502. doi:10.1080/08998280.2021.1907095
- Finkelman, F. D., Khodoun, M. V., and Strait, R. (2016). Human IgE-independent systemic anaphylaxis. *J. Allergy Clin. Immunol.* 137 (6), 1674–1680. doi:10.1016/j.jaci.2016.02.015
- Franceschini, A., Szklarczyk, D., Frankild, S., Kuhn, M., Simonovic, M., Roth, A., et al. (2013). STRING v9.1: Protein-protein interaction networks, with increased coverage and integration. *Nucleic Acids Res.* 41, D808–D815. doi:10.1093/nar/gks1094
- Freshour, S. L., Kiwala, S., Cotto, K. C., Coffman, A. C., McMichael, J. F., Song, J. J., et al. (2021). Integration of the drug-gene interaction database (DGIdb 4.0) with open crowdsourced efforts. *Nucleic Acids Res.* 49 (D1), D1144–D1151. doi:10.1093/nar/gkaa1084
- Galli, S. J., Gaudenzio, N., and Tsai, M. (2020). Mast cells in inflammation and disease: Recent progress and ongoing concerns. *Annu. Rev. Immunol.* 38, 49–77. doi:10.1146/annurev-immunol-071719-094903
- Galli, S. J., and Tsai, M. (2012). IgE and mast cells in allergic disease. *Nat. Med.* 18 (5), 693–704. doi:10.1038/nm.2755
- Gill, P., Jindal, N. L., Jagdis, A., and Vadas, P. (2015). Platelets in the immune response: Revisiting platelet-activating factor in anaphylaxis. *J. Allergy Clin. Immunol.* 135 (6), 1424–1432. doi:10.1016/j.jaci.2015.04.019
- Gossage, D. L., Cieslarova, B., Ap, S., Zheng, H., Xin, Y., Lal, P., et al. (2018). Phase 1b study of the safety, pharmacokinetics, and disease-related outcomes of the matrix metalloproteinase-9 inhibitor andecaliximab in patients with rheumatoid arthritis. *Clin. Ther.* 40 (1), 156–165.e5. doi:10.1016/j.clinthera.2017.11.011
- Goto, K., Kasama, S., Sato, M., and Kurabayashi, M. (2016). Myocardial scintigraphic evidence of Kounis syndrome: What is the aetiology of acute coronary syndrome? *Eur. Heart J.* 37 (14), 1157. doi:10.1093/eurheartj/ehv703
- Han, H., Cho, J. W., Lee, S., Yun, A., Kim, H., Bae, D., et al. (2018). TRRUST v2: An expanded reference database of human and mouse transcriptional regulatory interactions. *Nucleic Acids Res.* 46 (D1), D380–D386. doi:10.1093/nar/gkx1013
- Hikoso, S., Yamaguchi, O., Higuchi, Y., Hirotsani, S., Takeda, T., Kashiwase, K., et al. (2004). Pressure overload induces cardiac dysfunction and dilation in signal transducer and activator of transcription 6-deficient mice. *Circulation* 110 (17), 2631–2637. doi:10.1161/01.CIR.0000146798.70980.9A
- Irani, A. M., and Akl, E. G. (2015). Management and prevention of anaphylaxis. *F1000Res* 4, F1000. doi:10.12688/f1000research.7181.1
- Jonsson, F., Mancardi, D. A., Kita, Y., Karasuyama, H., Iannascoli, B., Van Rooijen, N., et al. (2011). Mouse and human neutrophils induce anaphylaxis. *J. Clin. Invest.* 121 (4), 1484–1496. doi:10.1172/JCI45232
- Keenan, A. B., Torre, D., Lachmann, A., Leong, A. K., Wojciechowski, M. L., Utti, V., et al. (2019). ChEA3: Transcription factor enrichment analysis by orthogonal omics integration. *Nucleic Acids Res.* 47 (W1), W212–W224. doi:10.1093/nar/gkz446
- Kelly, D., Khan, S. Q., Thompson, M., Cockerill, G., Ng, L. L., Samani, N., et al. (2008). Plasma tissue inhibitor of metalloproteinase-1 and matrix metalloproteinase-9: Novel indicators of left ventricular remodelling and prognosis after acute myocardial infarction. *Eur. Heart J.* 29 (17), 2116–2124. doi:10.1093/eurheartj/ehn315
- Kounis, N. G., and Zavras, G. M. (1991). Histamine-induced coronary artery spasm: The concept of allergic angina. *Br. J. Clin. Pract.* 45 (2), 121–128. doi:10.1111/j.1742-1241.1991.tb10251.x
- Lee, Y. N., Tuckerman, J., Nechushtan, H., Schutz, G., Razin, E., and Angel, P. (2004). c-Fos as a regulator of degranulation and cytokine production in FcεpsilonRI-activated mast cells. *J. Immunol.* 173 (4), 2571–2577. doi:10.4049/jimmunol.173.4.2571
- Li, J., Tan, Y., Passariello, C. L., Martinez, E. C., Kritzer, M. D., Li, X., et al. (2020). Signalosome-regulated serum response factor phosphorylation determining myocyte growth in width versus length as a therapeutic target for heart failure. *Circulation* 142 (22), 2138–2154. doi:10.1161/CIRCULATIONAHA.119.044805
- Li, J., Zheng, J., Zhou, Y., Liu, X., and Peng, W. (2018). Acute coronary syndrome secondary to allergic coronary vasospasm (Kounis syndrome): A case series, follow-up and literature review. *BMC Cardiovasc Disord.* 18 (1), 42. doi:10.1186/s12872-018-0781-9
- Lieberman, P., and Simons, F. E. (2015). Anaphylaxis and cardiovascular disease: Therapeutic dilemmas. *Clin. Exp. Allergy* 45 (8), 1288–1295. doi:10.1111/cea.12520
- Liu, Y., Shepherd, E. G., and Nelin, L. D. (2007). MAPK phosphatases--regulating the immune response. *Nat. Rev. Immunol.* 7 (3), 202–212. doi:10.1038/nri2035
- LoVerde, D., Iweala, O. I., Eginli, A., and Krishnaswamy, G. (2018). Anaphylaxis. *Chest* 153 (2), 528–543. doi:10.1016/j.chest.2017.07.033
- Maier, J. V., Brema, S., Tuckermann, J., Herzer, U., Klein, M., Stassen, M., et al. (2007). Dual specificity phosphatase 1 knockout mice show enhanced susceptibility to anaphylaxis but are sensitive to glucocorticoids. *Mol. Endocrinol.* 21 (11), 2663–2671. doi:10.1210/me.2007-0067
- Marone, G., Genovese, A., Varricchi, G., and Granata, F. (2014). Human heart as a shock organ in anaphylaxis. *Allergo J. Int.* 23 (2), 60–66. doi:10.1007/s40629-014-0007-3
- Mascareno, E., Dhar, M., and Siddiqui, M. A. (1998). Signal transduction and activator of transcription (STAT) protein-dependent activation of angiotensinogen promoter: A cellular signal for hypertrophy in cardiac muscle. *Proc. Natl. Acad. Sci. U. S. A.* 95 (10), 5590–5594. doi:10.1073/pnas.95.10.5590
- Mascareno, E., El-Shafei, M., Maulik, N., Sato, M., Guo, Y., Das, D. K., et al. (2001). JAK/STAT signaling is associated with cardiac dysfunction during ischemia and reperfusion. *Circulation* 104 (3), 325–329. doi:10.1161/01.cir.104.3.325
- Matsuyama, K., Yasue, H., Okumura, K., Matsuyama, K., Ogawa, H., Morikami, Y., et al. (1990). Effects of H1-receptor stimulation on coronary arterial diameter and coronary hemodynamics in humans. *Circulation* 81 (1), 65–71. doi:10.1161/01.cir.81.1.65
- Mikelis, C. M., Simaan, M., Ando, K., Fukuhara, S., Sakurai, A., Amornphimoltham, P., et al. (2015). RhoA and ROCK mediate histamine-induced vascular leakage and anaphylactic shock. *Nat. Commun.* 6, 6725. doi:10.1038/ncomms7725
- Miyake, Y., Toyonaga, K., Mori, D., Kakuta, S., Hoshino, Y., Oyama, A., et al. (2013). C-type lectin MCL is an FcγR-coupled receptor that mediates the adjuvant activity of mycobacterial cord factor. *Immunity* 38 (5), 1050–1062. doi:10.1016/j.immuni.2013.03.010
- Muraro, A., Worm, M., Alviani, C., Cardona, V., DunnGalvin, A., Garvey, L. H., et al. (2022). EAACI guidelines: Anaphylaxis (2021 update). *Allergy* 77 (2), 357–377. doi:10.1111/all.15032
- Newman, A. M., Liu, C. L., Green, M. R., Gentles, A. J., Feng, W., Xu, Y., et al. (2015). Robust enumeration of cell subsets from tissue expression profiles. *Nat. Methods* 12 (5), 453–457. doi:10.1038/nmeth.3337
- Orrem, H. L., Shetelig, C., Ueland, T., Limalanathan, S., Nilsson, P. H., Husebye, T., et al. (2018). Soluble IL-1 receptor 2 is associated with left ventricular remodelling in patients with ST-elevation myocardial infarction. *Int. J. Cardiol.* 268, 187–192. doi:10.1016/j.ijcard.2018.05.032



- Reddy, Y. N. V., Obokata, M., Koepp, K. E., Egbe, A. C., Wiley, B., and Borlaug, B. A. (2019). The beta-adrenergic agonist albuterol improves pulmonary vascular reserve in heart failure with preserved ejection fraction. *Circ. Res.* 124 (2), 306–314. doi:10.1161/CIRCRESAHA.118.313832
- Rijavec, M., Maver, A., Turner, P. J., Hocevar, K., Kosnik, M., Yamani, A., et al. (2022). Integrative transcriptomic analysis in human and mouse model of anaphylaxis identifies gene signatures associated with cell movement, migration and neuroinflammatory signalling. *Front. Immunol.* 13, 1016165. doi:10.3389/fimmu.2022.1016165
- Roumeliotis, A., Davlouros, P., Anastasopoulou, M., Tsigkas, G., Koniari, I., Mplani, V., et al. (2021). Allergy associated myocardial infarction: A comprehensive report of clinical presentation, diagnosis and management of Kounis syndrome. *Vaccines (Basel)* 10 (1), 38. doi:10.3390/vaccines10010038
- Ruiter, B., and Shreffler, W. G. (2012). The role of dendritic cells in food allergy. *J. Allergy Clin. Immunol.* 129 (4), 921–928. doi:10.1016/j.jaci.2012.01.080
- Rung, J., and Brazma, A. (2013). Reuse of public genome-wide gene expression data. *Nat. Rev. Genet.* 14 (2), 89–99. doi:10.1038/nrg3394
- Sakaue, T., Inaba, S., Sumimoto, T., and Saito, M. (2020). Intravascular ultrasound-confirmed plaque rupture following multiple bee stings. *Eur. Heart J.* 41 (13), 1374. doi:10.1093/eurheartj/ehz789
- Schreiber, S., Siegel, C. A., Friedenberg, K. A., Younes, Z. H., Seidler, U., Bhandari, B. R., et al. (2018). A phase 2, randomized, placebo-controlled study evaluating matrix metalloproteinase-9 inhibitor, andecaliximab, in patients with moderately to severely active Crohn's disease. *J. Crohns Colitis* 12 (9), 1014–1020. doi:10.1093/ecco-jcc/jjy070
- Shannon, P., Markiel, A., Ozier, O., Baliga, N. S., Wang, J. T., Ramage, D., et al. (2003). Cytoscape: A software environment for integrated models of biomolecular interaction networks. *Genome Res.* 13 (11), 2498–2504. doi:10.1101/gr.1239303
- Shimoda, K., van Deursen, J., Sangster, M. Y., Sarawar, S. R., Carson, R. T., Tripp, R. A., et al. (1996). Lack of IL-4-induced Th2 response and IgE class switching in mice with disrupted Stat6 gene. *Nature* 380 (6575), 630–633. doi:10.1038/380630a0
- Somuncu, M. U., Pusuroglu, H., Karakurt, H., Bolat, I., Karakurt, S. T., Demir, A. R., et al. (2020). The prognostic value of elevated matrix metalloproteinase-9 in patients undergoing primary percutaneous coronary intervention for ST-elevation myocardial infarction: A two-year prospective study. *Rev. Port. Cardiol. Engl. Ed.* 39 (5), 267–276. doi:10.1016/j.repc.2019.09.011
- Takeuchi, I., Yanagi, K., Takada, S., Uchiyama, T., Igarashi, A., Motomura, K., et al. (2023). STAT6 gain-of-function variant exacerbates multiple allergic symptoms. *J. Allergy Clin. Immunol.* 151 (5), 1402–1409.e6. doi:10.1016/j.jaci.2022.12.802
- Turner, P. J., Campbell, D. E., Motosue, M. S., and Campbell, R. L. (2020). Global trends in anaphylaxis epidemiology and clinical implications. *J. Allergy Clin. Immunol. Pract.* 8 (4), 1169–1176. doi:10.1016/j.jaip.2019.11.027
- van Ginkel, C. D., Pettersson, M. E., Dubois, A. E. J., and Koppelman, G. H. (2018). Association of STAT6 gene variants with food allergy diagnosed by double-blind placebo-controlled food challenges. *Allergy* 73 (6), 1337–1341. doi:10.1111/all.13432
- Walker, J. A., and McKenzie, A. N. J. T(H). (2018). T<sub>H</sub>2 cell development and function. *Nat. Rev. Immunol.* 18 (2), 121–133. doi:10.1038/nri.2017.118
- Wang, H. N., Ji, K., Zhang, L. N., Xie, C. C., Li, W. Y., Zhao, Z. F., et al. (2021). Inhibition of c-Fos expression attenuates IgE-mediated mast cell activation and allergic inflammation by counteracting an inhibitory AP1/Egr1/IL-4 axis. *J. Transl. Med.* 19 (1), 261. doi:10.1186/s12967-021-02932-0
- Warde-Farley, D., Donaldson, S. L., Comes, O., Zuberi, K., Badrawi, R., Chao, P., et al. (2010). The GeneMANIA prediction server: Biological network integration for gene prioritization and predicting gene function. *Nucleic Acids Res.* 38, W214–W220. Web Server issue. doi:10.1093/nar/gkq537
- Watson, C. T., Cohain, A. T., Griffin, R. S., Chun, Y., Grishin, A., Haczynska, H., et al. (2017). Integrative transcriptomic analysis reveals key drivers of acute peanut allergic reactions. *Nat. Commun.* 8 (1), 1943. doi:10.1038/s41467-017-02188-7
- Webb, C. S., Bonnema, D. D., Ahmed, S. H., Leonardi, A. H., McClure, C. D., Clark, L. L., et al. (2006). Specific temporal profile of matrix metalloproteinase release occurs in patients after myocardial infarction: Relation to left ventricular remodeling. *Circulation* 114 (10), 1020–1027. doi:10.1161/CIRCULATIONAHA.105.600353
- Wood, R. A., Camargo, C. A., Jr., Lieberman, P., Sampson, H. A., Schwartz, L. B., Zitt, M., et al. (2014). Anaphylaxis in America: The prevalence and characteristics of anaphylaxis in the United States. *J. Allergy Clin. Immunol.* 133 (2), 461–467. doi:10.1016/j.jaci.2013.08.016
- Xu, J., and Yang, Y. (2021). Integrated gene expression profiling analysis reveals potential molecular mechanisms and candidate biomarkers for early risk stratification and prediction of STEMI and post-STEMI heart failure patients. *Front. Cardiovasc Med.* 8, 736497. doi:10.3389/fcvm.2021.736497
- Yamamoto, H., Otake, H., Tanimura, K., and Hirata, K. I. (2022). Kounis syndrome leading to triple-vessel coronary artery ischaemia due to simultaneous coronary spasm, plaque erosion, and multiple stent thrombosis: A case report. *Eur. Heart J. Case Rep.* 6 (5), ytac178. doi:10.1093/ehjcr/ytac178
- Yu, G., Wang, L. G., Han, Y., and He, Q. Y. (2012). clusterProfiler: an R package for comparing biological themes among gene clusters. *OMICS* 16 (5), 284–287. doi:10.1089/omi.2011.0118
- Zhang, W., Zhu, B., Ding, S., Wang, X., Wu, J., Zhu, X., et al. (2020). Disruption of STAT6 signal promotes cardiac fibrosis through the mobilization and transformation of CD11b(+) immature myeloid cells. *Front. Physiol.* 11, 579712. doi:10.3389/fphys.2020.579712
- Zhu, L. L., Zhao, X. Q., Jiang, C., You, Y., Chen, X. P., Jiang, Y. Y., et al. (2013). C-type lectin receptors Dectin-3 and Dectin-2 form a heterodimeric pattern-recognition receptor for host defense against fungal infection. *Immunity* 39 (2), 324–334. doi:10.1016/j.immuni.2013.05.017





## OPEN ACCESS

## EDITED BY

Xianwei Wang,  
Xinxiang Medical University, China

## REVIEWED BY

Xiaolei Sun,  
Southwestern Medical University, China  
Zhengyang Bao,  
Wuxi Maternity and Child Health Care  
Hospital, China  
Ningning Wang,  
Dalian Medical University, China

## \*CORRESPONDENCE

Ming Liu,  
✉ mingliu14@fudan.edu.cn  
Hong Jiang,  
✉ jianghong\_@fudan.edu.cn

<sup>†</sup>These authors have contributed equally  
to this work

RECEIVED 12 March 2023

ACCEPTED 17 July 2023

PUBLISHED 01 August 2023

## CITATION

Zhang B-L, Yu P, Su E-Y, Zhang C-Y,  
Xie S-Y, Yang X, Zou Y-Z, Liu M and  
Jiang H (2023), Inhibition of GSDMD  
activation by Z-LLSD-FMK or Z-YVAD-  
FMK reduces vascular inflammation and  
atherosclerotic lesion development in  
ApoE<sup>-/-</sup> mice.  
*Front. Pharmacol.* 14:1184588.  
doi: 10.3389/fphar.2023.1184588

## COPYRIGHT

© 2023 Zhang, Yu, Su, Zhang, Xie, Yang,  
Zou, Liu and Jiang. This is an open-access  
article distributed under the terms of the  
[Creative Commons Attribution License  
\(CC BY\)](https://creativecommons.org/licenses/by/4.0/). The use, distribution or  
reproduction in other forums is  
permitted, provided the original author(s)  
and the copyright owner(s) are credited  
and that the original publication in this  
journal is cited, in accordance with  
accepted academic practice. No use,  
distribution or reproduction is permitted  
which does not comply with these terms.

# Inhibition of GSDMD activation by Z-LLSD-FMK or Z-YVAD-FMK reduces vascular inflammation and atherosclerotic lesion development in ApoE<sup>-/-</sup> mice

Bao-Li Zhang<sup>1†</sup>, Peng Yu<sup>2†</sup>, En-Yong Su<sup>1</sup>, Chun-Yu Zhang<sup>1</sup>,  
Shi-Yao Xie<sup>1</sup>, Xue Yang<sup>1</sup>, Yun-Zeng Zou<sup>1</sup>, Ming Liu<sup>3,4\*</sup> and  
Hong Jiang<sup>1,4\*</sup>

<sup>1</sup>Department of Cardiology, Shanghai Institute of Cardiovascular Diseases, National Clinical Research Center for Interventional Medicine, Zhongshan Hospital, Fudan University, Shanghai, China, <sup>2</sup>Department of Endocrinology and Metabolism, Fudan Institute of Metabolic Diseases, Zhongshan Hospital, Fudan University, Shanghai, China, <sup>3</sup>Department of Health Management Center, Zhongshan Hospital, Fudan University, Shanghai, China, <sup>4</sup>Shanghai Engineering Research Center of AI Technology for Cardiopulmonary Diseases, Zhongshan Hospital, Fudan University, Shanghai, China

Pyroptosis is a form of pro-inflammatory cell death that can be mediated by gasdermin D (GSDMD) activation induced by inflammatory caspases such as caspase-1. Emerging evidence suggests that targeting GSDMD activation or pyroptosis may facilitate the reduction of vascular inflammation and atherosclerotic lesion development. The current study investigated the therapeutic effects of inhibition of GSDMD activation by the novel GSDMD inhibitor N-Benzylloxycarbonyl-Leu-Leu-Ser-Asp(OMe)-fluoromethylketone (Z-LLSD-FMK), the specific caspase-1 inhibitor N-Benzylloxycarbonyl-Tyr-Val-Ala-Asp(OMe)-fluoromethylketone (Z-YVAD-FMK), and a combination of both on atherosclerosis in ApoE<sup>-/-</sup> mice fed a western diet at 5 weeks of age, and further determined the efficacy of these polypeptide inhibitors in bone marrow-derived macrophages (BMDMs). *In vivo* studies there was plaque formation, GSDMD activation, and caspase-1 activation in aortas, which increased gradually from 6 to 18 weeks of age, and increased markedly at 14 and 18 weeks of age. ApoE<sup>-/-</sup> mice were administered Z-LLSD-FMK (200 µg/day), Z-YVAD-FMK (200 µg/day), a combination of both, or vehicle control intraperitoneally from 14 to 18 weeks of age. Treatment significantly reduced lesion formation, macrophage infiltration in lesions, protein levels of vascular cell adhesion molecule-1 and monocyte chemoattractant protein-1, and pyroptosis-related proteins such as activated caspase-1, activated GSDMD, cleaved interleukin(IL)-1β, and high mobility group box 1 in aortas. No overt differences in plasma lipid contents were detected. *In vitro* treatment with these polypeptide inhibitors dramatically decreased the percentage of propidium iodide-positive BMDMs, the release of lactate dehydrogenase and IL-1β, and protein levels of pyroptosis-related proteins both in supernatants and cell lysates elevated by lipopolysaccharide + nigericin. Notably however, there were no significant differences in the above-mentioned results between the Z-LLSD-FMK group and the Z-YVAD-FMK group, and the combination of both did not yield enhanced effects. These findings indicate that suppression of

GSDMD activation by Z-LLSD-FMK or Z-YVAD-FMK reduces vascular inflammation and lesion development in ApoE<sup>-/-</sup> mice.

#### KEYWORDS

atherosclerosis, GSDMD, macrophage, pyroptosis, vascular inflammation, Z-LLSD-FMK, Z-YVAD-FMK

## 1 Introduction

Atherosclerosis is a chronic vascular inflammatory disorder in which lesions are formed in the arterial wall. With the progression of lesions, life-threatening manifestations of atherosclerotic cardiovascular diseases (ASCVDs) occur (Ahmadi et al., 2019). Currently the high mortality related to ASCVDs exceeds that attributable to cancer as a primary cause of death globally (Arai et al., 2019; Ma et al., 2020; Virani et al., 2020). Reducing lesion development would reportedly avoid the later stages, and thus prevent clinical manifestations and death. It is therefore of great importance to develop novel pharmacological therapeutic strategies to inhibit atherosclerotic lesion development.

It is well established that vascular inflammation makes a significant contribution to lesion development. It was recently demonstrated that pyroptosis is a pro-inflammatory form of programmed cell death, and gasdermin D (GSDMD), a pore-forming protein, is a final executor of pyroptosis (Shi et al., 2017). GSDMD is cleaved by caspase-1 activated by assembly of diverse canonical inflammasomes, like nucleotide-binding oligomerization domain-like receptor protein 3 (NLRP3), or by caspase-11 (or human caspases 4 and 5) activated by non-canonical inflammasome pathway, into N-terminal GSDMD fragments (GSDMD-N) (Shi J. et al., 2015). GSDMD-N oligomerizes to form pores in the cell membrane, resulting in the release of pro-inflammatory mediators such as cleaved interleukin(IL)-1 $\beta$  (He et al., 2015; Evavold et al., 2018) and high mobility group box 1 (HMGB1) (Volchuk et al., 2020), triggering a strong pro-inflammatory response (Broz et al., 2020). Deficiency of GSDMD in a low-density lipoprotein receptor (LDLr) antisense oligonucleotide-induced hyperlipidemic mouse model reportedly reduced inflammatory responses in the artery wall and limited lesion development (Opoku et al., 2021). The same effects are evidently induced by a lack of caspase-1 (Gage et al., 2012; Usui et al., 2012; Yin et al., 2015) or IL-1 $\beta$  (Kirii et al., 2003), and neutralization or inhibition of HMGB1 (Kanellakis et al., 2011; Liu et al., 2013) in ApoE<sup>-/-</sup> mice. Macrophages are the major immune cell population in atherosclerotic lesions (Xu et al., 2019), and play a central role in lesion development (Barrett, 2020; Willemsen and de Winther, 2020). Critically, in previous studies pyroptosis-related proteins such as caspase-1, IL-1 $\beta$  were mainly expressed in macrophages in carotid atherosclerotic plaques (Shi X. et al., 2015). Moreover, a previous study has indicated that reconstitution of LDLr<sup>-/-</sup> mice with bone marrow lacking IL-1 $\alpha$ /IL-1 $\beta$  can lead to decreased vascular inflammation and lesion sizes (Düewell et al., 2010). Hence pyroptosis—at least macrophage pyroptosis—plays an essential role in vascular inflammation and lesion development, and suppression of GSDMD activation or cleavage may be a promising strategy for reducing lesion development.

GSDMD binds directly to caspases 1, 4, 5, and 11 (Yang et al., 2018), and is specifically cleaved by them (Shi J. et al., 2015). A specific cleavage site peptide of human GSDMD is <sub>272</sub>FLTD<sub>275</sub> (Shi J. et al., 2015), and recently N-acetyl-Phe-Leu-Thr-Asp-chloromethylketone (Ac-FLTD-CMK), the human GSDMD inhibitor, has been designed and demonstrated to significantly block GSDMD cleavage and pyroptosis by potently inhibiting the enzymatic activities of caspases 1, 4, 5, and 11 (Yang et al., 2018). Its availability and specificity have also been demonstrated in a series of pharmacological and cellular assays (Yang et al., 2018). To date the therapeutic effects of Ac-FLTD-CMK on atherosclerosis have not been investigated. The specific cleavage site peptide of mouse GSDMD is <sub>273</sub>LLSD<sub>276</sub> (Shi J. et al., 2015), and based on above-mentioned studies, in the current study N-Benzoyloxycarbonyl-Leu-Leu-Ser-Asp(OMe)-fluoromethylketone (Z-LLSD-FMK), a novel mouse GSDMD inhibitor, was chemically designed to suppress mouse GSDMD cleavage. It has been reported that N-Benzoyloxycarbonyl-Tyr-Val-Ala-Asp(OMe)-fluoromethylketone (Z-YVAD-FMK) (Garcia-Calvo et al., 1998), a specific caspase-1 inhibitor, inhibited cleavage of GSDMD in HK-2 cells (Wen et al., 2022), reduced kidney injury in brain-dead rats (Liu et al., 2021), and mitigated lung injury caused by PM2.5-induced lung inflammation in mice by impeding pyroptosis (Li et al., 2021). However, the therapeutic effects of Z-YVAD-FMK on atherosclerosis remain unclear.

The aim of the present study was to investigate the therapeutic effects of inhibition of GSDMD activation by Z-LLSD-FMK, Z-YVAD-FMK, and the combination of both on vascular inflammation and atherosclerosis. Using *in vivo* and *in vitro* experiments, both Z-LLSD-FMK and Z-YVAD-FMK were found to observably inhibit GSDMD activation and pyroptosis, and reduce vascular inflammation and the lesion development, with no differences or synergies in their effects.

## 2 Materials and methods

### 2.1 Reagents

Z-LLSD-FMK (purity >98%) and Z-YVAD-FMK (purity >98%) were synthesized by GL Biochem Co., Ltd. (Shanghai, China). Dimethylsulfoxide (DMSO), hematoxylin and eosin (H&E), oil red O, lipopolysaccharide (LPS), and nigericin were purchased from Sigma-Aldrich (St. Louis, MO, United States). Paraformaldehyde (PFA) was purchased from Solarbio (Beijing, China). Phosphate-buffered saline (PBS) was purchased from HyClone (Logan, UT, United States). Bovine serum albumin (BSA) was purchased from Yeasen Biotechnology Co., Ltd. (Shanghai, China). Antifade mounting medium with 4'-6-diamidino-2-phenylindole (DAPI), propidium iodide (PI)/Hoechst 33342, and lactate dehydrogenase (LDH) cytotoxicity assay kits were purchased from Beyotime Biotechnology (Shanghai, China). Red blood cell lysis buffer was

purchased from Biolegend (San Diego, CA, United States). RPMI 1640 was purchased from Keygen BioTECH (Nanjing, China). Fetal bovine serum (FBS) was purchased from ThermoFisher Scientific (Waltham, MA, United States), and macrophage colony-stimulating factor (M-CSF) was purchased from Peprotech (Rocky Hill, NJ, United States). Mouse IL-1 $\beta$  enzyme-linked immunosorbent assay (ELISA) kits were purchased from R&D systems (Minneapolis, MN, United States). Phosphatase and protease antagonist cocktails were purchased from Sangon Biotech Co., Ltd. (Shanghai, China). Primary antibodies against EGF-like module-containing mucin-like hormone receptor-like 1 (F4/80<sup>+</sup>), HMGB1, caspase-1, GSDMD, and goat anti-rat IgG conjugated to Alexa Fluor 568 were purchased from Abcam (Cambridge, United Kingdom). Primary antibodies against NLRP3 were purchased from Cell Signaling Technology (Beverly, MA, United States), and primary antibodies against vascular cell adhesion molecule-1 (VCAM-1), monocyte chemoattractant protein-1 (MCP-1), and IL-1 $\beta$  were purchased from Wuhan Boster Bioengineering Ltd. (Wuhan, China). Horseradish peroxidase (HRP)-conjugated rabbit secondary IgG was purchased from Jackson ImmunoResearch Laboratories, Inc. (Philadelphia, PA, United States). RIPA lysis buffer, BCA protein assay kits, and enhanced chemiluminescent solutions were purchased from Pierce Biotechnology (Rockford, IL, United States). HRP-conjugated antibody against actin was purchased from Bioworld Technology, Inc. (Bloomington, MN, United States).

## 2.2 Mice and diets

ApoE<sup>-/-</sup> mice (male, C57BL/6 background, 5 weeks old) were provided by Shanghai Model Organisms Center, Inc. (Shanghai, China) and kept in microisolator cages with water and food available *ad libitum*, under specific pathogen-free conditions at the Shanghai Model Organisms Center. ApoE<sup>-/-</sup> mice were fed a western diet (21% fat, 0.15% cholesterol; SLAC, Shanghai, China) (Liu et al., 2013) from 5 weeks of age, and samples were collected at 6, 8, 11, 14, and 18 weeks of age (5 mice per group) to determine the timepoint and duration of pharmacological intervention. Thirty-six 5-week-old ApoE<sup>-/-</sup> mice were also fed the western diet, and at 14 weeks of age these mice were randomized into four groups. Treatments were administered to the four groups via intraperitoneal injection for 4 weeks, as follows: 1) control (vehicle, 0.25 mL, 2% DMSO/day), 2) Z-YVAD-FMK (Fu et al., 2019) (0.25 mL, 200  $\mu$ g/day), 3) Z-LLSD-FMK (0.25 mL, 200  $\mu$ g/day), and 4) Z-YVAD-FMK + Z-LLSD-FMK (0.25 mL, 200  $\mu$ g + 200  $\mu$ g/day). Mice were killed at 18 weeks of age. All mouse studies were approved by the Animal Ethics Committee of Zhongshan Hospital, Fudan University. All experimental procedures were performed in accordance with the guidelines for the Care and Use of Laboratory Animals published by the US National Institutes of Health (NIH Publication No. 85-23, revised 1996) (Zhang et al., 2021).

## 2.3 Lipid measurement

Blood was collected from the right ventricle of fasted mice after anesthesia. Plasma levels of triglycerides, total cholesterol, and high-density lipoprotein (HDL) were detected via colorimetric

enzymatic assays (Jinan Sysmex Limited Company, Jinan, China) in accordance with the manufacturer's instructions (Liu et al., 2017).

## 2.4 Quantification of atherosclerotic lesions

Atherosclerotic lesions were quantified as previously described (Liu et al., 2013; Liu et al., 2017). In brief, ApoE<sup>-/-</sup> mice were fasted for more than 4 h then anesthetized. Their hearts were removed, and the aortic arches were dissected. The aortic roots were then harvested and briefly fixed in ice-cold 4% PFA for 4 h. The fixed aortic roots were washed in PBS for 15 min three times, dehydrated in 30% sucrose overnight, then embedded in optimal cutting temperature compound (Sakura, Torrance, CA, United States) followed by snap freezing. Serial sections 10  $\mu$ m thick were cut from the first appearance of the aortic valve leaflets until the leaflets were no longer visible. Six sections were mounted onto each slide for a total of five slides. Sections were stained with H&E and oil red O, and quantification of the atherosclerotic lesion area was measured by a blinded observer using ImageJ v.1.42q software (National Institutes of Health, Bethesda, MD, United States).

## 2.5 Immunofluorescence

The immunofluorescence procedures applied to cryosections have been described previously (Liu et al., 2013; Liu et al., 2017). Briefly, after drying for 60 min, cryostat sections that had been fixed in 4% PFA were rehydrated in PBS, degreased in 95% ethanol for 10 min, and blocked with PBS containing 2% nonimmune serum solution and 5% BSA at room temperature for 30 min. The cryosections were then incubated with rat anti-F4/80<sup>+</sup> antibody (1:200) diluted in blocking reagent at 4°C overnight. Negative controls were run in parallel with the omission of primary antibodies. Subsequently, for visualization, sections that had been washed three times with PBS were incubated with goat anti-rat IgG conjugated to Alexa Fluor 568 (1:400) diluted in blocking reagent at room temperature for 2 h. After washing three times with PBS, sections were stained with antifade mounting medium with DAPI. Quantitative analysis of the F4/80-positive area in atherosclerotic lesions was conducted with ImageJ v.1.42q software.

## 2.6 BMDM culture and treatment

Murine BMDMs were obtained from 10 to 12-week-old C57BL/6 male mice and differentiated as described previously (Yanai et al., 2013). Briefly, bone marrow cells in bilateral hind femora and tibias from mice were gently flushed out with 20 mL sterile PBS and collected by centrifugation at 1,500 rpm for 5 min at 4°C. After lysing erythrocytes with red blood cell lysis buffer, cells were cultured and differentiated in 6-cm dishes or 24-well plates with RPMI 1640 supplemented with 10% (vol/vol) FBS and M-CSF (100 ng/mL) for 6 days in a humidified incubator with 5% CO<sub>2</sub> at 37°C. After the medium was replaced with fresh medium without FBS or M-CSF, BMDMs were pretreated with Z-YVAD-FMK (100  $\mu$ M), Z-LLSD-FMK (100  $\mu$ M), or Z-YVAD-FMK (100  $\mu$ M) + Z-LLSD-FMK (100  $\mu$ M) for 30 min, then primed with

LPS (500 ng/mL) for 4 h followed by nigericin (10  $\mu$ M) for 30 min (Rozman-Pungercar et al., 2003; Gicquel et al., 2015; Zhang et al., 2020). After treatment, supernatants were collected and centrifuged at 1,500 rpm for 5 min at 4°C to generate cell-free medium preparations. The cell-free supernatants and cells in 6-cm dishes or 24-well plates were then prepared to perform a series of assays.

## 2.7 Cell death assay

The percentage of BMDM death was measured via PI/Hoechst 33342 staining. Briefly, after treatment as described above, samples from each group were washed with PBS and stained with PI and Hoechst 33342 at 4°C for 30 min in the dark in accordance with the manufacturer's instructions. Cell images were visualized at  $\times 100$  magnification under a Leica microscope (Wetzlar, Germany) and analyzed using ImageJ v.1.42q software. The percentage of PI-positive cells was determined in five randomly selected image fields for each group.

LDH cytotoxicity assay kits were also used to evaluate cell death. This assay detects leakage of the intracellular enzyme LDH upon cellular injury. Briefly, after treatment, 120  $\mu$ L of cell-free supernatant collected from each well in each group was transferred to 96-well plates. Then, 60  $\mu$ L of the LDH cytotoxicity assay kit reagent mixture was added to each well in the 96-well plates and they were incubated for 30 min at room temperature in the dark. The absorbance signal was determined at 490 nm using a microplate reader (BioTek Instrumentals, Inc., Winooski, VT, United States). Results are shown as the percentage of the total amount of LDH. All of these procedures were performed in accordance with the manufacturer's instructions.

## 2.8 ELISA

ELISA kits were used to measure concentrations of IL-1 $\beta$  in cell-free supernatants from BMDM cultures, in accordance with the manufacturer's instructions.

## 2.9 Western blotting

As described previously (Liu et al., 2017), total proteins were extracted from aortic tissue and BMDMs in ice-cold RIPA lysis buffer with a phosphatase and protease antagonist cocktail and disruption by an ultrasonic homogenizer. Protein concentrations were detected with a BCA protein assay kit. Equal volumes of cell culture supernatants were concentrated by centrifugation at 4,000 rpm for 40 min at 4°C using an Amicon® Ultra-4 centrifugal filter with a 10-kDa cutoff (Millipore, Burlington, VT, United States). All of these procedures were conducted in accordance with the manufacturer's instructions. Equivalent quantities of homogenized aortal or cellular proteins or equal volumes of concentrated supernatants were separated on 15% SDS-PAGE gels by electrophoresis then transferred to polyvinylidene fluoride membranes (Millipore). The primary antibodies were directed against HMGB1 (1:3,000), caspase-1 (1:1,000), GSDMD (1:500),

NLRP3 (1:1,000), VCAM-1 (1:400), MCP-1 (1:400), and IL-1 $\beta$  (1:400). After blocking with 5% BSA at room temperature for 1.5 h, the membranes were incubated with the above-mentioned primary antibodies at 4°C overnight. On the second day, after washing three times in Tris-buffered saline with Tween 20 buffer the membranes were probed with HRP-conjugated rabbit secondary IgG antibody (1:20,000) at room temperature for 2 h. An enhanced chemiluminescent solution was used to visualize protein expression. Quantitative analysis of band density was conducted with Quantity One v.4.6.2 software (Bio-Rad, Berkeley, CA, United States). The bands were normalized to  $\beta$ -actin (1:20,000).

## 2.10 Statistical analysis

Data are expressed as the mean  $\pm$  the standard error of the mean (SEM). Statistical comparisons between multiple groups were performed by one-way analysis of variance followed by a *post hoc* Tukey's test. All statistical analyses and figure editing were conducted with GraphPad Prism v.6.01 software (GraphPad Software, Inc., La Jolla, CA, United States). Differences were considered significant if  $p < 0.05$ .

# 3 Results

## 3.1 GSDMD activation in atherosclerotic lesion development in ApoE<sup>-/-</sup> mice

We first examined atherosclerotic plaque formation in aortic roots, GSDMD activation, and caspase-1 activation in aorta tissue from 6 to 18-week-old ApoE<sup>-/-</sup> mice fed a western diet to determine the timepoint and duration of pharmacological intervention. Lesion formation in aortic roots was gradually increased from 6 to 18 weeks of age, and significantly increased lesion area was detected in 14 and 18-week-old ApoE<sup>-/-</sup> mice, whereas no significant plaque formation was evident in mice at 11 weeks of age compared with 6 or 8-week-old ApoE<sup>-/-</sup> mice (Figures 1A, B). Consistently, protein levels of activated GSDMD (GSDMD-N) and activated caspase-1 (p10) in aortas of ApoE<sup>-/-</sup> mice were also gradually increased during the development of atherosclerosis, and significant GSDMD activation and caspase-1 activation was observed in the 14 and 18-week-old ApoE<sup>-/-</sup> mice but not in 11-week-old mice compared with 6 or 8-week-old ApoE<sup>-/-</sup> mice (Figures 1C–E).

## 3.2 Inhibition of GSDMD activation reduced atherosclerotic lesion development in ApoE<sup>-/-</sup> mice

To determine the therapeutic effects of Z-LLSD-FMK (Figure 2A), Z-YVAD-FMK, and the combination of the two on atherosclerosis, an ApoE<sup>-/-</sup> mice model of atherosclerosis was used. The above-mentioned agents were administered to ApoE<sup>-/-</sup> mice at 14 weeks of age, and aortic sinus assays and plasma lipid measurement were performed at 18 weeks of age. The



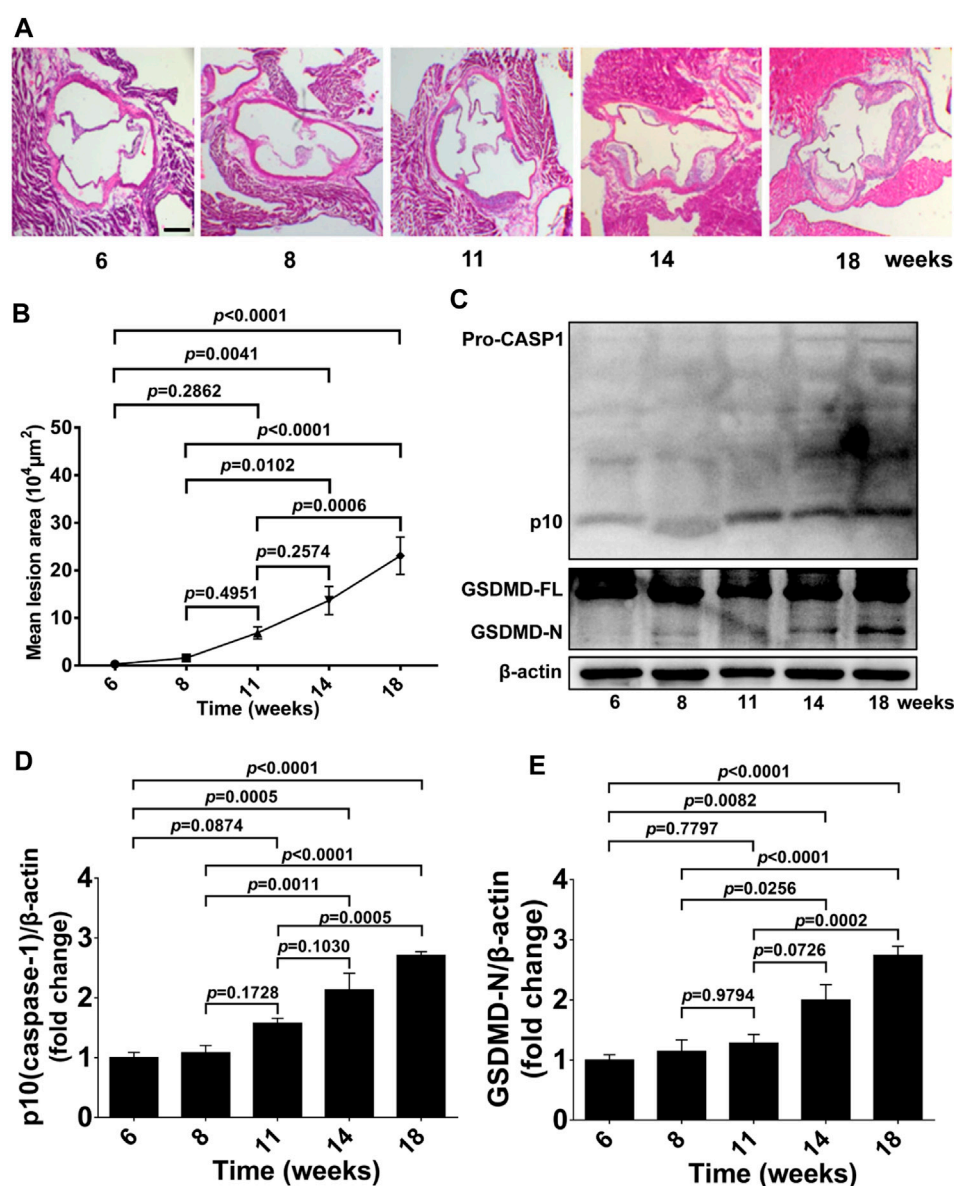


FIGURE 1

GSDMD activation in atherosclerotic lesion development in ApoE<sup>-/-</sup> mice. ApoE<sup>-/-</sup> mice were killed at the ages of 6, 8, 11, 14, and 18 weeks, and their aortas were harvested. (A) Representative aortic root cross-sections stained with H&E (scale bar = 200  $\mu\text{m}$ ). (B) Quantification of lesion area ( $n = 5$ ). (C) Representative images of western blots. (D,E) Quantification of protein expression of p10 (caspase-1) and GSDMD-N by Western blotting ( $n = 4$ ).  $\beta$ -actin served as the loading control. Data represent means  $\pm$  SEM.

corresponding *in vivo* protocol is presented in Figure 2B. H&E and oil red O staining of aortic root sections revealed that Z-YVAD-FMK, Z-LLSD-FMK, and the two combined markedly ameliorated atherosclerotic plaque development in ApoE<sup>-/-</sup> mice (Figures 2C, D). Aortic sections exhibited an approximately 49.01% decrease in atherosclerotic lesion area in the Z-YVAD-FMK group, a 47.10% decrease in the Z-LLSD-FMK group, and a 48.04% decrease in the Z-YVAD-FMK + Z-LLSD-FMK group, compared with the control (Figure 2D). Relative to the control group there were no significant differences in triglycerides, total cholesterol or HDL cholesterol in the three intervention groups (Figures 2E–G).

### 3.3 Inhibition of GSDMD activation alleviated vascular inflammation in ApoE<sup>-/-</sup> mice

To clarify the inhibitory effects of Z-LLSD-FMK, Z-YVAD-FMK, and the two combined on vascular inflammation, levels of macrophage infiltration and the two pro-inflammatory mediators VCAM-1 and MCP-1 were assessed. After 4 weeks of intervention there was an approximately 50.87% reduction in the positive area of F4/80<sup>+</sup> macrophages in the atherosclerotic lesions in the aortic sinus in the Z-YVAD-FMK group, a 53.78% reduction in the Z-LLSD-FMK group, and a 52.95% reduction in the Z-YVAD-FMK +



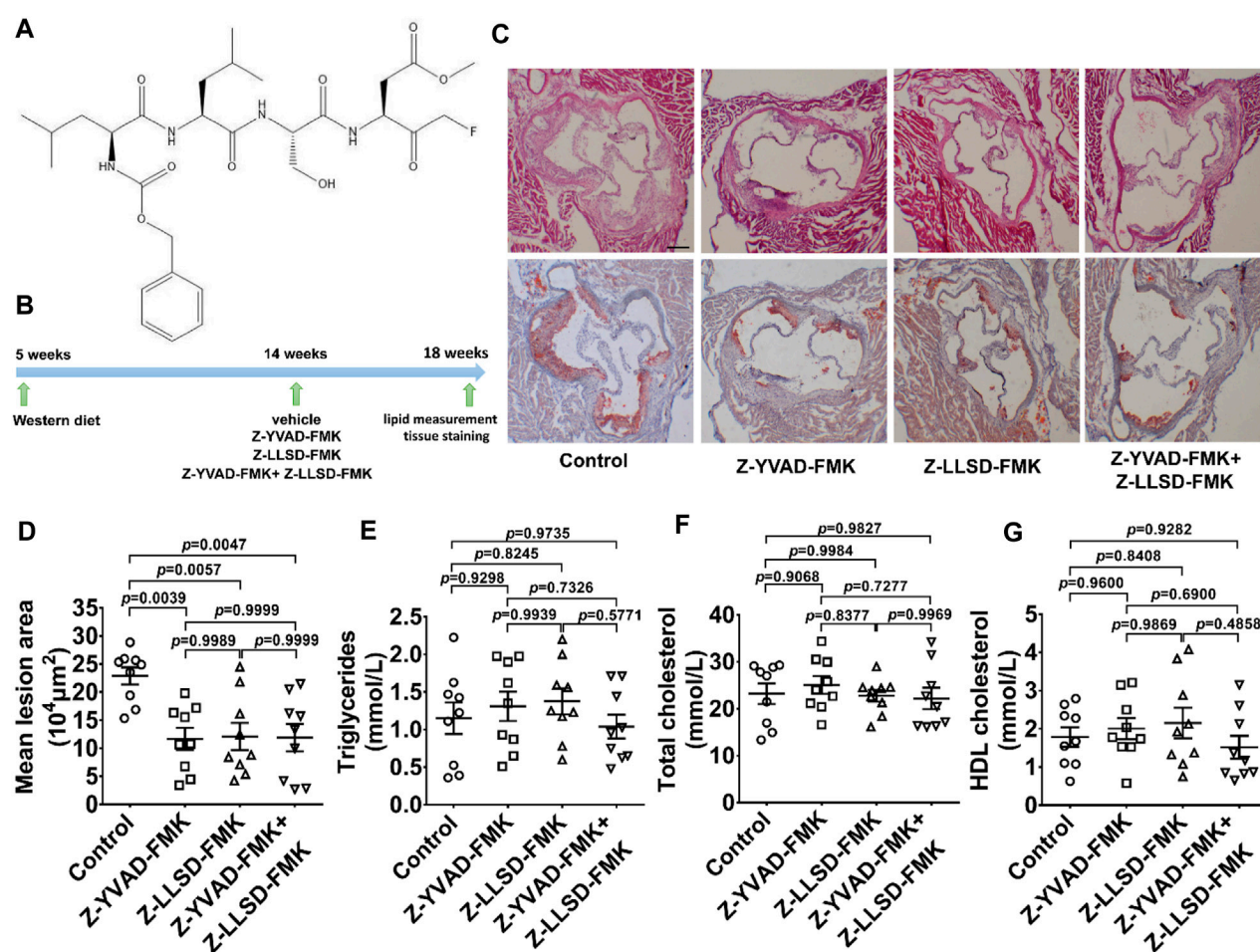


FIGURE 2

Inhibition of GSDMD activation reduced atherosclerotic lesion development in ApoE<sup>-/-</sup> mice. After 4 weeks of administration of Z-YVAD-FMK, Z-LLSD-FMK, or the two combined, the ApoE<sup>-/-</sup> mice were killed at 18 weeks. (A) Chemical structure of Z-LLSD-FMK (C<sub>29</sub>H<sub>43</sub>FN<sub>4</sub>O<sub>9</sub>). (B) Experimental protocol for the administration of Z-YVAD-FMK, Z-LLSD-FMK, and the two combined in ApoE<sup>-/-</sup> mice. (C) Representative images of aortic sinus sections stained with H&E and oil red O are shown (scale bar = 200 μm). (D) Quantitative analysis of atherosclerotic lesion area in the aortic sinus (n = 9). Plasma levels of triglycerides (E), total cholesterol (F), and HDL cholesterol (G) (n = 9).

Z-LLSD-FMK group, compared with the control group (Figures 3A, B). ApoE<sup>-/-</sup> mice treated with Z-YVAD-FMK, Z-LLSD-FMK, or the two combined expressed significantly lower protein levels of VCAM-1 and MCP-1 in aorta tissue than vehicle-treated ApoE<sup>-/-</sup> mice (Figures 3C–E), which corresponded with the decreases in atherosclerotic lesion area and macrophage infiltration (Figure 2D, Figure 3B).

### 3.4 Inhibition of GSDMD activation suppressed expression of pyroptosis pathway-related proteins in ApoE<sup>-/-</sup> mice

To confirm the suppressive effects of Z-LLSD-FMK, Z-YVAD-FMK, and the two combined on the expression of pyroptosis pathway-related proteins in ApoE<sup>-/-</sup> mice, expression of these proteins in whole aortas was assessed in each group. Protein levels of NLRP3 were slightly weakened by Z-YVAD-FMK, Z-LLSD-FMK, and the two combined, but protein levels of

activated caspase-1 (p10) and activated GSDMD (GSDMD-N) were remarkably reduced in ApoE<sup>-/-</sup> mice administered Z-YVAD-FMK, Z-LLSD-FMK, or the two combined, compared with ApoE<sup>-/-</sup> mice treated with vehicle (Figures 4A–D). Western blotting analysis also showed that the protein levels of cleaved IL-1β and HMGB1 were significantly decreased after administration of Z-YVAD-FMK, Z-LLSD-FMK, or the two combined relative to vehicle treatment (Figures 4A,E,F).

### 3.5 Z-LLSD-FMK or Z-YVAD-FMK restrained GSDMD activation or pyroptosis induced by LPS + nigericin in BMDMs

To further confirm the inhibitory effects of Z-LLSD-FMK, Z-YVAD-FMK, and the two combined on GSDMD activation or pyroptosis *in vitro*, BMDMs were pretreated with Z-LLSD-FMK, Z-YVAD-FMK, or both for 30 min then primed with LPS for 4 h followed by nigericin for 30 min. Cell death was then determined via

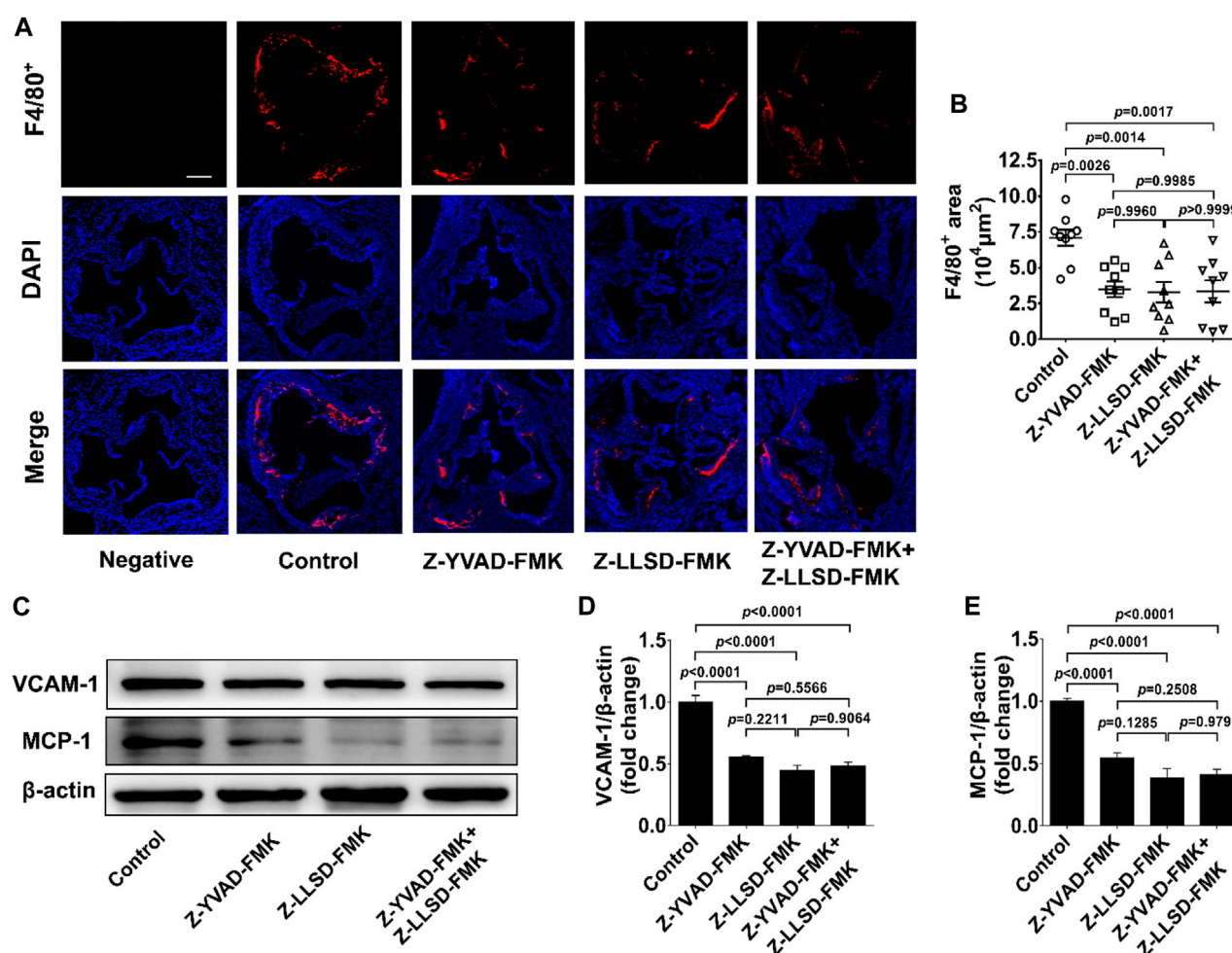


FIGURE 3

Inhibition of GSDMD activation alleviated vascular inflammation in ApoE<sup>-/-</sup> mice. The ApoE<sup>-/-</sup> mice were killed at 18 weeks and aortas were acquired. (A) Accumulation of macrophages in atherosclerotic lesions in the aortic sinus was detected by immunofluorescent staining of F4/80<sup>+</sup> (red) and DAPI (blue), and representative images are shown (scale bar = 200 μm). (B) Quantification of the positive area of F4/80<sup>+</sup> macrophages in atherosclerotic lesions ( $n = 9$ ). (C) Western blotting analysis was performed to examine the protein levels of VCAM-1 and MCP-1 in aortas from the indicated mice. (D,E) Quantitative analysis ( $n = 6$ ). β-actin served as a loading control. Data represent means ± SEM.

staining with PI/Hoechst 33342 and LDH release in supernatants. IL-1β release in supernatants and protein levels of pyroptosis pathway-related proteins both in supernatants and cell lysates were also detected. Compared with the vehicle-treated group, the percentage of PI-positive BMDMs, release of LDH and IL-1β in supernatants, and protein levels of NLRP3, p10 (caspase-1), GSDMD-N, cleaved IL-1β, and HMGB1 in supernatants and cell lysates were significantly elevated in the LPS + nigericin-stimulated group (Figures 5A–J). Remarkably, compared with the control group the percentage of PI-positive BMDMs, release of LDH and IL-1β, protein levels of NLRP3, p10 (caspase-1), GSDMD-N, cleaved IL-1β, and HMGB1 in supernatants, and protein expression of p10 (caspase-1), GSDMD-N, cleaved IL-1β, and HMGB1 in cell lysates were significantly lower in the LPS + nigericin-stimulated groups that were pretreated with Z-LLSD-FMK, Z-YVAD-FMK, or both (Figures 5A–J). However, compared with the control group, protein expression of NLRP3 in cell lysates was slightly decreased in the LPS

+ nigericin-stimulated groups pretreated with Z-LLSD-FMK, Z-YVAD-FMK, or both (Figures 5E, F).

## 4 Discussion

In the present study inhibition of GSDMD activation by a novel mouse GSDMD inhibitor, Z-LLSD-FMK, and a specific caspase-1 inhibitor, Z-YVAD-FMK, significantly suppressed the expression of pyroptosis pathway-related proteins, and reduced vascular inflammation and lesion development in an ApoE<sup>-/-</sup> mouse model of atherosclerosis. Both Z-LLSD-FMK and Z-YVAD-FMK markedly inhibited GSDMD activation and pyroptosis in a BMDM model stimulated by LPS + nigericin. There were no significant differences in plasma lipid levels between the control group and treatment groups. Moreover, there were no significant differences in the above-mentioned results between the Z-LLSD-FMK group and

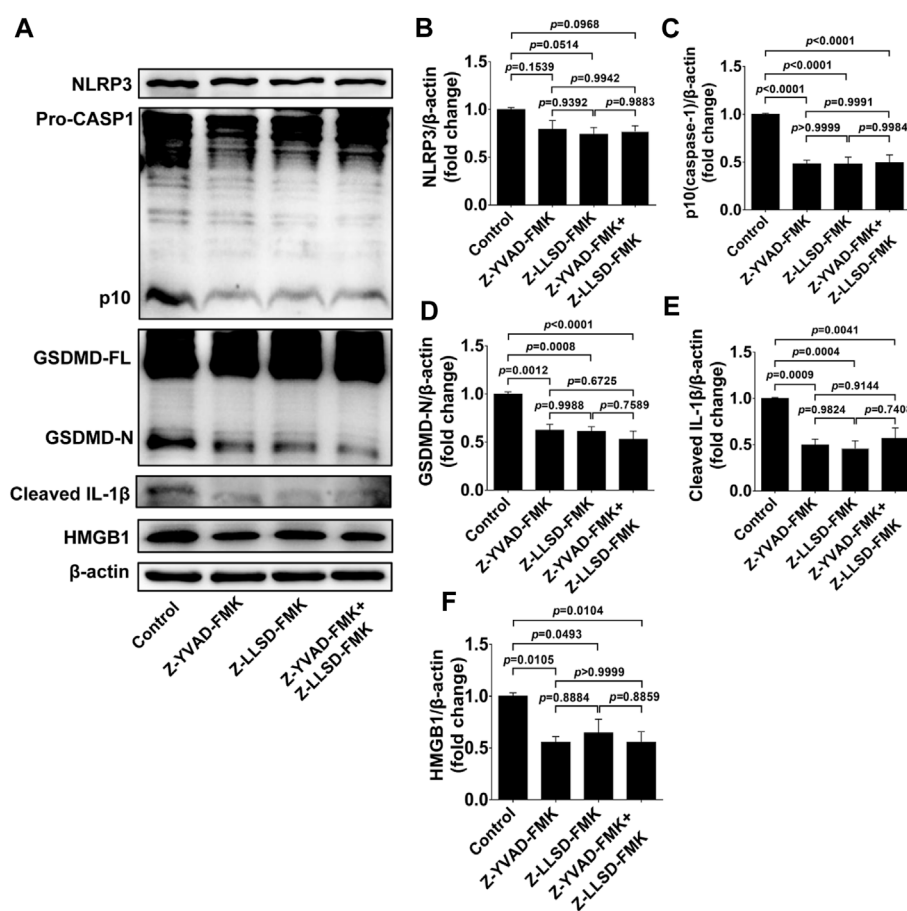


FIGURE 4

Inhibition of GSDMD activation suppressed the expression of pyroptosis pathway-related proteins in ApoE<sup>-/-</sup> mice. After 4 weeks of treatment the ApoE<sup>-/-</sup> mice were killed at 18 weeks. (A) Western blotting analysis was conducted to detect protein levels of NLRP3, caspase-1, GSDMD, cleaved IL-1β, and HMGB1 in the aorta. (B–F) Quantitative analysis of expression of NLRP3, p10 (caspase-1), GSDMD-N, cleaved IL-1β, and HMGB1 ( $n = 6$ ). β-actin served as the loading control. Data represent means  $\pm$  SEM.

the Z-YVAD-FMK group, and the combination of both Z-LLSD-FMK and Z-YVAD-FMK did not have enhanced effects. These results suggest that the canonical inflammasome pathway probably plays a more prominent role in vascular inflammation and lesion development in ApoE<sup>-/-</sup> mice, and that the novel human GSDMD inhibitor, Ac-FLTD-CMK, may be a novel and effective drug to treat atherosclerosis in the future.

The high mortality related to ASCVDs has been the leading cause of death worldwide (Libby, 2021). Limiting lesion development avoids the later stages of plaques, and thereby prevents clinical manifestations and death (Soehnlein and Libby, 2021). There is thus a great need to investigate potential pharmacological therapeutic strategies to decrease lesion development. Consistent with previous studies (Düwell et al., 2010; Yin et al., 2015; Su et al., 2022), we found that lesion formation in aortic roots and activated caspase-1 in aorta tissue were steadily increased with diet feeding. In the present study, plaque formation, GSDMD activation and caspase-1 activation were gradually increased from 6 to 18 weeks of age. All of them were dramatically increased at 14 and 18 weeks of age, but not at 11 weeks of age compared with 6 or 8 weeks of age. Consequently,

we administered Z-LLSD-FMK or Z-YVAD-FMK to ApoE<sup>-/-</sup> mice at 14 weeks of age, and therapeutic effects on atherosclerosis were detected at 18 weeks of age. Suppression of GSDMD activation by Z-LLSD-FMK or Z-YVAD-FMK remarkably reduced lesion development in ApoE<sup>-/-</sup> mice, suggesting that inhibition of GSDMD activation may be a promising strategy for the treatment of atherosclerosis.

In previous studies there were no overt differences in plasma levels of triglycerides or total cholesterol between littermate controls and atherosclerosis-prone mice deficient in GSDMD or caspase-1, but macrophage infiltration in lesions and expression of VCAM-1 and IL-1β in aorta tissue were significantly decreased in atherosclerosis-prone mice lacking GSDMD or caspase-1 (Gage et al., 2012; Usui et al., 2012; Yin et al., 2015; Opoku et al., 2021). Likewise, in the current study inhibition of GSDMD activation by Z-LLSD-FMK or Z-YVAD-FMK had the same above-described effects. We also observed that suppression of GSDMD cleavage by Z-LLSD-FMK or Z-YVAD-FMK markedly reduced the protein levels of MCP-1 and HMGB1 in aorta tissue in ApoE<sup>-/-</sup> mice. Suppression of GSDMD activation by Z-LLSD-FMK or Z-YVAD-FMK attenuated vascular inflammation. It is well-



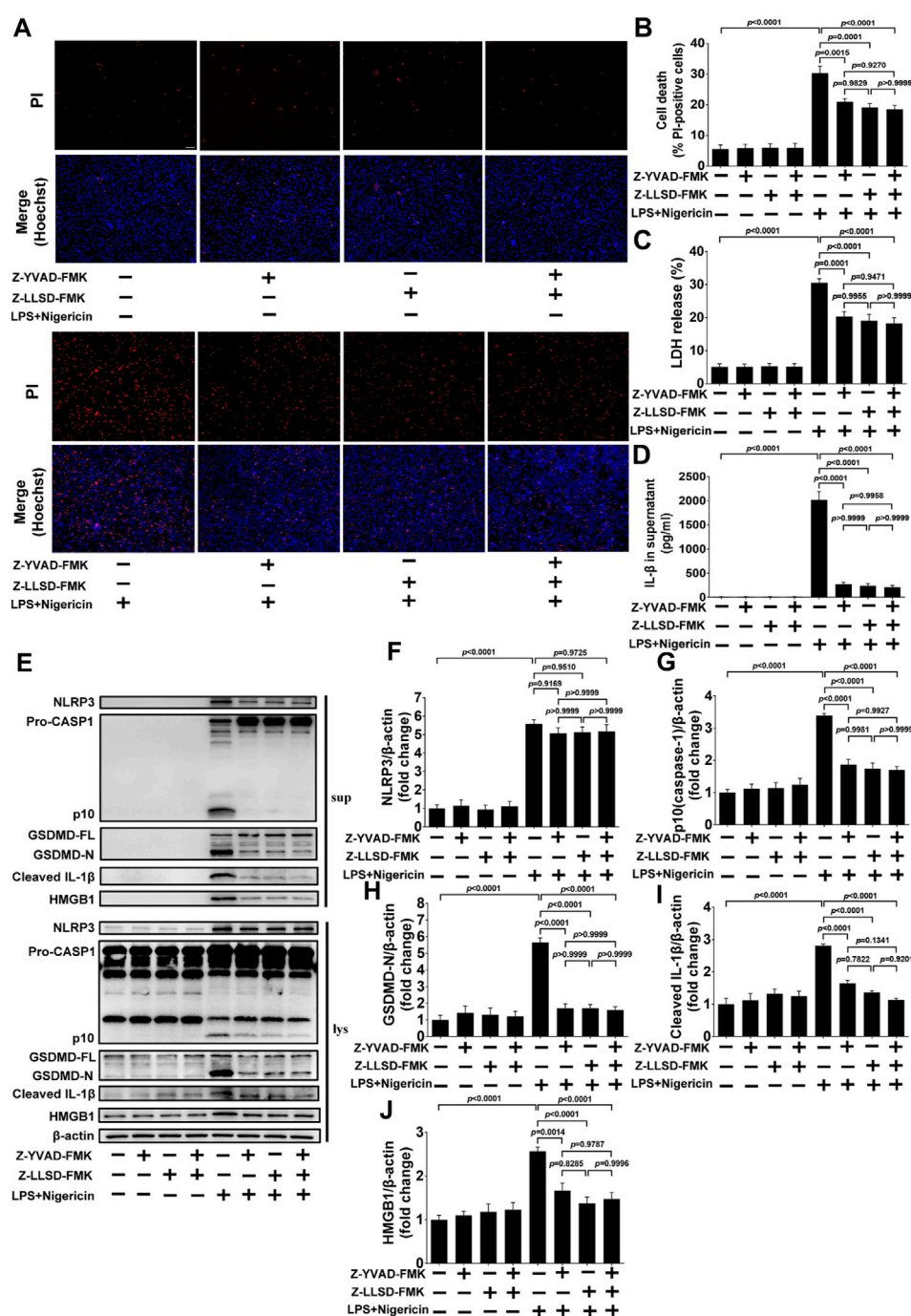


FIGURE 5

Z-LLSD-FMK or Z-YVAD-FMK inhibited GSDMD activation or pyroptosis induced by LPS + nigericin in BMDMs. BMDMs were primed with LPS for 4 h followed by nigericin for 30 min. Z-LLSD-FMK, Z-YVAD-FMK, and both combined were added 30 min before LPS + nigericin treatment. (A) Representative immunofluorescence images of cell death determination via PI (red) and Hoechst 33342 (blue) staining (scale bar = 75 μm). (B) The percentage of PI-positive BMDMs was calculated at five randomly selected image fields ( $n = 5$ ). (C) LDH release in supernatants ( $n = 5$ ). (D) IL-1β release in supernatants was analyzed by ELISA ( $n = 5$ ). (E) Western blotting analysis was performed to detect protein levels of NLRP3, caspase-1, GSDMD, cleaved IL-1β, and HMGB1 in supernatants and cell lysates. (F–J) Quantitative analysis of expression of NLRP3, p10 (caspase-1), GSDMD-N, cleaved IL-1β, and HMGB1 in cell lysates ( $n = 5$ ). β-actin served as the loading control. Data represent means  $\pm$  SEM.

established that imbalanced lipid metabolism and chronic vascular inflammation promote atherosclerosis (Bäck et al., 2019; Libby, 2021). The reduction in atherosclerotic lesion development in the present study was probably due to the relief of vascular

inflammation rather than lipid lowering. Previous studies also showed that in spite of optimal low LDL cholesterol concentrations, there is residual risk of ASCVDs during statin therapy (Johannessen et al., 2021). Thus, in addition to lipid-

lowering therapy, ameliorating vascular inflammation may also be a crucial strategy for treating atherosclerosis, and suppression of GSDMD activation may be a promising therapeutic strategy.

In the current study inhibition of GSDMD activation by Z-LLSD-FMK or Z-YVAD-FMK significantly reduced macrophage infiltration in lesions. It has previously been reported that a lack of GSDMD in mice or in BMDMs, and deficiency of caspase-1 in ApoE<sup>-/-</sup> mice, reduced the release or expression of IL-1 $\beta$  (Gage et al., 2012; Usui et al., 2012; Opoku et al., 2021). In other previous studies deficiency of GSDMD in BMDMs, or lack of caspase-1 either in mice or in BMDMs reduced the release of HMGB1 (Lamkanfi et al., 2010; Volchuk et al., 2020). Deficiency of IL-1 $\beta$  in ApoE<sup>-/-</sup> mice evidently reduced expression of VCAM-1 and MCP-1 (Kirii et al., 2003), whereas exposure of IL-1 $\beta$  caused expression of these molecules in human vascular smooth muscle cells (Wang et al., 1995). Moreover, neutralization or inhibition of HMGB1 in ApoE<sup>-/-</sup> mice reduced expression of VCAM-1 and MCP-1 (Kanellakis et al., 2011; Liu et al., 2013). Consistent with these studies, we found that suppression of GSDMD activation by Z-LLSD-FMK or Z-YVAD-FMK led to reduced expression or release of IL-1 $\beta$  and HMGB1, which reduced protein levels of both VCAM-1 and MCP-1. This may have led to reduced monocyte adhesion to the arterial wall and reduction in intraplaque macrophages, because MCP-1 is one of the most potent chemoattractants of monocytes, and VCAM-1 plays a critical role in the recruitment of monocytes. In this regard it has been established that inhibition of MCP-1 reduces macrophage levels in atherosclerotic lesions, and blocking VCAM-1 inhibits monocytes from entering the arterial wall (Huo et al., 2000; Inoue et al., 2002).

Previous studies have shown that activation of caspase-1 or the canonical inflammasome pathway is induced by infectious or non-infectious challenges (Shi et al., 2017), and the non-canonical pathway is activated by recognizing cytosolic LPS that originally exists in the cell wall of Gram-negative bacterium (Hagar et al., 2013), thereby inducing GSDMD cleavage or pyroptosis (Shi J. et al., 2015; Kayagaki et al., 2015; Aglietti et al., 2016). In the current study there were no significant differences between the Z-LLSD-FMK group and the Z-YVAD-FMK group in the lesion area, and the combination of both did not have enhanced effects. From our results, the canonical inflammasome pathway probably plays a more prominent role than the non-canonical pathway in promoting vascular inflammation and lesion development in ApoE<sup>-/-</sup> mice. Maybe it is because atherosclerosis is chronic sterile inflammation, and it has been reported that the effects of the non-canonical pathway are evident in acute infectious inflammation such as *Salmonella* infection (Broz et al., 2012) or LPS-induced sepsis (Napier et al., 2016). However, more further studies need to be undertaken to verify the effects of the non-canonical pathway in atherosclerosis in the future.

It has been verified that the cleavage site peptide of human GSDMD is <sup>272</sup>FLTD<sup>275</sup>, and Ac-FLTD-CMK, the human GSDMD inhibitor, has been designed and confirmed to markedly inhibit GSDMD cleavage in THP-1 cells (Yang et al., 2018). However, the therapeutic effects of Ac-FLTD-CMK on atherosclerosis have not been investigated. In the present study Z-LLSD-FMK, a novel mouse GSDMD inhibitor, was designed because the cleavage site peptide of mouse GSDMD is <sup>273</sup>LLSD<sup>276</sup>, and it has been shown to suppress GSDMD activation *in vivo* and *in vitro*, and more importantly, reduce atherosclerotic lesion development in ApoE<sup>-/-</sup> mice. GSDMD

cleavage leads to production of GSDMD-N that oligomerizes to form pores in membranes (Shi J. et al., 2015), which mediate the release of intracellular pro-inflammatory contents such as IL-1 $\beta$  (He et al., 2015; Evavold et al., 2018). In a previous study inhibition of GSDMD cleavage by Ac-FLTD-CMK reduced IL-1 $\beta$  release *in vitro* (Yang et al., 2018), and in the current study inhibition of GSDMD activation by Z-LLSD-FMK reduced IL-1 $\beta$  expression or release *in vivo* and *in vitro*. In human carotid or coronary atherosclerotic plaques, IL-1 $\beta$  levels were reportedly increased compared with normal arteries (Galea et al., 1996; Shi X. et al., 2015; Paramel Varghese et al., 2016). IL-1 $\beta$  inhibition by canakinumab evidently reduces inflammation in patients with atherosclerotic disease (Choudhury et al., 2016), and reduces recurrent cardiovascular events in stable patients with coronary artery disease (Ridker et al., 2017). Thus inhibition of GSDMD cleavage by Ac-FLTD-CMK may be of therapeutic benefit in ASCVD patients, and further studies in ASCVD patients need to be undertaken.

GSDMD is cleaved by inflammatory caspases (such as caspase-1) into GSDMD-N oligomerizing to form pores in membranes, thereby inducing pyroptosis (Yang et al., 2018). In this context, the deficiency of GSDMD had ameliorated vascular inflammation and reduced lesion development (Opoku et al., 2021). The same effects are induced by a lack of caspase-1 or other pyroptosis-related proteins (Kirii et al., 2003; Gage et al., 2012; Usui et al., 2012; Yin et al., 2015) in ApoE<sup>-/-</sup> mice. Inhibition of GSDMD activation may therefore be a promising and potential therapeutic target for treating atherosclerosis. A few inhibitors targeting the GSDMD activation pathway and GSDMD itself have been developed in recent years; these include Z-VAD-FMK and disulfiram. However, most of them have low specificity and are associated with a high risk of side effects. For example, Z-VAD-FMK was originally developed to restrain inflammatory caspases (Slee et al., 1996; Burdette et al., 2021) and it significantly inhibits GSDMD activation and pyroptosis in macrophages (Yang et al., 2018). Notably, Z-VAD-FMK does not specifically block only the inflammatory caspases; it also suppresses apoptotic caspases (Burdette et al., 2021). The lack of distinction between caspases leads to off-target effects, rendering it inappropriate for use as a drug (Slee et al., 1996; Ekert et al., 1999; Burdette et al., 2021). Moreover, disulfiram, an inhibitor of the enzyme acetaldehyde dehydrogenase, has been proven to effectively block GSDMD activation and GSDMD-induced pore formation; it inhibits pyroptosis in cells and LPS-induced septic death in mice (Hu et al., 2020; Burdette et al., 2021). Nevertheless, it has been found to have inhibitory effects on various proteins with diverse functions (Burdette et al., 2021). Reports therefore suggest that disulfiram has a considerable number of side effects (Watson et al., 1980; Christensen et al., 1984; Berlin, 1989). Ac-FLTD-CMK has been designed based on the specific cleavage site peptide of human GSDMD and has been proven to significantly block GSDMD cleavage and pyroptosis by potently and specifically inhibiting the enzymatic activities of caspases 1, 4, 5, and 11, but not the apoptotic caspases (such as caspase-3) (Yang et al., 2018). The specificity and availability of Ac-FLTD-CMK has been demonstrated by a series of pharmacological and cellular assays (Yang et al., 2018). In addition, polypeptide drugs are commonly and safely used in clinical practice (Lau and Dunn, 2018; Danielsen et al., 2022). Thus, in our study, Z-LLSD-FMK was designed as the specific cleavage site peptide of mouse GSDMD <sup>273</sup>LLSD<sup>276</sup>, and it was found to inhibit GSDMD



activation *in vivo* and *in vitro* and decrease lesion development in ApoE<sup>-/-</sup> mice. In addition to targeting the upstream pathways of GSDMD activation or GSDMD itself, IL-1 $\beta$  has also been evaluated in clinical studies for the treatment of ASCVDs and has been proven to be effective to a certain extent (Choudhury et al., 2016; Ridker et al., 2017). However, it is a downstream effector protein of pyroptosis; GSDMD, a final executor of canonical and non-canonical inflammasome activity or pyroptosis, is required for IL-1 $\beta$  secretion (He et al., 2015; Shi et al., 2017). Inhibition of GSDMD activation may be a better therapeutic strategy, as the pyroptosis pathway and inflammation are inhibited earlier upstream. Ac-FLTD-CMK may therefore be a promising and potential therapeutic drug for the treatment of atherosclerosis in the future.

Collectively the results of the present study indicate that suppression of GSDMD activation by the novel mouse GSDMD polypeptide inhibitor Z-LLSD-FMK and the specific caspase-1 inhibitor Z-YVAD-FMK significantly reduces vascular inflammation and atherosclerotic lesion development in ApoE<sup>-/-</sup> mice. Both of them markedly restrained GSDMD activation or pyroptosis in a BMDM model of LPS + nigericin. Our findings suggest that blocking GSDMD activation by the novel human GSDMD polypeptide inhibitor Ac-FLTD-CMK may be a novel and effective strategy for reducing atherosclerotic lesion development for the treatment of atherosclerosis.

## Data availability statement

The original contributions presented in the study are included in the article, further inquiries can be directed to the corresponding authors.

## Ethics statement

The animal study was reviewed and approved by Animal Ethics Committee of Zhongshan Hospital, Fudan University.

## References

- Aglietti, R. A., Estevez, A., Gupta, A., Ramirez, M. G., Liu, P. S., Kayagaki, N., et al. (2016). GsdmD p30 elicited by caspase-11 during pyroptosis forms pores in membranes. *Proc. Natl. Acad. Sci. U. S. A.* 113 (28), 7858–7863. doi:10.1073/pnas.1607769113
- Ahmadi, A., Argulian, E., Leipsic, J., Newby, D. E., and Narula, J. (2019). From subclinical atherosclerosis to plaque progression and acute coronary events: JACC state-of-the-art review. *J. Am. Coll. Cardiol.* 74 (12), 1608–1617. doi:10.1016/j.jacc.2019.08.012
- Arai, H., Mortaki, K., Rane, P., Quinn, C., Zhao, Z., and Qian, Y. (2019). Estimating years of life lost due to cardiovascular disease in Japan. *Circ. J.* 83 (5), 1006–1010. doi:10.1253/circj.CJ-18-1216
- Bäck, M., Yurdagül, A., Tabas, I., Öörni, K., and Kovanen, P. T. (2019). Inflammation and its resolution in atherosclerosis: Mediators and therapeutic opportunities. *Nat. Rev. Cardiol.* 16 (7), 389–406. doi:10.1038/s41569-019-0169-2
- Barrett, T. J. (2020). Macrophages in atherosclerosis regression. *Arterioscler. Thromb. Vasc. Biol.* 40 (1), 20–33. doi:10.1161/atvbaha.119.312802
- Berlin, R. G. (1989). Disulfiram hepatotoxicity: A consideration of its mechanism and clinical spectrum. *Alcohol Alcohol* 24 (3), 241–246.
- Broz, P., Pelegrin, P., and Shao, F. (2020). The gasdermins, a protein family executing cell death and inflammation. *Nat. Rev. Immunol.* 20 (3), 143–157. doi:10.1038/s41577-019-0228-2
- Broz, P., Ruby, T., Belhocine, K., Bouley, D. M., Kayagaki, N., Dixit, V. M., et al. (2012). Caspase-11 increases susceptibility to Salmonella infection in the absence of caspase-1. *Nature* 490 (7419), 288–291. doi:10.1038/nature11419
- Burdette, B. E., Esparza, A. N., Zhu, H., and Wang, S. (2021). Gasdermin D in pyroptosis. *Acta Pharm. Sin. B* 11 (9), 2768–2782. doi:10.1016/j.apsb.2021.02.006
- Choudhury, R. P., Birks, J. S., Mani, V., Biasioli, L., Robson, M. D., L'Allier, P. L., et al. (2016). Arterial effects of canakinumab in patients with atherosclerosis and type 2 diabetes or glucose intolerance. *J. Am. Coll. Cardiol.* 68 (16), 1769–1780. doi:10.1016/j.jacc.2016.07.768
- Christensen, J. K., Rønsted, P., and Vaag, U. H. (1984). Side effects after disulfiram. Comparison of disulfiram and placebo in a double-blind multicentre study. *Acta Psychiatr. Scand.* 69 (4), 265–273. doi:10.1111/j.1600-0447.1984.tb02496.x
- Danielsen, M., Hempel, C., Andresen, T. L., and Urquhart, A. J. (2022). Biopharmaceutical nanoclusters: Towards the self-delivery of protein and peptide therapeutics. *J. Control Release* 347, 282–307. doi:10.1016/j.jconrel.2022.04.050
- Duewell, P., Kono, H., Rayner, K. J., Sirois, C. M., Vladimer, G., Bauernfeind, F. G., et al. (2010). NLRP3 inflammasomes are required for atherogenesis and activated by cholesterol crystals. *Nature* 464 (7293), 1357–1361. doi:10.1038/nature08938
- Ekert, P. G., Silke, J., and Vaux, D. L. (1999). Caspase inhibitors. *Cell Death Differ.* 6 (11), 1081–1086. doi:10.1038/sj.cdd.4400594
- Evavold, C. L., Ruan, J., Tan, Y., Xia, S., Wu, H., and Kagan, J. C. (2018). The pore-forming protein gasdermin D regulates interleukin-1 secretion from living macrophages. *Immunity* 48 (1), 35–44.e6. doi:10.1016/j.immuni.2017.11.013

## Author contributions

The study was conceived and designed by B-LZ, Y-ZZ, ML, and HJ. B-LZ and PY performed most of the experiments. E-YS performed some of the experimental procedures. C-YZ, S-YX, and XY contributed to data acquisition. B-LZ and PY analyzed and interpreted the data. B-LZ wrote the manuscript. ML and HJ supervised the project. All authors contributed to the article and approved the submitted version.

## Funding

This study was supported by the National Natural Science Foundation of China (grant number 81970375).

## Acknowledgments

We acknowledge financial support from the National Natural Science Foundation of China, and thank Zhongshan Hospital, Fudan University for providing laboratory equipment.

## Conflict of interest

The authors declare that the research was conducted in the absence of any commercial or financial relationships that could be construed as a potential conflict of interest.

## Publisher's note

All claims expressed in this article are solely those of the authors and do not necessarily represent those of their affiliated organizations, or those of the publisher, the editors and the reviewers. Any product that may be evaluated in this article, or claim that may be made by its manufacturer, is not guaranteed or endorsed by the publisher.

- Fu, Q., Wu, J., Zhou, X. Y., Ji, M. H., Mao, Q. H., Li, Q., et al. (2019). NLRP3/Caspase-1 pathway-induced pyroptosis mediated cognitive deficits in a mouse model of sepsis-associated encephalopathy. *Inflammation* 42 (1), 306–318. doi:10.1007/s10753-018-0894-4
- Gage, J., Hasu, M., Thabet, M., and Whitman, S. C. (2012). Caspase-1 deficiency decreases atherosclerosis in apolipoprotein E-null mice. *Can. J. Cardiol.* 28 (2), 222–229. doi:10.1016/j.cjca.2011.10.013
- Galea, J., Armstrong, J., Gadsdon, P., Holden, H., Francis, S. E., and Holt, C. M. (1996). Interleukin-1 beta in coronary arteries of patients with ischemic heart disease. *Arterioscler. Thromb. Vasc. Biol.* 16 (8), 1000–1006. doi:10.1161/01.atv.16.8.1000
- Garcia-Calvo, M., Peterson, E. P., Leitinger, B., Ruel, R., Nicholson, D. W., and Thornberry, N. A. (1998). Inhibition of human caspases by peptide-based and macromolecular inhibitors. *J. Biol. Chem.* 273 (49), 32608–32613. doi:10.1074/jbc.273.49.32608
- Gicquel, T., Robert, S., Loyer, P., Vicioni, T., Bodin, A., Ribault, C., et al. (2015). IL-1 $\beta$  production is dependent on the activation of purinergic receptors and NLRP3 pathway in human macrophages. *Faseb J.* 29 (10), 4162–4173. doi:10.1096/fj.14-267393
- Hagar, J. A., Powell, D. A., Aachoui, Y., Ernst, R. K., and Miao, E. A. (2013). Cytoplasmic LPS activates caspase-11: Implications in TLR4-independent endotoxemic shock. *Science* 341 (6151), 1250–1253. doi:10.1126/science.1240988
- He, W. T., Wan, H., Hu, L., Chen, P., Wang, X., Huang, Z., et al. (2015). Gasdermin D is an executor of pyroptosis and required for interleukin-1 $\beta$  secretion. *Cell Res.* 25 (12), 1285–1298. doi:10.1038/cr.2015.139
- Hu, J. J., Liu, X., Xia, S., Zhang, Z., Zhang, Y., Zhao, J., et al. (2020). FDA-approved disulfiram inhibits pyroptosis by blocking gasdermin D pore formation. *Nat. Immunol.* 21 (7), 736–745. doi:10.1038/s41590-020-0669-6
- Huo, Y., Hafezi-Moghadam, A., and Ley, K. (2000). Role of vascular cell adhesion molecule-1 and fibronectin connecting segment-1 in monocyte rolling and adhesion on early atherosclerotic lesions. *Circ. Res.* 87 (2), 153–159. doi:10.1161/01.res.87.2.153
- Inoue, S., Egashira, K., Ni, W., Kitamoto, S., Usui, M., Otani, K., et al. (2002). Anti-monocyte chemoattractant protein-1 gene therapy limits progression and destabilization of established atherosclerosis in apolipoprotein E-knockout mice. *Circulation* 106 (21), 2700–2706. doi:10.1161/01.cir.0000038140.80105.ad
- Johannessen, C. D. L., Mortensen, M. B., Langsted, A., and Nordestgaard, B. G. (2021). Apolipoprotein B and non-HDL cholesterol better reflect residual risk than LDL cholesterol in statin-treated patients. *J. Am. Coll. Cardiol.* 77 (11), 1439–1450. doi:10.1016/j.jacc.2021.01.027
- Kanellakis, P., Agrotis, A., Kyaw, T. S., Koulis, C., Ahrens, I., Mori, S., et al. (2011). High-mobility group box protein 1 neutralization reduces development of diet-induced atherosclerosis in apolipoprotein E-deficient mice. *Arterioscler. Thromb. Vasc. Biol.* 31 (2), 313–319. doi:10.1161/atvbaha.110.218669
- Kayagaki, N., Stowe, I. B., Lee, B. L., O'Rourke, K., Anderson, K., Warming, S., et al. (2015). Caspase-11 cleaves gasdermin D for non-canonical inflammasome signalling. *Nature* 526 (7575), 666–671. doi:10.1038/nature15541
- Kirii, H., Niwa, T., Yamada, Y., Wada, H., Saito, K., Iwakura, Y., et al. (2003). Lack of interleukin-1 $\beta$  decreases the severity of atherosclerosis in ApoE-deficient mice. *Arterioscler. Thromb. Vasc. Biol.* 23 (4), 656–660. doi:10.1161/01.Atv.0000064374.15232.C3
- Lamkanfi, M., Sarkar, A., Vande Walle, L., Vitari, A. C., Amer, A. O., Wewers, M. D., et al. (2010). Inflammasome-dependent release of the alarmin HMGB1 in endotoxemia. *J. Immunol.* 185 (7), 4385–4392. doi:10.4049/jimmunol.1000803
- Lau, J. L., and Dunn, M. K. (2018). Therapeutic peptides: Historical perspectives, current development trends, and future directions. *Bioorg Med. Chem.* 26 (10), 2700–2707. doi:10.1016/j.bmc.2017.06.052
- Li, J., An, Z., Song, J., Du, J., Zhang, L., Jiang, J., et al. (2021). Fine particulate matter-induced lung inflammation is mediated by pyroptosis in mice. *Ecotoxicol. Environ. Saf.* 219, 112351. doi:10.1016/j.ecoenv.2021.112351
- Libby, P. (2021). The changing landscape of atherosclerosis. *Nature* 592 (7855), 524–533. doi:10.1038/s41586-021-03392-8
- Liu, M., Yu, P., Jiang, H., Yang, X., Zhao, J., Zou, Y., et al. (2017). The essential role of Pin1 via NF- $\kappa$ B signaling in vascular inflammation and atherosclerosis in ApoE(-/-) mice. *Int. J. Mol. Sci.* 18 (3), 644. doi:10.3390/ijms18030644
- Liu, M., Yu, Y., Jiang, H., Zhang, L., Zhang, P. P., Yu, P., et al. (2013). Simvastatin suppresses vascular inflammation and atherosclerosis in ApoE(-/-) mice by downregulating the HMGB1-RAGE axis. *Acta Pharmacol. Sin.* 34 (6), 830–836. doi:10.1038/aps.2013.8
- Liu, W., Yang, D., Shi, J., Wen, P., Zhang, J., Wang, Z., et al. (2021). Caspase-1 inhibitor reduces pyroptosis induced by brain death in kidney. *Front. Surg.* 8, 760989. doi:10.3389/fsurg.2021.760989
- Ma, L. Y., Chen, W. W., Gao, R. L., Liu, L. S., Zhu, M. L., Wang, Y. J., et al. (2020). China cardiovascular diseases report 2018: An updated summary. *J. Geriatr. Cardiol.* 17 (1), 1–8. doi:10.11909/j.issn.1671-5411.2020.01.001
- Napier, B. A., Brubaker, S. W., Sweeney, T. E., Monette, P., Rothmeier, G. H., Gertszov, N. A., et al. (2016). Complement pathway amplifies caspase-11-dependent cell death and endotoxin-induced sepsis severity. *J. Exp. Med.* 213 (11), 2365–2382. doi:10.1084/jem.20160027
- Opoku, E., Traugher, C. A., Zhang, D., Iacano, A. J., Khan, M., Han, J., et al. (2021). Gasdermin D mediates inflammation-induced defects in reverse cholesterol transport and promotes atherosclerosis. *Front. Cell Dev. Biol.* 9, 715211. doi:10.3389/fcell.2021.715211
- Paramel Varghese, G., Folkersen, L., Strawbridge, R. J., Halvorsen, B., Yndestad, A., Ranheim, T., et al. (2016). NLRP3 inflammasome expression and activation in human atherosclerosis. *J. Am. Heart Assoc.* 5 (5), e003031. doi:10.1161/jaha.115.003031
- Ridker, P. M., Everett, B. M., Thuren, T., MacFadyen, J. G., Chang, W. H., Ballantyne, C., et al. (2017). Antiinflammatory therapy with canakinumab for atherosclerotic disease. *N. Engl. J. Med.* 377 (12), 1119–1131. doi:10.1056/NEJMoa1707914
- Rozman-Pungercar, J., Kopitar-Jerala, N., Bogoy, M., Turk, D., Vasiljeva, O., Stefe, I., et al. (2003). Inhibition of papain-like cysteine proteases and legumain by caspase-specific inhibitors: When reaction mechanism is more important than specificity. *Cell Death Differ.* 10 (8), 881–888. doi:10.1038/sj.cdd.4401247
- Shi, J., Gao, W., and Shao, F. (2017). Pyroptosis: Gasdermin-Mediated programmed necrotic cell death. *Trends Biochem. Sci.* 42 (4), 245–254. doi:10.1016/j.tibs.2016.10.004
- Shi, J., Zhao, Y., Wang, K., Shi, X., Wang, Y., Huang, H., et al. (2015a). Cleavage of GSDMD by inflammatory caspases determines pyroptotic cell death. *Nature* 526 (7575), 660–665. doi:10.1038/nature15514
- Shi, X., Xie, W. L., Kong, W. W., Chen, D., and Qu, P. (2015b). Expression of the NLRP3 inflammasome in carotid atherosclerosis. *J. Stroke Cerebrovasc. Dis.* 24 (11), 2455–2466. doi:10.1016/j.jstrokecerebrovasdis.2015.03.024
- Slee, E. A., Zhu, H., Chow, S. C., MacFarlane, M., Nicholson, D. W., and Cohen, G. M. (1996). Benzoyloxycarbonyl-Val-Ala-Asp (OMe) fluoromethylketone (Z-VAD-FMK) inhibits apoptosis by blocking the processing of CPP32. *Biochem. J.* 315 (Pt 1), 21–24. doi:10.1042/bj3150021
- Soehnlein, O., and Libby, P. (2021). Targeting inflammation in atherosclerosis - from experimental insights to the clinic. *Nat. Rev. Drug Discov.* 20 (8), 589–610. doi:10.1038/s41573-021-00198-1
- Su, E., Yu, P., Zhang, B., Zhang, A., Xie, S., Zhang, C., et al. (2022). Endothelial intracellular ANG (angiogenin) protects against atherosclerosis by decreasing endoplasmic reticulum stress. *Arterioscler. Thromb. Vasc. Biol.* 42 (3), 305–325. doi:10.1161/atvbaha.121.317339
- Usui, F., Shirasuna, K., Kimura, H., Tatsumi, K., Kawashima, A., Karasawa, T., et al. (2012). Critical role of caspase-1 in vascular inflammation and development of atherosclerosis in Western diet-fed apolipoprotein E-deficient mice. *Biochem. Biophys. Res. Commun.* 425 (2), 162–168. doi:10.1016/j.bbrc.2012.07.058
- Virani, S. S., Alonso, A., Benjamin, E. J., Bittencourt, M. S., Callaway, C. W., Carson, A. P., et al. (2020). Heart disease and stroke statistics 2020 update: A report from the American heart association. *Circulation* 141 (9), e139–e596. doi:10.1161/cir.0000000000000757
- Volchuk, A., Ye, A., Chi, L., Steinberg, B. E., and Goldenberg, N. M. (2020). Indirect regulation of HMGB1 release by gasdermin D. *Nat. Commun.* 11 (1), 4561. doi:10.1038/s41467-020-18443-3
- Wang, X., Feuerstein, G. Z., Gu, J. L., Lysko, P. G., and Yue, T. L. (1995). Interleukin-1 $\beta$  induces expression of adhesion molecules in human vascular smooth muscle cells and enhances adhesion of leukocytes to smooth muscle cells. *Atherosclerosis* 115 (1), 89–98. doi:10.1016/0021-9150(94)05503-b
- Watson, C. P., Ashby, P., and Bilbao, J. M. (1980). Disulfiram neuropathy. *Can. Med. Assoc. J.* 123 (2), 123–126.
- Wen, S., Deng, F., Li, L., Xu, L., Li, X., and Fan, Q. (2022). VX-765 ameliorates renal injury and fibrosis in diabetes by regulating caspase-1-mediated pyroptosis and inflammation. *J. Diabetes Investig.* 13 (1), 22–33. doi:10.1111/jdi.13660
- Willemsen, L., and de Winther, M. P. (2020). Macrophage subsets in atherosclerosis as defined by single-cell technologies. *J. Pathol.* 250 (5), 705–714. doi:10.1002/path.5392
- Xu, H., Jiang, J., Chen, W., Li, W., and Chen, Z. (2019). Vascular macrophages in atherosclerosis. *J. Immunol. Res.* 2019, 4354786. doi:10.1155/2019/4354786
- Yanai, H., Matsuda, A., An, J., Koshiba, R., Nishio, J., Negishi, H., et al. (2013). Conditional ablation of HMGB1 in mice reveals its protective function against endotoxemia and bacterial infection. *Proc. Natl. Acad. Sci. U. S. A.* 110 (51), 20699–20704. doi:10.1073/pnas.1320808110
- Yang, J., Liu, Z., Wang, C., Yang, R., Rathkey, J. K., Pinkard, O. W., et al. (2018). Mechanism of gasdermin D recognition by inflammatory caspases and their inhibition by a gasdermin D-derived peptide inhibitor. *Proc. Natl. Acad. Sci. U. S. A.* 115 (26), 6792–6797. doi:10.1073/pnas.1800562115
- Yin, Y., Li, X., Sha, X., Xi, H., Li, Y. F., Shao, Y., et al. (2015). Early hyperlipidemia promotes endothelial activation via a caspase-1-sirtuin 1 pathway. *Arterioscler. Thromb. Vasc. Biol.* 35 (4), 804–816. doi:10.1161/atvbaha.115.305282
- Zhang, C., Zhao, C., Chen, X., Tao, R., Wang, S., Meng, G., et al. (2020). Induction of ASC pyroptosis requires gasdermin D or caspase-1/11-dependent mediators and IFN $\beta$  from pyroptotic macrophages. *Cell Death Dis.* 11 (6), 470. doi:10.1038/s41419-020-2664-0
- Zhang, L., Zhang, B., Yu, Y., Wang, J., Wu, J., Su, Y., et al. (2021). Angiotensin II increases HMGB1 expression in the myocardium through AT1 and AT2 receptors when under pressure overload. *Int. Heart J.* 62 (1), 162–170. doi:10.1536/ihj.20-384



## OPEN ACCESS

## EDITED BY

Xianwei Wang,  
Xinxiang Medical University, China

## REVIEWED BY

Tao You,  
Gansu Provincial Hospital, China  
Xuan Zheng,  
Wuhan University, China  
Siyi He,  
General Hospital of Western Theater  
Command, China

## \*CORRESPONDENCE

Jiang Li,  
✉ lijiangcs@csu.edu.cn

RECEIVED 12 June 2023

ACCEPTED 09 August 2023

PUBLISHED 28 August 2023

## CITATION

Luo J, Li Y, Chen J, Qiu H, Chen W, Luo X, Chen Y, Tan Y and Li J (2023), Evaluating the role of serum uric acid in the risk stratification and therapeutic response of patients with pulmonary arterial hypertension associated with congenital heart disease (PAH-CHD). *Front. Pharmacol.* 14:1238581. doi: 10.3389/fphar.2023.1238581

## COPYRIGHT

© 2023 Luo, Li, Chen, Qiu, Chen, Luo, Chen, Tan and Li. This is an open-access article distributed under the terms of the [Creative Commons Attribution License \(CC BY\)](https://creativecommons.org/licenses/by/4.0/). The use, distribution or reproduction in other forums is permitted, provided the original author(s) and the copyright owner(s) are credited and that the original publication in this journal is cited, in accordance with accepted academic practice. No use, distribution or reproduction is permitted which does not comply with these terms.

# Evaluating the role of serum uric acid in the risk stratification and therapeutic response of patients with pulmonary arterial hypertension associated with congenital heart disease (PAH-CHD)

Jun Luo, Yuanchang Li, Jingyuan Chen, Haihua Qiu, Wenjie Chen, Xiaoqin Luo, Yusi Chen, Yingjie Tan and Jiang Li\*

Department of Cardiovascular Medicine, The Second Xiangya Hospital, Central South University, Changsha, Hunan, China

**Background:** Pulmonary arterial hypertension (PAH) is a malignant pulmonary vascular disease that negatively impacts quality of life, exercise capacity, and mortality. This study sought to investigate the relationship between serum uric acid (UA) level and the disease severity and treatment response of patients with PAH and congenital heart disease (PAH-CHD).

**Methods:** This study included 225 CHD patients and 40 healthy subjects. Serum UA was measured in all patients, and UA levels and haemodynamic parameters were re-evaluated in 20 patients who had received PAH-specific drug treatment for at least  $7 \pm 1$  month.

**Results:** Serum UA levels were significantly higher in PAH-CHD patients than in CHD patients with a normal pulmonary artery pressure and normal subjects ( $347.7 \pm 105.7 \mu\text{mol/L}$  vs.  $278.3 \pm 84.6 \mu\text{mol/L}$ ;  $347.7 \pm 105.7 \mu\text{mol/L}$  vs.  $255.7 \pm 44.5 \mu\text{mol/L}$ ,  $p < 0.05$ ). UA levels in the intermediate and high risk groups were significantly higher than those in the low-risk group ( $365.6 \pm 107.8 \mu\text{mol/L}$  vs.  $311.2 \pm 82.8 \mu\text{mol/L}$ ;  $451.6 \pm 117.6 \mu\text{mol/L}$  vs.  $311.2 \pm 82.8 \mu\text{mol/L}$ ,  $p < 0.05$ ). Serum UA levels positively correlated with mean pulmonary arterial pressure, WHO functional class, pulmonary vascular resistance, and NT-proBNP ( $r = 0.343, 0.357, 0.406, 0.398$ ;  $p < 0.001$ ), and negatively with mixed venous oxygen saturation ( $\text{SvO}_2$ ) and arterial oxygen saturation ( $\text{SaO}_2$ ) ( $r = -0.293, -0.329$ ;  $p < 0.001$ ). UA significantly decreased from  $352.7 \pm 97.5$  to  $294.4 \pm 56.8 \mu\text{mol/L}$  ( $p = 0.001$ ) after PAH-specific drug treatment for at least 6 months, along with significant decreases in mean pulmonary arterial pressure and pulmonary vascular resistance and increases in cardiac index and mixed  $\text{SvO}_2$ .

**Conclusion:** Serum UA can be used as a practical and economic biomarker for risk stratification and the evaluation of PAH-specific drug treatment effects for patients with PAH-CHD.

## KEYWORDS

uric acid, congenital heart disease, pulmonary arterial hypertension, eisenmenger syndrome, risk stratification

# 1 Introduction

Pulmonary hypertension (PH) is a malignant pulmonary vascular disease that is characterized by a progressive increase in pulmonary vascular resistance (PVR) that can eventually lead to right heart failure and death (Galiè et al., 2015). PH is currently subclassified into five categories. PAH associated with congenital heart disease (PAH-CHD) is the first category of PH, and is primarily characterized by pulmonary arteriole remodeling (Galiè et al., 2015; Simonneau et al., 2019). Nearly 50% of PAH patients have idiopathic, heritable, or drug-induced PAH in Western countries (Simonneau et al., 2019). However, CHD is the most common cause of PAH in China (Jiang and Jing, 2013).

Most CHD patients are diagnosed late for many reasons, at which time the pulmonary vessels have already undergone irreversible remodeling and in some cases Eisenmenger syndrome (ES) is established. ES is not correctable surgically (Dimopoulos et al., 2014). While PAH-specific drugs improve survival (Galiè et al., 2015; Arnott et al., 2018), many patients continually deteriorate. In a Danish nationwide study, Schwartz found that the 1-, 5-, and 10-year mortality rates of PAH-CHD patients were 24%, 44%, and 52%, respectively (Schwartz et al., 2018). Early diagnosis, accurate and convenient disease severity assessment, and the ability to predict changes due to the disease are key prognostic factors for PAH-CHD patients.

The utility of serological biomarkers in PAH has been a recent subject of significant research. Brain natriuretic peptide (BNP), N-terminal pro BNP (NT-proBNP), troponin T (TNT), endothelin-1 (ET-1) and C-reactive protein (CRP) have all been associated with the development of PAH. However, only the measurement of BNP and NT-proBNP are recommended by clinical guidelines and widely used in practice (Nagaya et al., 2000; Leuchte et al., 2007; Foris et al., 2013; Galiè et al., 2015; Pezzuto et al., 2015).

Serum uric acid (UA) is the final product of purine metabolism and is a marker of low cardiac output (CO) and/or tissue hypoxia (Foris et al., 2013; Galiè et al., 2015; Pezzuto et al., 2015). UA plays an important role in the disease evaluation and prognosis of PAH patients with idiopathic PAH and that associated with connective tissue disease (Nagaya et al., 1999; Castillo-Martínez et al., 2016). However, the clinical significance of UA in patients with PAH-CHD has been poorly studied, and quantitative risk stratification of PAH using UA levels has never been attempted. This study aimed to analyze the role of UA in assessing the disease status, risk stratification, and treatment response of PAH-CHD patients to provide the basis for its clinical use.

## 2 Patients and methods

### 2.1 Study population

This study was performed at the Department of Cardiovascular Medicine of the Second Xiangya Hospital, Central South University, China. Two-hundred consecutive CHD patients diagnosed with PAH (PAH-CHD group) from July 2017 to June 2019 were enrolled. The inclusion criteria were: 1) a diagnosis of PAH, defined as an mPAP  $\geq 25$  mmHg, pulmonary artery wedge

pressure (PAWP)  $\leq 15$  mmHg, and PVR  $\geq 3$  Wood; 2) all measurements were performed via right heart catheterization (RHC). The exclusion criteria were: 1) any other cause of PH, including connective tissue disease, left heart disease, lung disease and/or hypoxia, and chronic thromboembolic disease; 2) patients with gout, liver disease, kidney disease, hypertension, coronary heart disease, an age  $< 18$  years old, missing data, a history of CHD surgery, or prior use of PAH-specific drugs. Twenty-five CHD patients with normal pulmonary arterial pressures (non-PAH-CHD group) and 40 healthy adults (normal group) were used as controls. The inclusion criteria for the healthy adult group were age older than 18 years old and no history of hypertension, obesity, diabetes, coronary heart disease, stroke, or other cardiovascular disease. The study protocol was approved by the ethics committee of The Second Xiangya Hospital of Central South University, and all participants provided informed consent before enrollment. The flow chart for this study was described in Figure 1.

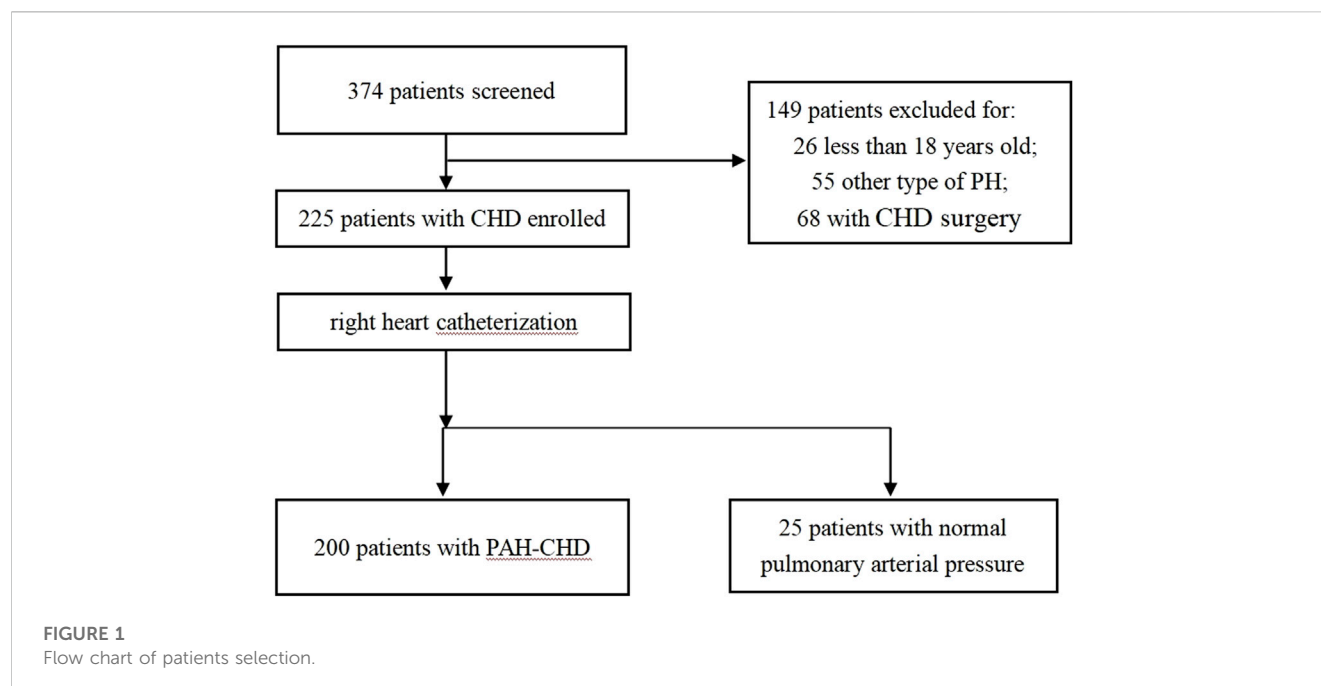
### 2.2 Clinical and laboratory data

Baseline clinical information, including gender, age, body mass index (BMI), systolic blood pressure (SBP), diastolic blood pressure (DBP), arterial oxygen saturation (SaO<sub>2</sub>), heart rate, WHO functional class, and previous medical history were collected. Blood samples were drawn from the unilateral cubital vein after an overnight fast and prior to RHC. Medications, including diuretics, cardiac inotropes, and targeted drugs, were initiated based on an adequate risk status assessment. This protocol was implemented to reduce the influence of medication regimen on baseline serum UA level to the greatest extent possible. A complete blood count was analyzed using a SYSMEX Blood Analyzer XN10 (Kobe, Japan). Serum UA levels were measured using the uricase-peroxidase method. Other biochemical parameters, including creatinine (Cr), alanine aminotransferase (ALT), aspartate aminotransferase (AST), direct bilirubin (DBIL), total bilirubin (TBIL), D-Dimer, and NT-proBNP, were analyzed using a Hitachi Automatic Biochemical Analyzer 7,600-020 (Tokyo, Japan) in the laboratory at The Second Xiangya Hospital of Central South University. The reference range for UA was 142.0–416.0  $\mu\text{mol/L}$ .

### 2.3 Echocardiography

An experienced cardiologist performed transthoracic echocardiography (TTE) on all patients using a commercially available device (Vivid 7, Vingmed, GE, United States of America). Using left ventricular (LV) long axis, LV short axis, and apical 4-chamber views, we evaluated and recorded the right atrial end-systolic diameter (RAS), right ventricular end-diastolic diameter (RVD), internal diameter of the pulmonary artery (PA), aortic inner diameter (AO), and left ventricular ejection fraction (LVEF). Systolic tricuspid regurgitation velocity (TRV) was calculated using continuous-wave Doppler echocardiography, and the peak TRV was used to estimate the peak tricuspid regurgitation pressure gradient (PTR) using a simplified Bernoulli equation. Systolic PA pressure (sPAP) was estimated by adding PTR to the





estimated right atrial pressure based on the size and change in diameter of the inferior vena cava during respiration.

## 2.4 Right heart catheterization

With the exception of healthy subjects, all patients underwent RHC via their right femoral vein at the Interventional Catheterization Centre of The Second Xiangya Hospital of Central South University. We used a Siemens Axiom Artis X-ray device (SIEMENS Co., Munich, Germany). Baseline haemodynamic parameters, including systolic pulmonary arterial pressure (SPAP), diastolic pulmonary arterial pressure (DPAP), mPAP, mean right atrial pressure (mRAP), PAWP, and oximetry samples of various heart chambers, were measured using a Swan-Ganz catheter. Cardiac index (CI) was calculated as CO based on Fick's principle divided by body surface area. PVR was calculated using the following formula:  $(mPAP - PAWP) / CO$ . We used Wood units as the units for PVR. ES was defined as  $Qp/Qs < 1.0$  and  $PVR > 10$  Wood. All studied patients were diagnosed with PAH-CHD via RHC according to the following standard criteria: an  $mPAP \geq 25$  mmHg and  $PVR > 3$  Wood units at rest in the presence of a normal PAWP ( $\leq 15$  mmHg).

## 2.5 Risk assessment

The pre-treatment risk assessment for the 200 PAH-CHD patients was based on the comprehensive risk stratification recommended by the European Heart Journal in 2018 (Kylhammar et al., 2018). This risk assessment strategy includes eight variables: World Health Organization functional class (FC), 6-min walking distance (6MWD), CI, right atrial pressure, NT-proBNP, mixed venous oxygen saturation ( $SvO_2$ ), right atrial area, and the presence of a pericardial effusion. All of the

aforementioned variables were a part of the risk assessment instrument proposed by the ESC/ERS 2015 guidelines (Galiè et al., 2015). Each variable was categorized as low, intermediate, or high risk based on pre-specified values and given one, two, or three points, respectively. We then divided the sum of all grades by the number of available variables for each patient, resulting in a mean grade. The risk group for each patient was defined by the mean grade rounded off to the nearest integer. PAH-CHD patients were categorized into three risk groups: low (PAH-CHD-L group), intermediate (PAH-CHD-M group), or high (PAH-CHD-H group).

## 2.6 Treatment and follow-up

Surgical indications at our center were a pulmonary-to-systemic flow ratio ( $Qp/Qs$ )  $\geq 1.5$  and a  $PVR \leq 3$  Wood. The 138 PAH-CHD patients who were not candidates for transcatheter closure or surgery received individualized treatments. In addition to conventional treatment, including oxygen, diuretics, or digitalis, patients with a positive acute pulmonary vasodilator test received a calcium channel blocker. Patients with a negative acute pulmonary vasodilator test received at least one disease-specific drug, such as an endothelin receptor antagonist (ERA), phosphodiesterase type 5 inhibitor (PDE-5i), or prostacyclin analogue (PGI<sub>2</sub>). We followed all PAH-CHD patients who received PAH-specific drug therapies. Twenty PAH-CHD patients underwent repeated RHC after an average follow-up period of  $7 \pm 1$  month. Additional information, including biochemical indicators and echocardiographic parameters, were also collected for these patients.

## 2.7 Statistical analysis

Statistical analyses were performed using the Statistical Package for Social Science version 22.0 for Windows (SPSS Inc., Chicago, IL,



United States). Quantitative data (Clinical features, biochemical indicators, echocardiography parameters, and haemodynamic variables) were described as means and standard deviations (normal or approximately normal distributions) or medians and interquartile ranges (IQR) (non-normal distributions). Normally distributed data were compared using a one-way analysis of variance for repeated measurement data, and non-normal distributions were compared using Friedman's M test. Qualitative data and ranked data (WHO FC) were described as a number and percentage. Ranked data were compared using Friedman's M test, and qualitative data were compared using Cochran's Q test. Correlation coefficients between two variables were calculated using Pearson's correlation. A receiver operating characteristic (ROC) curve was used to confirm the serum UA level that provided the best diagnostic significance for intermediate to high-risk PAH-CHD patients. A paired *t*-test was performed to compare baseline and post-treatment echocardiographic, haemodynamic, and serological features. Two-sided *p*-values less than 0.05 were considered statistically significant in all analyses.

## 3 Results

### 3.1 Baseline characteristics

This study included 200 PAH-CHD patients (mean age  $37.7 \pm 14.1$  years; range 15–72 years; 145 female). The PAH-CHD-L group had 94 patients (47.0%), the PAH-CHD-M group 88 (44.0%), and the PAH-CHD-H group 18 (9.0%). All PAH-CHD patients received standard therapy with diuretics. Compared with the nPAH-CHD group and the control group, the body weight and BMI of the PAH-CHD group were lower ( $p < 0.05$ ). There was no statistically significant difference in BMI between the low, medium, and high-risk patients in the PAH-CHD group ( $p > 0.05$ ). There were no significant differences in baseline ALT, AST, total bile acid (TBA), blood Urea Nitrogen (BUN), Cr, international standardized ratio (INR), and D-Dimer levels between groups. Airect bilirubin (DBIL), NT-proBNP, and platelet levels were higher in the PAH-CHD group than in the normal control and nPAH-CHD groups ( $p < 0.05$ ). Subgroup analysis showed that NT-proBNP and platelet levels in the PAH-CHD-M and PAH-CHD-H groups were significantly higher than in the PAH-CHD-L group ( $p < 0.05$ ), but there was no statistical difference between the two groups ( $p > 0.05$ ). The red blood cell distribution width (RDW) in the PAH-CHD group was equivalent to that of the non-PAH-CHD and control groups ( $p > 0.05$ ). However, our subgroup analysis showed that the RDW level of the PAH-CHD-H group was higher than that of the PAH-CHD-M group ( $p < 0.05$ ), but equivalent to the PAH-CHD-L group (Table 1).

### 3.2 Hemodynamic data

The mean RAS, RVD, PA, and TRV of the PAH-CHD (including all subgroups) and nPAH-CHD groups were significantly higher than those of the control group ( $p < 0.05$ ). The mean PA and TRV levels in the PAH-CHD group (including all subgroups) were both higher than those of the nPAH-CHD group ( $p < 0.05$ ) (Table 1).

Compared with the nPAH-CHD group, the PAH-CHD group (including all subgroups) had significantly increased pulmonary artery systolic pressure (SPAP), pulmonary artery diastolic pressure (DPAP), pulmonary artery mean pressure (mPAP), right ventricular mean pressure (mRVP), and total pulmonary resistance (PVR) ( $p < 0.05$ ). The levels of SPAP and mPAP in the PAH-CHD-H group were significantly higher than those of the PAH-CHD-M and PAH-CHD-L groups ( $p < 0.05$ ), but there was no statistically significant difference in SPAP between the PAH-CHD-M and PAH-CHD-L groups ( $p > 0.05$ ). The mean DPAP and mRVP of the PAH-CHD-H and PAH-CHD-M groups were higher than those of the PAH-CHD-L group ( $p < 0.05$ ). However, there was no statistically significant difference in DPAP and mRVP between the PAH-CHD-H and the PAH-CHD-M group ( $p > 0.05$ ). SvO<sub>2</sub> was significantly lower in the PAH-CHD group (including all subgroups), and decreased with increased PAH risk stratification level ( $p < 0.05$ ) (Table 1).

### 3.3 UA levels and ROC curve analysis

Baseline UA levels were significantly higher in PAH-CHD patients than in CHD patients with normal pulmonary pressures or normal control subjects (Table 1). Patients in the intermediate- and high-risk groups had significantly higher UA levels than low-risk patients (Figure 2). A total of 40 patients presented with hyperuricemia (UA  $> 416.0 \mu\text{mol/L}$ ), including 2 non-PAH-CHD patients, 10 PAH-CHD-L patients, 20 PAH-CHD-M patients, and 8 PAH-CHD-H patients, accounting for 8.0%, 10.6%, 22.7%, and 44.4% of each group. As no significant difference in UA levels was observed between the PAH-CHD-L and non-PAH-CHD groups, we performed ROC analysis and identified a cutoff serum UA level of  $330.9 \mu\text{mol/L}$  to achieve the maximum Youden index {sensitivity [65.1%]-[1-specificity (71.4%)]}. The area under the curve (AUC) was 0.706 (95% CI 0.638–0.773) for predicting intermediate-high risk PAH (Figure 3).

### 3.4 Correlations between serum UA levels and haemodynamic features and risk assessment variables

Table 2 presents correlations between serum UA levels and different variables. Serum UA levels were positively correlated with mPAP, SPAP, WHO functional class, NT-proBNP, and PVR, and a negatively correlated with SvO<sub>2</sub>, and SaO<sub>2</sub> (Figure 4) the influence of serum UA levels on clinical indicators.

The optimal cutoff value for UA diagnosis for medium to high-risk PAH-CHD patients was calculated using ROC curve analysis. This study divided PAH-CHD patients into UA  $> 330.9 \mu\text{mol}$  and UA  $\leq 330.9 \mu\text{mol}$  groups. Differences in patient characteristics, biochemical indicators, imaging measurements, and hemodynamic parameters were compared between the two groups. Cardiac function grading, NT-proBNP, RAS, RVD, mean PA, and PVR were significantly increased in the higher UA level group than the UA  $\leq 330.9 \mu\text{mol}$  group, while SaO<sub>2</sub>, SvO<sub>2</sub> and right CI were significantly decreased in the higher UA level group ( $p < 0.05$ ). These results indicate that high levels of UA can indicate more severe PAH and a worse prognosis in PAH-CHD patients (Table 3).

TABLE 1 Baseline patient characteristics.

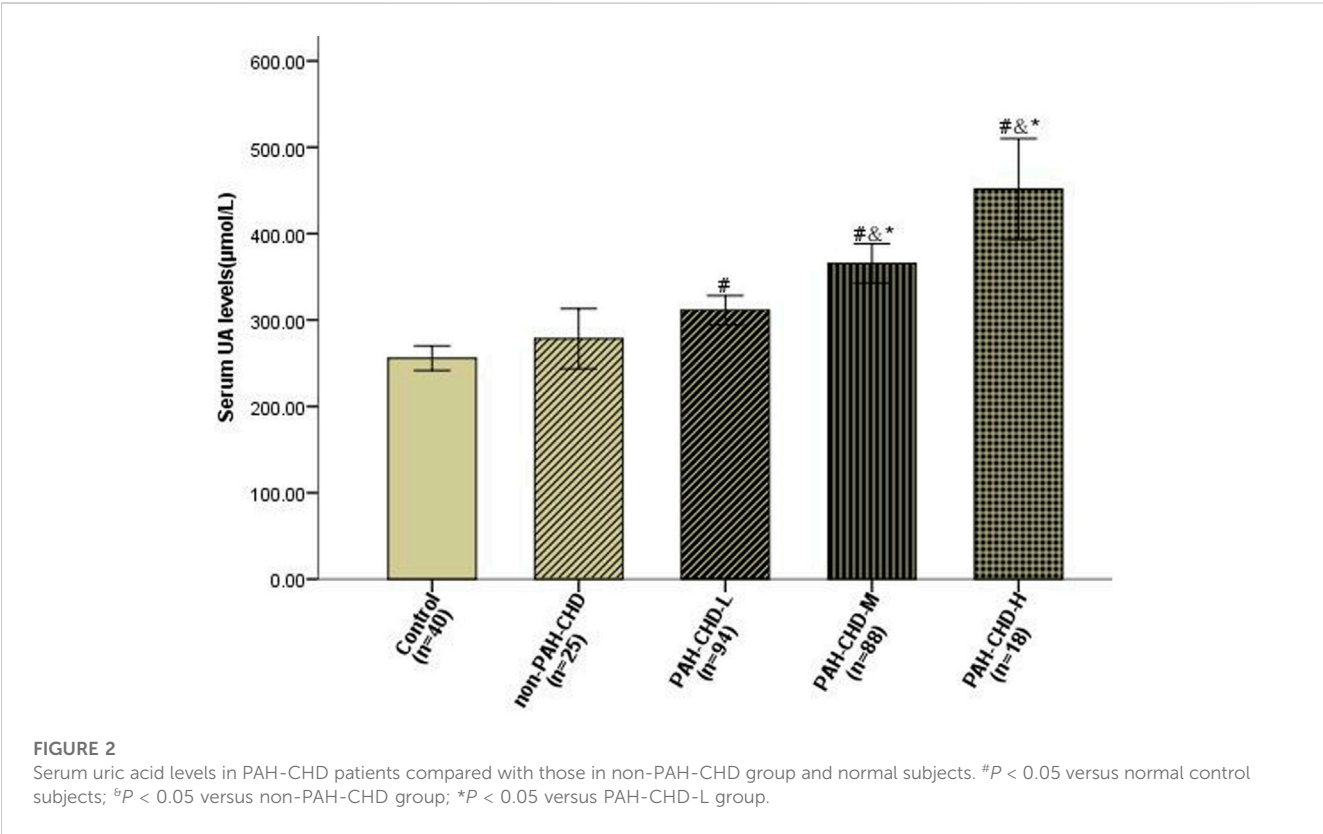
Characteristics	Normal ( <i>n</i> = 40)	Non-PAH-CHD ( <i>n</i> = 25)	PAH-CHD ( <i>n</i> = 200)	PAH-CHD-L ( <i>n</i> = 94)	PAH-CHD-M ( <i>n</i> = 88)	PAH-CHD-H ( <i>n</i> = 18)
<b>Clinical features</b>						
Male/Female( <i>n</i> )	14/26	5/20	55/145	19/75	30/58	6/12
Age (years)	41.9 ± 13.1	37.3 ± 12.6	37.7 ± 14.1	35.9 ± 13.9	39.8 ± 14.6	36.4 ± 12.0
BMI (kg/m <sup>2</sup> )	22.8 ± 3.8	21.4 ± 2.9	19.8 ± 3.3 <sup>#</sup>	20.2 ± 3.6 <sup>#</sup>	19.4 ± 2.8 <sup>#</sup>	19.4 ± 2.8 <sup>#</sup>
HR (beats/min)	81.9 ± 8.4	80.9 ± 13.3	84.4 ± 14.3	81.7 ± 14.2	86.8 ± 14.1*	87.2 ± 13.8
SaO <sub>2</sub> (%)	96.7 ± 1.3	96.3 ± 1.1	92.7 ± 5.5 <sup>#</sup>	93.9 ± 4.0 <sup>#</sup>	93.1 ± 4.4 <sup>#</sup>	84.3 ± 8.8 <sup>#</sup> ■
SBP (mmHg)	117.8 ± 9.1	113.6 ± 11.0	114.4 ± 14.4	114.1 ± 13.1	115.0 ± 15.6	113.1 ± 15.8
DBP (mmHg)	76.2 ± 7.9	74.8 ± 7.2	72.3 ± 10.5	71.6 ± 9.5	72.7 ± 10.7	74.1 ± 14.1
Cardiac diagnosis						
VSD		8	59	16	21	22
ASD		11	68	17	27	24
PDA		6	65	14	25	26
Atrioventricular septal defect			8	1	4	3
<b>Biomarkers</b>						
UA (μmol/L)	255.7 ± 44.5	278.3 ± 84.6	347.7 ± 105.7 <sup>#</sup>	311.2 ± 82.8 <sup>#</sup>	365.6 ± 107.8 <sup>#</sup> ■	451.6 ± 117.6 <sup>#</sup> ■
Cr (μmol/L)	59.6 ± 10.1	60.5 ± 12.9	61.4 ± 15.1	59.1 ± 14.8	64.0 ± 14.8	60.2 ± 17.0
ALT (u/L)	15.6 ± 6.3	14.1 ± 6.7	14.6 ± 6.0	15.2 ± 6.6	14.5 ± 5.6	12.9 ± 4.9
AST (u/L)	18.2 ± 5.7	17.9 ± 4.8	19.4 ± 4.5	19.7 ± 5.3	19.4 ± 3.7	18.4 ± 4.1
TBIL (μmol/L)	10.3 ± 4.5	11.8 ± 3.5	15.6 ± 7.1 <sup>#</sup>	11.7 ± 3.6	17.6 ± 6.9 <sup>#</sup> ■	26.4 ± 15.3 <sup>#</sup> ■
DBIL (μmol/L)	3.4 ± 1.9	3.8 ± 1.2	5.5 ± 3.8 <sup>#</sup>	4.0 ± 1.4	6.2 ± 3.1 <sup>#</sup> ■	9.7 ± 8.5
D-dimer (μg/mL)	0.2 ± 0.1	0.3 ± 0.1	0.3 ± 0.2	0.3 ± 0.2	0.3 ± 0.2	0.4 ± 0.3
NT-proBNP (pg/mL)	78.0 (38.9–121.0)	94.5 (56.8–166.1)	669.8 (213.6–1500.0) <sup>#</sup>	229.3 (135.3–594.4) <sup>#</sup>	1155.5 (562.1–2485.8) <sup>#</sup> ■	2301.5 (1464.6– 4,672.6) <sup>#</sup> ■
Hb (g/L)	135.0 ± 13.1	129.3 ± 11.2	146.0 ± 26.8 <sup>#</sup>	139.6 ± 23.3 <sup>#</sup>	146.5 ± 22.6 <sup>#</sup>	177.3 ± 39.0 <sup>#</sup> ■
PLT (×10 <sup>9</sup> /L)	228.1 ± 55.4	217.2 ± 61.6	177.9 ± 52.9 <sup>#</sup>	191.2 ± 50.6 <sup>#</sup>	170.7 ± 51.1 <sup>#</sup> ■	143.9 ± 53.9 <sup>#</sup> ■
RDW-CV (%)	12.7 ± 0.6	12.8 ± 0.6	14.4 ± 8.6	14.6 ± 12.3	13.6 ± 1.3 <sup>#</sup>	17.3 ± 3.9 <sup>#</sup> ■
<b>TTE variables</b>						
RAS (mm)	29.3 ± 2.3	38.0 ± 9.2 <sup>#</sup>	42.1 ± 8.8 <sup>#</sup>	39.8 ± 6.9 <sup>#</sup>	44.7 ± 9.4 <sup>#</sup> ■	41.3 ± 11.4 <sup>#</sup>
RVD (mm)	29.3 ± 2.1	39.2 ± 9.0 <sup>#</sup>	43.3 ± 9.4 <sup>#</sup>	41.8 ± 8.6 <sup>#</sup>	45.2 ± 9.6 <sup>#</sup>	41.9 ± 10.9 <sup>#</sup>
LVEF (%)	61.6 ± 3.6	63.1 ± 4.9	62.1 ± 8.1	63.4 ± 7.6	61.7 ± 8.6	57.8 ± 7.3
PA (mm)	20.8 ± 1.6	25.6 ± 6.0 <sup>#</sup>	34.7 ± 7.5 <sup>#</sup>	35.1 ± 8.1 <sup>#</sup>	34.9 ± 7.3 <sup>#</sup>	31.3 ± 4.1 <sup>#</sup> ■
TRV (m/s)	2.0 ± 0.4	2.7 ± 0.7 <sup>#</sup>	4.2 ± 0.9 <sup>#</sup>	4.1 ± 0.9 <sup>#</sup>	4.2 ± 0.9 <sup>#</sup>	4.3 ± 0.9 <sup>#</sup>
<b>Haemodynamic variables</b>						
SPAP (mmHg)	NA	30.2 ± 4.5	89.4 ± 28.7 <sup>#</sup>	82.0 ± 27.0 <sup>#</sup>	92.6 ± 28.0 <sup>#</sup>	112.6 ± 26.4 <sup>#</sup> ■
mPAP (mmHg)	NA	20.5 ± 2.7	59.4 ± 21.2 <sup>#</sup>	53.8 ± 19.4 <sup>#</sup>	61.6 ± 20.4 <sup>#</sup>	78.1 ± 22.3 <sup>#</sup> ■
mRAP (mmHg)	NA	9.4 ± 3.7	10.9 ± 5.8	9.3 ± 4.1	12.8 ± 6.7 <sup>#</sup> ■	10.1 ± 6.5
PVR (Wood)	NA	2.3 ± 0.6	11.8 ± 9.8 <sup>#</sup>	8.4 ± 5.6 <sup>#</sup>	11.4 ± 6.9 <sup>#</sup> ■	31.9 ± 14.7 <sup>#</sup> ■

(Continued on following page)

TABLE 1 (Continued) Baseline patient characteristics.

Characteristics	Normal (n = 40)	Non-PAH-CHD (n = 25)	PAH-CHD (n = 200)	PAH-CHD-L (n = 94)	PAH-CHD-M (n = 88)	PAH-CHD-H (n = 18)
CI (L/min/m <sup>2</sup> )	NA	3.7 ± 0.8	3.1 ± 0.9 <sup>§</sup>	3.2 ± 1.0	2.8 ± 0.6 <sup>§*</sup>	1.8 ± 0.4 <sup>§**</sup>
SvO <sub>2</sub> (%)	NA	75.3 ± 5.7	66.2 ± 8.6 <sup>§</sup>	70.4 ± 6.0 <sup>§</sup>	64.2 ± 7.8 <sup>§*</sup>	53.8 ± 8.3 <sup>§**</sup>

BMI, body mass index; HR, heart rate; SaO<sub>2</sub>, arterial oxygen saturation; SBP, systolic blood pressure; DBP, diastolic blood pressure; UA, uric acid; Cr, creatinine; ALT, alanine aminotransferase; AST, aspartate aminotransferase; TBIL, total bilirubin; DBIL, direct bilirubin; NT-proBNP N-terminal pro-brain natriuretic peptide; Hb, haemoglobin; PLT, platelet; RDW-CV, red blood cell distribution width; RAS, right atrial end-systolic diameter; RVD, right ventricular end-diastolic diameter; LVEF, left ventricular ejection fraction; PA, pulmonary artery; TRV, tricuspid regurgitant velocity; SPAP, systolic pulmonary arterial pressure; mPAP, mean pulmonary arterial pressure; mRAP, mean right atrial pressure; PVR, pulmonary vascular resistance; CI, cardiac index; SvO<sub>2</sub>, venous oxygen saturation; ASD, atrial septal defect; VSD, ventricular septal defect; PDA, patent ductus arteriosus; NA, no data available. <sup>§</sup>*p* < 0.05 versus normal subjects; <sup>§</sup>*p* < 0.05 versus non-PAH-CHD, group; <sup>\*</sup>*p* < 0.05 versus PAH-CHD-L, group; <sup>\*\*</sup>*p* < 0.05 versus PAH-CHD-M, group.



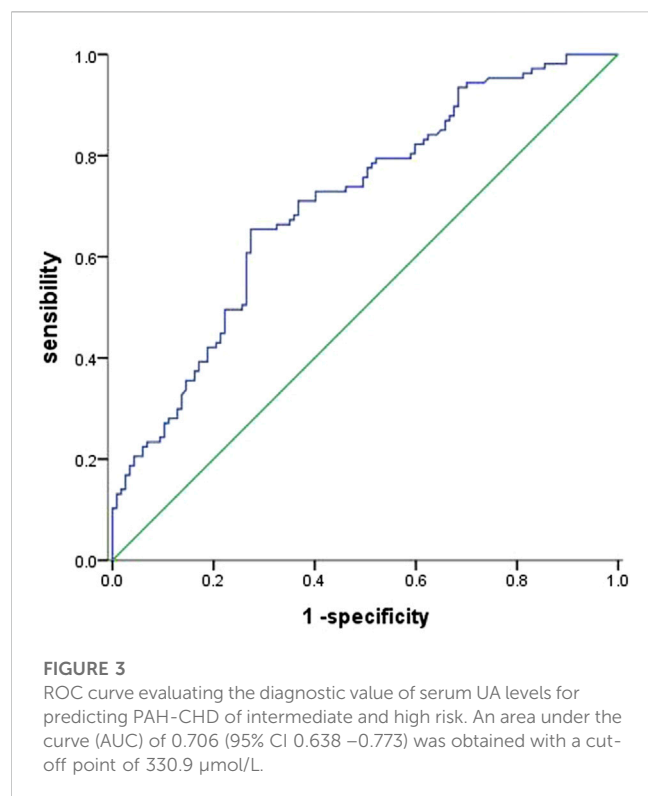
3.5 Changes in echocardiographic, haemodynamic, and serologic parameters following vasodilator treatment

All PAH-CHD patients were treated with one or two targeted drugs. Twenty patients followed up for an average of 7 ± 1 month and underwent repeat RHC. During that follow-up period, 10 of the 20 patients received an ERA combined with a PDE-5i, 5 received an ERA with PGI<sub>2</sub>, 1 received a PDE-5i with PGI<sub>2</sub>, 1 received PGI<sub>2</sub> monotherapy, and the remaining three received ERA monotherapy. After at least 6 months of therapy, serum UA level and other clinical variables were re-examined. Changes in serum UA levels, echocardiographic data, and haemodynamic parameters are presented in Table 4. Haemodynamic and echocardiographic parameters, such as RAS, RVD, sPAP, mPAP, and PVR were significantly decreased, while CI and mixed SvO<sub>2</sub> significantly

improved after vasodilator treatment. Serum UA levels significantly decreased after vasodilator treatment, from 352.7 ± 97.5 μmol/L to 294.4 ± 56.8 μmol/L (*p* = 0.001). However, no significant decrease in mRAP was observed after treatment.

4 Discussion

To the best of our knowledge, most of the current research on the role of serum UA levels in PAH has focused on patients with connective tissue diseases and IPAH. The present study found that serum UA levels were significantly elevated in intermediate and high-risk PAH-CHD patients, suggesting that UA is predictive of disease severity. We also found that serum UA levels positively correlated with mPAP, SPAP, WHO functional class, and PVR, and negatively correlated with CI, mixed SvO<sub>2</sub>, and SaO<sub>2</sub>. Serum UA



levels also significantly decreased following treatment with PAH-specific drugs. These results suggest that serum UA levels have the potential to serve as an indicator of disease severity and treatment response in PAH-CHD patients.

#### 4.1 Increased serum UA levels in PAH-CHD patients

UA levels are affected by a diverse range of factors, such as gender, age, race, and diet. Hyperuricemia is common in PAH (Nagaya et al., 1999; Voelkel et al., 2000; Dimitroulas et al., 2011).

Nagaya et al. (1999) found that increased serum UA levels in idiopathic PAH patients are negatively correlated with CO, and constitute an independent risk factor for long-term mortality. Dimitroulas et al. (2011) reported that systemic sclerosis patients with PAH had higher serum UA levels than those without PAH, and that serum UA levels correlated with 6-min walking and other functional capacity tests. A study conducted on patients with primary and secondary PAH found that serum UA levels were higher in patients with severe PAH (Voelkel et al., 2000).

The results of our research are in agreement with these studies. We found that serum UA levels were significantly higher in patients with PAH-CHD than in non-PAH-CHD patients or healthy subjects. We also noted that hyperuricemia in the present study was mainly present in high-risk PAH-CHD patients.

Although the exact mechanism as to why PAH patients have elevated serum UA levels is unclear, tissue ischaemia and/or hypoxia may play an important role. CHD patients with ES have hypoxic exacerbations due to right-to-left shunting, which may lead to increased serum UA levels (Fathallah and Krasuki, 2018). We hypothesized that the differences in serum UA levels observed within the PAH-CHD group may be due to the higher incidence of ES in the intermediate and high-risk groups. SaO<sub>2</sub> levels were lowest in PAH-CHD-H patients, and UA levels were negatively correlated with SaO<sub>2</sub>, SvO<sub>2</sub>, and CI, suggesting that uric acid overproduction reflects damage to oxidative metabolism.

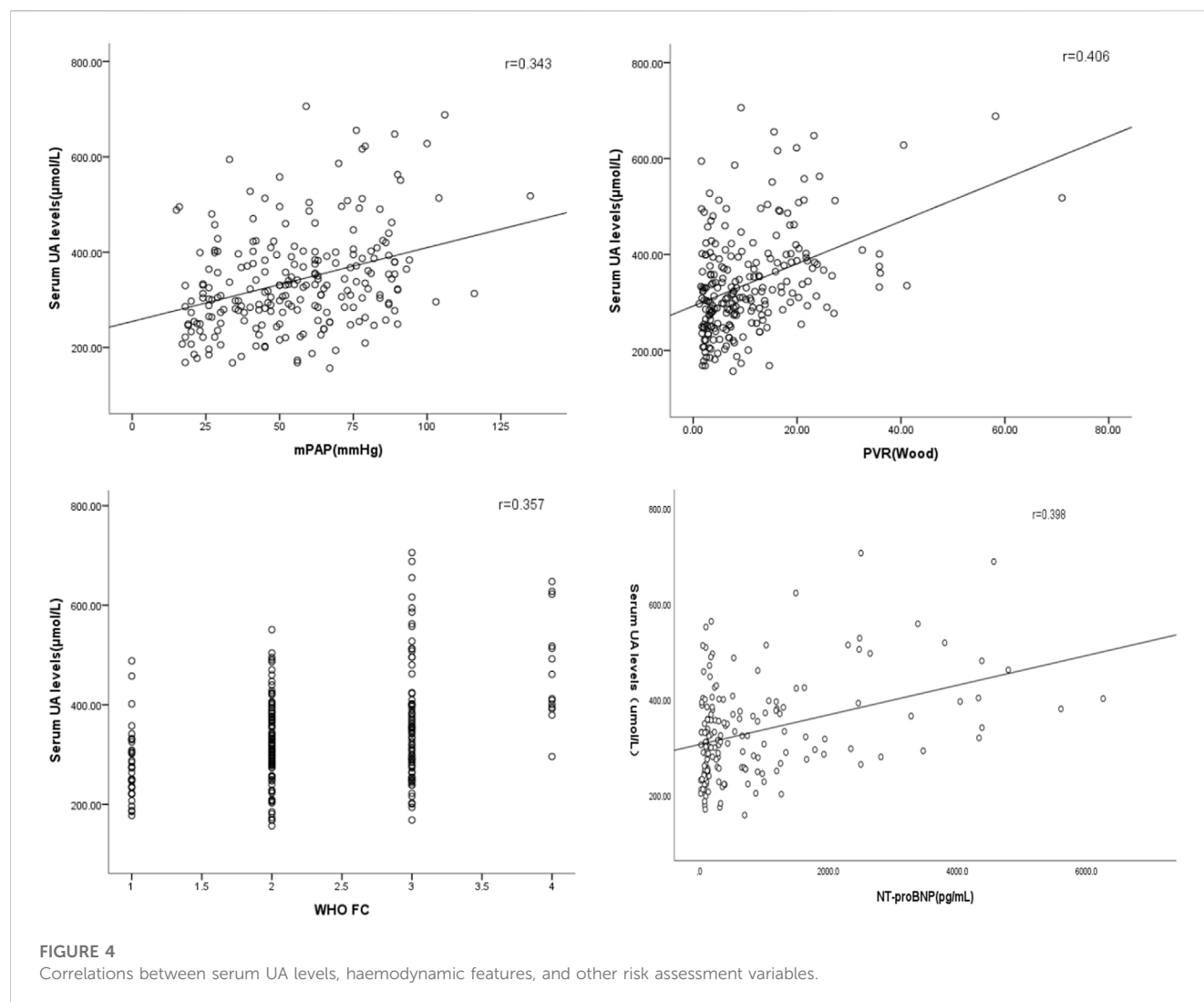
Reduced CI and renal perfusion may also be responsible for the elevated serum UA levels. A study by Ross et al. (1986) found that elevated UA levels in ES patients were due to inappropriately low uric acid excretion and enhanced urate reabsorption. Bendayan et al. (2003) reported that hyperuricemia in patients with worsening PAH is caused by impaired renal excretion of UA, which was associated with decreased CO and renal perfusion pressure (Prince et al., 2012). Although serum UA levels were negatively correlated with right CI in the present work, no statistically significant association was found with either serum Cr or LVEF in any of the five groups. These results suggest that patients with normal intrarenal dynamics can appropriately manage elevated UA levels.

Hoeper et al. (1999) found a strong association between serum UA levels and mRAP. This was not the case in our study, although

TABLE 2 Associations between serum UA levels and other variables.

Variables	Correlation coefficient	95% confidence interval	p-Value
SPAP	0.261	0.105 to 0.386	<0.001
mPAP	0.343	0.156 to 0.454	<0.001
mRAP	0.047	−0.105 to 0.260	0.488
PVR	0.406	0.225 to 0.550	<0.001
WHO FC	0.357	0.156 to 0.419	<0.001
NT-proBNP	0.398	0.204 to 0.464	<0.001
CI	−0.183	−0.374 to −0.152	0.006
SvO <sub>2</sub>	−0.293	−0.387 to −0.008	<0.001
SaO <sub>2</sub>	−0.329	−0.411 to −0.127	<0.001

WHO FC, WHO functional class; for others, see Table one.



intermediate-risk PAH-CHD patients higher mRAP than CHD patients with normal pulmonary artery pressures. Interestingly, no increases in mRAP were observed in high-risk PAH-CHD patients, which may be explained by right-to-left shunting reducing right atrial pressure.

Diuretic therapy is known to increase serum UA levels by stimulating urate reabsorption in the proximal tubule. All PAH patients received diuretics in our study. However, their baseline renal function was normal, so no significant differences were found between groups. We therefore believe that diuretic use cannot explain the elevated UA level observed in PAH-CHD patients.

## 4.2 Is UA a pathogenic factor in PAH?

While the degree to which elevated UA levels contribute to the development of PAH is unknown, several mechanisms may be proposed to this regard. First, persistent hyperuricemia may result in endothelial dysfunction, which in turn may lead to PAH progression through the promotion of oxidative stress. Besides being a key enzyme for UA production, xanthine

oxidoreductase (XOR) is closely related to vascular oxidative stress, plausibly through the generation of reactive oxygen species (ROS) (Berry and Hare, 2004). ROS produced by increased XOR activity may exceeds cellular antioxidant capacity, inducing oxidative stress and endothelial dysfunction (Cai and Harrison, 2000). Second, disruption of NO signaling pathways by UA may be related to the pathobiology of PAH. Pulmonary vasodilation by synthesizing NO through the L-arginine-eNOS pathway, a complex process that is catalyzed by eNOS with arginine as a substrate (Zharikov et al., 2008). Third, elevated UA levels stimulate the release of a variety of inflammatory mediators and induce smooth muscle cell proliferation, thereby promoting the development and progression of pulmonary vascular disease (Rao et al., 1991; Kanellis et al., 2003; Kang et al., 2005). The present study lacked a long follow-up time or the use of cardiovascular events as endpoints, but it did find that serum UA levels significantly correlated with prognostic parameters. UA levels may therefore indirectly reflect hemodynamic status, thereby assessing the severity of PAH-CHD.



**TABLE 3** The influence of serum UA levels on clinical indicators.

	UA ≤ 330.9 μmol/L	UA > 330.9 μmol/L	<i>p</i> -Value
	( <i>n</i> = 122)	( <i>n</i> = 103)	
General data			
Age (year)	37.5 ± 12.6	37.8 ± 15.4	0.843
Female (%)	88.5	55.2	<0.001
HR (times/min)	83.8 ± 14.2	84.2 ± 14.2	0.835
SaO <sub>2</sub> (%)	94.6 ± 3.6	91.4 ± 6.4	<0.001
cardiac function III-IV(%)	28.7	54.4	<0.001
Biochemical data			
NT-proBNP(pg/mL)	300.0 (132.4-855.9)	977.5 (241.3-2379.8)	<0.001
Echocardiographic parameters			
RAS (mm)	39.5 ± 8.2	44.1 ± 9.2	<0.001
RVD (mm)	40.8 ± 9.0	45.1 ± 9.3	0.001
TRV (m/s)			
LVEF (%)	62.9 ± 7.6	61.4 ± 7.9	0.151
Right Heart Catheter Parameters			
mPAP (mmHg)	49.1 ± 22.4	62.2 ± 22.7	<0.001
mRAP (mmHg)	10.5 ± 5.8	10.9 ± 5.4	0.610
PVR (Wood)	7.5 ± 5.6	14.6 ± 12.0	<0.001
CI(L/min/m <sup>2</sup> )	3.4 ± 0.9	2.9 ± 0.9	<0.001
SvO <sub>2</sub> (%)	69.0 ± 7.6	65.1 ± 9.6	0.001

**TABLE 4** Changes in clinical parameters due to treatment.

Parameters	Baseline	After therapy	<i>p</i> -Value
RAS (mm)	45.7 $\pm$ 6.0	41.0 $\pm$ 4.4	0.006
RVD (mm)	47.4 $\pm$ 7.8	42.4 $\pm$ 5.6	0.011
sPAP (mmHg)	91.2 $\pm$ 22.1	70.7 $\pm$ 19.8	<0.001
SPAP (mmHg)	95.5 $\pm$ 20.3	78.9 $\pm$ 21.2	<0.001
mPAP (mmHg)	60.3 $\pm$ 14.1	50.9 $\pm$ 14.8	<0.001
mRAP (mmHg)	9.7 $\pm$ 4.1	9.4 $\pm$ 3.8	0.786
PVR (Wood)	9.9 $\pm$ 6.9	4.5 $\pm$ 1.5	0.001
CI (L/min/m <sup>2</sup> )	2.9 $\pm$ 0.7	4.5 $\pm$ 1.0	<0.001
SvO <sub>2</sub> (%)	65.2 $\pm$ 5.4	69.0 $\pm$ 5.6	0.003
UA ( $\mu\text{mol/L}$ )	352.7 $\pm$ 97.5	294.4 $\pm$ 56.8	0.001

sPAP, systolic pulmonary arterial pressure estimated by echocardiography. For other abbreviations see [Table 1](#).

All 20 patients who received PAH-specific therapy for at least 6 months demonstrated significant improvements in their WHO functional class, echocardiographic parameters, and haemodynamic

variables. Serum UA levels decreased and mixed SvO<sub>2</sub> and right heart CI increased. Oya et al. found that serum UA levels vary in ES patients, with reduced PVR after treatment with PGI<sub>2</sub> (Oya et al.,

2000). These results suggest that serum UA levels may serve as a useful indicator of disease progression and treatment efficacy in PAH-CHD patients.

### 4.3 Targeted therapies in PAH-CHD patients

PAH-CHD is a heterogeneous patient population with various phenotypes of pulmonary vascular disease that range from increased pulmonary blood flow to Eisenmenger physiology with shunt reversal due to supra-systemic pulmonary pressures and right-to-left shunting. There is now additional evidence that PAH-targeted therapies are of benefit to patients with PAH-CHD, and that these therapies are commonly used in this patient population (Rosenkranz et al., 2015; Hidayati et al., 2020; Kaemmerer et al., 2021). This study followed 20 PAH-CHD patients who were re-catherized after at least 6 months of targeted drug treatment. We found that right heart size was significantly improved and hemodynamic indicators, including PVR and PAP, were significantly decreased. This suggests that targeted drug treatment can improve the symptoms and reduce the incidence of cardiovascular events in patients with PAH-CHD. We look forward to a further confirming the role of targeted drugs in congenital heart disease with PH with a larger scale clinical study.

### 4.4 Clinical implications

Serum UA levels are simple to measure in a non-invasive and inexpensive manner. Several additional biochemical markers, including BNP, TNT, ET-1, and CRP, have been proposed, (Nagaya et al., 1999; Leuchte et al., 2007; Castillo-Martínez et al., 2016; Kylhammar et al., 2018), but serum UA may be superior in that it performs as a predictor of the disease severity and mortality of patients with PAH-CHD over long-term follow-up. The present work also found that serum UA levels decreased following PAH-specific drug therapy. Based on these findings, we suggest that serum UA levels be repeatedly measured to evaluate the treatment response of PAH-CHD patients in both the outpatient and inpatient settings.

### 4.5 Limitations

The findings of the present work have to be interpreted in the context of its limitations. First, this is a single center study. Second, although this study had a relatively large sample size compared with related studies in the literature, it was still small for stratified analysis. A larger multi-center prospective study is necessary to further refine our findings. Third, only a few patients underwent repeated RHC after treatment with PAH-specific drugs. The current data can only partially reflect the relationship between decreased UA levels and improved haemodynamic indicators. Fourth, this study lacked a long follow-up time and the use of cardiovascular events as endpoints. We also failed to confirm that whether serum UA levels could act as an independent risk factor for CHD patients with PAH.

## 4.6 Conclusion

In conclusion, we associated serum UA levels with clinical and haemodynamic severity in PAH-CHD patients. Serum UA levels may be a practical biomarker for assessing risk stratification in patients with PAH, and for evaluating treatment response to PAH-specific drugs. Further studies with larger sample sizes are necessary to confirm the results of this study.

## Data availability statement

The raw data supporting the conclusion of this article will be made available by the authors, without undue reservation.

## Ethics statement

The studies involving humans were approved by The Second Xiangya Hospital of Central South University. The studies were conducted in accordance with the local legislation and institutional requirements. The participants provided their written informed consent to participate in this study.

## Author contributions

JL and YL did the literature search, data collection, study design, analysis of data and manuscript preparation. JC, HQ, and WC designed the study, analysed the data and reviewed the manuscript. XL, YC, and YT designed the study and prepared and reviewed the manuscript. JL analysed the data. All authors contributed to the article and approved the submitted version.

## Funding

This work was supported by National Natural Science Foundation of China (Project 81870233 and 81600249), Natural Science Foundation of Hunan Province (2022JJ30823), Hunan Provincial Health Commission Foundation of China (Project 202103010961), Natural Science Foundation of Changsha city (Project kq2202392) and China International Medical Foundation (2022-N-01-23).

## Acknowledgments

The authors express their gratitude to all the participants for their cooperation.

## Conflict of interest

The authors declare that the research was conducted in the absence of any commercial or financial relationships that could be construed as a potential conflict of interest.

## Publisher's note

All claims expressed in this article are solely those of the authors and do not necessarily represent those of their affiliated

organizations, or those of the publisher, the editors and the reviewers. Any product that may be evaluated in this article, or claim that may be made by its manufacturer, is not guaranteed or endorsed by the publisher.

## References

- Arnott, C., strange, G., Bullock, A., Kirby, A. C., Donnell, C., Radford, D. J., et al. (2018). Pulmonary vasodilator therapy is associated with greater survival in Eisenmenger syndrome. *Heart* 104, 732–737. doi:10.1136/heartjnl-2017-311876
- Bendayan, D., Shitrit, D., Ygla, M., Huerta, M., Fink, G., and Kramer, M. R. (2003). Hyperuricemia as a prognostic factor in pulmonary arterial hypertension. *Respir. Med.* 97 (2), 130–133. doi:10.1053/rmed.2003.1440
- Berry, C. E., and Hare, J. M. (2004). Xanthine oxidoreductase and cardiovascular disease: molecular mechanisms and pathophysiological implications. *J. Physiol.* 555 (3), 589–606. doi:10.1113/jphysiol.2003.055913
- Cai, H., and Harrison, D. G. (2000). Endothelial dysfunction in cardiovascular diseases: the role of oxidant stress. *Circ. Res.* 87 (10), 840–844. doi:10.1161/01.res.87.10.840
- Castillo-Martínez, D., Marroquín-Fabián, E., Lozada-Navarro, A. C., Mora-Ramírez, M., Juárez, M., Sánchez-Muñoz, F., et al. (2016). Levels of uric acid may predict the future development of pulmonary hypertension in systemic lupus erythematosus: a seven-year follow-up study. *Lupus* 25 (1), 61–66. doi:10.1177/0961203315600539
- Dimitroulas, T., Giannakoulas, G., Dimitroula, H., Sfetsios, T., Parcharidou, D., Karvounis, H., et al. (2011). Significance of serum uric acid in pulmonary hypertension due to systemic sclerosis: a pilot study. *Rheumatol. Int.* 31 (2), 263–267. doi:10.1007/s00296-010-1557-4
- Dimopoulos, K., Wort, S. J., and Michael, A. (2014). Pulmonary hypertension related to congenital heart disease: a call for action. *Euro Heart J.* 35 (11), 691–700. doi:10.1093/eurheartj/ehz437
- Fathallah, M., and Krasuki, R. A. (2018). A multifaceted approach to pulmonary hypertension in adults with congenital heart disease. *Prog. Cardiovasc. Dis.* 61 (3–4), 320–327. doi:10.1016/j.pcad.2018.07.017
- Foris, V., Kovacs, G., Tscherner, M., Olschewski, A., and Olschewski, H. (2013). Biomarkers in pulmonary hypertension: what do we know? *Chest* 144 (1), 274–328. doi:10.1378/chest.12-1246
- Galiè, N., Humbert, M., Vachiery, J. L., Gibbs, S., Lang, I., Torbicki, A., et al. (2015). 2015 ESC/ERS guidelines for the diagnosis and treatment of pulmonary hypertension: the joint task force for the diagnosis and treatment of pulmonary hypertension of the European society of cardiology (ESC) and the European respiratory society (ERS): endorsed by: association for European paediatric and congenital cardiology (AEPC), international society for heart and lung transplantation (ISHLT). *Eur. Respir. J.* 46 (4), 903–975. doi:10.1183/13993003.01032-2015
- Hidayati, F., Gharini, P. P. R., Hartopo, A. B., Anggrahini, D. W., and Dinarti, L. K. (2020). The effect of oral sildenafil therapy on health-related quality of life in adults with pulmonary arterial hypertension related to uncorrected secundum atrial septal defect: a quasi experimental study. *Health Qual. Life Outcomes* 18 (1), 278. doi:10.1186/s12955-020-01498-7
- Hoepfer, M. M., Hohlfield, J. M., and Fabel, H. (1999). Hyperuricaemia in patients with right or left heart failure. *Eur. Respir. J.* 13, 682–685. doi:10.1183/09031936.99.13368299
- Jiang, X., and Jing, Z. C. (2013). Epidemiology of pulmonary arterial hypertension. *Curr. Hypertens. Rep.* 15 (6), 638–649. doi:10.1007/s11906-013-0397-5
- Kaemmerer, A. S., Gorenflo, M., Huscher, D., Pittrow, D., Ewert, P., Pausch, C., et al. (2021). Medical treatment of pulmonary hypertension in adults with congenital heart disease: updated and extended results from the international COMPERA-CHD registry. *Cardiovasc. Diagn. Ther.* 11 (6), 1255–1268. doi:10.21037/cdt-21-351
- Kanellis, J., Watanabe, S., Li, J. H., Kang, D. H., Li, P., Nakagawa, T., et al. (2003). Uric acid stimulates monocyte chemoattractant protein-1 production in vascular smooth muscle cells via mitogen-activated protein kinase and cyclooxygenase-2. *Hypertension* 41 (6), 1287–1293. doi:10.1161/01.HYP.0000072820.07472.3B
- Kang, D. H., Park, S. K., Lee, I. K., and Johnson, R. J. (2005). Uric acid-induced C-reactive protein expression: implication on cell proliferation and nitric oxide production of human vascular cells. *J. Am. Soc. Nephrol.* 16 (12), 3553–3562. doi:10.1681/ASN.2005050572
- Kylhammar, D., Kjellström, B., Hjalmarsson, C., Jansson, K., Nisell, M., Söderberg, S., et al. (2018). A comprehensive risk stratification at early follow-up determines prognosis in pulmonary arterial hypertension. *Euro Heart J.* 39 (47), 4175–4181. doi:10.1093/eurheartj/ehx257
- Leuchte, H. H., Nounou, M. E., Tuerpe, J. C., Hartmann, B., Baumgartner, R. A., Vogeser, M., et al. (2007). N-terminal pro-brain natriuretic peptide and renal insufficiency as predictors of mortality in pulmonary hypertension. *Chest* 131 (2), 402–409. doi:10.1378/chest.06-1758
- Nagaya, N., Nishikimi, T., Uematsu, M., Satoh, T., Kyotani, S., Sakamaki, F., et al. (2000). Plasma brain natriuretic peptide as a prognostic indicator in patients with primary pulmonary hypertension. *Circ* 102 (8), 865–870. doi:10.1161/01.cir.102.8.865
- Nagaya, N., Uematsu, M., Satoh, T., Kyotani, S., Sakamaki, F., Nakanishi, N., et al. (1999). Serum uric acid levels correlate with the severity and the mortality of primary pulmonary hypertension. *Am. J. Respir. Crit. Care Med.* 160 (2), 487–492. doi:10.1164/ajrccm.160.2.9812078
- Oya, H., Nagaya, N., Satoh, T., Sakamaki, F., Kyotani, S., Fujita, M., et al. (2000). Haemodynamic correlates and prognostic significance of serum uric acid in adult patients with Eisenmenger syndrome. *Heart* 84 (1), 53–58. doi:10.1136/heart.84.1.53
- Pezzuto, B., Badagliacca, R., Poscia, R., Ghio, S., D'Alto, M., Vitulo, P., et al. (2015). Circulating biomarkers in pulmonary arterial hypertension: update and future direction. *J. Heart Lung Transpl.* 34 (3), 282–305. doi:10.1016/j.healun.2014.12.005
- Prince, L. C., Wort, S. J., Perros, F., Dorfmueller, P., Huertas, A., Montani, D., et al. (2012). Inflammation in pulmonary arterial hypertension. *Chest* 141 (1), 210–221. doi:10.1378/chest.11-0793
- Rao, G. N., Corson, M. A., and Berk, B. C. (1991). Uric acid stimulates vascular smooth muscle cell proliferation by increasing platelet derived growth factor A-chain expression. *J. Biol. Chem.* 266 (13), 8604–8608. doi:10.1016/s0021-9258(18)93017-6
- Rosenkranz, S., Ghofrani, H. A., Beghetti, M., Ivy, D., Frey, R., Fritsch, A., et al. (2015). Riociguat for pulmonary arterial hypertension associated with congenital heart disease. *Heart* 101 (22), 1792–1799. doi:10.1136/heartjnl-2015-307832
- Ross, E. A., PerloV, J. K., Danovitch, G. M., Child, J. S., and Canobbio, M. M. (1986). Renal function and urate metabolism in late survivors with cyanotic congenital heart disease. *Circ* 73 (3), 396–400. doi:10.1161/01.cir.73.3.396
- Schwartz, S. S., Madsen, N., Laursen, H. B., Hirsch, R., and Olsen, M. S. (2018). Incidence and mortality of adults with pulmonary hypertension and congenital heart disease. *Am. J. Cardiol.* 121 (12), 1610–1616. doi:10.1016/j.amjcard.2018.02.051
- Simonneau, G., Montani, D., Celermajer, D. S., Denton, C. P., Gatzoulis, M. A., Krowka, M., et al. (2019). Haemodynamic definitions and updated clinical classification of pulmonary Hypertension. *Eur. Respir. J.* 53 (1), 1801913. doi:10.1183/13993003.01913-2018
- Voelkel, M. A., Wynne, K. M., Badesch, D. B., Groves, B. M., and Voelkel, N. F. (2000). Hyperuricemia in severe pulmonary hypertension. *Chest* 117 (1), 19–24. doi:10.1378/chest.117.1.19
- Zharikov, S., Krotova, K., Hu, H., Baylis, C., Johnson, R. J., Block, E. R., et al. (2008). Uric acid decreases NO production and increases arginase activity in cultured pulmonary artery endothelial cells. *Am. J. Physiol. Cell. Physiol.* 295 (5), C1183–C1190. doi:10.1152/ajpcell.00075.2008

# Frontiers in Pharmacology

Explores the interactions between chemicals and living beings

The most cited journal in its field, which advances access to pharmacological discoveries to prevent and treat human disease.

## Discover the latest Research Topics

[See more →](#)

### Frontiers

Avenue du Tribunal-Fédéral 34  
1005 Lausanne, Switzerland  
[frontiersin.org](https://frontiersin.org)

### Contact us

+41 (0)21 510 17 00  
[frontiersin.org/about/contact](https://frontiersin.org/about/contact)



### Frontiers in Pharmacology

